POLITECNICO DI TORINO

Collegio di Ingegneria Chimica e dei Materiali

Master of Science Course
In Material Engineering

Master of Science Thesis

Development of “e-noses” for VOCs sensing

Relator
Prof. Marco SANGERMANO
Dr. Tim ERDMANN

Candidate
Michael ZANON

March 2019

POLITECNICO DI TORINO

Abstract

COLLEGIO DI INGEGNERIA CHIMICA E DEI MATERIALI

DISAT

Master of Science Course in Materials Engineering

Development of polymeric VOCs sensors

Michael Zanon

The human nose is still the primary `instrument' used to assess the smell of various industrial products today, despite considerable and sustained attempts to develop new electronic instrumentation capable of mimicking its remarkable ability . The development of a gas sensor able to detect a wide range of chemical substances is considered to be a potential way to provide a solution to this need. Especially VOCs compound, due to their eventual not human-detectable smell , poisoning properties and common utilization, are an important class of analytes needed to be detected even at really low concentrations. In this thesis an investigation on VOCs polymeric chemiresistors, a type of gas sensors, is presented. The sensors are fabricated from the synthesis of the polymer to the final testing on the selected gases. The main aim of this thesis was to build a sensor able to present high values of sensitivity, exploring various types of polymers, selecting the most promising one and functionalize it. Between the three polymers tested, the results showed superiors performances of polyaniline in terms of sensibility, even compared with a commercially available sensor, and a certain degree of selectivity referring to polypyrrole end PEDOT:PSS.

AKLOWLEDGEMENTS

Firstly, I want to thank my professor, Marco Sangermano, for his support on every occasion. His availability was a rare gift and I am truly happy that I had the possibility to meet a so wonderful person, as much in the professional sector as in the personal life.

I would like to reserve a special thanks to Dr. Tim Erdmann, my mentor during the 5 months spent at IBM In the United States. I want to thank him for his continuous support, his assistance and availability. However, his advices were the most precious gift he could ever gave me, improving myself as a researcher. I would be happy if one day I could be just a similar researcher as he is.

I'm grateful to Dr. Andrea Fasoli and Dr. Luisa Bozano and to the sensor team all for the splendid opportunity provided to me.

This thesis, though, is not just the result of the 5 months spent in America at IBM Almaden Research Center but rather of two years and a half full of difficulties of all kinds. A special thanks is then also to all the persons who followed me and were by my side during the all path.

To Ross and Vivien, to the time spent together, to the trips around the west coast, to the IPA (too many), to the walks around IBM and to the funny visits to the museums. I could not ask anything better because: "All that I can see is just a yellow lemon tree".

To Mauro, Maria, Nicola and Rosario. I arrived in Turin by myself, I was ***1****, and you all with your strength, your affection, your presence made me that* ***+1****, different but never less. It was the only thing I wished for.*

To Andrea and Laura, my best friends. All that I said goes for you and even more. Our path started so many years ago that I have even lost the count. It is so strange how certain people meet during the path and never leave themselves anymore, no matter how far they are. We were meant to be together and we will be for so long again. Thanks guys.

To Lissa, Federico, Carla and the rest of the people I've met in those two years. It is so incredible how so many persons can enter in your life and enrich it in ways you cannot even image, you too were part of this adventure and I would like to say thanks to you all, from the first to the last.

To Sergio, the most complicated thanks of all. It is useless to say that in these two years you were the most important person to me, it is useless to say that you were like a lifebelt in a stormy sea, it is useless to say that you healed me, it is useless to say many things about you. To you because this goal it could not be achieved without you, to you because even if it is useless again, you will be the first person on the line whenever I will remember of this path. Thank you.

To my sisters, Jessica and Sofia. To you that are an integral part of myself, different sides of the same coin, so different but so equal, united by love. To you that are the only thing in my life that will never change.

To my dad. To you that, despite all the difficulties, were there to support me and understand even when nobody else could.

Finally, to my mum, to her who is everything to me. My rock, my force, the person that since my childhood I always tried to emulate and the person I want to be in my future. To you mum, this is yours more than mine. Congratulations.

Contents

RIASSUNTO

Sin dagli albori dell'antichità, una delle caratteristiche che hanno reso il genere umano la specie dominante è stata la presenza e lo sviluppo sinergico di tutti e cinque gli organi di senso. Tra di essi due sono quelli imputabili al nutrimento, l'olfatto e il gusto. Nonostante questo, l'olfatto è un fattore dominante nella nostra percezione degli odori ed è impiegato, spesso singolarmente, per profilare gli aromi di vari prodotti e la loro qualità. Il senso dell'olfatto parte dalla stimolazione del nervo olfattivo, tramite l'adsorbimento di molecole odorose emesse da un oggetto sulla superficie di speciali recettori sensoriali, presenti nella cavità interna del naso, chiamate ciglia. Il segnale elettrico che si sviluppa è in grado di essere codificato e processato dal cervello in modo da fornire una risposta precisa sulla natura della molecola odorosa inalata. Tuttavia, l'uso del naso umano presenta delle limitazioni dovute sia al tipo di molecola inalata che alle condizioni soggettive della persona interessata.

In questo ambito entrano dunque tutte quelle tecnologie denominate "sensi elettronici" che sono in grado di emulare gli organi di senso umani tramite l'utilizzo di un insieme di singoli sensori e di un sistema di ricognizione dell'impronta elettronica delle molecole odorose oggetto di studio. In questa direzione sono stati sviluppati un insieme di dispositivi dove al nome dell'organo riprodotto è anteposta la lettera "e"; Un esempio fra tutti l'"e-nose". Questa tecnologia è, in molti casi, ancora nelle fasi iniziali ed il nome di sensori di gas è tuttavia preferito ed è di questo argomento che tratterà la seguente tesi di laurea. La realizzazione di questi dispositivi, parte dagli anni 50 del 1900, ma solo nel 1988 Gardner ha fornito una definizione univoca come strumento che comprende una matrice di sensori dotati di una specificità parziale collegata ad un sistema di riconoscimento capace di identificare fragranze, siano esse semplici o complesse. Ogni sensore è tuttavia sensibile non ad un singolo analita (come lo sono invece le ciglia) ma ad un'ampia gamma di molecole che possono in alcuni casi dare risposte del tutto simili le une alle altre. Questo è il motivo per cui diversi sensori, anche di diversi materiali, devono essere impiegati congiuntamente in una matrice al fine di avere un'impronta del tutto unica per il gas o la fragranza che si vuole analizzare. Sarà successivamente il sistema centrale di analisi (l'equivalente del nostro cervello) a processare tramite algoritmi i risultati tramite varie tecniche, tra cui un'analisi grafica, un'analisi delle componenti principali (PCA) oppure utilizzando il machine learning tramite un analisi neuronale di un network precedentemente aggiornato (ANN).

Varie sono le applicazioni per questo genere di dispositivi e in vari settori, da quello medico a quello aerospaziale, dall'alimentare a quello militare. In ambito medico l'analisi dei prodotti volatili delle urine o dei sottoprodotti di importanti e gravi malattie, quali il cancro al polmone, può portare ad una diagnosi tempestiva e ipoteticamente al salvataggio di una vita umana. In ambito ambientale potrebbe rendere possibile la rilevazione di inquinanti atmosferici, con un tempo di lettura e un ingombro spaziale estremamente inferiori alle tecniche generalmente

utilizzate oggi giorno. Inoltre, la rilevazione di sostanze pericolose alla vita umana, anche alle basse concentrazioni non percepibili ma letali per l'uomo, è una delle direzioni in cui la ricerca si sta muovendo. L'ambito più promettente è, al momento, quello alimentare. Di fatti questo genere di sensori è già utilizzato per un controllo qualità dei prodotti, per la rintracciabilità della provenienza geografica del cibo e per l'adulterazione di bevande. Di fatti, l'applicazione di sensori di dimensioni ridotte e a basso costo nei pressi del cibo nei supermercati oppure all'interno degli Smart-phone potrebbe risultare nei prossimi anni una delle frontiere più promettenti per il mondo della ricerca.

Il metodo di funzionamento di questi dispositivi si basa dunque sulla rilevazione di speciali molecole (una o centinaia combinate insieme) in grado di volatilizzare a relativamente basse temperature, per cui dotate di un'alta pressione di vapore a temperatura ambiente. Queste molecole, chiamate VOCs (volatile organic compound) possono essere di origine naturale (come ad esempio l'odore del succo d'arancia) come artificiale (come un'ampia gamma di solventi, l'acetone ne è un esempio). In questa tesi un totale di 15 solventi sono stati testati, in ordine di polarità, da molecole completamente apolari come il cicloesano fino all'acqua.

Un sensore è un dispositivo, nella sua definizione più ampia, che è in grado di realizzare un cambiamento delle sue proprietà a seguito di una variazione nelle condizioni ambientali nel suo attorno. Pure in questo caso, un sensore di gas è un dispositivo nel quale, a fronte di una differente concentrazione di una particolare specie chimica nel suo attorno, cambierà una delle sue caratteristiche intrinseche. Numerosi per cui sono i sensori sviluppati, ognuno in grado di variare una particolare proprietà. Tra i dispositivi più utilizzati vi sono i sensori piezoelettrici, i sensori ottici, i transistor, i pellistori e i chemi-resistori. I sensori piezoelettrici abbinano all'adsorbimento delle molecole sulla superficie o nel bulk e all'applicazione di un potenziale oscillante un cambio nella frequenza di risonanza del materiale stesso, diversa in base all'analita adsorbito. Per quanto riguarda i sensori ottici sono le proprietà ottiche quali la fluorescenza o l'adsorbanza a cambiare mentre per i transistor, di cui i MOSFET sono la categoria più sviluppata, c'è una variazione nella funzione lavoro. Le ultime due categorie sono i pellistori, sensori che si basano sul cambiamento del calore di reazione dovuta all'adsorbimento, e i chemi-resistori, una delle categorie più importanti e oggetto di questo lavoro.

Questi sensori si basano su una variazione della resistenza elettrica a seguito dell'applicazione di un voltaggio e di nuovo, all'adsorbimento di un analita sulla superficie del dispositivo. Sono dispositivi testati sia tramite corrente alternata (AC) che diretta (DC, come in questo lavoro). L'architettura classica presuppone un substrato di materiale semi-conduttore, silicio generalmente, su cui sono applicati tramite fotolitografia degli elettrodi conduttivi, ad esempio d'oro. Questi elettrodi presentano (vedi figura 1.7) dei gap sul quale il materiale selezionato per il sensing è applicato. Successivamente un voltaggio è applicato tra gli elettrodi e viene misurata la variazione nella resistenza del materiale oggetto di studio. La curva caratteristica ottenibile tramite questo genere di sensori è riportata in figura 1.13 in cui si relazionano la resistenza elettrica (e la sua variazione) e il tempo durante il quale l'analita è fatto fluire sulla superficie del materiale. Una delle caratteristiche è la presenza di una baseline indicata relazionando conduttività elettrica al tempo di esposizione dell'analita, ove la conduttività (e di conseguenza la resistenza elettrica, misurata tramite la formula 1.1) decresce durante il tempo di esposizione. Un plateau è generalmente raggiunto dopo un determinato tempo di sensing per il desorbimento delle specie precedentemente adsorbite sul materiale a seguito della "pulizia" della superficie tramite aria secca o altri mezzi. La sensing curve presenta numerosi picchi, nel momento stesso in cui le molecole vengono in contatto con la superficie del dispositivo e l'entità di questi ultimi tramite la formula 1.4 è in grado di fornire la risposta del materiale a quell'analita e a quella concentrazione. Di conseguenza risulteranno molto importanti tutti quei parametri tempo-dipendenti che forniranno una risposta univoca per tutte le concentrazioni di analita testate. Questi parametri, consultabili in figura 1.15, sono chiamati:

- Tempo di stabilizzazione; il tempo che impiega la variazione di resistenza elettrica per stabilizzarsi in un nuovo plateau.
- Tempo di risposta o tempo di esposizione; il tempo totale durante il quale l'analita è in contatto con il sensore.
- Tempo di recovery; il tempo impiegato per far tornare il sensore al valore di resistenza della baseline precedente all'esposizione dell'analita.

Numerosi sono i materiali utilizzabili in questa classe di sensori, dai MOS (metal-oxide semiconductors) che operano ad alta temperatura tramite la reazione degli gli ioni ossigeno presenti sulla loro superficie con le molecole di analita, a nanomateriali come il grafene, che operano in maniera analoga ai MOS ma con un rapporto superficie-volume estremamente più elevato. Altra classe sono i compositi a matrice polimerica caricati con filler conduttivi; in questo caso tramite il rigonfiamento della matrice successiva all'adsorbimento dell'analita nel bulk, il percorso conduttivo tra i filler o percolazione viene a mancare e si nota una crescita nella resistenza elettrica.

È evidente che tutti i materiali considerati presentino proprietà quali resistenza elettrica intrinseca, permittività elettrica, fattore di dissipazione elettrica e resistenza dielettrica adeguate all'impiego di questa tecnologia. Nonostante questo, il requisito di basso prezzo, flessibilità e alta reattività a numerosi analiti ha portato la scelta a ricadere su una classe di materiali, poco conosciuti e da poco scoperti ma con numerosissime potenzialità, ovvero i polimeri conduttori (ICP). Normalmente i polimeri sono considerati dielettrici poiché presentano un gap tra LUMO e HOMO superiore ai 5eV tanto da non permettere il salto degli elettroni in condizioni stardard. Questo porta a valori di resistenza elettrica molto alti (~ MΩ-GΩ), tuttavia negli anni '70 Heeger, MacDiarmid e Shirakawa scoprirono che, dopando il poliacetilene con iodio, questo presentava valori di conduttività nell'ordine degli Ω-KΩ con band gap comparabili a quelli dei semiconduttori. Da allora numerosi altri polimeri sono stati scoperti presentare queste proprietà e tra i più utilizzati ci sono polianilina (PAni), polipirrolo (PPy) e politiofene (PTh). Le loro proprietà elettriche sono dovute innanzitutto all'alternanza di legami singoli e legami doppi in modo tale da permettere la formazione di stati elettronici delocalizzati e alla creazione di sistemi di polaroni-bipolaroni. Questa struttura insatura può portare ad avere elettroni π disaccoppiati a muoversi lungo le catene polimeriche e, tramite effetto tunnelling, a saltare tra una catena e l'altra all'interno del random coil polimerico, aumentando la mobilità elettronica e riducendo il band gap. Nonostante in questi polimeri coniugati ci sia, dunque, un'alta mobilità a mancare sono i portatori di carica in quanto impegnati nel legame doppio o aromatico. E dunque sempre necessario un processo di doping in grado di fornire questi portatori di carica tramite un doping di tipo p o di tipo n. Nel caso di doping di tipo n sono degli extra elettroni a essere inseriti nella catena mentre per il tipo p delle lacune, permettendo a questo punto il passaggio di corrente e una resistenza elettrica adeguata; questo processo è chiamato doping primario. A questo punto se il gas adsorbito è un ossidante acquista elettroni dalla catena polimerica, riducendo la resistenza nel caso di polimeri p-doped e aumentandola nel caso degli n-doped. Al contrario se è riducente cederà elettroni aumentando la resistenza nei p e aumentandola negli n; questo è chiamato doping secondario. In entrambi i casi quello che verrà rilevato dal sensore sarà un cambio nella resistenza elettrica intrinseca. Polimeri conduttori di tipo n sono però estremamente suscettibili all'ossidazione e dovrebbero, per la maggior parte, essere utilizzati in atmosfere inerti o in vuoto; Per questo motivo la maggior parte dei polimeri utilizzati in questa tecnologia e in questa tesi sono di tipo p, come polipirrolo, polianilina e PEDOT:PSS. Il processo di doping secondario è inoltre reversibile, in quanto scatenato dall'adsorbimento dell'analita sulla superfice dell'active layer e per cui, una volta rimosso si ritorna a livelli di resistenza precedenti all'esposizione. È necessario specificare in ogni caso che il principio conduttivo di questi materiali non è del tutto compreso fino a fondo e i risultati ottenibili sono scanditi pure da numerosissime altre variabili. Infatti, la teoria si rifà a una catena polimerica esente da difetti, prerogativa impensabile all'interno di un polimero ed inoltre la diffusione dell'analita all'interno del random coil polimerico può portare ad un fenomeno di rigonfiamento della struttura allontanando le catene fra di loro e non permettendo effetti di tunneling fra le macromolecole. Tutto questo si può tradurre, in alcuni casi, a risultati opposti a quelli teorizzati.

Ogni sensore, sia esso polimerico o un ossido di metallo, necessita di raggiungere determinate performance che sono scandite da quelle che sono chiamate le "3 S", che rappresentano i tre principali requisiti; Queste proprietà sono sensibilità, selettività e stabilità. La sensibilità è un numero puro che rappresenta la bontà della risposta associata alla variazione del segnale di output rispetto al valore reale della proprietà fisica considerata. Maggiore risulterà questo valore quindi, più sarà minore la quantità di analita rilevabile. La selettività invece è la capacità di un sensore di discriminare verso differenti gas o fragranze, fornendo la risposta corretta ad ogni evenienza. La stabilità, infine, indica il grado di deterioramento funzionale del dispositivo rapportato al suo uso e al tempo di utilizzo. Mentre il naso umano è in grado di soddisfare efficacemente i tre parametri, i sensori elettronici di gas necessitano di un compromesso tra le tre variabili. La scelta su quale parametro ottimizzare varierà di conseguenza in base all'applicazione. Nel caso dei polimeri più specificatamente, quello che si nota sono relativamente alti valori di sensibilità (dovuti alle facili reazioni con gli analiti considerati), ragionevole grado di selettività ma livelli di stabilità abbastanza bassi.

Per fare questo si è proceduto alla fabbricazione del sensore dalle fasi iniziali, ovvero dalla sintesi dei tre polimeri utilizzati, al coating dello strato attivo e fino alle fasi di test finali. L'attività si è inoltre concentrata sullo studio dei metodi di funzionamento della tecnologia e delle interazioni che intercorrono fra i gas e il materiale attivo per stabilire le relazioni esistenti tra le proprietà fisico-chimiche e la risposta elettrica. Inoltre, una parte di programmazione si è richiesta necessaria in modo da discriminare, analizzare e processare l'altissimo numero di dati in ingresso; Questo è stato possibile tramite uno script IGORPro, un programma in grado di analizzare e processare una grande mole di dati dando come output tutta la gamma di grafici necessaria. L'obiettivo è quello di giungere alla fabbricazione di semplici chemi-resistori polimerici che ottimizzino almeno due delle tre proprietà principali. In particolare, alti valori di sensibilità sono stati ricercati come target principale e, ove possibile, adeguati livelli di selettività all'interno delle specie chimiche testate.

Questo progetto è stato realizzato nell'ambito di una collaborazione fra il Politecnico di Torino, l'università madre dell'autore della tesi, e il centro di ricerca di IBM Almaden a San Jose in California, ove tutto il lavoro sperimentale è stato effettuato. Cinque fasi sono necessarie per lo studio:

- Sintesi del polimero
- Ottenimento della piattaforma del sensore
- Coating del polimero nel gap fra gli elettrodi
- Fase di testing
- Fase di processo dei dati

La fabbricazione del dispositivo parte dalla sintesi dei tre polimeri testati. Tuttavia, mentre la sintesi di polianilina e polipirrolo è stata effettuata dal sottoscritto, per quanto concerne alla sintesi del PEDOT:PSS essa era stata effettuata precedentemente all'interno dei laboratori del centro di ricerca. La sintesi del polimero è un processo abbastanza semplice, ottenuta in laboratorio tramite la miscelazione di tutti gli ingredienti necessari alla polimerizzazione del monomero e al successivo doping primario. Nel caso della polianilina la sintesi procede tramite la creazione di un radicale libero sul monomero di anilina con una successiva addizione continua di monomero e la creazione della catena polimerica. In questo caso la sintesi necessita di:

- Il monomero di anilina, generalmente 102 mg (1.10 mmol, 1.0 eq.)
- Un ossidante, come il persolfato di ammonio o altri.
- Un eventuale co-ossidante, l'ipoclorito di sodio, generalmente 1 ml (in una soluzione acquosa del 6% di cloro attivo)
- Un dopante, l'acido cloridrico, generalmente 12 ml.

Mentre il monomero e il dopante sono allo stato liquido, l'ossidante necessita della solubilizzazione all'interno del dopante in modo da essere aggiunto successivamente alla soluzione. In questo modo, inoltre, una prima dissociazione dell'ossidante in due radicali ha inizio. Successivamente il tutto viene aggiunto all'interno di un piccolo baker, posizionato sopra un sistema di mescolamento magnetico e con uno stirrer al suo intero. Questi radicali ossideranno la polianilina in forma di pristine e creeranno la forma emeraldine a cui poi si aggiungera il protone dissociato dall'acido cloridrico in modo da creare il sale di emeraldine, la forma conduttiva e dopata di polianilina. Il parametro principale da seguire durante la polimerizzazione è il colore del polimero, in quanto la presenza di numerosi anelli aromatici ridurrà il band gap fra HOMO e LUMO e facendo cadere la transizione dell'elettrone a seguito dell'assorbimento di un fotone nello spettro viola-verde del visibile. La reazione è lasciata continuare per un tempo minimo di 30 minuti dopo i quali viene eliminato l'ossidante e il dopante manualmente e sostituiti con acqua. Vari step di lavaggio-precipitazione vengono effettuati successivamente fino a ottenere una soluzione stabile di polimero in acqua.

La reazione del polipirrolo è invece di tipo cationico ed è l'ossidante che è in grado di strappare elettroni all'anello aromatico del monomero creando un catione che poi si accoppierà con un successivo e formerà la catena polimerica. Gli stessi ingredienti sono stati utilizzati pure in questa reazione. La procedura eseguita nel caso della polianilina è seguita pure in questo caso fino ad ottenere una soluzione stabile. In tutti i casi i provini seguono una numerazione basata sul nome del polimero stesso, seguita dalle iniziali di nome e cognome di chi ha effettuato la sintesi, dal libro ufficiale di IBM ove le concentrazioni utilizzate sono riportate e dal numero di pagina; Un esempio di questo è il provino PAni TE-I-70.

Successivamente è la piattaforma di silicio provvista di elettrodi che viene fabbricata. Mentre il piatto di silicio è comprato precedentemente, ottenuto tramite la crescita a singolo cristallo di Czochralki e all'esposizione di un flusso di ossigeno o azoto in modo da ottenere uno strato superficiale di silice o nitruro di silicio per evitare perdite di corrente tra gli elettrodi e il substrato. Processi di pulizia sono i primi step effettuati all'interno dei laboratori per eliminare eventuali residui organici dalla superficie. Dopodiché è applicato tramite spin coating uno strato di resist polimerico, chiamato KRS, sulla superficie della piattaforma di silicio, aiutata all'adesione da una molecola di esametildisilisano (HMDS). Lo step successivo vede l'utilizzo della fotolitografia ove il resist viene depolimerizzato selettivamente e all'applicazione dello strato di oro che formerà poi gli elettrodi. La fase finale vede la solubilizzazione del resist rimasto e l'ottenimento della geometria finale degli elettrodi, generalmente con un gap fra elettrodi di 100 nm.

Il seguente step è la fase di coating, performata in questo lavoro tramite differenti tecniche in base al polimero considerato. La maggior polarità di polianilina e polipirrolo rendeva difficile il rivestimento sul gap tra gli elettrodi tramite blow-coating in quanto la soluzione tendeva ad avere un'alta bagnabilità sul substrato di silice e a spandersi non coprendo perfettamente la zona da rivestire; In questi casi la tecnica utilizzata è stata quella del drop-casting. Nel caso del blade-coating un macchinario progettato e sviluppato all'interno del centro di ricerca è stato utilizzato avendo come parametri principali la velocità della spatola, la distanza fra la spatola e il substrato siliceo e la quantità di soluzione applicata sulla spatola. Il processo è seguito tramite l'utilizzo di un computer che regola pure la distanza in cui la spatola si fermerà. Diverse velocità e gap fra spatola e substrato sono state testate in modo da raggiungere valori di spessore del film il quanto più bassi possibili. Lo spessore dello strato attivo risulta infatti, all'interno del sensore, un parametro fondamentale in quanto può influenzare la risposta del dispositivo. Presupponendo infatti diversi spessori ma uno stesso tempo di esposizione all'analita, come visibile in figura 3.18, e presupponendo uno stesso grado di diffusione nel bulk della specie chimica analizzata risulta chiara una maggior risposta dell'analita nel caso di spessori minori. Per questa tecnologia di coating, inoltre, una ricerca effettiva volta all'ottimizzazione dei parametri operativi è stata necessaria in quanto lo spessore ha un andamento di tipo trapezoidale rispetto alla velocità della spatola. Valori di 3000 cm/min di velocità hanno dunque portato ad uno spessore del film di 20 nm mentre valori di 30'000 a uno spessore di 150 nm. Il gap è stato fatto variare fra valori di 3 fino a 10 μm mentre la quantità di soluzione posta sulla lama è stata costante durante tutti i test, pari a 2.5 μl.

Per quanto riguarda il drop-casting, una quantità di 0.7 μl di soluzione è stata applicata sui vari provini tramite una siringa di precisione esattamente sul gap tra gli elettrodi. Questa tecnica presenta la criticità del controllo dello spessore ottenibile; di fatti la tecnica è abbastanza manuale e approssimativa e non permette un efficace controllo; Questa affermazione è totalmente supportata dai valori di spessore ottenuti, che vanno dai 1.5 μm fino ai 100 nm. L'unico parametro utilizzato è stata la diluizione della soluzione di partenza con più o meno solvente in modo da avere più o meno polimero solubilizzato al suo interno. Un'altra tecnica utilizzata è stato lo spray-coating, ma dovuto a problemi tecnici e di riproducibilità dei risultati è stata abbandonata.

Come da protocollo IBM su ogni provino, una volta effettuato il coating, è stata misurato lo spessore del film tramite un profilometro e ottenuta un'immagine tramite un microscopio della zona di coating. Questa procedura si è resa necessaria in modo da capire successivamente quali parametri variare e come lo strato attivo cambiava nel tempo, oltre a capire la forma del film polimerico e in particolare la sua omogeneità. Infatti, la presenza marcata di "coffee spot", ovvero di maggior concentrazione di polimero ai bordi della goccia, può portare a spessori totalmente differenti rispetto al centro e a risultati successivi non del tutto attendibili, grazie ad un adsorbimento preferenziale delle molecole di analita.

Una volta terminata la fabbricazione di questi dispositivi elettronici, i sensori sono stati testati elettricamente nel laboratorio del centro di ricerca dell'IBM con un sistema ivi realizzato per produrre e fornire al campione determinate concentrazioni di gas in modo controllato ed affidabile. Questo sistema vedeva la presenza di:

- Un sistema di trasporto dell'analita in fase gassosa.
- Una camera ove il dispositivo era posizionato
- Un Keithley model 6430 Source Meter R
- Un Keithley Switch System
- Un computer

Nel sistema di trasporto, composto da diversi tubi che formano una linea per la distribuzione del gas quasi perfettamente stagna, un flusso di aria secca proveniente dalla fonte generale di aria compressa del laboratorio è utilizzata sia come gas carrier che come gas di diluizione. Il flusso principale è diviso in due getti regolati dalla presenza di due Mass Flow Controller forniti dalla MKS e chiamati MFC Solvente e MFC Carrier. Il flusso di aria secca, controllato dal MFC Solvente, scorre dentro un tubo di PE collegato ad un bubbler all'interno di un contenitore termostatico Dewar, usato per mantenere la temperatura. L'aria secca, fluendo attraverso al bubbler si saturerà dell'analita e procederà ad un sistema di mixing, chiamata camera di miscelazione, dove il flusso di aria saturo si miscela a sua volta con un flusso di aria secca proveniente dal MFC Carrier, raggiungendo la concentrazione finale richiesta. Dalla camera di miscelazione il flusso è in grado, grazie ad un ulteriore tubo di PE di arrivare in una camera di acciaio inox, accuratamente serrata tramite delle viti e chiamata Polymer Chamber, ove il sensore è stato posto, reagendo con esso e cambiandone le proprietà. Il cambio di resistenza è rilevato tramite una misura a due punte, dove una è utilizzata per applicare il voltaggio e l'altra è usata come ground. Un Keithley model 6430 Source Meter R viene utilizzato per applicare una tensione variabile fra 1 e 0.1 V e allo stesso tempo per misurare la corrente che attraversa il campione. Un sistema di cambio del voltaggio Keithley Switch System allo stesso tempo applica il voltaggio per un tempo precisato ai diversi elettrodi sul sensore, per un tempo che va dai 0.05 ai 0.1 s. Durante l'esperimento i dati acquisiti dal Keithley vengono automaticamente salvati su di un personal computer e processati da un programma scritto con Python che plotta in tempo reale l'andamento della corrente, che è strettamente legata alla resistenza elettrica. Il sistema è controllato tramite un protocollo .txt precedentemente creato ove vengono indicati i valori di exposure time, 3 minuti, e recovery time, 10 minuti; All'interno del file sono inoltre indicati i valori portata di flusso di aria con cui controllare i Mass Flow Controller, riportati in sccm (centimetri cubici standard per minuto) con cui viene impartito il grado di diluizione dell'analita con il flusso centrale di aria secca. Alcuni parametri devono essere accuratamente controllati perché in base ai valori di resistenza del dispositivo testato la misurazione potrebbe presentare valori di rumore di fondo, imputabili al Source Meter Keithley, così elevati da rendere il test nullo. Questi parametri sono la soglia massima di voltaggio applicabile, il range di voltaggio all'interno del quale si effettua la misura, il tempo di misurazione individuale di ogni cella e il numero di punti che vengono mediati in una singola misurazione. In particolare, è stato notato come un troppo alto numero di punti mediati porti a curve caratteristiche del tutto simili fra loro, una troppo bassa soglia porti alla non misurazione in caso sia superata, un range troppo alto e una tempo di misurazione toppo basso portino ad un rumore di fondo eccessivo. Nei due ultimi casi questo comportamento è dovuto al gap troppo elevato tra il range e la misurazione effettiva (facendo salire sullo stesso piano le misurazioni e il rumore) e all'impossibilità dello strumento di raggiungere un valore stabile della risposta. Gli analiti testati sono 14, ovvero, in ordine di polarità:

1. Cicloesano
2. Ottano
3. Toluene
4. Etilacetato
5. Cloroformio
6. Di-etiletere
7. 2-butanone
8. Acetone
9. Acetonitrile
10. 2-propanolo
11. 1-propanolo
12. Etanolo
13. Metanolo
14. Acqua

Considerando l'alto numero di dati ottenuti come output dal sistema di misura, circa 500'000 per ogni sensore prendendo in considerazione il totale di 14 analiti oggetto di studio, si è resa necessaria la creazione di uno script che fosse in grado di analizzare e processare i dati per conto dell'utente, salvando il tempo di processing individuale. I dati ottenuti, ovvero la corrente elettrica al variare del tempo, sono dunque processati da uno script IGORPro innanzitutto per caricare i dati e ottenere i valori di resistenza elettrica al variare del tempo tramite la prima legge di Ohm. A partire dai valori di resistenza della baseline precedente ad ogni picco il programma è in grado di calcolare in maniera autonoma i valori di risposta ad ogni concentrazione grazie alla formula 1.4. Inoltre, considerando le diverse pressioni parziali caratteristiche di ogni solvente è stato necessario ricavare le costanti semi-empiriche di Antoine, alle condizioni di temperatura ambiente e pressione atmosferica. Il programma, indicate le costanti caratteristiche e caricando il protocollo .txt è in grado, utilizzando la formula 3.5, di calcolare le concentrazioni specifiche di prova (in ppm). L'output di questa feature sono un insieme di funzioni, chiamate waves, che sono l'oggetto di base del programma e tramite il quale i grafici necessari saranno poi forniti. I grafici ottenibili sono:

- la resistenza al variare de tempo di analisi, sia a partire dai dati reali che da dati mediati.
- La corrente al variare del tempo di analisi, sia a partire dai dati reali che da dati mediati.

- La derivata prima della resistenza al variare del tempo di analisi, sia a partire da dati reali che dati mediati.
- La risposta del materiale al variare della concentrazione di analita, sia per ogni cella che il totale di 8 celle insieme.
- Il confronto della risposta del materiale al variare della concentrazione per un determinato analita rispetto al totale di campioni testati.
- Il confronto della risposta de materiale al variare della concentrazione per un determinato campione rispetto al totale degli analiti testati.

Per quanto riguarda i risultati essi sono stati strutturati in modo tale da analizzare per prima cosa i risultati di ogni materiale in modo tale da comprendere i valori di risposta generali. Il seguente passo è stata la variazione di alcuni parametri sullo stesso materiale in modo tale da ottimizzare le performance di risposta ricercate. Per ultimo viene fatto un confronto fra i diversi materiali testati in modo tale da ottenere un profilo più dettagliato delle caratteristiche di sensing di ogni polimero. Una delle caratteristiche simili a tutti i campioni testati è risultata la forma della curva di sensing, infatti in tutti i casi si è notata un andamento lineare per la prima parte della curva, ovvero per le basse concentrazioni, e un andamento tendente al logaritmico in maniera graduale con l’incremento della concentrazione di analita. Questo comportamento è probabilmente dovuto a una graduale saturazione della superficie dello strato attivo.

Il primo polimero testato in ordine cronologico è stato il PEDOT:PSS. Una prima misurazione sul campione TE-I-59 ha mostrato valori di risposta generalmente bassi (inferiori al 1% di variazione di resistenza) con un picco del valore medio di risposta rapportato alle 8 celle nel loro totale di 0.24% per l’acqua. Un altro fenomeno osservato all’interno di tutti i campioni è la risposta più pronunciata delle celle 4, 5 e 7. La risposta a questo quesito è stata imputata non tanto alla maggior reattività di queste celle ma al metodo di diffusione del gas all’interno della Polymer Chamber; È possibile infatti che il gas raggiunga prima queste celle e con una concentrazione maggiore rispetto alle altre. Visti i risultati deludenti una riduzione dello spessore del film polimerico è stata ricercata raggiungendo, tramite blade-coating, spessori dell’ordine di 15-30 nm. In questo nuovo campione, nominato TE-II-31, vista l’elevata differenza di resistenza e i parametri del Source Meter Keithley da rispettare si è reso necessaria la misurazione solamente delle celle 1, 5, 7 and 8. Un importante risultato è stato notato nella forma della baseline. Con uno spessore molto sottile si è evidenziato un comportamento opposto della baseline rispetto all’andamento tradizionale, ovvero una caduta di resistenza (sintomo di un accresciuta conduttività elettrica). Il comportamento è probabilmente dovuto ad un differente grado di desorbimento sulla superficie sottile, mancando in questo caso un bulk capace di supportare una eventuale diffusione interna del solvente. Inoltre, la risposta ha presentato valori superiori fino al 140%.

Per quanto riguarda il polipirrolo le prime misurazioni, effettuate solamente su 6 analiti, hanno dimostrato una risposta maggiore che nel caso del PEDOT:PSS ma di nuovo sotto il 2% alle basse concentrazioni (massimo di 1.52% nel caso dell’etilacetato). In questo caso due campioni sono stati portati alla fase finale di testing, TE-II-20 e TE-II-24. Mentre il secondo ha evidenziato valori di risposte che, seppur bassi, sono in linea con quelli dei materiali precedentemente testati, il primo ha mostrato valori di risposta molto confusi. Infatti, per la maggior parte delle celle, un vero e proprio trend della risposta non era presente. Tuttavia, analizzando in maniera più approfondita il campione si è notato un andamento di alcune celle, ed in particolare della 1, in cui nella sensing curve a determinate concentrazioni differenti per ogni analita, era presente un'inversione del picco caratteristico. Questo riportato sul diagramma della risposta al variare delle concentrazioni faceva risultare andamenti delle curve differenti per ogni analita testato, quindi un certo grado di selettività.

L'ultimo materiale studiato è stata la polianilina. Questo polimero ha mostrato, tramite il campione TE-I-70, livelli di risposta alle basse concentrazioni nettamente superiori a quelle dei materiali precedenti, con un massimo toccato nel caso del toluene a 6.26%. L'incremento rispetto agli altri polimeri si è sempre attestato a valori superiori al 100%, con un massimo del 19'200% nel caso dell'etilacetato comparato con il PEDOT:PSS. Inoltre, confrontando il sensore fabbricato con un sensore in commercio a base di polimeri caricati con particelle di carbon black (Cyranose 320) è stata dimostrata una risposta estremamente superiore della polianilina. Questo dimostra che gli sforzi compiuti nella direzione dei polimeri conduttivi sono in grado di dare performance migliori rispetto a tutti gli altri materiali organici. Per questo motivo la maggior parte di ottimizzazione sui materiali è stata effettuata sulla polianilina. Successivamente è stata testata una polianilina ottenuta con due differenti ossidanti, dimostrando un incremento della risposta nell'utilizzo del persolfato di ammonio su una media del 30%. Un altro parametro testato è stata la differenza di spessore nel gap fra gli elettrodi. Il campione, TE-II-5, presentava gap accoppiati per celle contigue e in particolare 1 μm per le celle 1 e 4, 2 μm per le celle 2 e 5, 5 μm per le celle 3 e 7 e 10 μm per le celle 4 e 8. Nessun segno di dipendenza dal gap è stato tuttavia notato. L'ultima strada per aumentare le performance è stata tramite l'aggiunta di nanoparticelle conduttive di oro che, in quanto elettron-donatori, potevano facilitare l'adsorbimento di gas sulla loro superficie aumentando la risposta del materiale, creando il campione TE-II-16. Queste particelle, comprate dalla BBI Solutions, sono state aggiunte in fase di polimerizzazione tramite 3 ml di una soluzione acquosa contenente nanoparticelle di oro della dimensione di 10 nm nella concentrazione di $5.70 \times 10^{12}\ \frac{perticles}{ml}$. Un miglioramento è stato effettivamente notato ma la spiegazione può ricadere sia nelle nanoparticelle che nello spessore più sottile presentato da questo campione. In ogni caso un massimo di un 42% di incremento è stato notato per il toluene.

In conclusione, a questo lavoro di tesi, la polianilina risulta il materiale con le migliori performance di sensibilità a basse concentrazioni ma una discriminazione verso differenti analiti non è stata possibile in quanto non sono state evidenziati diversi comportamenti del dispositivo in termini di risposta o forma dei picchi caratteristici. Al contrario, polipirrolo e PEDOT:PSS presentano valori di risposta a basse concentrazioni così bassi che potrebbero essere confusi con il rumore di fondo del macchinario Keithley. Nonostante questo, ottimizzando la sintesi del polipirrolo ottenuto senza acido cloridrico e uno studio più approfondito del PEDOT:PSS con spessore limitato (grazie al diverso andamento della baseline) può portare ad un livello di selettività ai diversi VOC maggiore e più specifica. In particolare, l'applicazione dei tre materiali su un unico sensore sarebbe in grado di dare risultati molto più approfonditi sia sulla concentrazione rilevabile che sulla tipologia di analita. Inoltre, uno studio più approfondito su tutti e tre le proprietà principali dei sensori, ovvero sensibilità, selettività e stabilità necessita in ogni caso di ulteriori studi. Di fatti, durante il soggiorno ad IBM la ricerca di concentrazioni ancora minori è stata effettuata utilizzando un forno a temperatura e portata controllata. L'utilizzo di questo strumento avrebbe potuto portare a concentrazioni dell'ordine di decine di ppm, ma a causa di problemi tecnici, ottenute le concentrazioni desiderate, non è stato possibile utilizzarlo. Altre soluzioni per incrementare la performance potrebbero essere la funzionalizzazione del polimero con gruppi altamente reattivi e selettivi o l’aggiunta di differenti nanoparticelle. Il problema maggiore dei polimeri risulta tuttavia la stabilità, per cui ulteriori test eseguiti alle stesse condizioni operative sono necessari, anche utilizzando un certo grado di umidità (generalmente deleteria per questa classe di materiali). Molte altre proprietà sono modificabili, come la morfologia del polimero, la composizione e le condizioni operative, tutte caratteristiche intimamente legate alle performance del sensore. Inoltre, la combinazione di polimeri conduttivi con altre tipologie di materiali, potrebbe garantire un giorno la fabbricazione di un vero e proprio e-nose capace di fornire un impronta univoca per ogni VOC ed, applicato con un sistema di riconoscimento del segnale, la possibilità di affianco alla sua controparte naturale: il naso umano.

CHAPTER 1

INTRODUCTION

There are three sensory systems in humans which contribute to the sensation of flavour . These three chemical senses are olfaction (the sense of smell), gustation (the sense of taste) and the trigeminal sense (responsive to irritant chemical species) . However, smell is the dominant factor in our sensation of flavour and so can often be used alone to profile the flavour of various products. The sense of smell arises from the stimulation of the human olfactory system by odorant molecules emitted from an object. In this sector enters the gas sensors technologies, to give a solution to the need of a miniature and portable device able to detect analytes, and especially VOCs, in real time with good sensing performances. This investigation is the starting point, leading in the future to a real electronic nose based on the human counterpart, with a large range of applications such as military, security, safety, food quality control, environment control and disease diagnosis. Polymer-based sensors are already widely used due to their versatility, flexibility, low energy consumption, easy synthesis and inexpensive cost and on this material will be focused this work.

In this framework the project is inserted, a joint venture between the Politecnico di Torino and IBM Almaden Research center, where all the thesis work was carried out. The total amount of time spent for this internship was 5 months with the major aim of a fabrication of a VOCs sensor able to detect low concentrations of analyte, comparing different types of polymer and optimizing them. Eventually selectivity toward different analytes was researched in order to meet the three main goal for any kind of sensors: selectivity, sensibility and stability.

This thesis is divided on 5 chapter where all the aspect of the technology investigated were reported and discussed in detail:

1. The first chapter treats about the e-nose devices in all the aspects. A first discussion on what the technology is and on what is it based is reported, followed by the classical structure of these devices and the possible applications. Then the various types of devices are listed with a special focus on chemiresistors (the sensor treated in this thesis). Afterward the various types of material employed for this class of sensors are listed, together with the sensing curve and the important parameters needed to know. A final specification on the objective of the thesis is then reported.
2. On chapter 2 the material selected to employ in these devices are discussed, so that conductive polymers. A first part concerning the conductive principles and the electrical properties required is followed by the doping procedure needed for this class of organic material. Then

it follows a discussion on the three polymers selected: polyaniline, polypyrrole and poly(3,4-ethylenedioxythiophene):polystyrene sulfonate (PEDOT:PSS).

3. The third chapter treats the experimental work. The first part treats about the polymer synthesis, followed by the experimental set-up preparation and discussion, such as the coating or the electronic set-up parameters optimization. The last part talks about the implementation of an IGORPro script able to analyse and process all the data achieved as output by the computer connected with the experimental apparatus.
4. On chapter 4 the results are presented, divided by material with comparison between the three polymers. A final part of further investigations on polyaniline is reported.
5. The last chapter is dedicated to the conclusions and on future outlook of the technology treated.

1.1. The electronic nose

Over the last decades, “electronic sensing” technologies have shown important developments in the commercial and technical fields, granting meaningful efforts and attention from all the research world as well as support and funds by all the major companies operating in the sector.

The expression of “electronic sensing” refers to the capacity of reproducing human senses employing sensor arrays and pattern recognition systems. Nowadays there are many devices emulating the all spectrum of human senses where the name of the sensing organ is preceded by the vowel “e”, a short term for “electronic”. In this respect, it does not have to sound unusual hearing about “e-tongues”, “e-eyes” or “e-noses”.

For instance, to recreate the sense of taste, “e-tongues” are available on the market. These devices are able to measure and compare tastes and are applied in many sectors, from the flavour aging to the quality of extra-virgin olive oil [1].

The sense of smell is one of the most complicated and mysterious senses because of its link to memory and emotions. The perfume industry is built around this connection, with perfumers developing fragrances that seek to convey a vast array of emotions and feelings; from desire to power, vitality to relaxation. [2]

It is not surprising, therefore, the aspiration given in these years towards the creation of an instrument able to reproduce the exact working principle of one of the most challenging human organs, the nose.

By “electronic Nose” or “e-nose” is meant a device which can permit the detection and the recognition of gaseous substances, whether they are odorous or odourless.

In particular, the effort is target on some kind of substances called VOC (Volatile organic compounds); These molecules are generally organic chemicals that have a high vapor pressure at ordinary room temperature, resulting from a relatively low boiling point. The class includes numerous species of compounds both human-made and natural. The importance of this class of substances results even more clear considering their large usage as solvents. In fact, acetone, ethanol, 2 propanol and ethil acetate gelong to this group.

The name “e-nose” was firstly coined in 1988 by Gardner who defined it as [3]:

”an instrument which comprises an array of electronic chemical sensors with partial specificity and an appropriate pattern recognition system, capable of recognizing simple or complex odours”

It is inferable from the Gardner definition that for a detection device to be considered an electronic nose it must contain an intelligent chemical-array sensor system that reproduces the mammalian olfactory system. The implication is that all sensing devices that have only one sensor or can detect only one compound or aroma cannot, by definition, be considered electronic noses. Thus, electrochemical cells (ECs) that detect only one specific gas are not electronic noses according to the Garner definition.

Even if the common name used to refer to the device comes from the late ’80s, the fist idea of an electronic system able to work as an artificial olfaction device is associated to Hartman in 1954 and the first rudimental instrument to Wilkens and Hartman in 1964. Later, in 1982, Persaud and Dodd [4] introduced the concept of an array of sensor that, working together, grant and reproduce the sensing principle of the human nose.

The key to understand the working method of this device is based on how the human nose can sense and recognize the different odorous molecules contained in the air.

There are different steps that characterize all the process from the odorous molecule detection to the brain response. With references to the Figure 1.1 it is clear that all the process starts from the inhalation of the sample molecule.

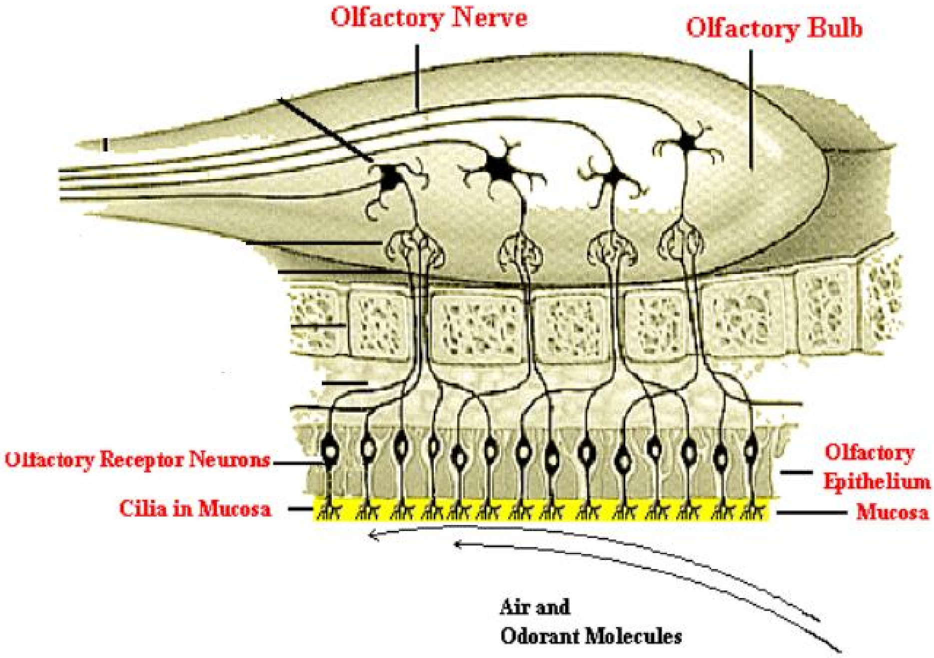

Figure 1.1: Human nose anatomy. Adapted from [5].

Those molecules are volatile chemical compounds that are carried by inhaled air to the upper part of the nose, located in the roof of the two nasal cavities of the human nose, just below and between the eyes. In this region there are special receptors called “cilia” where molecular reception occurs, and sensory transduction starts. To grant the binding of the molecules, the cilia are immersed into a layer of mucus; This mucus layer is a lipid-rich secretion that bathes the surface of the receptors at the epithelium surface and assists in transporting the molecules. As only volatile materials that are soluble in the mucosa can interact with the olfactory receptors and produce the signals that the brain interprets as odour, extremely polar and lipophobic compounds cannot be detected by the human nose (this is the reason why humans can't smell water). Above the mucus layer is based the olfactory epithelium where the olfactory receptor neurons are able to create bindings between the odorous molecules and the related binding protein on the neurons. There are more than 100 million protein receptors of about 1000 different types, each one able to interact with a specific odorant [6]. The olfactory receptor neurons turnover approximately every 40 days granting new cells to replace the old degradated ones [7]. Thanks to many nervous filaments the signal is then sent to the olfactory bulb that processes the information sending it directly to the higher levels of the central nervous system where the signaling process is decoded, olfactory interpretated and the response occurs.

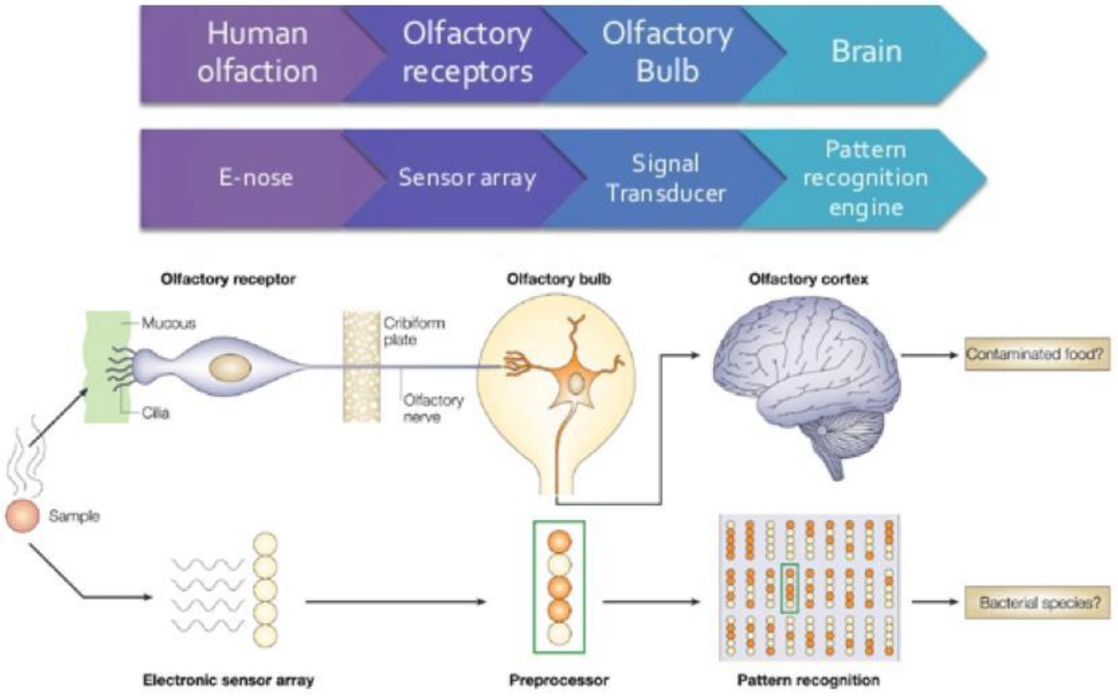

Figure 1.2: Analogy between the working principle of the human nose and the e-nose technology [8].

Likewise, the electronic version includes an array of different sensors, possibly even of different materials, where the adsorption on the surface of the incoming odorant occurs. In this case, having not a lipid-rich layer designated to trap the odorous molecules, this device is able to detect almost all the spectrum of reactive gases or vapors with the sensor material surface. On the other hand, the majority of these sensors are not selective towards just one analyte, but they present a certain degree of response when exposed to any odorant. When the adsorption occurs a certain property on the sensor material changes and the alteration is processed and sent to the central computer that interprets and codifies the response. In this sense, even though a signal is always present in any sensor, a data-crossing and a pattern recognition could grant a codification of the sensed adorous molecule. This alteration on the properties, so then the electrical signal, is time dependent and the rise and decay time will depend upon many different parameters [3]:

1. The flow delivery system that carries the odour from the source to the sensor array, e.g., the flow profile and type of carrier gas;
2. The nature of the odour, e.g., type, concentration;
3. The reaction kinetics of the odour and the active material;
4. The diffusion of the odour within the active material;
5. The nature of the sensing material, e.g., physical structure, porosity, thermal time-constant;
6. The nature of the substrate supporting the active material, e.g., thermal conductivity, acoustic impedance;
7. Ambient conditions, e .g., temperature of active material, carrier gas, humidity, pressure.

The lifetime of the sensors, however, needs to be much longer than his biological counterpart in order to return economically the investment made.

An "electronic nose" system typically consists, as shown in Figure 1.2, of a multisensor array, an information-processing unit or processor such as an artificial neural network (ANN), software with digital pattern-recognition algorithms, and reference-library databases [9]. The cross-reactive sensor array is composed of incrementally-different sensors chosen to respond to a wide range of chemical classes and discriminate diverse mixtures of possible analytes. The output from individual sensors are collectively assembled and integrated to produce a distinct digital response pattern. Identification and classification of an analyte mixture is accomplished through recognition of this unique aroma signature (electronic fingerprint) of collective sensor responses. The identity of a simple or complex mixture represented by a unique aroma signature pattern may be determined without having to separate the mixture into its individual components prior to or during analysis. A reference library of digital aroma signature patterns for known samples is constructed prior to analysis of unknowns. The ANN is configured through a learning process (neural net training) using pattern recognition algorithms that look for differences between the patterns of all analyte types included in the reference library. This process continues until a previously selected level of discrimination is met. The results are validated and assembled into the reference library to which unknown samples can be compared. Identification of unknowns is based on the distribution of aroma attributes or elements that the analyte pattern has in common with patterns present in databases of the reference library.

1.2. Structure of the sensor, commercial e-noses and applications

Even though every kind of electronic nose has different features, some similarities upon all the instruments are always present. Gardner and Bartlett [3] provided a basic requisite definition of an electronic-nose device with a list of necessary components (as follows):

1. An aroma delivery system, which transfers the volatile aromatic molecules from the source material to the sensor array system;
2. A chamber where sensors are housed: this has usually fixed temperature and humidity, which otherwise would affect the aroma molecules adsorption;

3. An electronic transistor which converts the chemical signal into an electrical signal, amplifies and conditions it;
4. A digital converter that converts the signal from electrical (analog) to digital;
5. A computer microprocessor which reads the digital signal and displays the output after which the statistical analysis for sample classification or recognition is done. Generally, the digital output information generated by the e-nose are studied and interpreted using three types of analysis techniques [9]:
    - **a.** Graphical analysis: bar chart, profiling, polar and offset polar plots;
    - **b.** Multivariate data analysis: principal component analysis (PCA), canonical discriminate analysis (CDA), featured within (FW) and cluster analysis (CA);
    - **c.** Network analyses: artificial neural network (ANN) and radial basis function (RBF);

    Among all the analysis techniques the artificial neural network (ANN) is the best known and most evolved analysis techniques utilized in statistical software packages for commercially-available electronic noses. To reproduce the cognitive processes of the human brain, ANN contains interconnected data processing algorithms that work in parallel. Various instrument-training methods are employed through pattern-recognition algorithms that look for similarities and differences between identification elements of known aroma patterns found in an analyte-specific reference library. The training process is a machine-learning technique that requires a discrete amount of known sample data to train the system and is very efficient in comparing unknown samples to known references. The result of ANN data analysis usually is in the form of a percentage match of identification elements in the sample with those of aroma patterns from known sources in the reference library.

Considering the multipurpose function of the sense of smell and the fundamental role in human development and social interactions, a device capable to reproduce and improve this behavior lends itself to a wide application range. Due to the high demanding on devices with these characteristics, “electronic noses” are already commercially available with different levels of accuracy. A summary of some of the most widely used electronic noses with manufacturers, models available and technological basis are listed on Table 1.2.1.

Instrument type	Manufacturer	Models produced	Technology basis
Single-technology (e-nose sensors only)	Airsense Analytics	i-Pen, PEN2, PEN3	MOS sensors
	Alpha MOS	FOX 2000, 3000, 4000	MOS sensors
	Applied Sensor	Air quality module	MOS sensors
	Chemsensing	ChemSensing Sensor array	Colorimetric optical
	CogniScent Inc.	ScenTrak	Dye polymer sensors
	CSIRO	Cybernose	Receptor-based array
	Dr. Födisch AG	OMD 98, 1.10	MOS sensors
	Forschungszentrum Karlsruhe	SAGAS	SAW sensors
	Gerstel GmbH Co.	QSC	MOS sensors
	GSG Mess- und Analysengeräte	MOSES II	Modular gas sensors
	Illumina Inc.	oNose	Fluorescence optical
	Microsensor Systems Inc	Hazmatcad, Fuel Sniffer, SAW MiniCAD mk II	SAW sensors
	Osmetech Plc	Aromascan A32S	Conducting polymers
	Sacmi	EOS 835, Ambiente	Gas sensor array
	Scensive Technol.	Bloodhound ST214	Conducting polymers
	Smiths Group plc	Cyranose 320	Carbon black-polymers
	Sysca AG	Artinose	MOS sensors
	Technobiochip	LibraNose 2.1	QMB sensors

Table 1.1: Manufacturer, models produced and technology basis of the most common commercial electronic noses. Adapted from [9]

The uses of electronic noses have grown rapidly as new applications have been discovered. The numbers of e-noses sold by various manufacturers has largely depended on the technology basis of individual instruments, costs per unit, and specific application needs. In 1997, there were about 500 total analytical instruments units sold worldwide with an approximate market value of 30 million euros. Within the past ten years, the Applied Sensor Company has sold the most units (> 100,000) of their e-nose (the Air Quality Module electronic nose) [9]; primarily used to maintain ambient or environmental air quality by detection of odors, VOCs and carbon dioxide within living spaces. The Cyranose 320 developed by Sensigent is a portable electronic-nose system which component technology consists of 32 individual polymer sensors blended with carbon black composite and configured as an array [10]. When the sensors are exposed to vapors or aromatic volatile compounds they swell, changing the conductivity of the carbon pathways and causing an increase in the resistance value that is monitored as the sensor signal. The resistance changes across the array are captured as a digital pattern that is representative of the test smell. The sensor technology yields a distinct response signature for each vapor regardless of its complexity; the overall response to a particular sample produces a “smell print” specific to a single stimulus. On Figure 1.3 are reported an image of the sensor (Figure 1.2.1.A) and a classical response plot of the device (Figure 1.3.B). A comparison between the response given by Cyranose 320 and the following paperwork will be discussed more in details on chapter 4.

5.

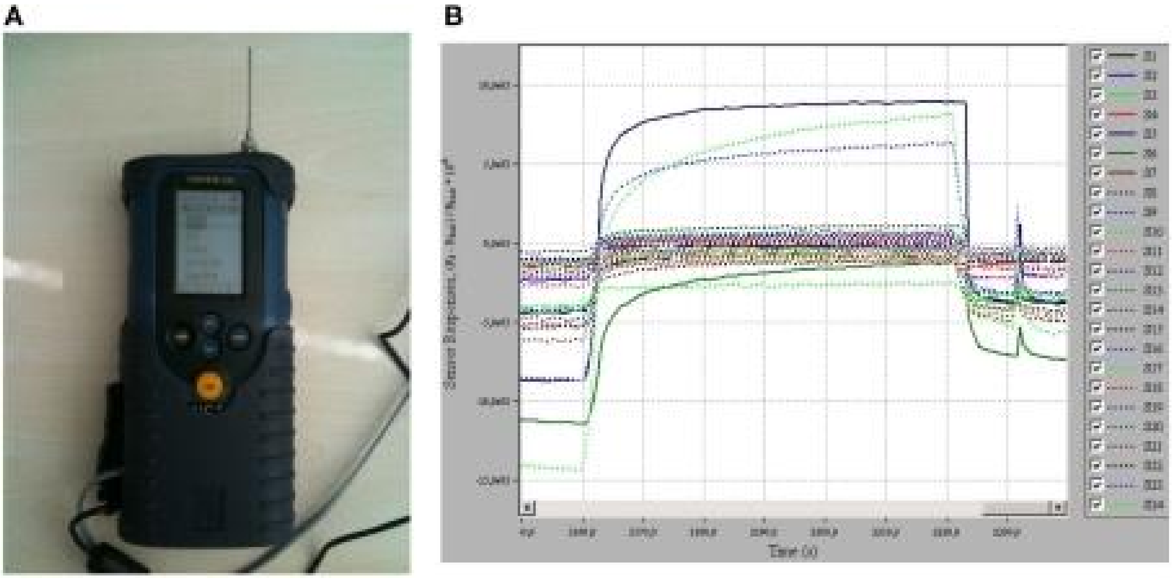

Figure 1.3: Cyranose sensor (A) and response plot (B). Adapted from [10]

Electronic Noses system has been designed specifically to meet a wide range of necessities and purposes. The most obvious application where the device can be employed is to detect and classify the smell (or flavor) in the food and beverage industry.

Within food, a major part of the current publications is focused on the meat spoilage. Spoilage of meat is a sensory quality and is usually detected when looking for off-odors and discoloration. The emission of the off-odors is usually caused by the presence of spoiling bacteria and the discoloration is, usually, a following consequence of the previous factor [11]. Moreover, spoilage of meat can also be chemical, not just microbial. Autoxidation of lipids and the production of free radicals affect fatty acids and lead to oxidative deterioration of the product [12]. Most of the time, during both the microbiological and chemical spoilage, some chemical compounds are released and can be detected by the electronic nose, giving an idea of the meat quality. Some of these chemical markers are reported on Table 1.2.1.

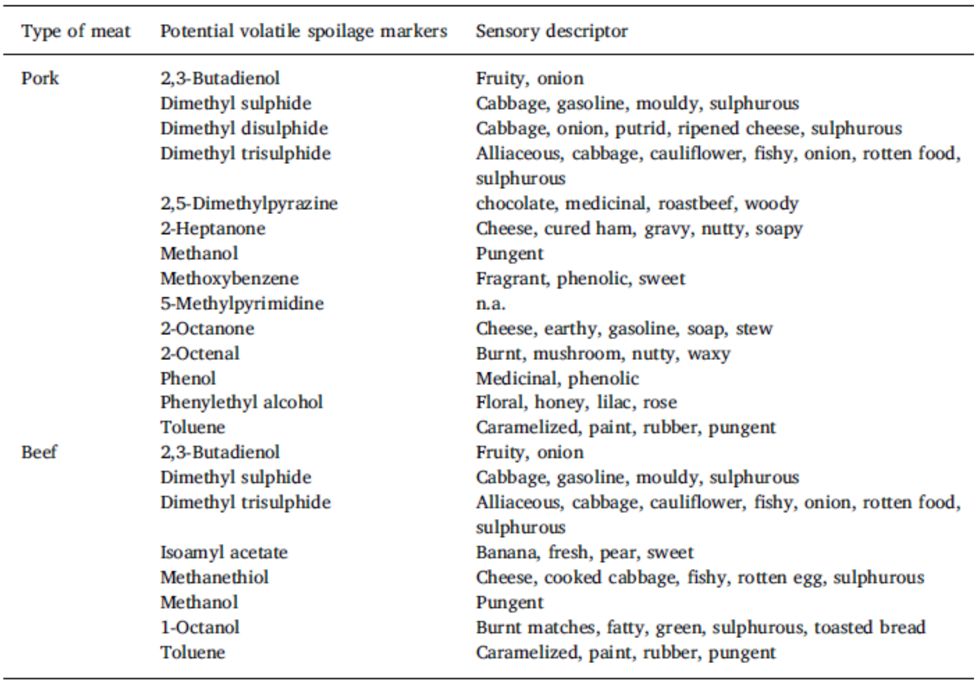

Type of meat	Potential volatile spoilage markers	Sensory descriptor
Pork	2,3-Butadienol	Fruity, onion
	Dimethyl sulphide	Cabbage, gasoline, mouldy, sulphurous
	Dimethyl disulphide	Cabbage, onion, putrid, ripened cheese, sulphurous
	Dimethyl trisulphide	Alliaceous, cabbage, cauliflower, fishy, onion, rotten food, sulphurous
	2,5-Dimethylpyrazine	chocolate, medicinal, roastbeef, woody
	2-Heptanone	Cheese, cured ham, gravy, nutty, soapy
	Methanol	Pungent
	Methoxybenzene	Fragrant, phenolic, sweet
	5-Methylpyrimidine	n.a.
	2-Octanone	Cheese, earthy, gasoline, soap, stew
	2-Octenal	Burnt, mushroom, nutty, waxy
	Phenol	Medicinal, phenolic
	Phenylethyl alcohol	Floral, honey, lilac, rose
	Toluene	Caramelized, paint, rubber, pungent
Beef	2,3-Butadienol	Fruity, onion
	Dimethyl sulphide	Cabbage, gasoline, mouldy, sulphurous
	Dimethyl trisulphide	Alliaceous, cabbage, cauliflower, fishy, onion, rotten food, sulphurous
	Isoamyl acetate	Banana, fresh, pear, sweet
	Methanethiol	Cheese, cooked cabbage, fishy, rotten egg, sulphurous
	Methanol	Pungent
	1-Octanol	Burnt matches, fatty, green, sulphurous, toasted bread
	Toluene	Caramelized, paint, rubber, pungent

Table 1.2: Meat, relative odorous molecules emitted and sensor description. Adapted from [11]

Despite the freshness and the spoilage rate is one of the most important factors in the food and beverage industries, another characteristic that can be evaluated with this technology is the adulteration. Adulteration in food is a menace, which all of us face since the beginning of civilization, as it not only decreases the quality of food products but also results in a continuing problem with significant consequences for human health and economic damage. Tighter controls need to be performed in the future in order to ensure the food and beverage quality. This problem is particularly pronounced in countries like Italy where the sector counts for a big percentage of the annual GDP; The economic loss on the tax revenue in the country was evaluated of 5,7 billion just in the year of 2016 [13].

One example was tested adulterating four fresh squeezed orange juices with a different ratio of concentrated juices, from 10 to 30% of volume. After all the test, the electronic nose showed more than 70 volatile compounds in total with differences in relative abundance of VOC's between the fresh tester and the mix fresh-concentrated juices, suggesting and proving the adulteration of the last ones [14].

Nowadays this technology can be applied also to track the geographical origin of different product. For instance, it was possible, combining the electronic nose with an electronic tongue to localize the exact region of production of various types of tea leaves [15].

Another application pursued by many researchers is the detection of the indoor air quality [16] and hazardous, toxic gases [17] or pollution.

Many publications pointed out the effectiveness of the electronic nose in health-care as an early diagnosis thanks to the microorganism or VOC's liberated by the bodily fluids or the breath. In urinary tract infections e-noses were used to analyze urine samples directly or after short incubations in test tube systems containing complex media, being able to distinguish between uninfected and infected urine [18]. Prospective studies have been performed to determine whether exhaled gas or breath analysis using an e-nose correlates with lung cancer. The results show good correlation with clinical diagnosis and provide new potential for diagnostic analysis [19].

Different companies are trying to miniaturize these sensors in order to integrate them into smartphones. In this way wireless gas detection with a smartphone via radio frequency communication will be possible [20].

The potential for future developments of innovative e-nose applications is enormous as researchers in many fields of scientific investigation and industrial development become more aware of the capabilities of the electronic nose. The current trend is aiming towards the development of electronic noses for specific purposes or a narrow range of applications. This strategy increases e-nose efficiency by minimizing the number of sensors needed for discriminations, reducing instrument costs, and allowing for greater portability through miniaturization. On table 1.2.3 are reported some other fields and possible applications.

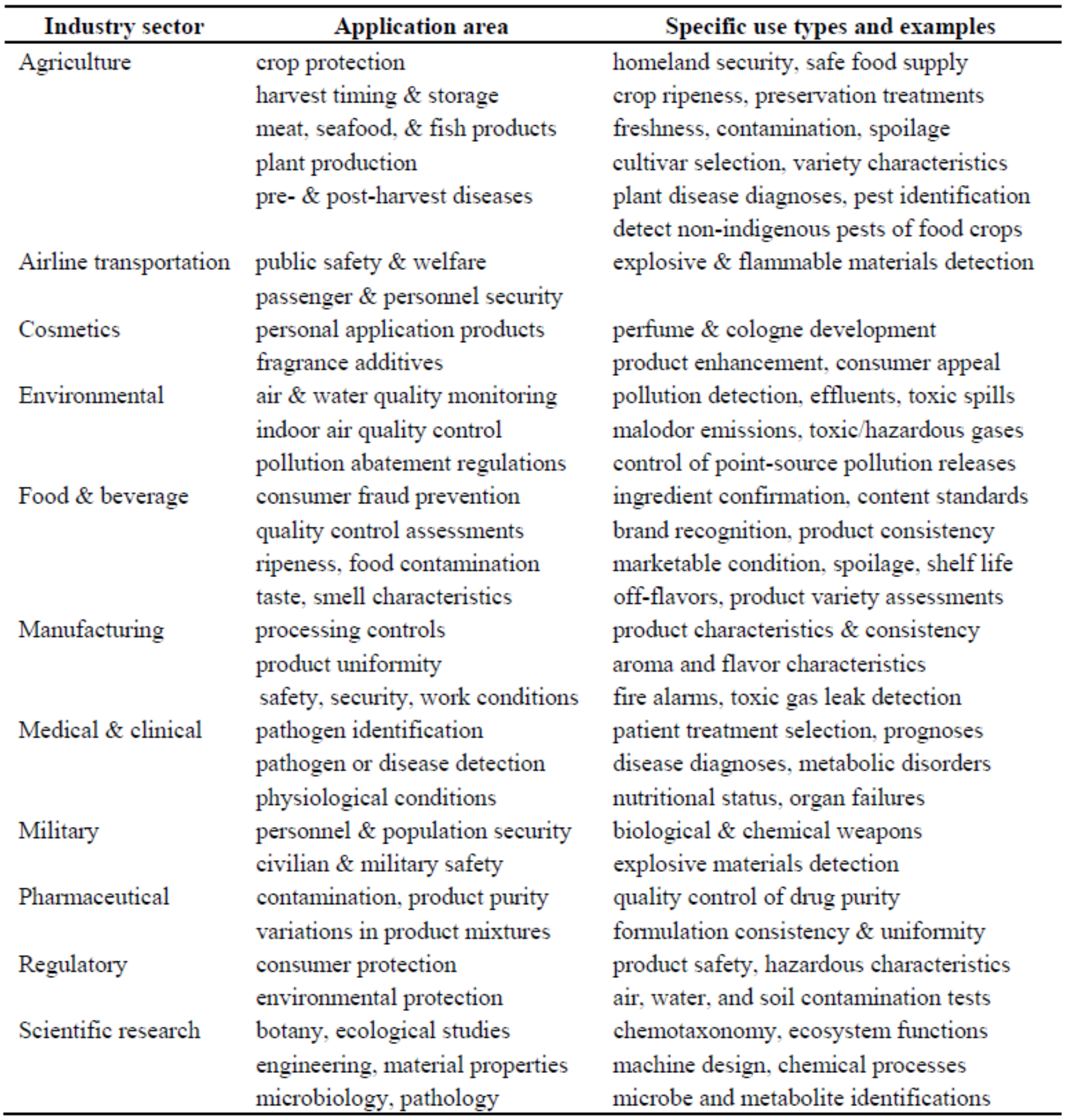

Industry sector	Application area	Specific use types and examples
Agriculture	crop protection	homeland security, safe food supply
	harvest timing & storage	crop ripeness, preservation treatments
	meat, seafood, & fish products	freshness, contamination, spoilage
	plant production	cultivar selection, variety characteristics
	pre- & post-harvest diseases	plant disease diagnoses, pest identification
		detect non-indigenous pests of food crops
Airline transportation	public safety & welfare	explosive & flammable materials detection
	passenger & personnel security	
Cosmetics	personal application products	perfume & cologne development
	fragrance additives	product enhancement, consumer appeal
Environmental	air & water quality monitoring	pollution detection, effluents, toxic spills
	indoor air quality control	malodor emissions, toxic/hazardous gases
	pollution abatement regulations	control of point-source pollution releases
Food & beverage	consumer fraud prevention	ingredient confirmation, content standards
	quality control assessments	brand recognition, product consistency
	ripeness, food contamination	marketable condition, spoilage, shelf life
	taste, smell characteristics	off-flavors, product variety assessments
Manufacturing	processing controls	product characteristics & consistency
	product uniformity	aroma and flavor characteristics
	safety, security, work conditions	fire alarms, toxic gas leak detection
Medical & clinical	pathogen identification	patient treatment selection, prognoses
	pathogen or disease detection	disease diagnoses, metabolic disorders
	physiological conditions	nutritional status, organ failures
Military	personnel & population security	biological & chemical weapons
	civilian & military safety	explosive materials detection
Pharmaceutical	contamination, product purity	quality control of drug purity
	variations in product mixtures	formulation consistency & uniformity
Regulatory	consumer protection	product safety, hazardous characteristics
	environmental protection	air, water, and soil contamination tests
Scientific research	botany, ecological studies	chemotaxonomy, ecosystem functions
	engineering, material properties	machine design, chemical processes
	microbiology, pathology	microbe and metabolite identifications

Table 1.3: Industry sector, application area and examples of utilization of electronic noses. Adapted from [11].

1.3. Sensors

In the broadest definition, a sensor is a device whose purpose is to detect changes in its environment and send the information to other electronics. The choice of an adequate sensor for a given application should be dictated by conditions in which the measurement will be carried out. Things to consider should be cost, durability of the sensors and also the composition of the gaseous mixture to be analyzed. Among all the sensors, the devices and techniques following listed are some of the mostly common sensor types used to perceive the smells and fragrances.

1.3.1. Piezoelectric crystal sensors

The main property of piezoelectric materials is to produce a voltage when a mechanical stress is applied and, equally, deform if a voltage is applied. This behaviour would not detect any kind of odorous molecule adsorbed on the surface but, when a waving potential is applied at a frequency near the resonant frequency of a piezoelectric crystal, an oscillating circuit is formed. The device is then coated with a material, such as a polymer, that adsorb the organic molecules from the gas phase changing the resonant frequency of the piezoelectric crystal. There are two main categories of these sensors, the surface acoustic wave resonators (SAW) and the quartz crystal microbalance sensors (QCM). QCM sensors typically operate at frequencies from 5 to 30 MHz, while SAW devices between 100 and 400 MHz [21] and the substrate material is generally ZnO, $LiNbO_3$ or quartz.

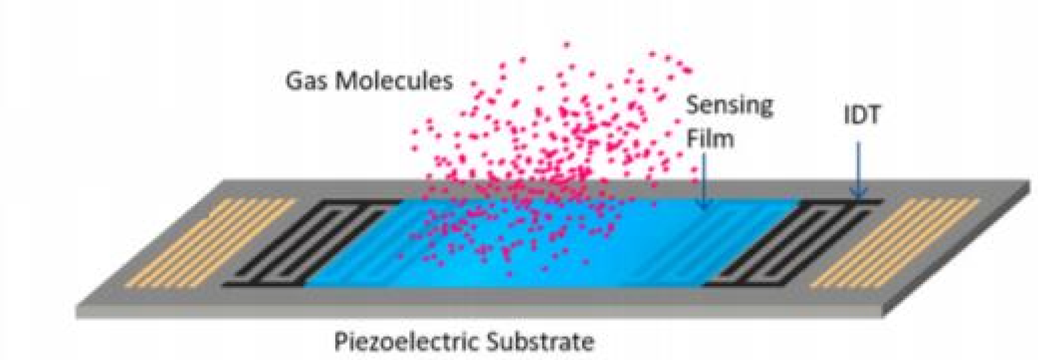

Figure 1.4: SAW sensor architecture. Adapted from [22].

The difference between the two sensors is that in the QCM sensor the acoustic wave propagates through the bulk while in the SAW resonator the motion occurs only at the surface; These waves propagate along the surface of a material and decay exponentially into the depth of the material (penetration depth ~ 1 wavelength) so that most of their energy density is localized in the near surface region. They propagate with a velocity slightly less than that of transverse waves in the material (and ~ 10−5 times the velocity of electromagnetic waves) [22].

The SAW resonator consists in a thin piezoelectric substrate, where, thanks to lithography it is possible to realize interdigit transducers (IDTs) where the voltage is applied; One of the IDTs will be the input and the other the output. On top of them a very thin film of the sensing material is coated to permit the adsorption. When the voltage is applied, it is possible to measure the shift on the resonant frequency. The QCM sensor follows the same working principle but as shown in Figure 1.5 the acoustic wave needs to penetrate through the piezoelectric substrate and the signal measured by the output electrode [23].

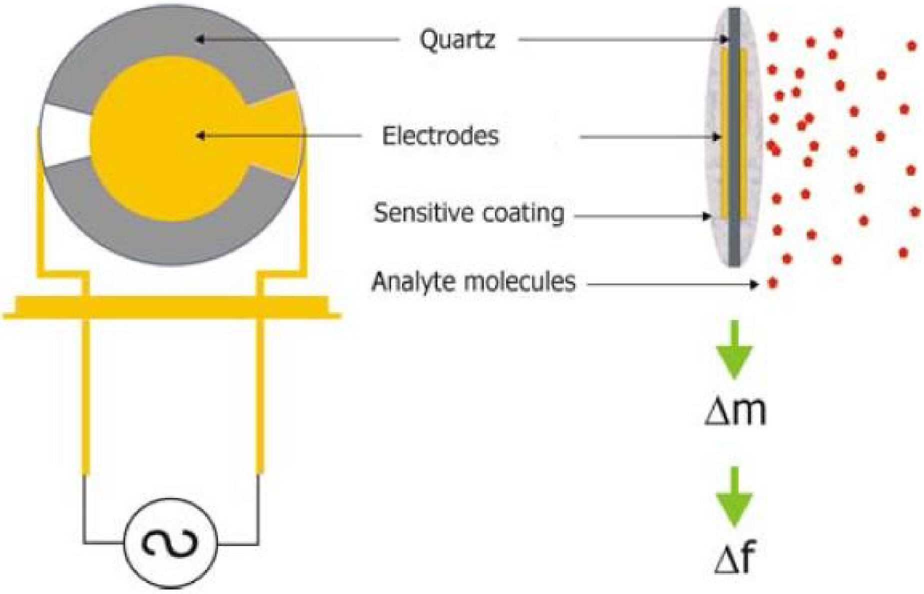

Figure 1.5: QCM sensor architecture. Adapted from [23].

1.3.2. Optical sensors

A multitude of transduction mechanisms may be utilized for detecting the analyte, including fluorescence intensity and lifetime, polarization, spectral shape, absorbance, wavelength and reflectance. One of the technologies used is the polymer-deposited optical sensor arrays; Solvatochromic (term used to describe the phenomenon that is observed when the color due to a solute is different when that solute is dissolved in different solvents) fluorescent dyes are immobilized in various polymer layers to produce a sensor array for detecting organic vapors. The interaction between the immobilized sensing dyes and the analyte generates local fluorescence signals that can be monitored over time. For example, the dye exhibits large shifts in its emission wavelength maximum with changes in local polarity. Typically, when exposed to solvents with increasing polarity, solvatochromic indicators will exhibit progressively more red-shifted absorption and/or emission spectra [24]. It's a unique technique because it is possible to obtain multiple information simultaneously, including fluorescence lifetime, the spectral shape, the wavelength and changes in intensity with a high accuracy and fast response. On the contrary, even if the different coatings are available with many different dyes, the fabrication process is expensive, and the interface circuitry is quite complex. The stability is another drawback because the lifetime of these devices is reduced due to the photobleaching effect.

1.3.3. Spectrometry-based sensors

Another class of devices utilized in gases smelling sensing are all these instruments based on spectrometric arrays. Within this group, gas chromatography (GC) and mass spectrometry (MS) are the two most common and famous techniques. In gas chromatography, the mobile phase (or "moving phase") is a carrier gas, usually an inert gas such as helium or an unreactive gas such as nitrogen. The stationary phase is a microscopic layer of liquid or polymer on an inert solid support, inside a piece of glass or metal tubing called a column. The instrument used to perform gas chromatography is called a gas chromatograph (or "aerograph", "gas separator"). The gaseous compounds being analyzed interact with the walls of the column, which is coated with a stationary phase. This causes each compound to elute at a different time, known as the retention time of the compound. The comparison of retention times is what gives GC its analytical usefulness and from there the chemical species is detected [25].

In a typical MS procedure, a sample, which may be solid, liquid, or gas, is ionized, for example by bombarding it with electrons. This may cause some of the sample's molecules to break into charged fragments. These ions are then separated according to their mass-to-charge ratio, typically by accelerating them and subjecting them to an electric or magnetic field: ions of the same mass-to-charge ratio will undergo the same amount of deflection. The ions are detected by a mechanism capable of detecting charged particles, such as an electron multiplier. Results are displayed as spectra of the relative abundance of detected ions as a function of the mass-to-charge ratio. The atoms or molecules in the sample can be identified by correlating known masses (e.g. an entire molecule) to the identified masses or through a characteristic fragmentation pattern [26].

The accuracy of the measurements is unreachable by other techniques but the processing time, the complexity of the system and the size of the instrument make these techniques not appropriate for anything else than scientific purposes.

1.3.4. Transistor sensors

Metal-oxide semiconductor field effect transistors (MOSFET) are the most famous and employed sensors within this class. The MOSFET structure consists of a metal gate on top of an oxide layer, typically $\mathrm{SiO_2}$, and a p-type silicon base with n-doped channels on either side of the gate (Figure 1.6). The surface potential, φ_s, of the semiconductor layer is dependent on the applied gate voltage V_g and the work function of both the metal, W_m, and semiconductor, W_s, materials [24] (q is the electric charge).

$$\varphi_s = f\left(V_g - \frac{W_{ms}}{q}\right) \tag{1.1}$$

$$W_{ms} = W_m - W_s \tag{1.2}$$

To maintain a constant surface potential, the applied gate voltage must be adjusted in relation to the change in the work function. The odorant adsorbs on the metal gate that has to be porous to permit the diffusion of the gaseous molecules at the oxide layer (the gate insulator) interface where a dipole layer is created. The reaction between these molecules and the catalyst gate alters the electric charge modifying the conducting channel current, allowing the detection of the odorant.

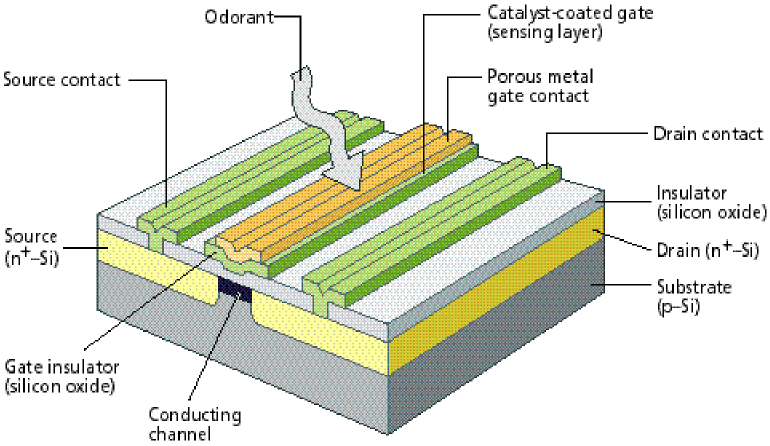

Figure 1.6: MOSFET sensor architecture. Adapted from [6].

1.3.5. Pellistor sensors

Pellistor sensors are devices employed to detect combustible gases or gases with high difference in thermal conductivity from the molecules studied with air. This type of sensors based on the thermo-catalytic principle detect the heat of reaction. For this purpose, a noble-metal catalyst is electrically heated to operating temperatures between 200 and 600°C. Chemical power, caused by the oxidation of combustible gases imbalances the equilibrium of electrical heat supply and thermal loss, allowing the detection of the gas studied [27].

1.3.6. Chemiresistors

This class of sensors, resistance-based, are a group of devices where, upon the exposure and the adsorption of the analyte on the surface of the coated material, a variation on the film intrinsic electrical resistance/impedance occurs; if the system is measured on direct current (DC) the resistance is measured, on the contrary if is performed on alternate current (AC) it is the impedance to be measured. The name chemiresistor is due to the fact that there is a direct chemical interaction between the sensing material and the analyte and this interaction can be through covalent bonding, hydrogen bonding of dipole-dipole interactions. Depending on this interaction, the desorption needs more or less energy to occur. A basic voltage is applied on the circuit and the charge or intensity of current is subsequently measured using an ohmmeter or a digital multimeter, revealing the reaction of the VOC's exposed with the active material layer [28].

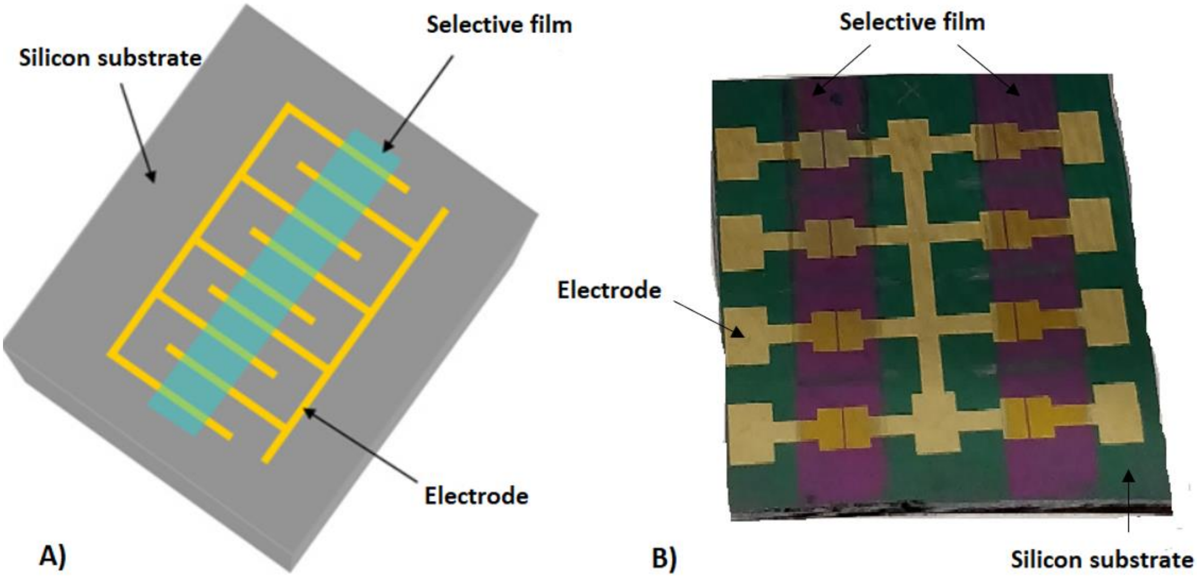

Figure 1.7: model and real chemiresistor architecture. Adapted from [28]

A basic chemiresistor architecture consists on interdigitated electrodes (usually) with a thin film of sensing material which is able to bridge the gap between the pair of electrodes, everything on top of a silicon wafer (the substrate). One electrode is the input, where the voltage is applied, while the other is the output, where the circuit is grounded. Electrodes are typically made of conductive metals, such as gold that ensure a good contact with the film. The coated material can be a conductor or semiconductor; the main classes of material used on VOCs sensing are listed in the following subchapters.

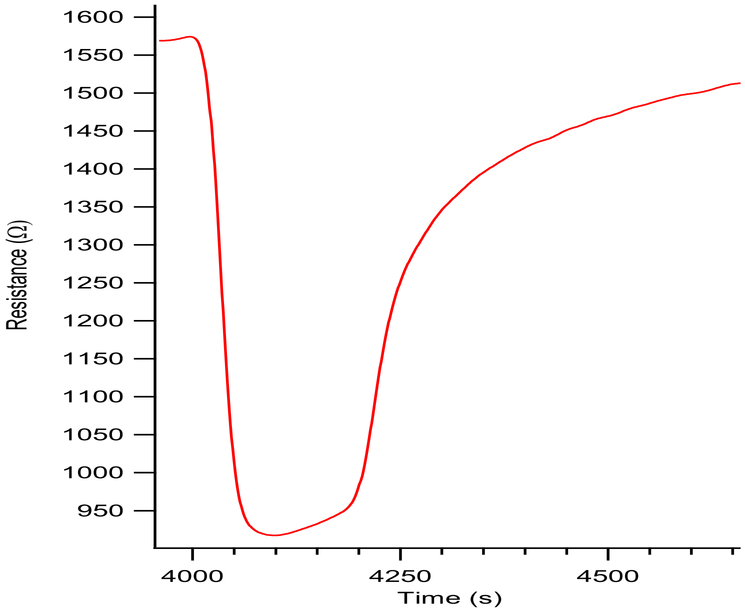

Figure 1.8: Resistance variation over the exposure time of the analytes

1.3.6.1. Metal-Oxide Semiconductors (MOS)

Metal-oxide sensors are most commonly a ceramic based material, the insulator, coated with a layer of semiconductor oxides (typically $\mathrm{SnO_2}$, $\mathrm{TiO_2}$, ZnO). On side of the sensitive material, the device is equipped with two electrodes, the input and the output, where the voltage is applied. On the bottom of all the instrument a heating system is present, generally a platinum coil, able to heats up to 500°C [29]. The sensing mechanism is believed to occur through chemi-adsorption of oxygen at the surface of the MOS element at elevated temperatures of 300°C-500°C. Molecular oxygen traps electrons from the semi-conductor's conduction band forming O_2^- or the atomic forms O^- adsorbed at the surface of the semiconductor material. The presence of such ions on the surface of the semiconductor particle grains creates a depletion layer boundary (Schottky barrier) that alters the electrical conductance of the device. If a reactive gas is introduced, this gas may react with the oxygen ions and electrons (or alternatively holes) at the surface of the semi-conductor. This chemical reaction directly affects the surface coverage and depletion layer and leads to a measurable change in the device's electrical conductivity. The user simply needs to monitor the conductivity (or resistance) of the MOS sensing element. This is often accomplished by placing the MOS device in a voltage divider with a fixed value resistor. Typically, the change in resistance is not linearly proportional to gas concentration. MOS devices are conceptually simple for the end-user, can often be acquired for <$20USD [30].

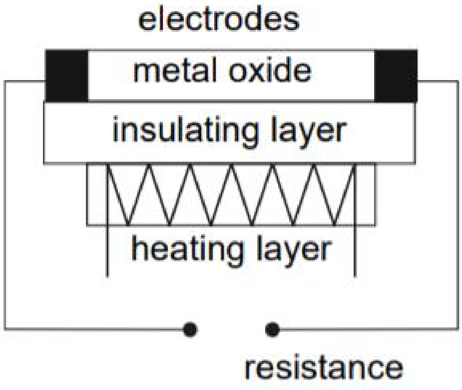

Figure 1.9: MOS sensor architecture. Adapted from [24].

Selectivity and sensitivity of the sensor depend on the type of semiconductor chosen. The sensitive layer can be modified by doping with precious metals (Pt, Pd, Cu, Au) reducing the impact of fluctuations of temperature and humidity on the obtained results [31]. The catalyst sensitive metal-oxide can be designed with a certain degree of porosity. This architecture of the sensor is performed to obtain a higher degree of superficial area, improving the adsorption of the molecules so that the sensitivity of the sensor. The major drawback of these class of material is the high-power consumption (due to the heater) which limits the potential application in portable and hand-held devices.

1.3.6.2. Nanomaterials

Nanomaterials describe in general, materials where at least one of three spatial dimensions is in the scale of nanometers (10^{-9} m). The definition given by the EU is:

“A natural, random or produced material which contains single or aggregated particles where more than the 50% of the distribution of the order of magnitude is in the range of 1 nm – 100 nm”

In this thesis, by nanomaterials are considered all the range of carbon nanostructured material such as graphene or carbon nanotubes.

Especially graphene, graphene oxide and reduced graphene oxide have emerged as fascinating candidates for sensing applications, because of their superior electronic, chemical, mechanical and thermal properties. The extraordinary surface area of graphene together with its exceptional electronic properties as well as its intrinsically low electrical noise has made it to be highly sensitive to the surface adsorption of gas molecules.

The sensor architecture consists in a silicon substrate on which platinum or gold electrodes were deposited. Then graphene or his oxides are dispersed in a solution and coated on the electrodes gaps and dry up in an oven to evaporate the solvent. A heating system is generally sited on the bottom of the silicon substrate to prevent the desorption problems also present on the MOS sensors. The main drawbacks in graphene are generally the fact that the differences in the sensed response are small and the gas discrimination is random. This behaviour of graphene can be a big problem is the e-nose technology, but it is also true that the response silhouette using graphene show a completely different trend, granting a good selectivity in the odorant sensing employing these sensors together with other different material sensors [32].

1.3.6.3. Composite Materials

A composite material is a heterogeneous compound where different phases, with different physique properties, are mixed and combined together in order to improve the performances of the material on a level absent on the starting material.

In the electronic nose applications, the composite materials normally used are loaded polymers. The architecture of the sensor is typically the same as the previous cases considered. An insulating matrix is charged homogenously with a conductive filler, such as carbon black (CB) particles or carbon nanotubes (CNTs) or other intrinsically conductive polymers or metal particles. While the transducing principle with a conductive polymer filler is quite complex and will be discussed more in detail on chapter 2, the carbon-based nanofiller base the sensing mechanism on swelling. Upon the exposure of the analyte, a swelling occurs, decreasing the conductivity (and increasing the resistance) when a voltage is applied. This phenomenon is due because the particles are introduced in order to touch each other creating a pathway or percolation threshold where the electrons can hop from a chain to the next one, thanks to the tunnelling effect. During the adsorption of the odorant, the odorous molecules diffuse between the polymer macromolecules breaking the entanglements previously created, increasing the free volume and interrupting the connection between the conductive fillers, avoiding or making difficult for the electron to flow from one electrode to the other. It is clear then that, to achieve a good conductivity, all the particles need to be connected so that a level of percolation is required. This percolation threshold ϕ_C, if reached, can improve up to ten times the conductivity (so decrease the resistance) [33].

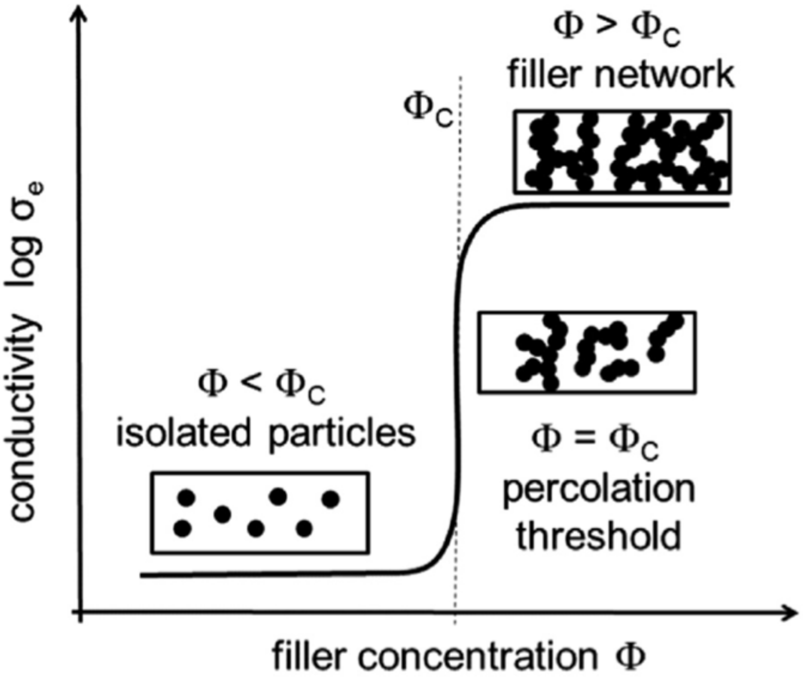

Figure 1.10: Percolation curve. Adapted from [33].

All the process is, though, reversible because the molecules once are diffused inside of the matrix do not chemically bound and so they can desorb, allowing the regeneration of the pathway. These devices are more sensitive and efficient at high temperature and close to the threshold [34].

1.3.6.4. Conductive Polymers

Polymers are usually considered as insulating materials and, for this reason, applied in numerous fields where conducing electricity is an issue. This is due to their low dielectric constant and the charge transport mechanism that does not allow the conduction of electric current. In fact, polymers usually show a very high resistance ($\simeq$ MΩ-GΩ), an irreconcilable property with the electronic nose technology. However, in 1977, Heeger, MacDiarmid and Shirakawa reported an oxidized iodine-doped polyacetylene showing a really high conductivity. This discovery granted them the Nobel Prize in Chemistry for the development of electrically conductive polymers thanks for the future applications that this new material can give. This new class of materials are called “intrinsically conductive polymers” or ICP and a common characteristic showed is the presence of conjugated bonds.

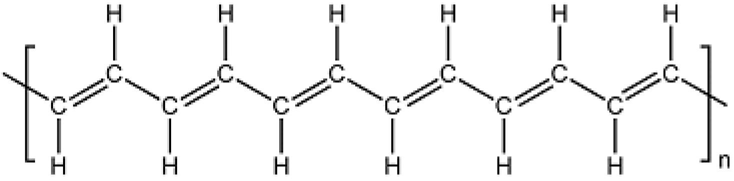

Figure 1.11: Polyacetylene

They are characterized by a backbone consisting of σ bonds and a system of p orbitals, orthogonal to the first, forming π bonds. Increasing the number of π bonds, the energy between the valence band and the conduction band decrease making the material as a semiconductor. Even though the energy to permit to jump in the conductive band decrease sensibly, at room temperature the excitement of the electron is still not possible; For this reason, is necessary to dope the polymer reducing the band gap, introducing new energetic levels necessary for the electron to move. A better and more comprehensive explanation of the process will be discussed on chapter 2.

1.3.6.5. Chemiresistor sensing curve and other important parameters

Once all the class of sensor material are be listed, another important factor to understand in this class of sensors is how the sensing curve looks like and the parameters associated to it.

The first useful concept is the baseline because it is the starting point to lately calculate the response value of the sensor. The importance of the baseline in this class of sensor is even more important for conductive polymers where the baseline keep changing over the time, sometimes without reaching a plateau as it shows on Figure 1.12. The continuous decrease on the baseline is still not well understood because it is strictly connected to the conducing principle of the material (especially for CP). Nevertheless, one possible reason, at least for conductive polymers, of this behaviour can be attributed to the de-doping caused by the desorbing of volatile molecules on the surface and on the bulk (that is the reason because the baseline needs much time to reach a plateau) of the active layer upon exposure of a dry air flow.

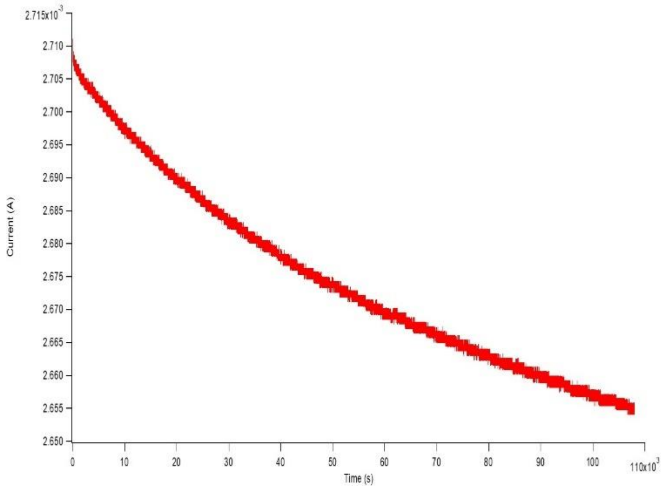

Figure 1.12: Classic baseline curve

Defined the baseline, it is important to visualize how the curve change upon the exposure of the sensing analyte. Even though the baseline is usually reported considering the change on current intensity [35], the sensing curve for chemiresistors, as reported generally on literature [36], is plotted in change on resistance over time following the formula (V is the voltage applied):

$$R = \frac{V}{I} \tag{1.3}$$

As can be noticed on Figure 1.13 several peaks are present on the curve; These peaks are the variation on resistance upon the exposure of the sensing analyte and the bigger results the peak the bigger is the concentration of the analyte or the percentage of the analyte on the total gaseous flow.

The importance of these peaks is because by the variation of resistance the response of the device is evaluated; two concepts need to be defined in order to understand what the response is: R_0, the value of resistance right before the beginning of the resistance drift attributed to the analyte, and R_1, the maximum value of the peak. There are various types of response evaluation with respect to the baseline (because of its drift) and this process compensate for noise, drift and also for inherently large or small signals. The three most common method used are [37]:

- Differential: The baseline (R_0) is subtracted from the peak maximum (R_1). This process eliminates intrinsic constant machine noise δ evaluating the response R indicated in Ohm by:

$$R = (R_1 + \delta) - (R_0 + \delta) = R_1 - R_0 \tag{1.4}$$

- Relative: The peak maximum (R_1) is divided by the baseline (R_0). This process eliminates multiplicative drift σ and a dimensionless response R is obtained.

$$R = \frac{R_1(1+\sigma)}{R_0(1+\sigma)} = \frac{R_1}{R_0} \tag{1.5}$$

- Fractional: The baseline R_0 is subtracted from the maximum peak R_1 and divided by the baseline. A normalized, dimensionless response R is obtained, compensating for inherently large or small signals.

$$R = \frac{R_1 - R_0}{R_0} \tag{1.6}$$

Usually the response is lately multiplied per 100 in order to obtain a percentage response. The choice of baseline manipulation depends on the sensor type, the application and also the researcher's preference; In this thesis the fractional method was selected.

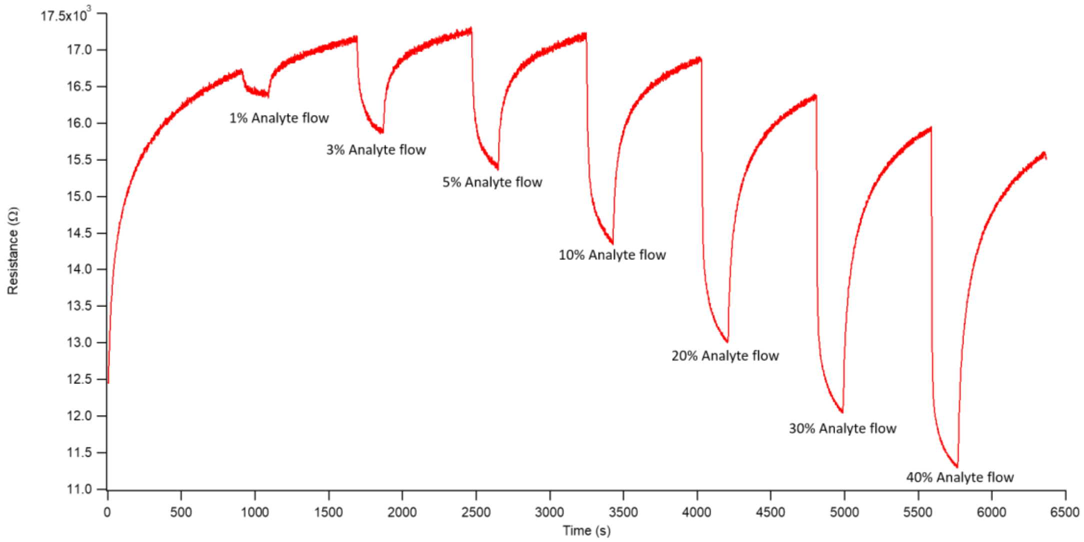

Figure 1.13: Chemiresistor sensing curve with the percentage of analyte on the total volume of gas flow indicated.

Other important parameters are all connected to the time; In particular, stabilization time, response time and recovery time.

The stabilization time or rise time, generally, can be assumed by the interval required by the output signal of a chemiresistor to display a change in the resistance and to reach a semi-constant value after exposure of the analyte. The definition of semi-constant behaviour is highly discussable; In fact, the point where the value starts to show a plateau can be set to a different percentage of variation. In Figure 1.14 the value was taken at 90% of variation.

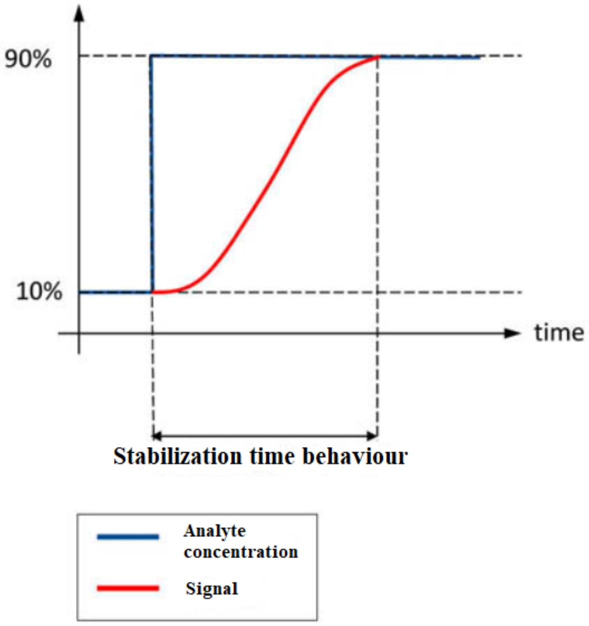

Figure 1.14: Stabilization time illustration. Adapted from [38].

The response time or exposure time is defined as the time during which the considered output property keeps changing. In the case of chemiresistors the response time can be assumed by the time within which the analyte flow is blown on the system and the molecules adsorb on the surface and diffuse on the bulk of the active layer variating the resistance of the device. Given the definition it is clear that a certain overlap between this time and the stabilization time is evident and need to be understood.

The last time parameter considered is the recovery time that is the time during which the output signal return to the value before of the variation of the considered property. In chemiresistors, the recovery time is the time within which the signal return approximately to the previous baseline value after the exposition of the analyte. This time depends highly on the material selected because is correlated with the desorption of the molecules adsorbed in and on the surface. For instance, MOS sensor usually present high recovery time because of the strong bonds that the molecules can make with the sensor material [39]. At the same way as stabilization time was defined, also the value of the recovery time does not need to return exactly to the baseline before-exposure value, but a certain percentage of return is admitted. On Figure 1.15 this value was set to 10% of property variation.

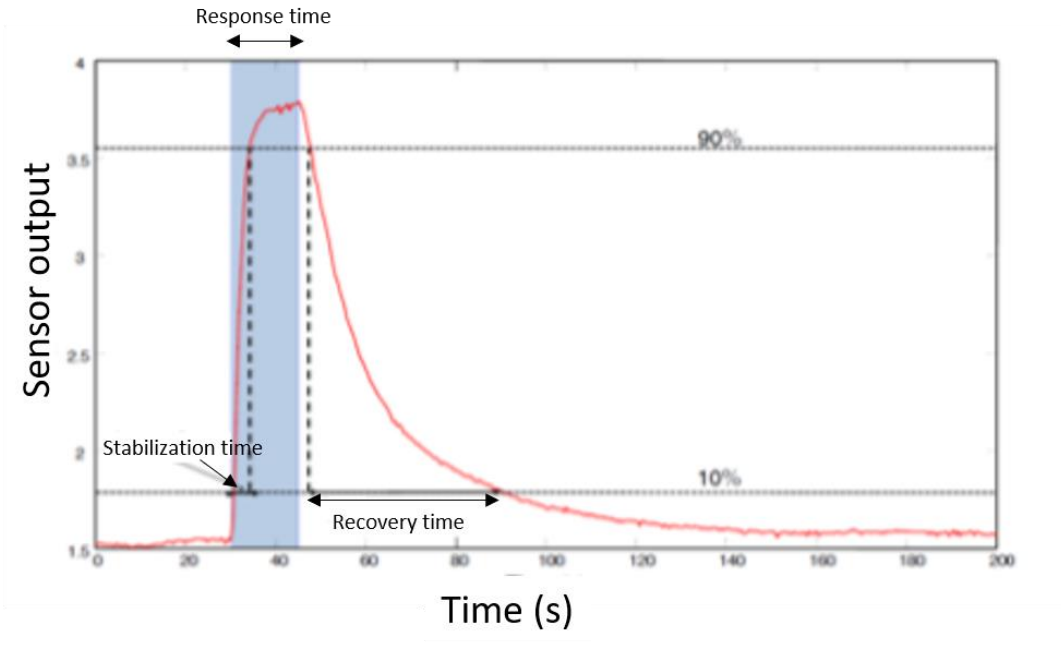

Figure 1.15: Sensing curve with the time parameters indicated. Adapted from [39].

However, the fundamental parameters researched when e-nose technology are developed are what are called by “3 S’s” which are sensitivity, selectivity and stability.

Sensitivity, in an electronical device, is the ratio between the variation of the measured value and the real value of the considered physical quantity. It does not have to be confused with responsivity, which is the variation of the measured value on the initial value, but rather the tangent curve of the responsivity. Despite the definition could fit in every occasion, the technology so that the instrument with the test are performed need to be considered. There is, in fact, a variation of the real value of the physical quantity that cannot be recorded, or it is confused with the intrinsic noise of the device; in this case the minimum sensibility of the system is reached.

Selectivity is a very important parameter in sensing technology because is the ability of the device to discriminate between different gases and fragrances. The parameter is related with the different interaction that the odorous molecules have with the sensing layer, from the bonding to the bulk diffusion. It is clear then that, changing the functional groups or adding different chemical species on the sensor may lead to a different response over different analytes. Even if some overlapping in the sensing of different analytes may occur, the aim is to have specific trend for the same analytes over many sensors.

The last parameter considered is the stability; this variable is generally really important, even more in case of polymeric sensing layers, since it is able to describe the tendency of the material to deteriorate, reducing the required sensing properties. It is usually expressed by lifetime, but it can also be reported by the number of cycles before replacement.

1.4. Thesis objective and IBM project

The development of a sensor able to detect and select the right chemical specie and give a strong and unique fingerprint is the main aim by all the major team of researcher working around the world.

The IBM sensor group at Almaden research center enters in this framework investigating over different analytes and different material. Within the group are present various sub-groups focused on different material such as MOS sensors, IC polymers, BioChemical sensing as well as different sensing principle such as chemiresistor or SAW.

The aim of this thesis was to investigate intrinsically conductive polymers as active sensing material in chemiresistor for the detection of VOCs with special focus on sensitivity and selectivity. The objective was to build a chemiresistor starting from the synthesis, through the coating and the measurement of the device over a class of 14 different analytes. Every sensor analysed was produced with different methods, changing the synthesis parameters, adding different species on the sensing layer or changing the coating procedure.

Subsequently, a script was written to record and analyse the results obtained, able to show rapidly and clearly the sensitivity for every measurement carried out and to discriminate, where possible, toward a difference in the sensing for different odorant.

CHAPTER 2

CONDUCTIVE POLYMERS

Since their discovery, conductive polymers have attracted much interest by the academic field; Electronic nose devices based on this category of materials were developed from the early 1980s [40]. In fact, there are numerous advantages on employing e-noses made with this material instead of MOS or metal, first of all the extremely inexpensive cost, both for the raw material and processing. Using this class of materials can lead to high sensitivities to a wide range of analytes, short response time, an easy synthesis, good mechanical properties and low power consumption since they operate mostly at room temperature [41]. By contrast, metal-oxides or graphene-based sensors must operate at high temperature and have much more limited range of detectable analytes [9]. On Table 2.1 are displayed the advantages and disadvantages of various classes of electronic nose materials.

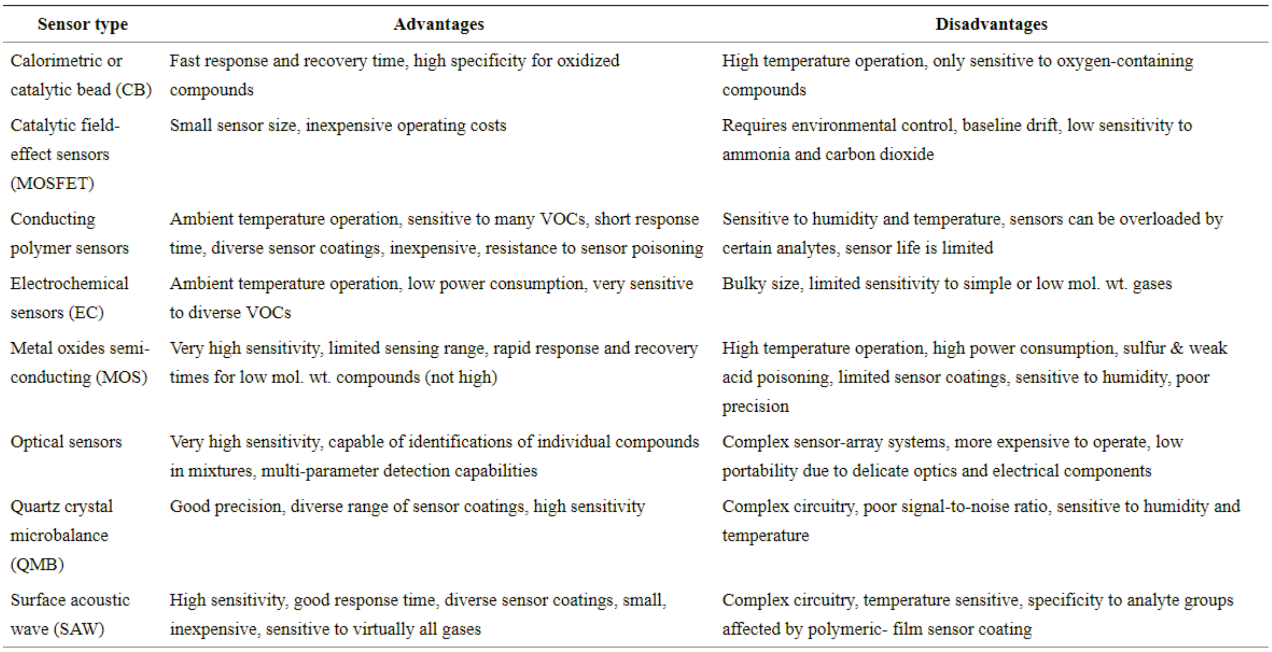

Sensor type	Advantages	Disadvantages
Calorimetric or catalytic bead (CB)	Fast response and recovery time, high specificity for oxidized compounds	High temperature operation, only sensitive to oxygen-containing compounds
Catalytic field-effect sensors (MOSFET)	Small sensor size, inexpensive operating costs	Requires environmental control, baseline drift, low sensitivity to ammonia and carbon dioxide
Conducting polymer sensors	Ambient temperature operation, sensitive to many VOCs, short response time, diverse sensor coatings, inexpensive, resistance to sensor poisoning	Sensitive to humidity and temperature, sensors can be overloaded by certain analytes, sensor life is limited
Electrochemical sensors (EC)	Ambient temperature operation, low power consumption, very sensitive to diverse VOCs	Bulky size, limited sensitivity to simple or low mol. wt. gases
Metal oxides semi-conducting (MOS)	Very high sensitivity, limited sensing range, rapid response and recovery times for low mol. wt. compounds (not high)	High temperature operation, high power consumption, sulfur & weak acid poisoning, limited sensor coatings, sensitive to humidity, poor precision
Optical sensors	Very high sensitivity, capable of identifications of individual compounds in mixtures, multi-parameter detection capabilities	Complex sensor-array systems, more expensive to operate, low portability due to delicate optics and electrical components
Quartz crystal microbalance (QMB)	Good precision, diverse range of sensor coatings, high sensitivity	Complex circuitry, poor signal-to-noise ratio, sensitive to humidity and temperature
Surface acoustic wave (SAW)	High sensitivity, good response time, diverse sensor coatings, small, inexpensive, sensitive to virtually all gases	Complex circuitry, temperature sensitive, specificity to analyte groups affected by polymeric- film sensor coating

Table 2.1: Summary of advantages and disadvantages of different class of material employed for electronic nose technologies. Adapted from [9].

According to this little introduction, from now on, this thesis will be focused on this class of materials. To have a better knowledge of the material is essential to understand the entity of electrical properties required for the application and the conductive principle.

2.1. Electrical properties of polymers

The electronic nose is a device where, upon the application of a voltage so then the conduction of electricity, the studied analyte is detected and analysed. The electrical properties are, therefore, an extremely important guide to the choice of the right polymer for the appropriate application. The most important electrical properties for organic materials are the electrical resistance, the electrical permittivity, the electrical dissipation factor and the dielectric strength.

1. The specific electric resistance is the attitude of a material to oppose resistance to the passage of the electric charges. It is measured in Ohm and is defined as:

$$R = \rho \frac{L}{S} \tag{2.1}$$

   Where ρ is the static resistivity (Ωm) and is a quantity independent to the geometry of the sample considered; L is the distance (m) between the two point where the current is measured; S is the area (m^2) of the section of the sample perpendicular at the direction of the current. The definition on resistance given is, however, complex and not really easy to apply. Usually, when electricity is involved, the voltage is applied and there is a multimeter appointed to measure the current; in this case a better definition of resistance is given by the Ohm law:

$$R = \frac{V}{I} \tag{2.2}$$

   Where V is the voltage (V) and I is the intensity of current (A). Not variating the voltage, the maximum conductivity (so the maximum intensity of current) is achieved by low resistances.

2. The electrical permittivity is a physical quantity which describe the behaviour of a dielectric material when exposed to an electric field; it measures the predisposition of the mentioned material to be polarized. Supposing to apply a voltage between two plates of a capacitor separated by vacuumed space, a certain charge quantity q is created and can be theorized as:

$$q = C_0 V \tag{2.3}$$

   Where C_0 is the capacity of the capacitor and V the voltage. If a polar layer is positioned between the two plates the constant C is substituted by the electrical permittivity:

$$\varepsilon = \frac{C}{C_0} \tag{2.4}$$

Considering C as the capacity of the introduced layer.

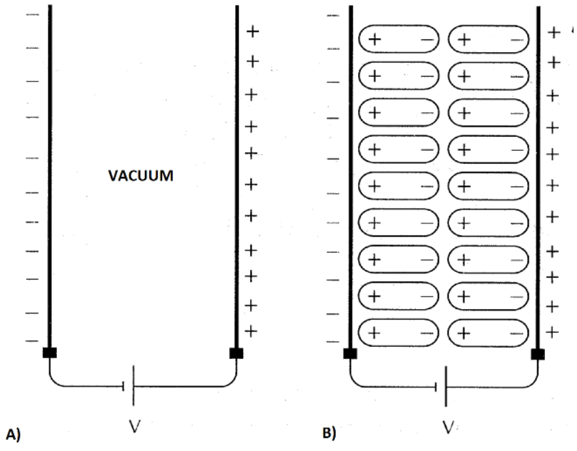

Figure 2.1: Charged plates with vacuum (A) and charged plates with polar molecules (B). Adapted from [42].

In this case the molecules tend to align the dipoles in the direction of the electric field, reducing the electric charge on the plate walls. Supposing the quantity of charge constant, the variable that change is the permittivity ε. A relatively high electrical permittivity is, therefore, needed to allow the conduction.

3. The electrical dissipation factor is a constant able to quantify the entity of the Joule effect. It is, generally, explained by the molecular friction and tends to be higher when the conductivity is low.

4. The dielectric strength is the variable that esteem the maximum potential delta that the organic material is able to support before of break. Increasing the conduction, the dielectric strength increase itself.

According to the mentioned properties, a proper made e-nose device show low resistance and high electrical permittivity, dissipation factor and dielectric strength.

2.2. Band theory

Not just the electrical properties are needed to understand what kind of organic material is suitable for the devices studied in this thesis, in fact the electric behaviour of polymers is highly connected to their electronic structure. According to the LCAO approximation, the wave functions of molecular orbitals are obtained by linear combination of the overlapped initial wave functions of the atoms (on Figure 3.3, Ψ_A and Ψ_B respectively) so that adding or subtracting them. If the molecular orbital is the product of the addition, show a lower energy than the initial wave functions, and in this case is called bonding orbital and present an increased symmetric interatomic electronic density. By contrast, if the molecular orbital is the product of the subtraction an antibonding orbital with higher energy is created and the interatomic electronic density is void. These orbitals or energetic levels are lately occupied by the electrons according to the Aufbau principle, from the less energetic to the more ones. The eventual promotion of one electron from the highest occupied molecular orbital (HOMO) to the lowest unoccupied molecular orbital (LUMO) is generally responsible for the conduction. An example with H_2 is showed on Figure 3.3.

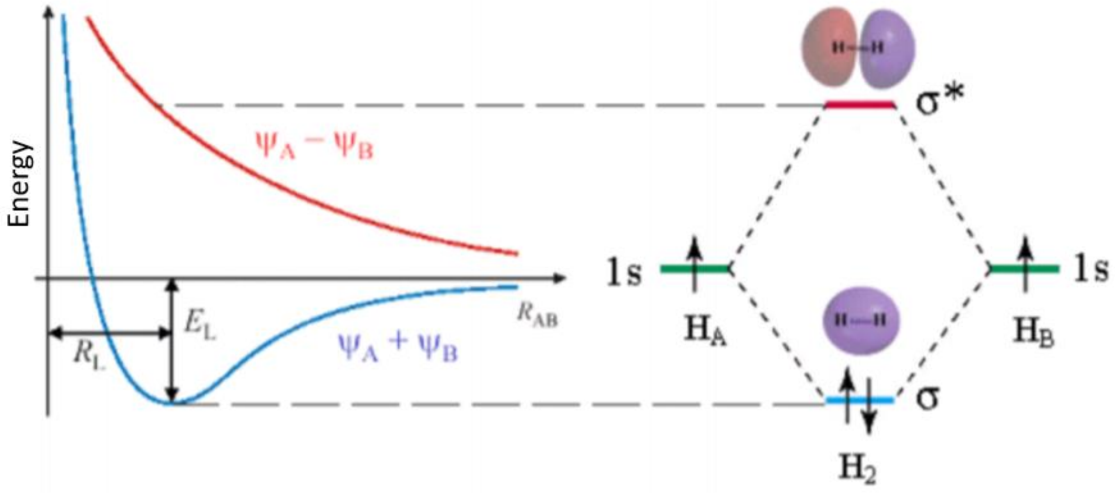

Figure 2.2: Bonding and antibonding energy against interatomic distance; Hydrogen energetic levels and bonding. Adapted from [43].

Referring to semiconductor or inorganic materials in general, instead of HOMO the referment is to valence band and instead of LUMO to conduction band. In metals or conducing materials, the conduction and valence bands are overlapped thanks to the high mobility of electrons given by the metallic bond. On semiconductors, the two bands are separated by an energetic gap; this gap has to be less than 1.5 eV in order to permit a partial passage of current otherwise a doping is needed in order to create intermediate energetic level, promoting the hopping of the electron. If the gap is greater of 3 eV the material is considered insulator; that's the case of most polymers. In case of organic material, however, the definition of bands loses all his meaning and the referment is to LUMO and HOMO.

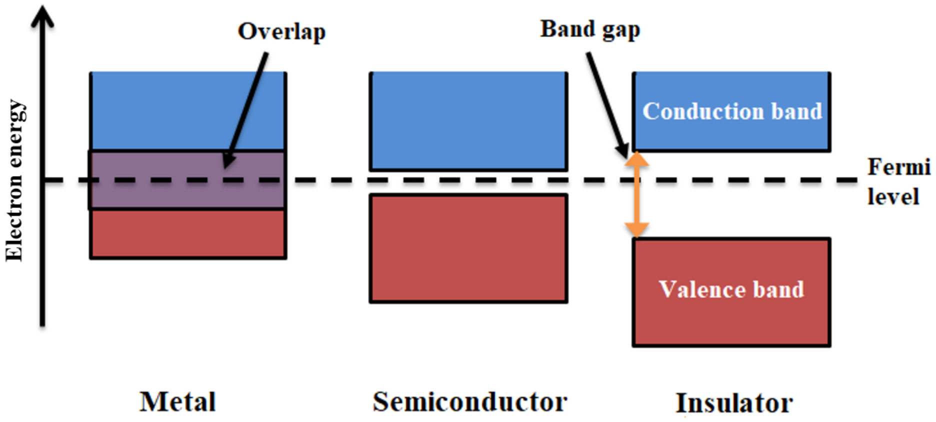

Figure 2.3: Bands scheme for metals, semiconductor and insulators. Adapted from [44].

2.3. Conductive principles

The conductive principle for ICPs is quite difficult and still not well known, numerous studies have been reported since the 1970s [45] trying to understand the exact mechanism but nowadays the reasons are not exhaustive.

The most accredited theory is based on the excitation of the macromolecule as a result of an applied voltage; in this case the molecule organise its steric structure based of the current direction creating positive or negative charged zones. The conduction is essentially based on the movement of the electrons paired to create the π bonds so that the presence of double bonds is required to permit the phenomenon of conduction. There are two excitation conformation, the degenerate and not degenerate, responsible for the conduction.

If the state of the excitation is degenerate (mostly on linear ICPs, such as polyacetylene) and there is a charge carrier, two isoenergetic phases of resonance are created on the macromolecule, visible on Figure 2.4.

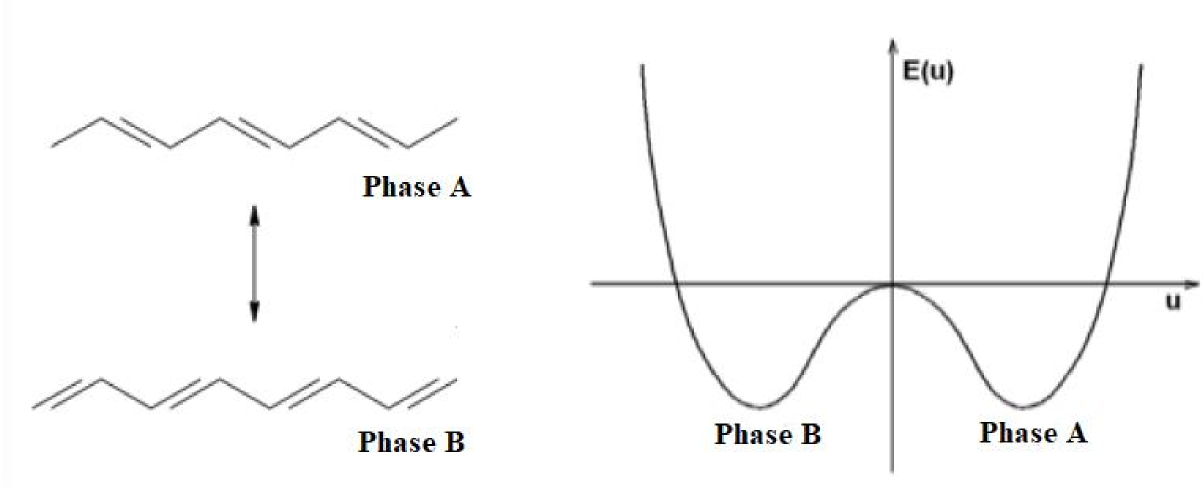

Figure 2.4: resonance phases of polyacetylene and potential energy over movement of the electron for degenerate excitation. Adapted from [46].

It is noticeable that the phase A and the phase B are spaced from a point where the energy is zero; In this transition point a soliton, a self-reinforcing solitary wave that maintains its shape while propagating at constant velocity without spin, is formed. The formation of this quasi-particle enables the positioning of a Fermi level between the HOMO and LUMO reducing the gap between the π bonding orbital and the π^* antibonding orbital.

The not degenerate is common to all the ICPs that present aromatic rings or rings with at least two double bonds on the backbone (such as polyaniline or polypyrrole).

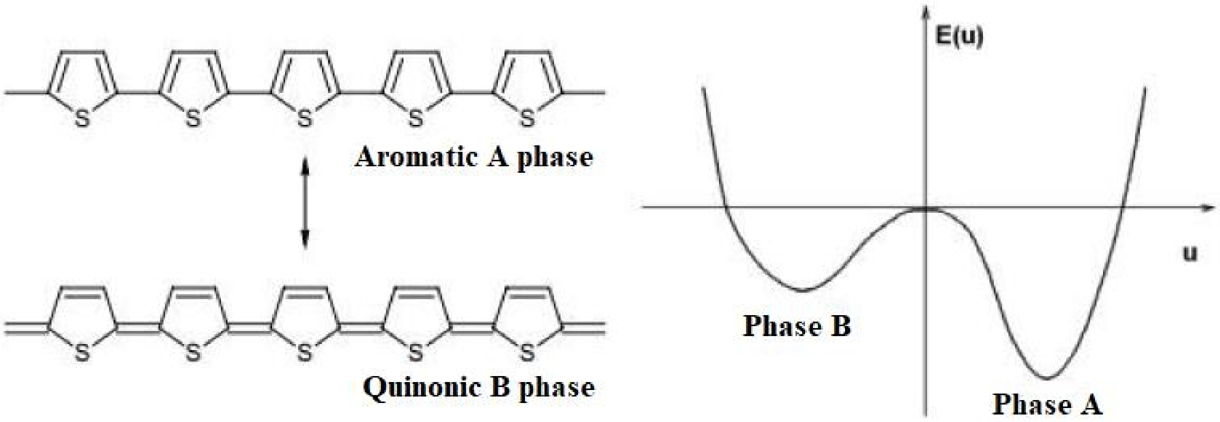

Figure 2.5: Resonance phases and potential energy over movement of the electron for not degenerate excitation. Adapted from [46].

In this case the two phases created are not isoenergetic but there is an A phase, aromatic, and a B phase, quinoic. The formation of these phases leads to the formation of multiple polaronic bands in between the HOMO and LUMO. The polarons, quasi-particles made up of an electron and a polarization field that moving on the backbone shifts the atoms from their equilibrium position in order to screen the electron, are formed when an electron is removed or added in the system deforming the polymeric crystalline lattice and generating an electromagnetic field. In some cases, a high doping of the polymer for example, a bi-polaron can be formed (a molecule containing two positive charge in a conjugated system) granting a most effective distortion of the lattice and the formation of two polarons, decreasing extremely the band gap and increasing the conduction.

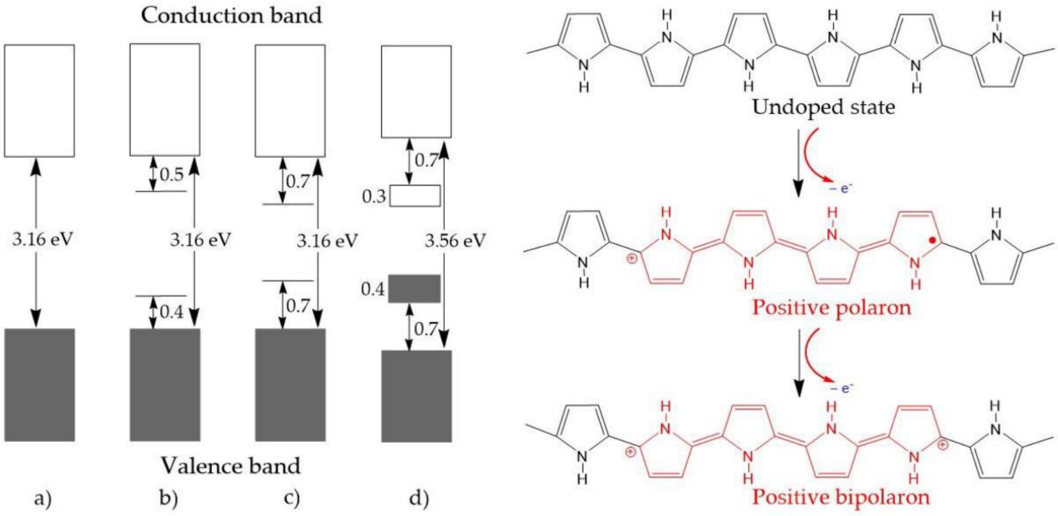

Figure 2.6: Electronic bands and chemical structure of polypyrrole illustrating (a) undoped; (b) polaron; (c) bipolaron; (d) fully doped state. Adapted from [47].

The problem with this discussion is that the presence of a crystalline polymeric lattice is theorized. Polymers, however, are always amorphous so that means that defect, such as not continuous double bonds, are always present inside of the backbone. These defects are able to introduce extra energetic levels or increase the gap between the HOMO and LUMO orbitals. Considering their presence, the conduction is not only carried out by the lowering of the band gap, but a phenomenon of tunnelling effect is needed to explain the conductivity of this class of conductive organic materials, both of for interchain defects and for conduction between different chains. The electrons are able, thus, to hop between one chain and the contiguous increasing the mobility of the charge carriers and making the material more conductive.

Another effect visible on this kind of materials is the swelling; in fact, when the molecules adsorb on the surface of the active layer it is possible that, after enough exposure time, they can diffuse through the bulk of the coated polymer occupying the intrinsic free volume. Once the analytes sit on these spots, they distort the characteristic structure of random coil, pulling away the chains one from the others. In this case all the phenomenon of tunnelling effect is avoided, and the analysis show a fall in the conductivity. An efficient prediction for the diffusion of the studied analytes can be done by the second law of Fick; a resolved version of the mentioned constituent equation (considering the appropriates boundary conditions) is reported below:

$$\frac{C_x - C_0}{C_s - C_0} = 1 - \mathrm{erf}\left(\frac{x}{2\sqrt{Dt}}\right) \qquad (2.5)$$

Where C_x is the concentration on the considered point x of the bulk, C_0 the concentration on the bulk of the active layer, C_s the concentration of the surface, D is the diffusion coefficient and t the time.

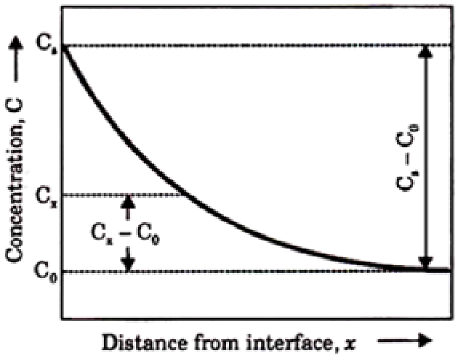

Figure 2.7: Second law of Fick resolved, Concentration over the distance from the interface. Adapted from [46].

2.4. Doping

Pure organic semiconductors are a class of materials that show good values of conductivity and electron mobility if compared to other polymers, such as polyethylene. Nevertheless, the intrinsic conductivity of these materials would not suit with the application they are thought for, essentially because of the leak of charge carriers. In order to increase the conductivity extra charge carriers need to be added, modifying the molecule; This is called primary doping. One example can be the polyacetylene before and after the doping with I_2; the initial conductivity is on the order of magnitude of $10^{-9}\Omega^{-1}\text{cm}^{-1}$ while after the doping it is around $200\ \Omega^{-1}\text{cm}^{-1}$ [48]. In general, however, the conductivity arises from values in a range of $10^{-15} - 10^{-5}\Omega^{-1}\text{cm}^{-1}$ till values that can reach $10^{3}\Omega^{-1}\text{cm}^{-1}$.

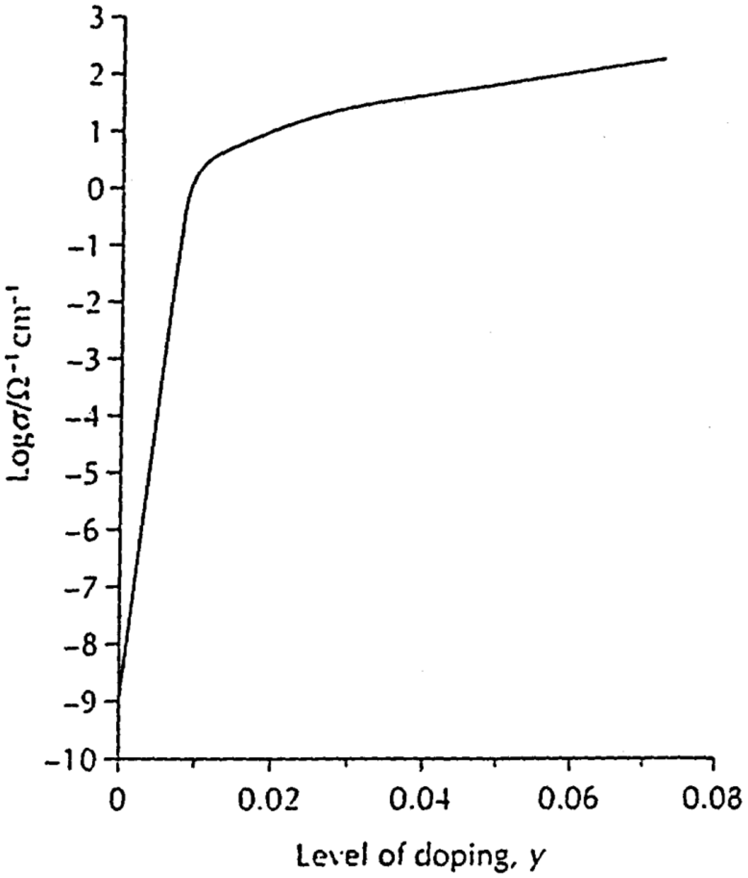

Figure 2.8: Increasement of conductivity over the level of doping for polyacetylene. Adapted from [42].

In fact, most of the time is the doping itself that, distorting the organic crystalline lattice is able to favourite the formation of polarons and bi-polarons. There are several methods to carry out the doping of the macromolecule:

1. Chemical and/or electrochemical doping: the dopant compounds are added during the polymerization and then the electrical conductivity or the electrochemical potential are controlled. It leads to a permanent induced electrical conductivity.
2. Photo-doping: the polymers, during the application, is irradiated by a beam of light that promote the hop of the charge carrier to the LUMO orbital. It leads to a transient electrical conductivity.
3. Charge injection: electrons are injected in the polymer backbone only as long as the biasing voltage is applied. It leads to a transient electrical conductivity.

A summary of the doping methods and the application for each technology are reported on figure 2.9.

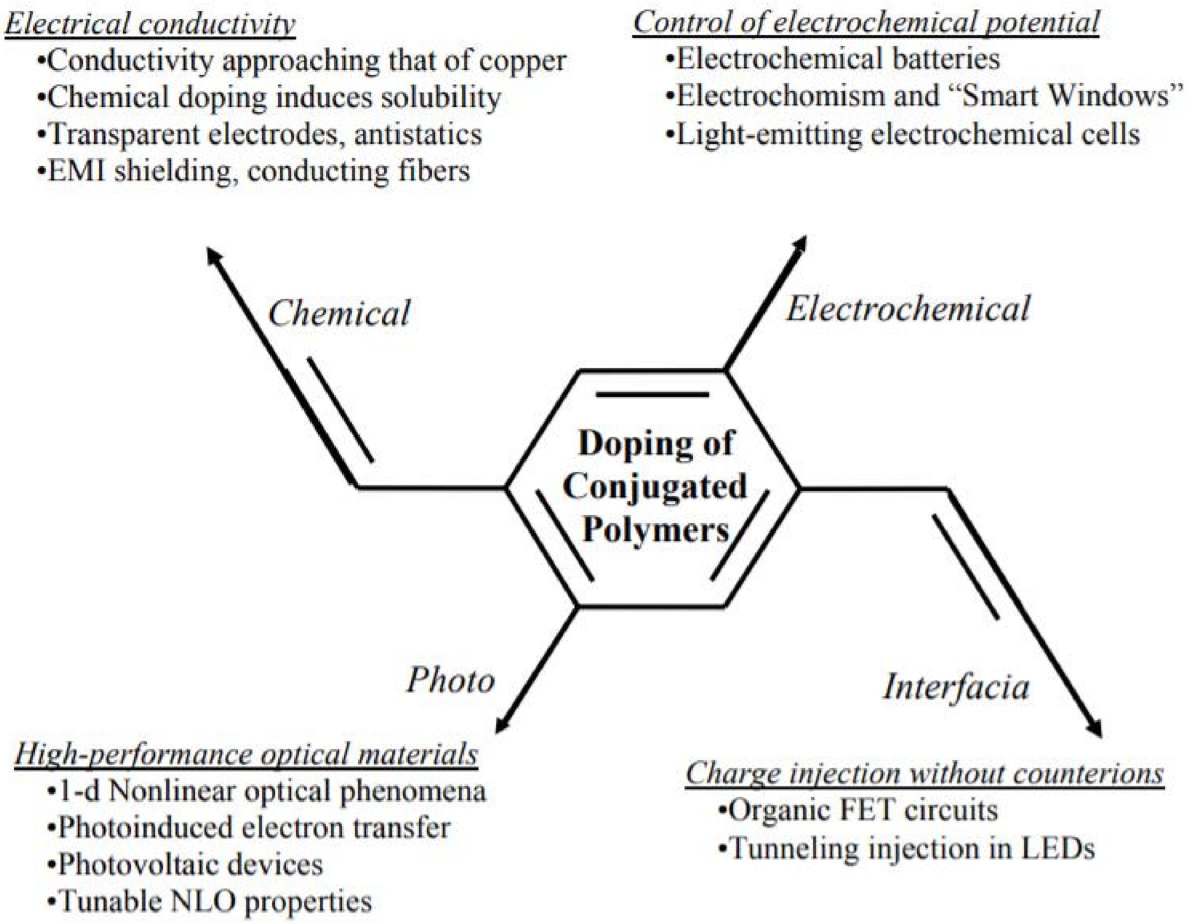

Figure 2.9: Doping methods and applications on conjugated polymers. Adapted from [46].

In this work, only chemical doping was performed; the reason is due to the more suitable and effective procedure of this technique compared to the others, in particular because of the permanent increasement od conductivity.

Doping can also be classified in two categories, based on what kind of charge carrier is added to the system:

1. n-type doping; the dopant compound in this case is able to add extra negative charge carriers, such as electrons, to the material.

   $$CP + ne^- \rightarrow (C^+)_n \, CP^{n-} \tag{2.6}$$

   Where for CP is indicated the conductive polymer, e are the electrons and C is the counter-cation associated to the negative charged macromolecule.

2. p-type doping; The dopant compound is able to add extra positive charge carriers, such as holes, to the material.

   $$CP \rightarrow CP^{n+}(A^-)_n + ne^- \tag{2.7}$$

Where for CP is indicated the conductive polymer, e are the electrons and A is the counter-anion associated to the positive charged macromolecule.

This universal definition can be adapted to organic materials considering the HOMO and LUMO orbitals. From an energetic point of view, n-type doping consists in adding a chemical species whose HOMO energy level is higher than the LUMO energetic level of the undoped polymer. By contrast, p-type doping consists in adding a molecule that, dissociating, has a LUMO energetic level lower than the equivalent HOMO on the organic material. Both techniques, increasing the charge carrier's density, add extra energetic levels on the gap between the HOMO and LUMO of the polymeric material considered, facilitating the movement of the charge carrier responsible of the conduction.

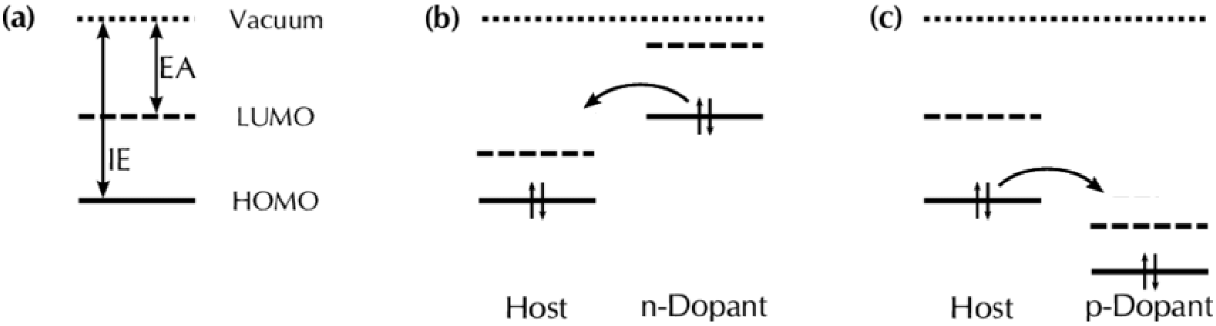

Figure 2.10: energetic levels and working principle if n-type and p-type polymers. Adapted from [49].

Examples of p-dopant could be all the chemicals species that can handle the extraction of electron from the polymeric chain; fluorine-based dopants are one of the categories mostly used, such as tetrafluoro-tetracyanoquinodimethane. Strong acid compounds, such as HCl, can also be employed according to the extremely powerful redox reaction occurring in their presence. Examples of n-type dopant are di-metal complexes of chromium or tungsten with the anion of 1,3,4,6,7,8-hexahydro-2H-pyrimido[1,2-a] pyrimidine [49]. As these compounds easily oxidize in air, thanks to the presence of oxygen, they have to be handled in an inert gas atmosphere or vacuum. Furthermore, finding a n-type dopant that is able to reduce significantly the gap between the HOMO of the dopant molecule and the LUMO of the organic material and able to resist to oxidation, is extremely complicated and that is the reason why n-type doped materials are usually considered not stable [52].

For this reason, all the polymer studied and analysed in this work are p-type doped material.

Once the polymer is doped the variation on resistance registered by the device is highly dependent on the adsorbed odorous molecule. In fact, if an extra hole is added (p-type doping) and the selected VOC for testing is an oxidizer, the adsorbed specie is able to withdraw electrons, increasing the number of holes and increasing the conductivity; In this case the e-nose will reveal a reduction of resistance. By contrast, if the VOC tested is a reducer it donates electrons to the macromolecule, decrease the conductivity and registering a step up on the resistance measurements. N-type doped polymers react oppositely so that oxidizer and reducers VOCs are able to increase and decrease the resistance, respectively. This behaviour, called secondary doping, is caused by redox reactions that occur on the surface of the material, even at room temperature.

It is important to understand, anyway, that the reactive mechanism and the variation on resistance are not still well known (due to the numerous conductive principles cooperating together) and the expected behaviour of the device can change strongly from the prediction; supporting this statement studies testing ammonia on a p-type doped e-nose showed a reduction of resistance, even though ammonia should react as an electron donor [41].

2.5. Polyaniline

Polyaniline is an amine-based conductive polymer that has been studied extensively for gas senses technologies. The reason of this interest falls on its outstanding properties, perfectly suitable for the e-nose sensing technologies.

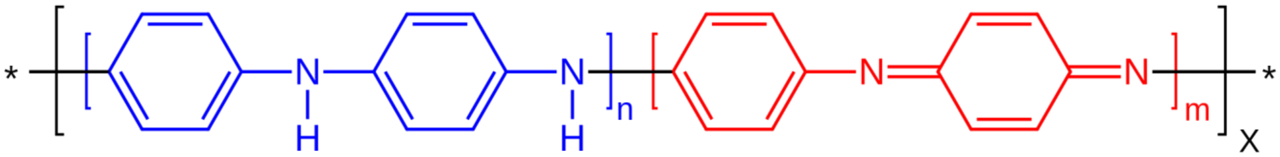

Figure 2.11: polyaniline pristine structure. In the image are expressed the benzenoid group (blue) and the quinoid (red).

The polymer shows high electroactivity, high resistance to corrosion, high doping level, excellent thermal stability and a high specific capacitance (400–500 F g−1 in an acidic medium). In addition, it has good environmental stability, controllable electrical conductivity (around 0.1 S cm−1 in the doped state with a Li dopant but can range from around 0.1 to 5 S cm−1) and can be easily processed [53]. The conductivity mentioned can be reached by a p-type doping in order to protonate the macromolecule: generally, a really acid solution is used, such as HCl, in order to add extra holes on the polymer chain. The process is controlled operating on the pH of the solution, adding different quantities of dopant. By contrast, polyaniline (PAni) exhibits poor physical and mechanical properties [54].

The general structure of the polymer, called pristine, shows two different structural units randomly placed within the backbone; One of the two units shows a quinoic group and the other a benzenoid group.

The polymerization starts from the aniline monomer and PAni presents different and distinct oxidation forms such as fully reduced leucoemeraldine base (LEB), the half oxidized emeraldine base (EB) and the fully oxidized pernigraniline base (PNB); every type of polyaniline present different physio-chemical property but just the EB shows a good electrical conductivity.

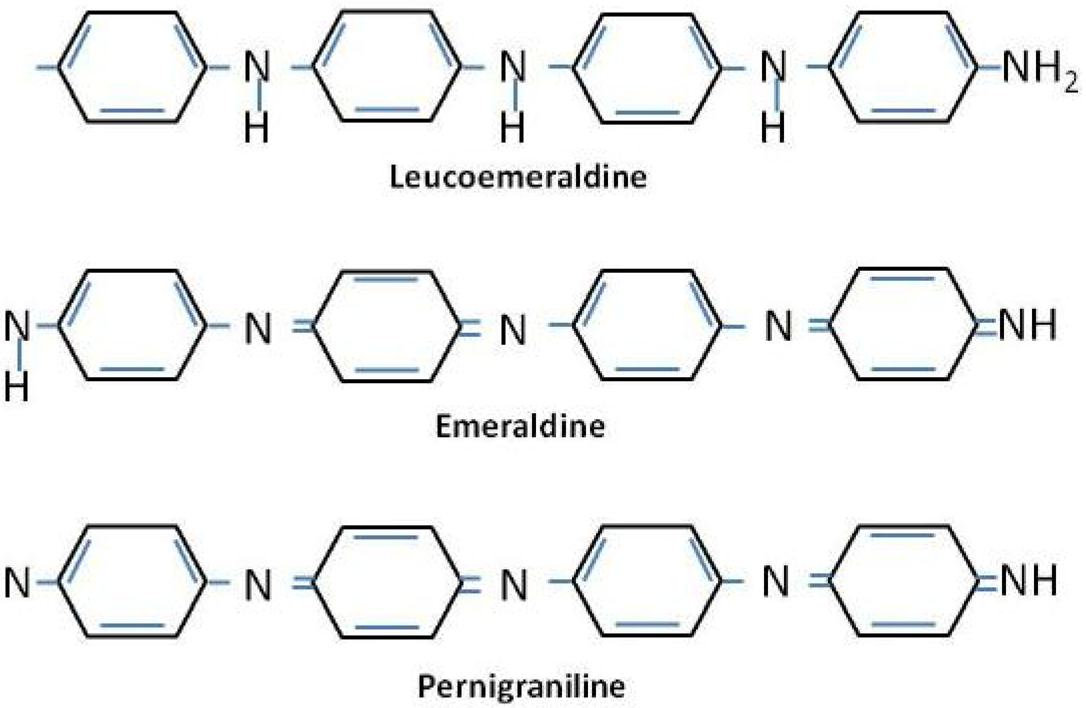

Figure 2.12: Different structures of polyaniline. Adapted from [55]

Although the oxidized emeraldine base, obtained starting from the aniline monomer and an oxidant, has a substantial good electrical conductivity a following step of doping is needed to achieve a conductivity in the order of magnitude of 1 S cm−1. The doping, normally carried out with aqueous protonic or functionalized acids, causes proton to be added to the -N= sites introducing energetic states within the forbidden gap; the material obtained is, therefore, a p-type doped polymer also called emeraldine salt (ES). Nevertheless, acid solution are not the only species able to dope PAni; for example, a doping with diphenyl H-phosphonate (DPPH) was carried out leading to a conductivity of 0.23 S cm−1 [56].

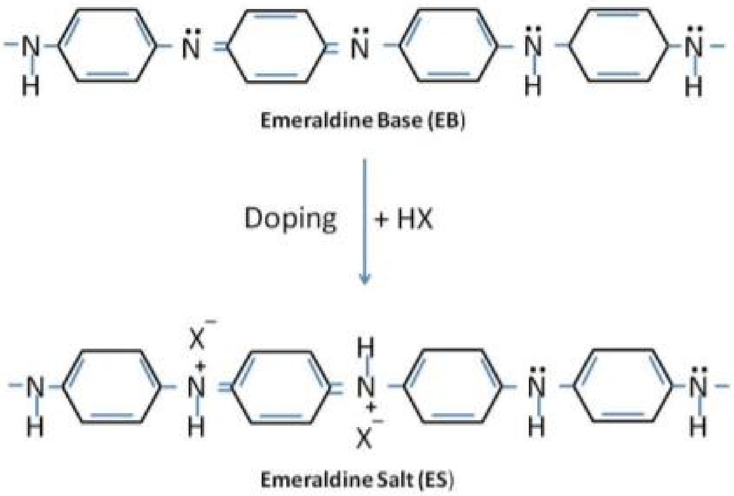

Figure 2.13: Doping process of the emeraldine base PAni. Adapted from [55]

Protonated PAni or emeraldine salt is conductive when a ratio of 3:1 between Benzenoid and Quinoid is achieved. This kind of configuration cannot be obtained with LEB and PNB and that's the reason why, even after doping with an acid, they present a low conductivity [55].

Not just the conductivity is important in gas sensing, another parameter that can enhance the response and the sensitivity toward different analytes is the surface-to-volume ratio. In fact, the odorous molecules need to adsorb on the surface of the active layer, the polyaniline coating in this case, and it is clear that the wider is the surface exposed the bigger will be the resistance variation, granting numerous adsorption sites. The aim is to create PAni nanofibers with the minimum diameter and the maximum length achievable. The ratio is generally optimized operating on the pH and the deposition time [57].

2.6. Polypyrrole

Polypyrrole (PPy) is an example of heterocyclic conductive polymer consisting in a long chain of pyrrole, a cyclic, aromatic and planar molecule. is especially promising for commercial applications because of its good environmental stability, facile synthesis, and higher conductivity.

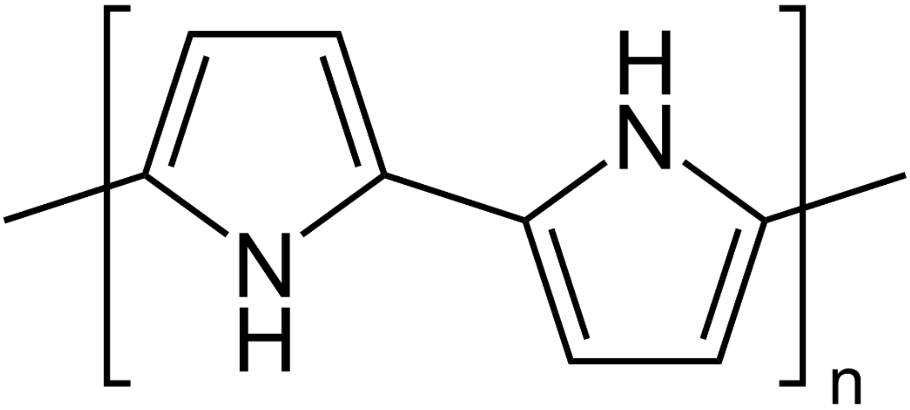

Figure 2.14: Polypirrole structural unit.

In fact, as the conductivity of the pure conducting polymer is rather low, in order to achieve the high conductivity suitable for sensing applications, a doping process is necessary. The typical conductivity of polypyrrole prepared by the oxidation of pyrrole with iron salts is 10^{-2} S cm^{-1}. When the polypyrrole was prepared in the presence of surfactants, the conductivity was higher by about two orders of magnitude and reached 3.1 S cm^{-1} for sodium dodecylbenzenesulfonate and 42 S cm^{-1} in the presence of sodium *n*-alkylnaphthalenesulfonate [58]. Even a simple doping with HCl can lead to an increment of conductivity suitable for gas sensing; The acid solution, thus, is able to attack the aromatic ring extracting electrons, creating a p-type conductive polymer. Electrical and mechanical properties of the polypyrrole depend heavily on the counter-ion used so that on the dopant. For instance, using perchlorate instead of oxalate can increase its conductivity by 10 times [59].

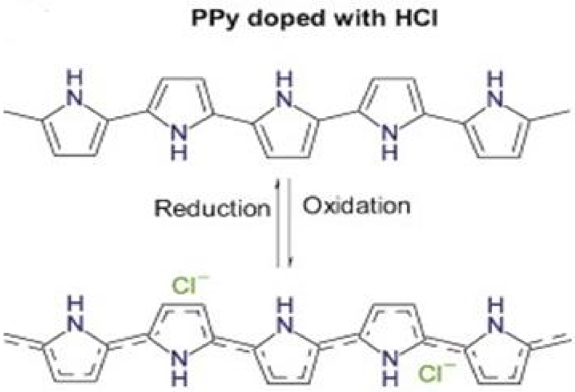

Figure 2.15: Doping/de-doping of polypyrrole achieved with HCl. Adapted from [59].

As much as the polyaniline case, also for polypyrrole an optimal surface-to-volume ratio can increase the sensitivity. Unlike the polyaniline, in this case getting polypyrrole nanofibers is rather difficult. The general conformation of PPy is globular but several studies have been carried out in order to achieve polypyrrole fibers. Skodovà et al. on 2013 found a way to obtain polypyrrole nanotubes when the polymer is prepared in presence of a dye, such as methyl orange [60].

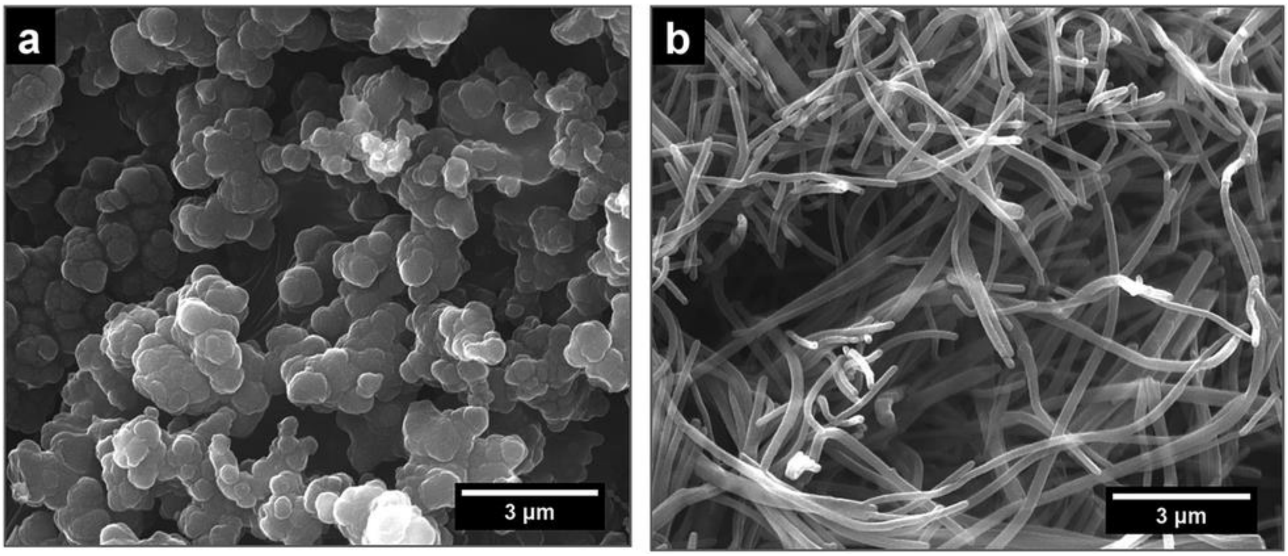

Figure 2.16: Globular polypirrole (a) and PPy nanotubes (b) images captured on SEM. Adapted from [58].

2.7. PEDOT:PSS

Differently to the other organic materials considered, PEDOT:PSS is not a simple polymer but rather a blend of two polymers combined together, Poly(3,4-ethylenedioxythiophene) (PEDOT) and Polystyrene sulfonate (PSS). PEDOT is a polymer based on polythiophene, an organic material that present a descent on conductivity after long periods, mining its application on gas sensing. Nevertheless, the stability can be increased lowering its oxidation potential by the addition of an electron-donor group, such as an alkoxy ring.

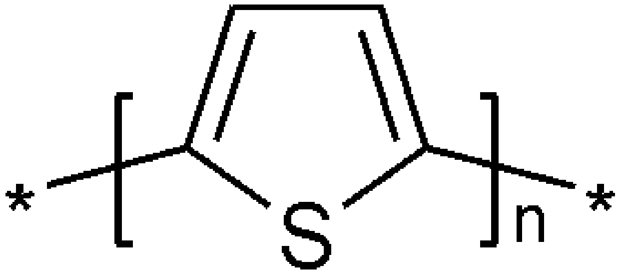

Figure 2.17: Polythiophene structural unit.

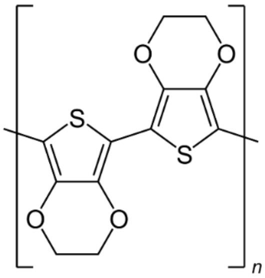

Figure 2.18: PEDOT structural unit.

Pure PEDOT is, however, insoluble in any media and need a counter-ion in order to create a conductive salt. PSS, a synthetic aromatic hydrocarbon deprotonated with a molecule of sulfonate which makes the macromolecule negatively charged, is one of the widely used counter-ions. The following doping of PEDOT, thanks to the reactions with PSS, is carried out to extract an electron from the sulphur leading to the creation of weak polar bonds between the two compounds.

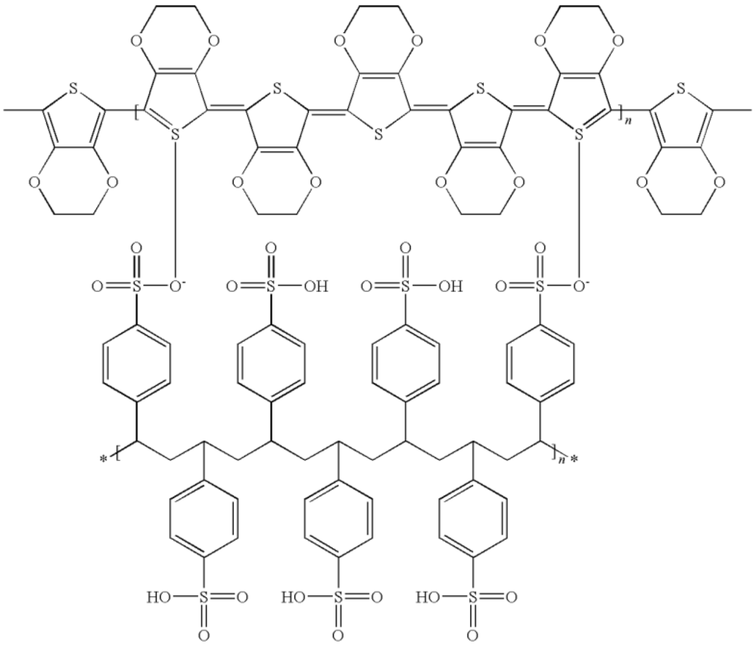

Figure 2.18: PEDOT:PSS structure; the polar bonds between the molecules are reported in the figure. Adapted from [61].

Generally, the doping is realized in excess of PSS; More in details the molar ratio between the thiophen group and the sulfonic acid variate between 1:1,9 to 1:15,2, corresponding a variation from 6 to 46 times more of PSS in the solution [61].

Similarly, to polypyrrole, nanofibers of PEDOT:PSS are extremely difficult to obtain and, generally, the only result achievable is a homogeneous film.

However, PEDOT:PSS shows the best conductivity between all the other polymers treated in this work thanks to the high number of charge carriers formed on the backbone. Saghaei et al. discovered a level of conductivity of 930 S/cm-1 when the polymer is treated with 2-Methylimidazole in order to keep the optical transparency loosed in the polymerization [62]. In addition, the polymer shows a thermic stability up to 200°C (at higher temperature the evaporation of PSS begins), high flexibility, easy synthesis and low cost.

CHAPTER 3

EXPERIMENTAL SET-UP

The aforesaid work is a joint venture project carried out from several years between the Turin Politecnico DISAT department and the IBM Almaden Research center. The device fabrication is explained in this section, trying to give a general idea of how the sensor is made, starting from the synthesis of the treated polymers, the coating and the measurements of the performances.

3.1. Synthesis

The first step is the synthesis of the three different polymers. In the following paragraphs just the preparation of polyaniline and polypyrrole are reported becouse PEDOT:PSS was made before of the arrival at the research center of the author of this thesis. The synthesis of this class of organic material is pretty easy and employ just the monomer, an oxidizer and eventually a co-oxidizer and the dopant.

The samples are named by: the shortened name of the polymer (e.g. PAni, PPy or PEDOT:PSS) followed by the initials of the person who made it (e.g. T.E. or M.Z.) and the book (I or II) and the page in the book where the synthesis parameters are. One example can be PAni TE-I-70.

3.1.1. Polyaniline

The synthesis of the polymer employs:

- The monomer: Aniline
- The oxidizer: Ammonium persulfate (APS) or other oxidizers
- An eventual co-oxidizer: Sodium hypochlorite (NaOCl)
- The dopant: HCl

More in details four samples are subsequently reported and studied on the results chapter. The samples are PAni TE-I-70, PAni TE-II-5, PAni TE-II-10 and PAni TE-II-16.

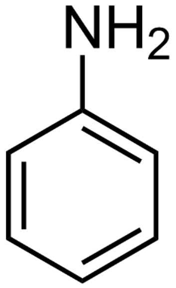

Figure 3.1: Aniline monomer.

PAni TE-I-70 was coated with two different solution, one from cell 1 to 4 and the other on cell 5 to 8. On the first 4 cells and also later on PAni TE-II-5, the synthesis of the solution started from a glass vial charged with 102 mg (1.10 mmol, 1.0 eq.) of aniline and dissolved on 11 ml of 1M HCl. Then to solubilize the oxidizer, 0.274 mmol and 0.25 eq. of a persulfate-based oxidizer was added to 1 ml of 1M of HCl. Under stirring, the oxidizer solution and the co-oxidizer NaOCl (1 ml of an aqueous solution of NaOCl with 6% of active chlorine) were added to the initial vial after 1 hour. After 30 minutes of reaction, the mixture was centrifuged at 20'000 rpm for 5 minutes, the supernatant removed, and the precipitates washed with ultrapure water. This procedure is repeated three times and then the stable solution is stored. From cell 5 to 8 the solution was synthesised at the same way with the same amount of monomer, dopant and co-oxidizer. The difference is in the addition of the ingredients; In this case they were added simultaneously and, subsequently, the stirring stopped. The reaction in this case was carried out over 1 hour and then washed at the same way as the first 4 cells.

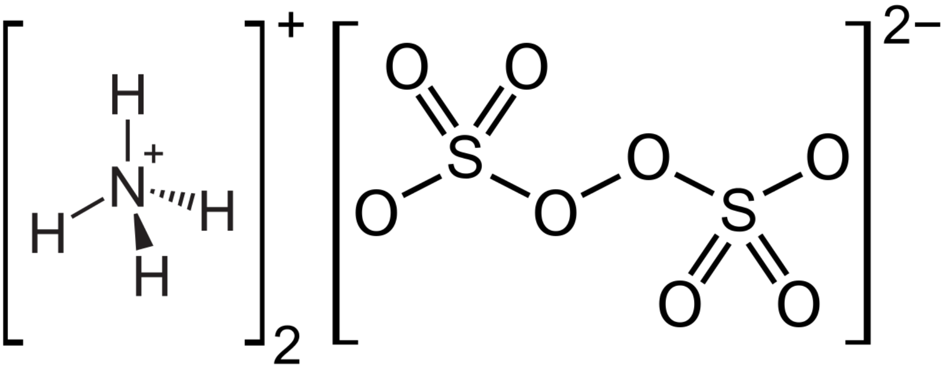

Figure 3.2: Ammonium persulfate oxidant (APS).

TE-II-10 cells 1 to 4, was prepared starting from a vial where 102 mg (1.10 mmol, 1.0 eq.) of aniline monomer and dissolved on 11 ml of 1M of HCl were mixed. After adding a solution of persulfate-based oxidizer (1.10 mmol, 1.0 eq.) in 1.5 ml of 1M of HCl the total solution was stirred for few seconds (20 seconds) and stopped. After 40 min of reaction, the supernatant was removed, and the solution centrifuged at 20'000 rpm for 5 minutes. Again, this procedure was repeated three times and the stable solution stored. The rest of the 4 cells were prepared with the same procedure but 125 mg (0.51 mmol, 0.5 eq.) of APS was used as oxidizer.

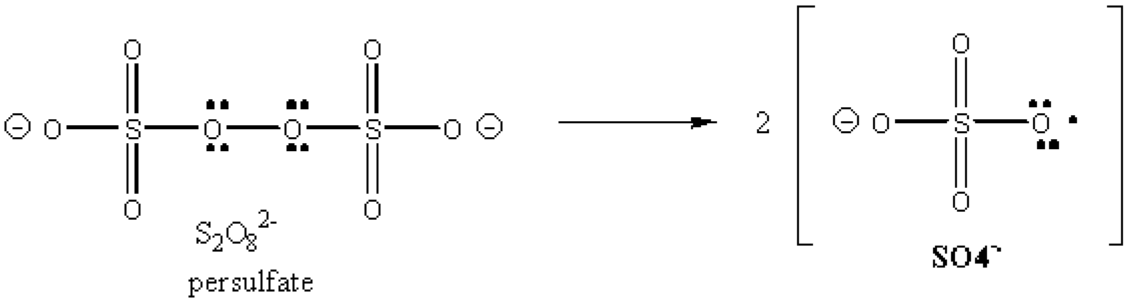

Figure 3.3: Dissociation of the APS oxidant in two radicals. Adapted from http://tutaba16.soup.io/post/389854667/none

The last sample, TE-II-16, was also coated with two different solution from cells 1 to 4 and cells 5 to 8. The only different between the two solutions coated was the stirring, stopped right after the reaction on cells 1 to 4 and carried out over the all-time of reaction for cells 5 to 8. A solution of 28 mg (0.30 mmol, 1.0 eq.) of aniline monomer was added on 3 ml of 1M of HCl and mixed with a solution of 34 mg of APS (0.15 mmol, 0.5 eq.) and 1 ml of 1M HCl. At the same time 3 ml of 10 nm gold nanoparticles were added during the polymerization. The gold nanoparticles, bought from BBI Solutions, are dispersed inside an aqueous solution with a concentration of 5.70×〖10〗^12 particles/ml. Both of the reactions were carried out during 55 min.

Figure 3.4: Live polymerization of polyaniline at different time. It can be noticed that just after 50 seconds the colour of the solution is already green.

An important factor to understand the right evolution of the polymerization is the solution colour. The conductive polymers studied in this thesis present all a typical colour purple or dark green. The reason of this colour stays on the energy gap between HOMO and LUMO; Generally, for a single bond this energy gap is pretty large, and the energy needed for the electron to jump in the more energetic orbital fall in the UV spectrum. If double bonds or benzenic group are present in the molecule the energy gap gradually decrease, falling into the visible spectrum. All the three conductive polymers considered in this thesis have a large number of benzenic groups, so the energy required by the electrons fall in the green or purple zone of the visible spectrum.

3.1.2. Polypyrrole

In the case of polypyrrole the procedure followed is the same as polyaniline. Also, the chemical species used are the same, except for the monomer, pyrrole. The reaction is initiated by the oxidation of monomer into radical cations, which combine to form dimers. Continuation of the process leads to formation of insoluble oligomers in solution, which deposit on the bottom of the vial. Due to low oxidation potential of pyrrole, a wide range of oxidizing agents can be used to initiate polymerization. Oxidant salts such as ferric chloride (FeCl3) function as both the oxidant and the dopant agent, and hence the polymer is obtained in the conducting form [63]. In this case HCl was used as dopant and APS as oxidizer.

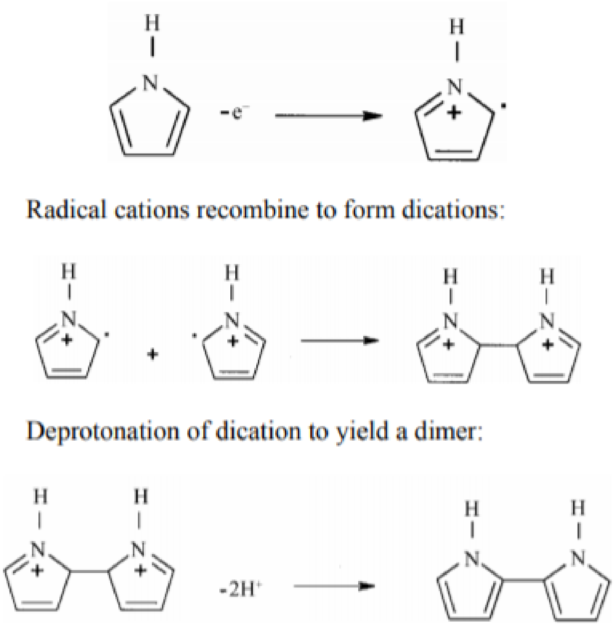

Figure 3.5: Polymerization of pyrrole. Adapted from [63].

Two sample are reported on the final chaper, PPy TE-II-20 and PPy TE-II-24. TE-II-20 was prepared staring from 55 mg (0.82 mmol, 1.0 eq.) of pyrrole monomer and dissolved on 8 ml of ultrapure water, used as solvent in this case. Under stirring, a solution of 211 mg (0.93 mmol, 1.13 eq.) of APS on 4.4 ml ultrapure water was added rapidly. After 30 min the reaction mixture was centrifuged at 4400 rpm for 5 minutes, the supernatant removed and the precipitates washed with ultrapure water. The procedure was repeated three times and the stable solution was stored. In this case, APS worked both as oxidizer and dopant. For TE-II-24 the only difference was the solvent used, 4.4 ml of 1M HCl.

3.2. Sensor platform

The sensor platforms, equipped with gold electrodes, is a delicate procedure involving several steps consisting essentially on cleaning, thermal evaporation and electron beam lithography. The all fabrication is usually carried out by the material team in at IBM Almaden Research center. The platform consists in a silicon wafer with a electrodes system. The geometry of the electrodes presents various gold plates (2 cm x 3 cm) connected by gold canals; The sides plates are the input, where the higher voltage is applied by a conductive cable, while the central two plates are the output or the grounded plates. Between these couple of plates are visible other smaller discontinuous plates; The gap is the space where the conductive polymer active layer will be placed. An array of 8 sensors is therefore created for each device.

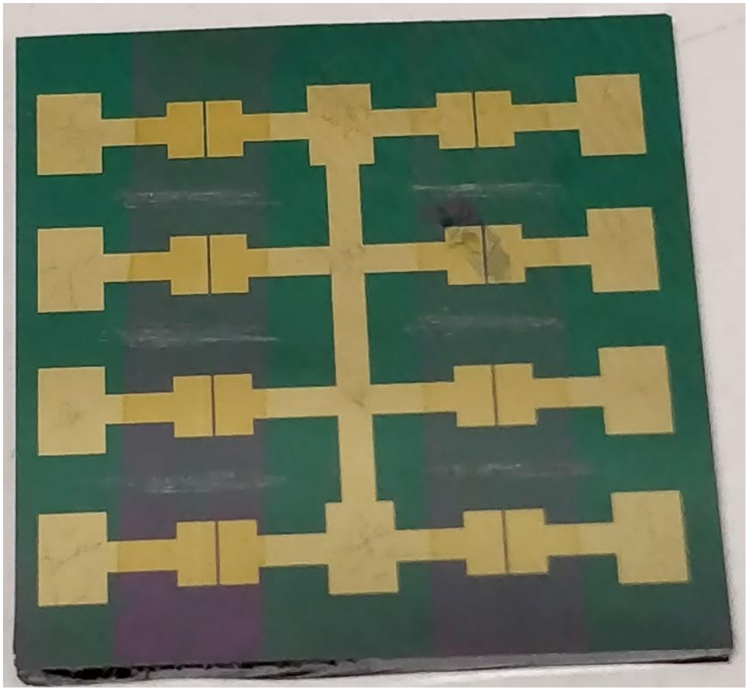

Figure 3.6: Sensor platform

To proceed to the electron beam lithography a first step of oxygen plasma cleaning is performed to remove completely every trace of organic residues from the previous processes and to avoid eventually any contamination. The electron beam lithography is a technique where, upon the exposure of an electron beam, the ray is carefully scanned on the surface only in a specific areas depolymerizing/polymerizing the resist previously coated on the surface of the wafer; the precision can be imputable to the precision of the machine (using a CAD pattern specifically drawn) or to a mask that is able to screen the electron beam. There are two types of electron beam lithography, negative and positive. In the positive technique the resist is a polymer and the ray are able to depolymerize the invested zone, degrading and making soluble the macromolecule that is lately remove by a solvent. In negative electron beam lithography, instead, the resist is a monomer and the ray give the necessary energy to start the polymerization; the remaining monomer is lately, at the same way, removed by an appropriate solvent.

The first step after the plasma cleaning is, therefore, the resist coating of the silicon wafer. Because of the existing silanols on the wafer surface, hydrogen bonding with the atmospheric water vapour is really easy to happen, making difficult the adhesion of the resist. An intermediate step of dehydrating in a oven at 150°C for 20 minutes is then performed. The same silanols are lately used to improve the adhesion of the resist on the silica layer spraying previously pure hexamethyldisilizane (HMDS); this molecule breaks the nitrogen bond in the middle creating two $Si(CH_3)_3$ molecules bonding with the oxygen of the silanols, exposing the favourable methyl group, and releasing ammonia.

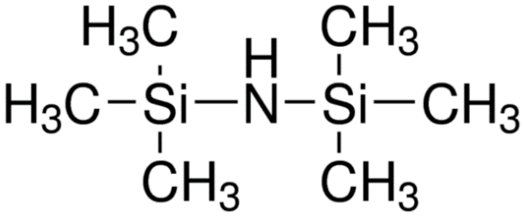

Figure 3.7: Hexamethyldisilazane molecule.

Subsequently the resist, called KRS and developed on IBM laboratories, is spin coated at 1500 rpm for 60 second and lately baked to dry the solvent where the resist is solubilized.

The next step is the electron beam lithography where the resist is depolymerized selectively and washed with an alkaline solution of tetramethylammonium hydroxide (TMAH) for 60 seconds. A security following step of oxygen plasma cleaning is performed to assure the removal of the spare resist.

After that the metal is deposited on the resist/no resist surface, sublimating the electrode material (Gold in this thesis) in a custom-made electron beam evaporation room and making it deposit lately on the resist layer; the thickness achieved and controlled leads to a 60 nm layer approximatively.

The last step is the lift off, where all the resist is removed by baths of N-Methyl-2-pyrrolidone at different temperatures (including the resist coated with the gold layer, recycled in a second moment) leaving just the initially designed electrodes geometry.

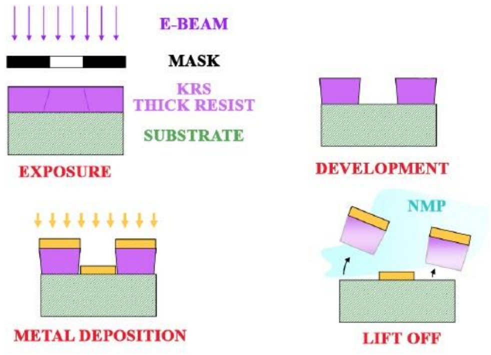

Figure 3.8: Electron beam lithography main steps. Adapted from [50].

3.3. Coating

Different coating technique have been tried in this thesis work in order to obtain the thinner and more homogeneous film possible. It has been seen that the coating step is highly dependent on the material selected for the procedure and on its wettability. The issue with the wettability is imputable to the fact that the solution coated (polymer + solvent, generally water) can spread excessively on the platform if the property is too high, not covering the gaps homogeneously; This characteristic is important because a not homogeneous film can lead to zone with a really low or void conductivity. This behaviour has been seen in the case of blade-coated polypyrrole and polyaniline; The reason has to be searched into the really polar ammine group that, reacting with the silanols groups by hydrogen bonding of the silicon wafer, make the aqueous solution spread extensively. The solution was to drop-cast the solution directly on the electrode's gaps, losing the thinner film achieved with the previous technique. To prove the above-mentioned behaviour, it was seen that the wettability was increasing after an oxygen plasma cleaning on the silicon wafer (cause of the creation of more polar group on the surface) and the spread wasn't occurring on PEDOT:PSS, where the ammine group is not present. Spray coating was also performed to achieve a thin film but, again, the wettability was too high in the two ammine-based polymers.

3.3.1. Drop-casting

Drop casting is a basic and low-cost method for the production of a inter-gap film. This technique remembers the spin coating process with the difference that the spinning of the substrate is not required. The film thickness in this case highly depend on the volume of the dispersion and the concentration of the macromolecules on the solvent. Other parameters noteworthy are the substrate wettability, the rate of evaporation of the solvent and the drying process. In fact, volatile solvents are generally preferred cause of the faster evaporation rate. The major advantage of this technique, compared to spin coating, is the absence of material wastage. On the other hand, a defect is the difficulty in controlling the film thickness.

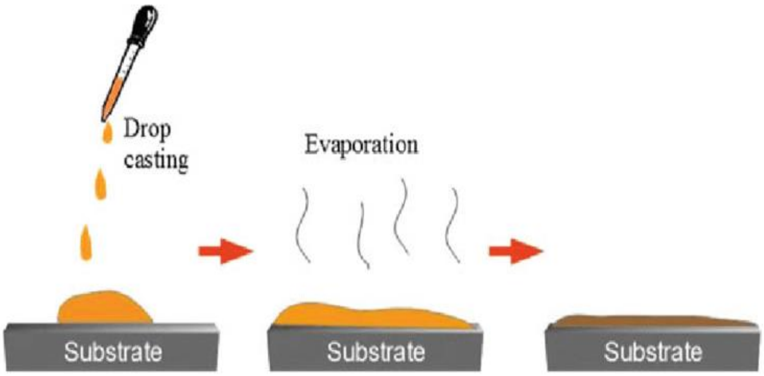

Figure 3.9: drop-casting main stages. Adapted from [64].

In this work the starting material is the polymer (PAni and PPy only) fining disperse in an aqueous solution. At this point the solution is draw into a precision syringe; lately 0.7 µl of solution are drop-casted directly on the electrode gaps being careful to not let the droplet spread on the silicon wafer. The coated device is then let rest overnight in order to make the water evaporate.

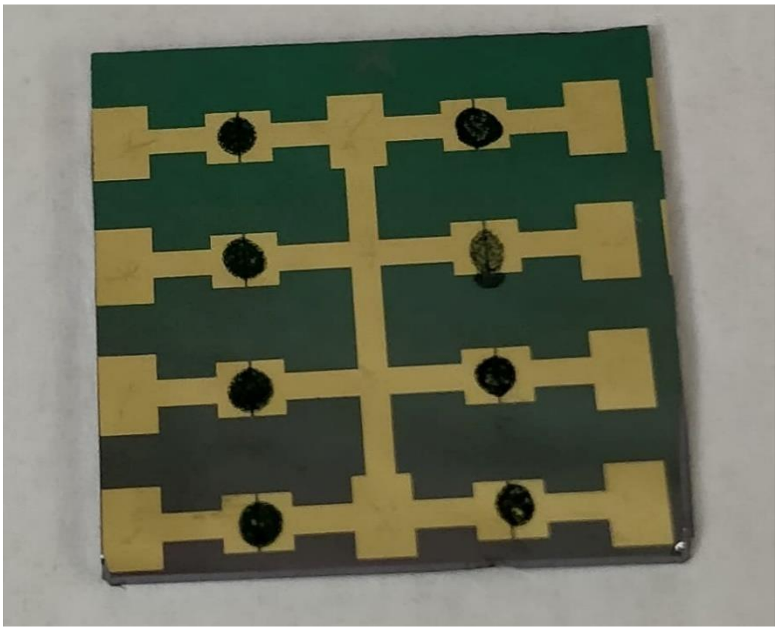

Figure 3.10: Drop-casted sensor platform

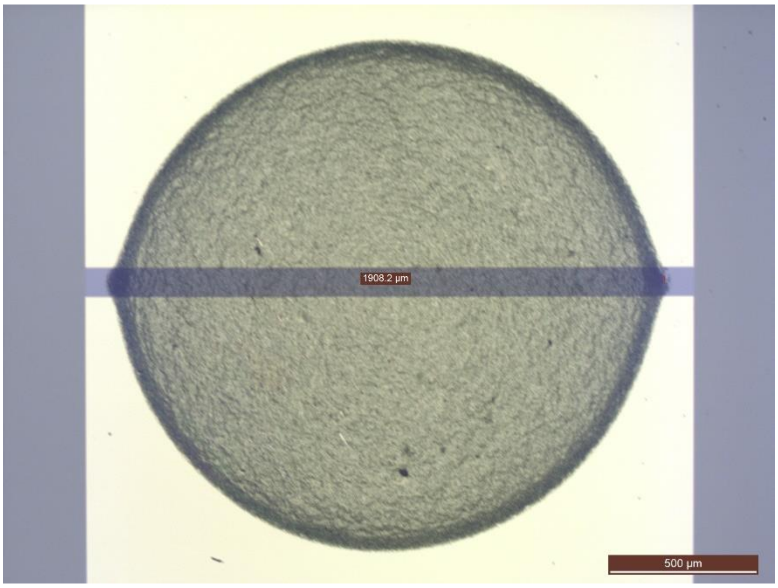

Figure 3.11: Droplet zoom-in image

3.3.2. Blade coating

Blade coating is a popular technique to generate thin (5-200 nm) films of active layers. In this coating procedure a reservoir of the solution chosen to be deposit is placed between a quasi-horizontal blade and a horizontal support in a way which a space between the two surfaces is granted; the reservoir is generally able to wet the surface of the materials and get trapped between the two interfaces. The blade is designed to be able to move in one direction and the solution is forced to follow it. During the movement a certain part of the coating fluid leaves the reservoir, wetting the surface of the substrate and spreading to create a thin solution layer. Finally, giving the time to the solvent to evaporate (volatile solvents are, thus, preferred) or baking the product, the final device is achieved. A useful scheme of the technique is shown on Figure 3.13.

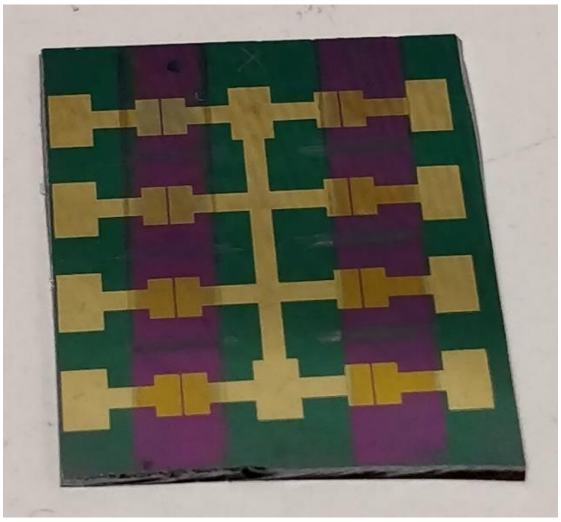

Figure 3.12: blade-casted sensor platform

There are several adjustable mechanical parameters to control the process. The custom-made machine owned by IBM Almaden Research Center is equipped by a “mechanical arm” with different turning dials responsible for various parameters. Turning one dial, the perpendicular direction then on the coating direction can be adjusted; another dial is the lever in charge to optimize the gap between the blade and the substrate. The last parameters, controlled by a computer, is the velocity of movement of the blade because the angle of the blade is not regulable. Furthermore, various blade with different blade-width are available.

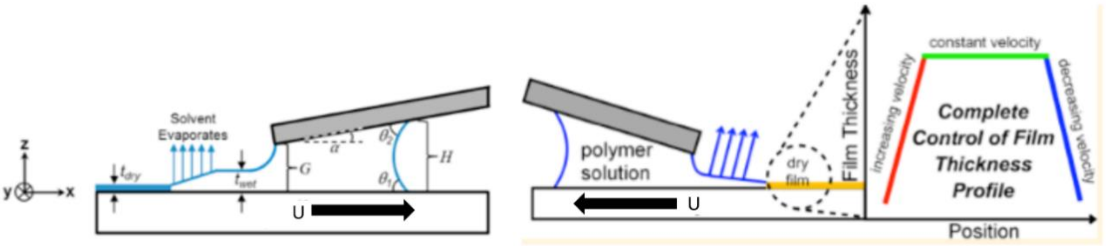

Figure 3.13: Blade coating scheme with parameters indicated. Adapted from [65].

The blade coating in this work is just performed for the solution PEDOT:PSS-water because, as already said, the two other polymers possess a too high wettability. A 2.5 µl of solution is placed on the gap with a precision syringe so that the droplet is able to flow in the inter-surfaces space. The gap between the surfaces was variated in a range between 3 to 10 µm and the velocity between 3000 to 30000 cm/min. As it can be seen on Figure 3.13 the velocity is an important parameter to characterize the film thickness profile; In fact, contrarily on what it can be thought, increasing the velocity does not lead always to a thicker film but the behaviour is more suitable with a trapezoidal profile [65]. With the polymer and the velocities considered in this thesis, a decrease on velocity was leading to a thinner film; in particular a velocity of 3000 showed a PEDOT:PSS film of around 20 nm while a velocity of 30000 leaded to a thickness of 150 nm.

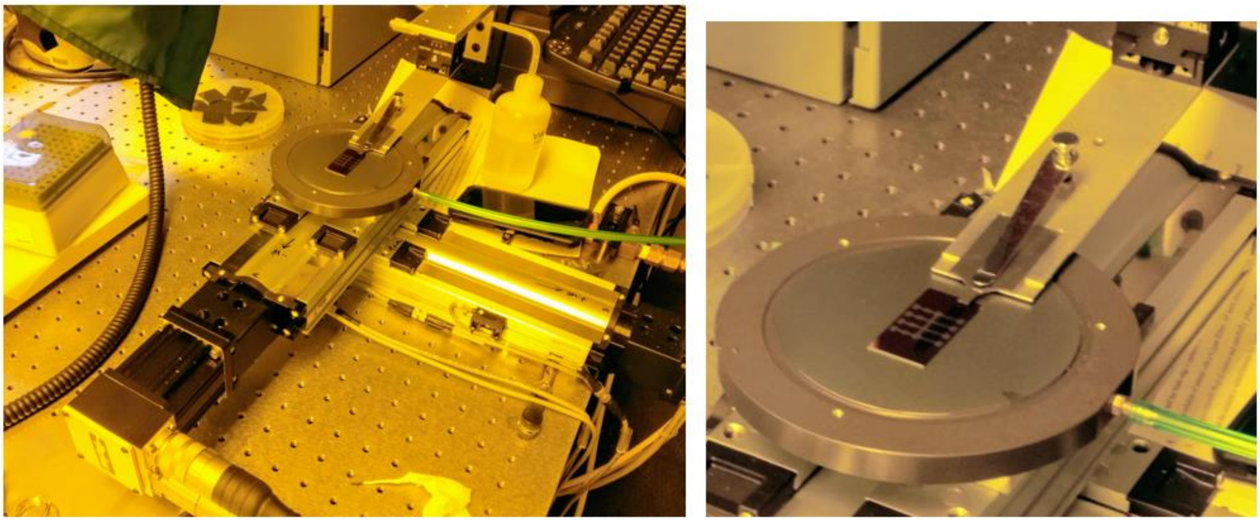

Figure 3.14: custom-made blade IBM blade coating instrument.

3.3.3. Spray coating

Spray coating is a processing technique being considered in research to prepare thin and thick films, especially starting from a polymer-solvent solution. The advantage of using this technique is the very low-cost processing method, the simplicity and the capacity to obtain relatively thin coatings.

Typical spray coating equipment consists of an atomizer, a precursor solution (polymer and water in this case) connected to the atomizer and a plate under the atomizer where a substrate can be placed. The air/nitrogen blast is the most commonly used atomizer and it is connected to an air/nitrogen compressor in order to furnish the gas carrier to spray the droplets. The atomizer consists in a tube connected with two canals where the solution and the gas carrier are forced to flow; Within this tube an adjustable needle is placed, and with a rotating dial, the height of the needle is regulated to let pass more or less mix of solution-gas. The spray time is defined by a computer.

The parameters are the needle height, the distance of the gun from the plate, the spray time, the fluid and gas pressure and the concentration and type of solvent of the solution.

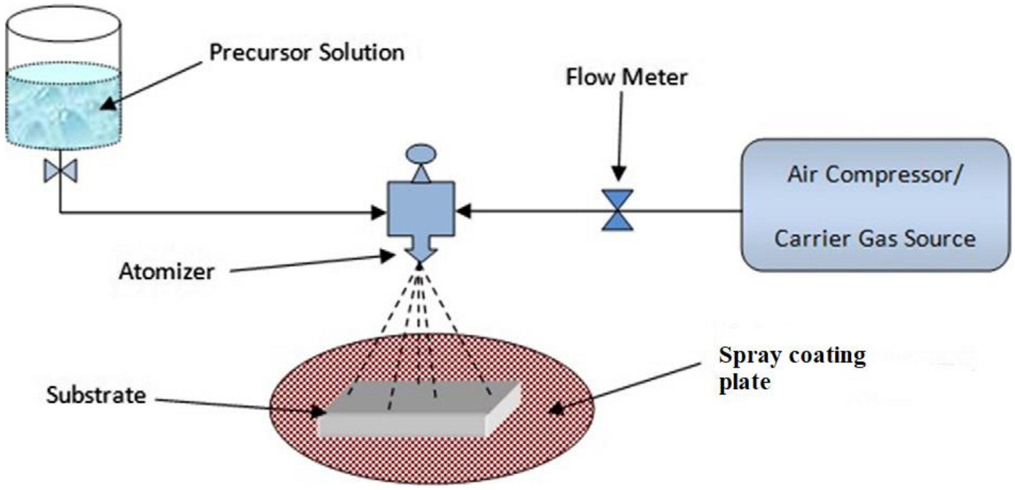

Figure 3.15: Spray coating scheme. Adapted from [66].

Within IBM Almaden Research Center an hand-made spray coating has been made. The variation of parameters in this thesis was limited to the height of the needle and the distance while the fluid pressure was 3 $\frac{Kg}{cm^2}$ and the gas pressure 14 psid. After numerous tests a selected height of the needle and distance from the substrate were chosen and marked on the instrument. Another important parameter, in order to create a round droplet on the electrode gap on the device was the mask; Different mask with different round holes were available and the mask with the diameter of 2 mm was selected.

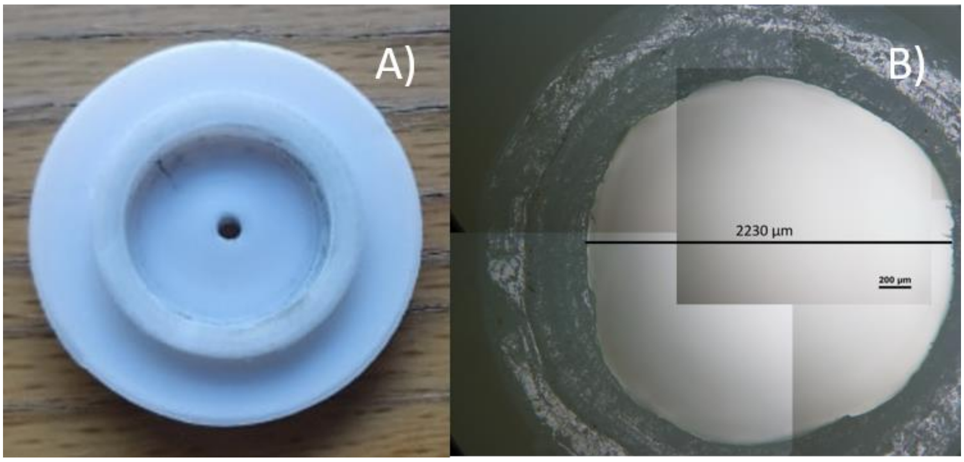

Figure 3.16: Mask image (A) and mask hole (B)

This technique, however, was not performed in order to coat the device since the droplet size was around double of the diameter of the mask hole (a problem that could be solved manufacturing a mask with a smaller dimension of the hole) and because the concentration of the polymer once the solvent was evaporated. In fact, because of the higher weight of the macromolecules compared to the solvent (water) and the centrifugal force during the spray time, a tendency of a “coffee spot” was noticed leaving all the center of the droplet empty of polymer. The solution in this case can be to increase the concentration of the polymer on the solution loosing, however, the thin thickness achievable with this technique.

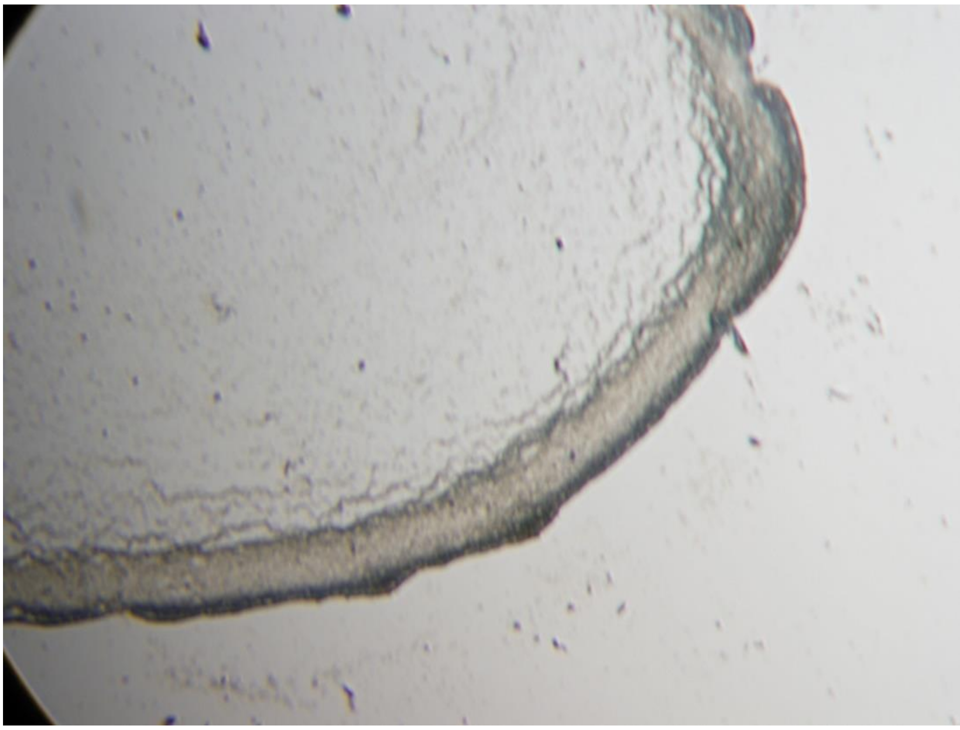

Figure 3.17: "coffee spot" behaviour of a spray coated droplet

3.4. Profilometer and microscope

A profilometer is a measuring instrument employed to quantify the superficial rugosity; Taking advantage of this function is possible to use the technology to measure the step between the silicon wafer substrate and the active layer quantifying the film thickness for every single coating. The resolution of the technique is generally really accurate and can detect variation on the thickness till some tens of nanometres. Two classes of profilometer exist, with or without contact; in this thesis the contact profilometer was used to track the film thickness.

The contact profilometer set-up employ a diamond tip movable vertically till the contact with the analysed surface and laterally in order to track the rugosity/thickness along a line for a previously decided distance. The tip is forced to impart a constant force to the surface and the analogic signal, generated by the height of the tip, is converted into a digital signal, lately stored and displayed on a computer.

The reason why the thickness is an important parameter is to be researched on the change on resistance of the active layer. As mentioned before the analytes, once reached the surface of the polymeric film, do not just adsorb but also diffuse into the bulk. The change on resistance is strongly dependent on the reaction that the analyte has with the organic material, so it is legitimate supposing that the deeper the molecule is able to arrive, the higher will be the variation on the intrinsic resistance of the material.

Now supposing two different active layers with two different thickness and supposing r_0 a standard measure of length , it is possible to theorize one active layer with a depth of $3r_0$ and one with a depth of $2r_0$. Supposing also that the analyte, once adsorbed can diffuse in the bulk of a depth of r_0 reducing the resistance from a value of R_0, still maintained on the active layer depth not reached by the analyte, to a value of R_1.

$$R_1 < R_0$$

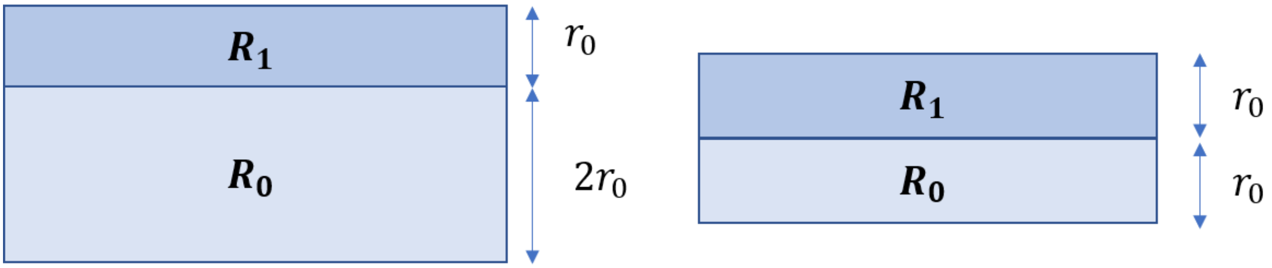

Figure 3.18: Resistance variation model supposing R1 and R0 two different resistance on the same active layer. On the left is shown a thicker layer while at the right a thin one.

Supposing now to weight the value of resistances on their thickness of competence it is clear that the value of resistance assigned to the thicker film is higher than the thinner one.

$$R_{tot(a)} = \frac{R_1 * r_0 + R_0 * 2r_0}{3r_0} \qquad > \qquad R_{tot(b)} = \frac{R_1 * r_0 + R_0 * r_0}{2r_0} \tag{3.1}$$

A higher resistance leads to a lower ΔR so that the change in resistance between $R_{tot(a)}$ and R_0 results lower; A less pronounced ΔR means less response and less sensitivity of the sensor. In other words, if the final objective is to create sensitive sensor devices a film as thin as possible is required.

Not just the thickness of the active layer is important but also a really homogenous film is needed. In order to have a closer view of the coating a simple optical microscope paired with a computer where the selected image is displayed, was been employed to characterize all the 8 active layer films of all the devices tested.

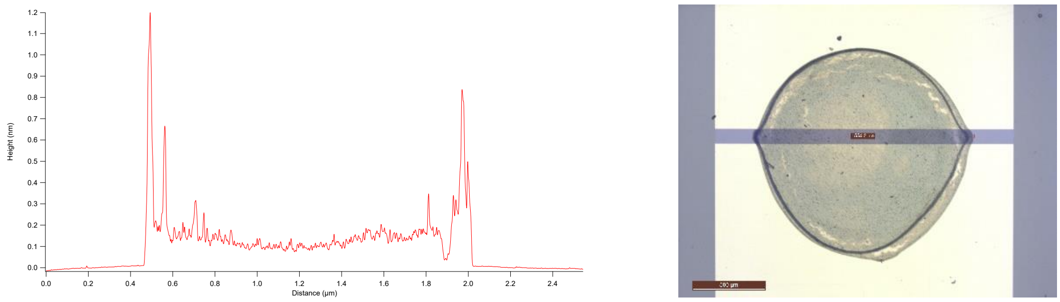

Figure 3.19: Thickness over active layer width and image of the drop-casted film on cell 1 on PAni MZ-1

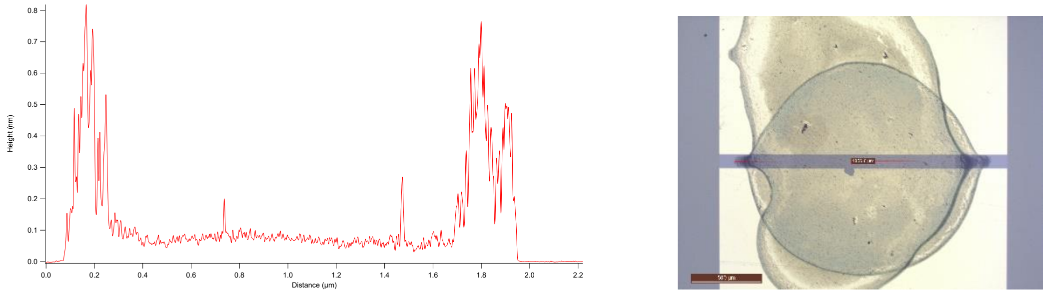

Figure 3.20: Thickness over active layer width and image of the drop-casted film on cell 2 on PAni MZ-1

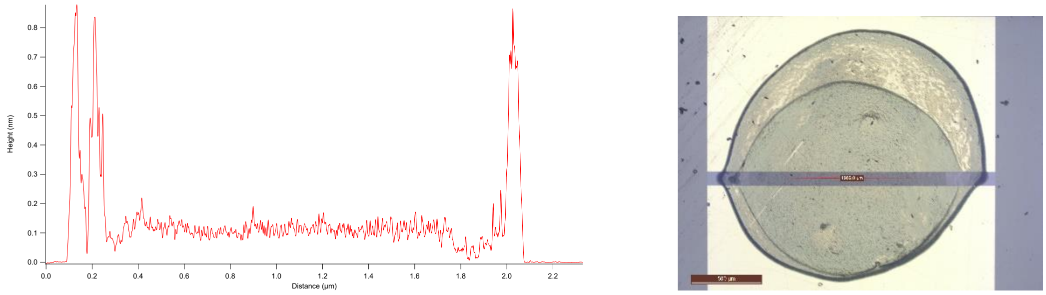

Figure 3.21 Thickness over active layer width and image of the drop-casted film on cell 3 on PAni MZ-1

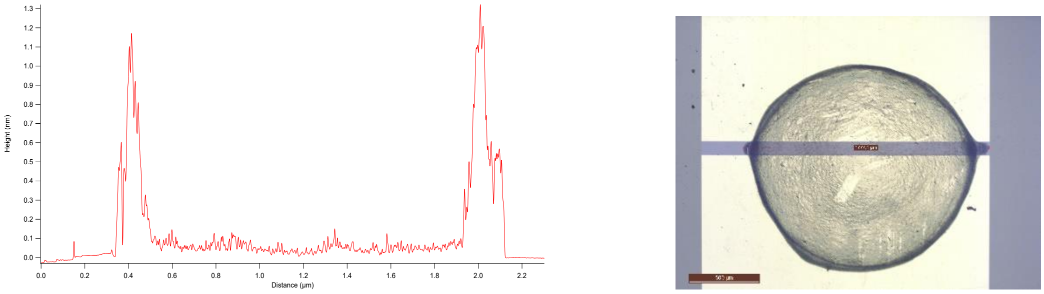

Figure 3.22: Thickness over active layer width and image of the drop-casted film on cell 4 on PAni MZ-1

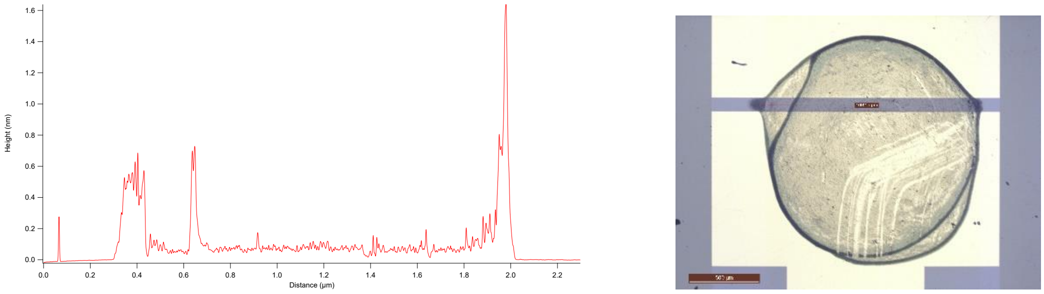

Figure 3.23: Thickness over active layer width and image of the drop-casted film on cell 5 on PAni MZ-1

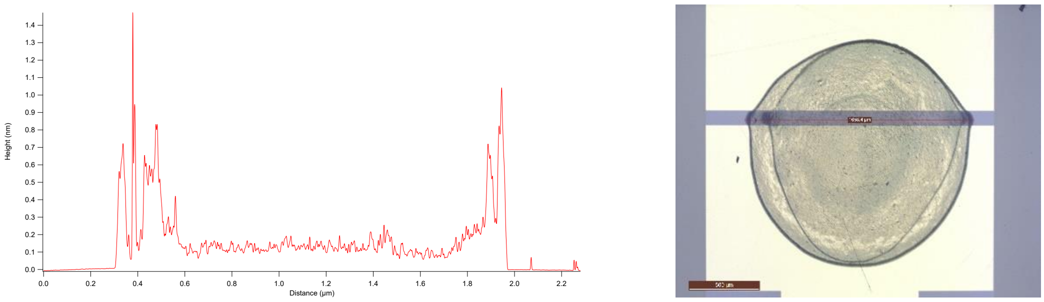

Figure 3.24: Thickness over active layer width and image of the drop-casted film on cell 6 on PAni MZ-1

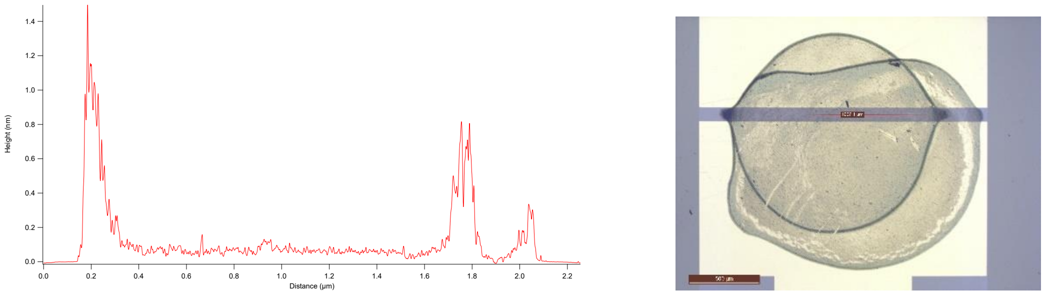

Figure 3.25: Thickness over active layer width and image of the drop-casted film on cell 7on PAni MZ-1

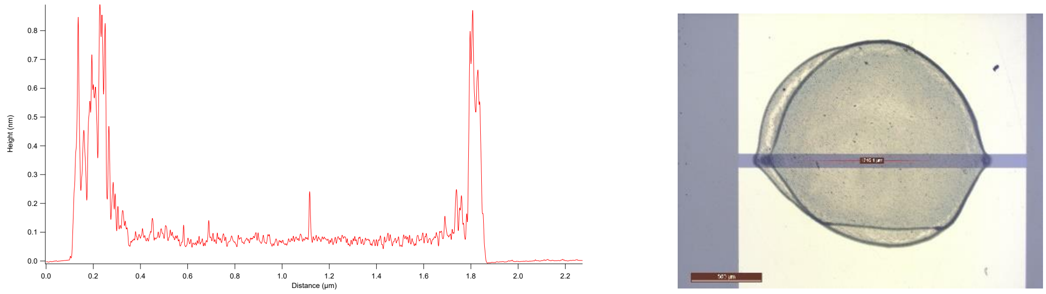

Figure 3.26: Thickness over active layer width and image of the drop-casted film on cell 8 on PAni MZ-1

3.5. Measuring system

Once the device is ready, the testing phase need to be carried out to prove the real performance of the sensor. IBM Almaden Research Center researcher and technical staff built his own measuring system adapting it to the various needs required. It is important to say, in fact, that the gas line do not serve just the system used for this thesis work but numerous set-ups of other different material sensing teams.

The set-up used for this work employs a:

1. Gas delivery system
2. Polymer chamber
3. Source unit
4. Switch system
5. Computer

3.5.1. Gas delivery system

The gas delivery system, electronically controlled by a Python script, is able to carry out the pressurized air flow from a central system to the testing device. It consists in a sealed tubing system connected with:

1. One dry air mass flow controller (MFC) purchased by MKS, with a maximum flow achievable of 2000 sccm.
2. One gas analyte mass flow controller purchased by MKS, with a maximum flow achievable of 200 sccm.
3. One wet ait mass flow controller purchased by MKS, with a maximum flow achievable of 2000 sccm.
4. One water bubbler right after the wet air mass flow controller to provide the wet air.
5. One analyte bubbler just after the analyte mass flow controller to provide the analyte air flow.

6. One mixing chamber where all the three different flow coming from the different MFCs mix, providing the final gas testing flow.
7. One oven downstream of the analyte mass flow controller to achieve very low concentration.

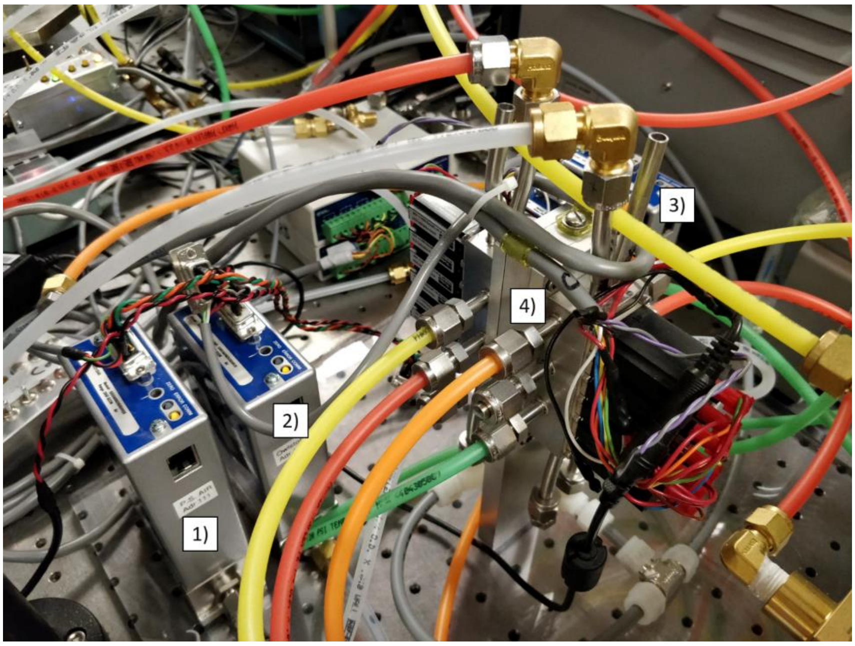

Figure 3.27: Gas delivery system. In the image are displayed the dry MFC (1), the analyte MFC (2), the wet MFC (3) and the mixing chamber (4)

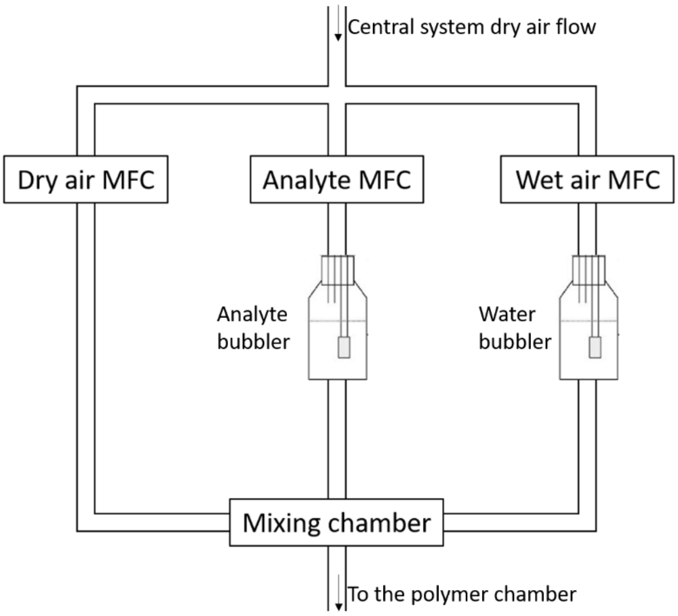

Figure 3.28: Gas delivery system scheme

The analyte flow is obtained by a bubbler. In this configuration a dry air flow, coming from the central pressured dry air system and upon the regulation of the flow given by the analyte mass flow controller, pass through the bubbler achieving different concentration. In fact, the concentration obtained is highly dependent on the input flow. The bubbler is a 30 cm long and 3 cm large glass container filled with analyte with one inlet port, where the dry air arrive and an outlet port, where the analyte saturated air comes out. The bubbler is placed in a thermal bath in order to keep the temperature of the studied substance constant.

The saturation or analyte concentration of the dry air flow depends on different parameters such as the temperature of the thermal bath, the input air flow and the analyte vapor pressure. The concentration achieved in this thesis are in the order of part per million (ppm); lower concentration could have been obtained with the oven set-up but, due to some technical problem the test could not be performed.

Considering the air flow as an ideal gas:

$$PV = nRT \tag{3.2}$$

And the concentration of the analyte on the dry air flow is proportional to the number of mole ratio:

$$C \, \alpha \, \frac{n_a}{n} = \frac{P^*}{P} \tag{3.3}$$

Where C is the concentration achieved, n_a is the number of moles of the gaseous analyte, n is the number of moles of dry air, P is the input air pressure (the atmospheric pressure in this case, controlled every time by a barometer placed before of the dry air inlet port), P^* is the analyte partial pressure.

P^* is calculated using the semi-empirical Antoine equation:

$$P^* = 10^{A - \frac{B}{C+T}} \tag{3.4}$$

Where A, B and C are empirical values dependent on the temperature and pressure considered. These constants depend strongly on the range of temperature and the pressure considered; The sensor studied was tested at room temperature, 20 °C, and atmospheric pressure reported on KPa or mmHg (101.325 and 760 respectively).

Once all the parameters are available, the concentration was evaluated by:

$$C_{ppm} = \left(\frac{P^*}{P} \frac{f}{F}\right) 10^6 \tag{3.5}$$

Where f is the input flow in sccm controlled by the analyte mass flow controller and F is the total flow (dry air, wet air and analyte saturated air). This ratio is, in fact, a dilution ratio.

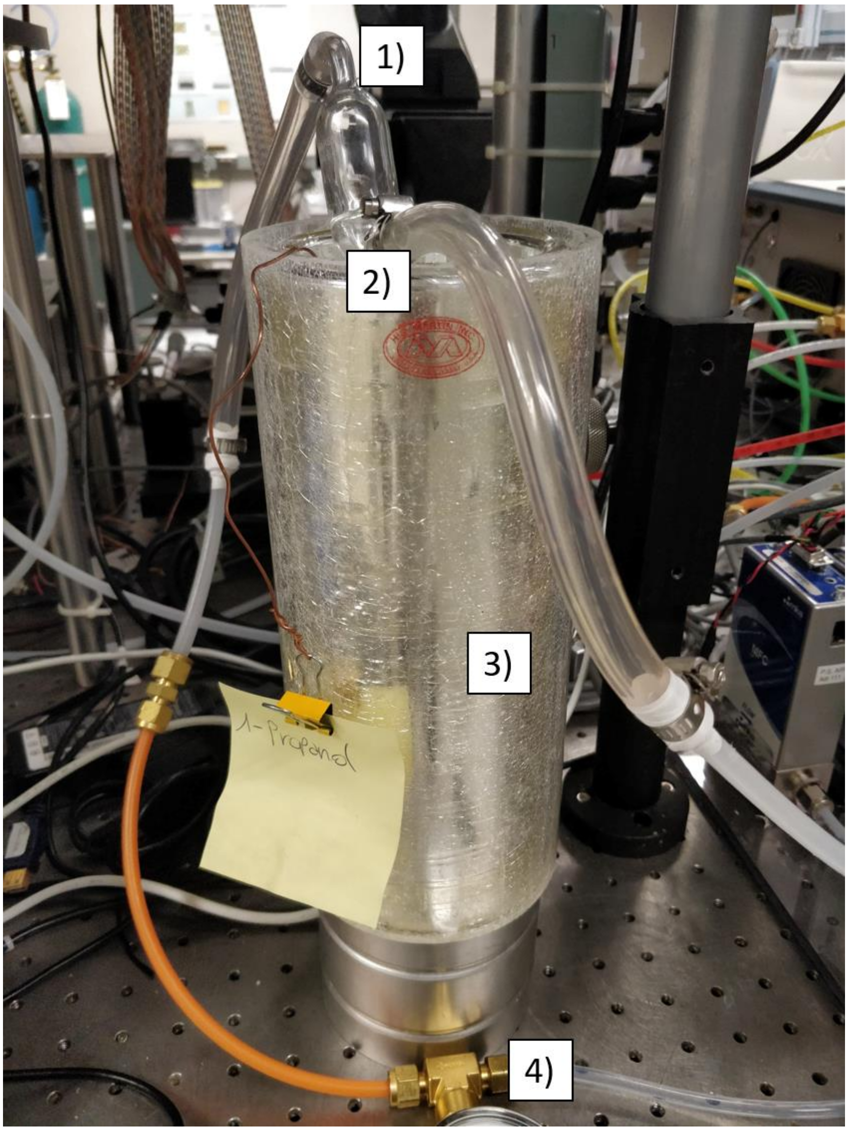

Figure 3.29: Testing bubbler. In the image are reported the inlet port (1), the outlet port (2), the thermal bath (3) and the barometer (4)

3.5.1.1. Analytes

All the analytes considered are, as previously mentioned, volatile organic compound so that means are substances able to evaporate relatively easily at room temperature. The importance of these VOC is because, the majority of them, can be dangerous for human being, animals and plants causing chronical health diseases [67]. 14 analytes with different levels of polarity were tested, from cyclohexane to water. Not all the analytes were tested on all the samples due to the short time of the experience and the long-time of the experiments; Nevertheless, at least six substances were tested for every sample, ordered by polarity. The analytes present on all the measurements are Octane (low polarity), Toluene (due to the benzenic group), Ethyl acetate, Acetone, 2-propanol and water.

A table with all the VOCs tested showing their relative polarity, partial pressure and boiling point is reported below:

Analyte	Relative polarity	Vapor pressure at 20°C (KPa)	Boiling point (1 Atm)
Cyclohexane	0.006	104	81 °C
Octane	0.044	14	126 °C
Toluene	0.099	29	111 °C
Ethyl acetate	0.228	97	77 °C
Chloroform	0.259	210	61 °C
Diethyl ether	0.275	59	35 °C
2-butanone	0.327	105	80 °C
Acetone	0.355	240	56 °C
Acetonitrile	0.460	97	82 °C
2-propanol	0.546	44	83 °C
1-propanol	0.617	20	98 °C
Ethanol	0.654	59	78 °C
Methanol	0.762	128	65 °C
Water	1.000	234	100 °C

Figure 3.1: Studied analyes ordered by relative polarity. Data obtained by https://sites.google.com/site/miller00828/in/solvent-polarity-table

Cyclohexane C_6H_{12}: Cyclohexane is a cycloalkane, colourless and a flammable liquid at room temperature with a distinctive detergent-like odour. It is produced generally by hydrogenation of benzene. The permissible exposure limit is 300 ppm [68] and Potential symptoms of overexposure to cyclohexane for humans are irritation of eyes, skin and respiratory system; drowsiness; dermatitis; narcosis and coma although cyclohexane generally has low acute toxicity.

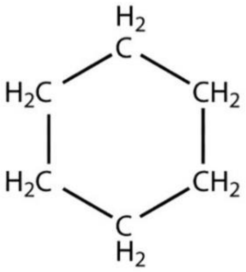

Figure 3.30: Cyclohexane molecule

Octane C_8H_{18}: Octane is a hydrocarbon alkane, colourless, volatile and flammable in its liquid state. The molecule is an important component of gasoline and present various isomeric forms. The form used in this thesis has a permissible exposure limit of 500 ppm [68]. The symptoms of overexposure on humans are the same as cyclohexane.

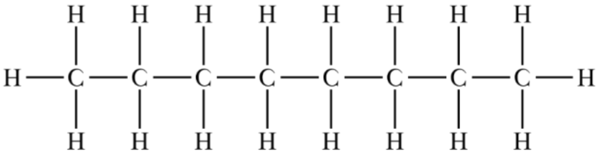

Figure 3.31: Octane molecule

Toluene C_7H_8: Toluene is an aromatic hydrocarbon, colourless liquid with a sweet, pungent odour. It is a common solvent used in paints and its permissible exposure limit is 200 ppm [68]. Exposure to toluene can cause eye and nose irritation, tiredness, confusion, euphoria, dizziness, headache, dilated pupils, tears, anxiety, muscle fatigue, insomnia, nerve damage, inflammation of the skin, and liver and kidney damage.

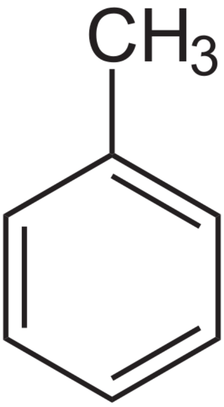

Figure 3.32: Toluene molecule

Ethyl acetate $C_4H_8O_2$: Ethyl acetate is an organic compound, colourless liquid with a characteristic sweet smell commonly used in glues. It is also manufactured on large scale for use as a solvent. The permissible exposure limit is around 400 ppm [68] and a prolonged or repeated skin contact may cause drying with cracking, irritation and possible dermatitis following.

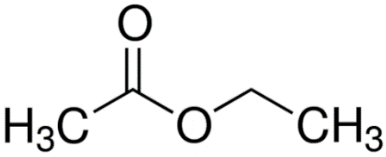

Figure 3.33: Ethyl acetate molecule

Chloroform $CHCl_3$: Chloroform is an organic compound, colourless, dense and sweet-smelling liquid, precursor to various refrigerant. It is a powerful anaesthetic, euphoriant, anxiolytic and sedative when inhaled or ingested. The analyte is highly dangerous [67] and the permissible exposure limit is around 50 ppm [68]. The most outstanding effect of acute exposure is depression of the central nervous system. Furthermore, vomiting and gastrointestinal upset may be observed and exposure to high concentration can lead to liver and kidney injury.

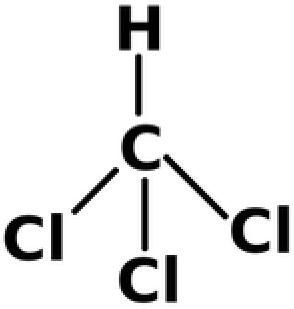

Figure 3.34: Chloroform molecule

Diethyl ether $C_4H_{10}O$: Diethyl ether is an organic compound, colourless, volatile and flammable liquid. It is employed as a common solvent in laboratories and previously as a general anaesthetic (before non-flammable drugs were developed). The permissible exposure limit is 400 ppm [68] and an overexposure to the substance can lead to headache, eyes and skin irritation but even to nausea or vomiting.

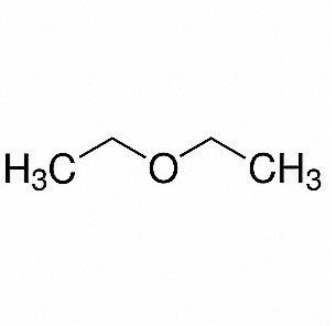

Figure 3.35: Diethyl ether molecule

2-butanone $C_4H_{10}O$: 2-butatone, also known as methyl ethyl ketone (MEK) is an organic compound, colourless liquid with a sharp, sweet odour. It is produced industrially on a large scale as solvent and present good solubility in water. The permissible exposure limit is 200 ppm [68] and acute (short-term) inhalation exposure to methyl ethyl ketone in humans results in irritation to the eyes, nose, and throat.

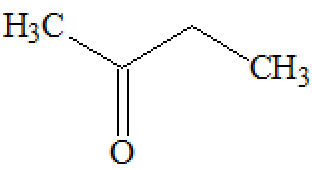

Figure 3.36: 2-butanone molecule

Acetone $(CH_3)_2CO$: Acetone is an organic compound, colourless and flammable liquid. It is also known to be the smallest ketone. It is one of the most used solvent, covering a large amount of purposes (it is also easily miscible in water) including cleaning in laboratories. The permissible exposure limit is quite high, 1000 ppm [68] also because acetone is produced and disposed of in the human body through normal metabolic processes. The problem related with a high exposure can lead to reproductivity diseases.

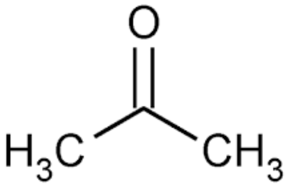

Figure 3.37: Acetone molecule

Acetonitrile CH_3CN: This organic compound is the simplest nitrile, colourless and flammable liquid with an aromatic odour. In laboratories it is used as medium polar organic solvent. Its permissible exposure limit is 40 ppm [68]. The problem with human health is the production by the metabolism of hydrogen cyanide, highly dangerous for the body. The symptoms, which do not usually appear for several hours after the exposure, include breathing difficulties, slow pulse rate, nausea, and vomiting. Convulsions and coma can occur in serious cases, followed by death from respiratory failure.

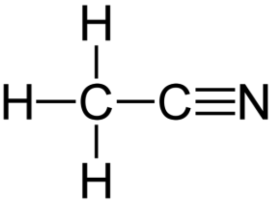

Figure 3.38: Acetonitrile molecule

2-propanol C_3H_8O: 2-propanol is a colourless, flammable chemical organic compound with a strong odour. It is a secondary alcohol and it is used in the manufacture of wide variety of industrial and household chemicals such as antiseptics, disinfectant and detergent as well as cleaning purposes in laboratories. The permissible exposure limit is 400 ppm [68].

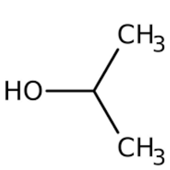

Figure 3.39; 2-propanol molecule

1-propanol C_3H_8O: 1-propanol is simplest one of the isomers of 2-propanol. The permissible exposure limit is 200 ppm [68].

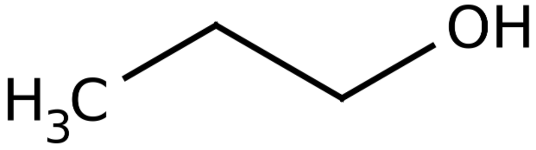

Figure 3.40: 1-propanol molecule

Ethanol C_2H_6O: Ethanol is a volatile, flammable and colourless liquid with a slight characteristic vinous odour. It is a psychoactive substance and is the principal type of alcohol found in alcoholic drinks. The permissible exposure limit is 1000 ppm [68]. Can lead, upon high and prolongate exposition (especially if ingested), to headache or liver damage.

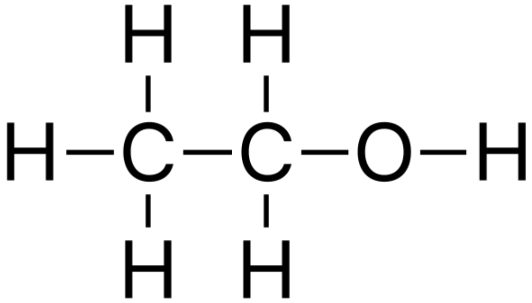

Figure 3.41: Ethanol molecule

Methanol CH_3OH: Methanol is the simplest alcohol, consisting of a methyl group linked to a hydroxyl group. It is a volatile, colourless and flammable liquid with an odour similar to ethanol. His toxicity is, however, far more dangerous than ethanol and, for this reason, the permissible exposure limit is 200 ppm [68]. One of the main problems of methanol ingestion is the permanent blindness caused by the destruction of the optic nerve; Furthermore, the ingestion of 30 mL of methanol can be fatal.

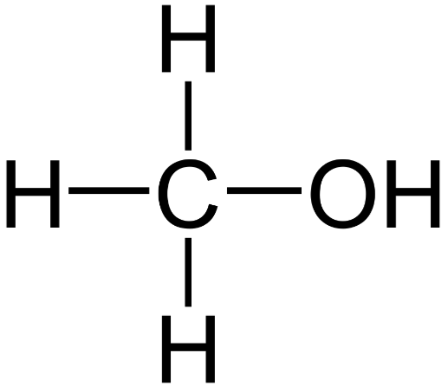

Figure 3.42: Methanol molecule

Water H_2O: Polyaniline and in general conductive polymer-based sensors are generally really sensitive to environmental humidity, affecting the sensing performances toward other analytes. This is due to the polar group present on the CP backbones that react easily with the aqueous vapour in the environment. That means that, however, CP sensors are really sensible to water and in fact numerous sensors have been developed toward this direction [69]. Nevertheless, sensors integrating a hydrophobic layer on the surface have been developed to resist to water response up to 350 ppm [70].

Concentrations (ppm)

Analyte	*1% volume*	*3% volume*	*5% volume*	*10% volume*	*20% volume*	*30% volume*	*40% volume*
Cyclohexane	973	2918	4864	9728	19456	29184	38912
Octane	119	358	596	1193	2387	3581	4775
Toluene	271	815	1359	2719	5439	8159	10878
Ethyl acetate	923	2770	4616	9233	18467	27701	36935
Chloroform	1964	5892	9820	19640	39280	58920	78560
Diethyl ether	5223	15669	26115	52230	104461	156692	208923
2-butanone	995	2985	4976	9952	19905	29858	3810
Acetone	2322	6966	11611	23222	46445	69668	92891
Acetonitrile	910	2732	4553	9106	18213	27320	36427
2-propanol	395	1185	1975	3950	7901	11851	15802
1-propanol	174	524	874	1748	3497	5245	6994
Ethanol	545	1636	2728	5456	10912	16368	21824
Methanol	1214	3644	6074	12149	24298	36447	48596
Water	216	648	1080	2160	4320	6480	8641

Table 3.2: Concentrations of the different analytes at different degree of volume % of the solvent in the sensing gas.

3.5.1.2. Measuring protocol

Once all the set-up is available and installed, the necessity of a central system who controls the measurements is needed. For this purpose a computer is installed right next to the system to start and control the test. A phyton script is responsible to control the input flow of the mass flow controllers thanks to a txt file where the time of exposure, the time of recovery and the different sccm (square cubic centimetres per minute) of air are reported.

As it can be noticed the timings are on chronologic order (until the value reported on the txt file) and not indicated just by the total amount of seconds. After a 15 initial minutes of dry air exposure, in order to “clean” the device from previous tests or humidity adsorbed on the surface, the protocol alternate 3 minutes of analyte exposure to 10 minutes of recovery time achieved by blowing dry air on the surface of the sensor. On the other side, the values of air blown are written to grant an increase on the analyte concentration over the total volume of air; starting from a 1% in the configuration 5-495 to a 30% on the configuration 150-350. The other concentrations are 3%, 5%, 10% and 20%.

Many other protocols were used, to achieve a bigger concentration of analyte for example or to create the baseline (blowing just dry air in this case), but the general and most used txt file is reported below:

Time (s)	Analyte flow	Dry air flow	Wet air flow
900	0	500	0
1080	5	495	0
1680	0	500	0
1860	15	485	0
2460	0	500	0
2640	25	475	0
3240	0	500	0
3420	50	450	0
4020	0	500	0
4200	100	400	0
4800	0	500	0
4980	150	350	0
5580	0	500	0
5590	0	0	0

Table 3.3: General measuring protocol

3.5.2. Polymer Chamber, source unit and switch system

Once the flow is mixed in the mixing chamber a tubing system is responsible to carry on the flow to the device. The device is placed in the polymer chamber that is a screw sealed box with different cables connected to the electrodes from one side and to the switch system and the source unit to the other side that apply the voltage and ground the system; It is really important in this configuration to place the device correctly inside of the chamber with the cables touching the electrodes otherwise no response will be reported. The flow is constantly removed from the system by an outgoing tube that connect the polymer chamber with a central exhaust line, preventing the mixture gas to stationing excessively on sensing.

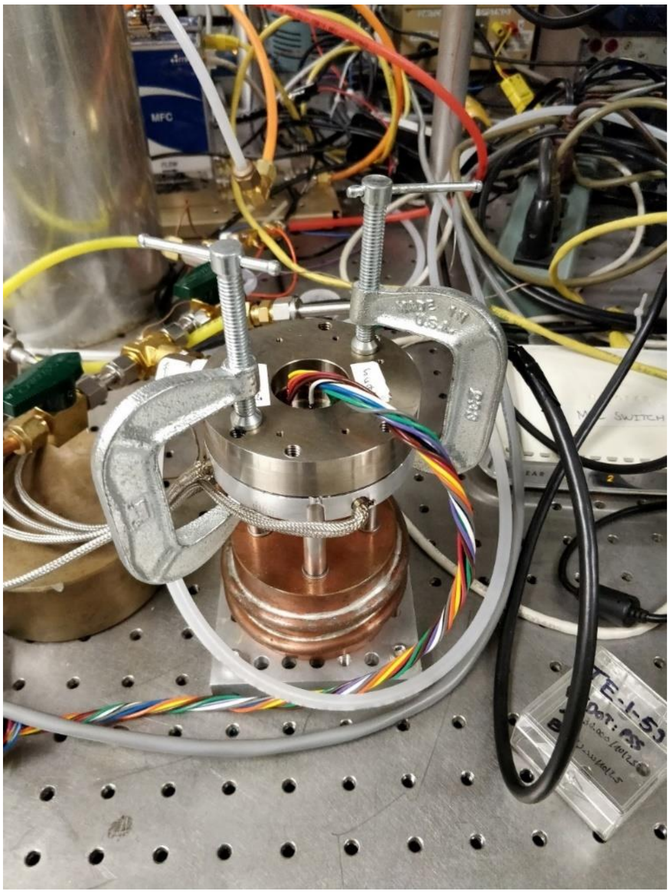

Figure 3.43: Polymer chamber. the sealing screws, the cables and the exhaust line (yellow tube) are visible on the image.

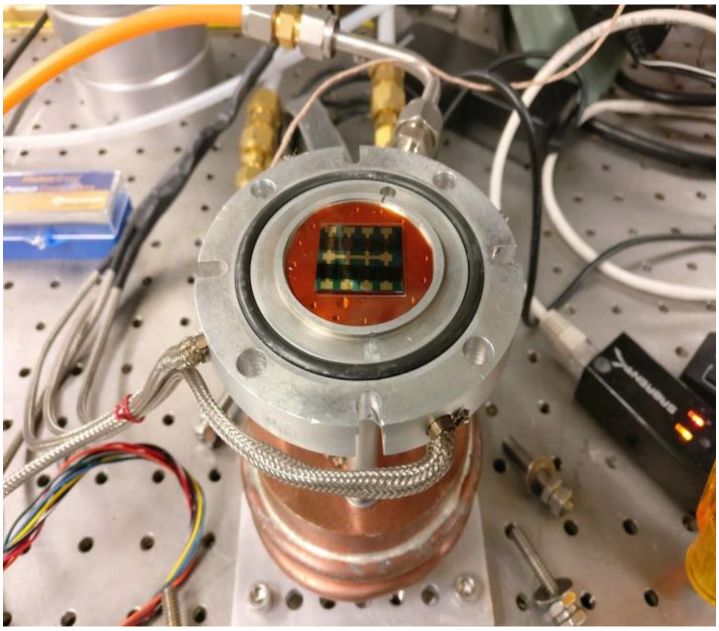

Figure 3.44: Opened polymer chamber with the device placed in

The Keithley 236 source unit is responsible to apply the voltage to the electrodes. The voltage is previously set by the phyton script and need to be selected carefully according to the different resistance of the sensor. This instrument is also responsible for the compliance; in fact, from the script other parameters need to be selected to have a clear output signal. The previously mentioned compliance is one of them and it is responsible for the superior value of current measurable; other parameters are the averaging point function, to average and smooth all the current output achieved and the current range, to set the maximum range within the source unit can work for the selected device.

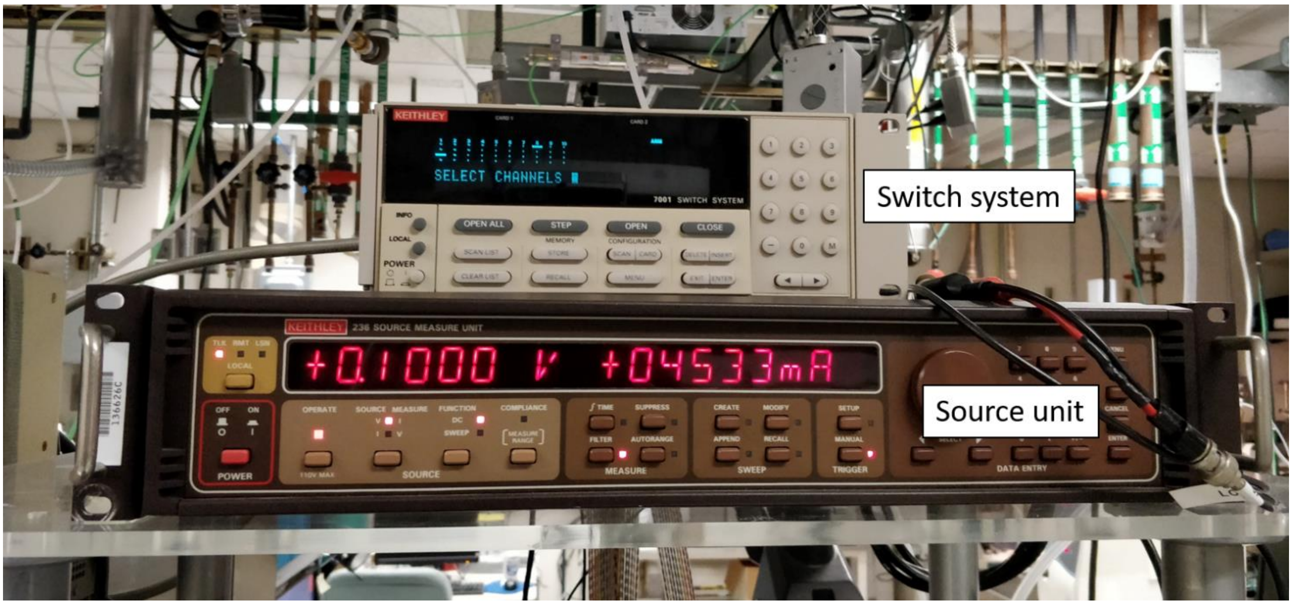

Figure 3.45: Switch system and source unit

The Keithley switch system is the organ responsible to close the circuit to every single sensor on the array, switching the voltage applied from the source unit electrode to electrode. An important parameter for this instrument is the wait time, so the time during which the voltage is applied in every single input cable and the data is collected. To better understand the speed of the system, the average order of magnitude of the time is between 0.05 to 0.1 seconds.

Those parameters are quite important because a not suitable values for the test performed can lead to a high noise in the data points achieved. In particular, it was seen that:

- High number of data points averaged lead to a lower noise but, at the same time, all the response curves tend to be equal and the response itself gets lower.
- The compliance does not play any role on response or noise, but if the measured value exceeds the compliance set, the following curve will be cut on that value.
- A too high range, compared to the current measurement tested, leads to a high noise. The reason can be found on the extreme high gap between the actual current and the current able to be measured.
- A too low wait time lead to higher noise because the machine is not able to end up to the set regime of the instrument.

Every step of the process, so that every parameter is previously chosen and indicated on the phyton script, is controlled by a computer which act like a central unit. Once the current DC measurements are achieved, they are sent to the same computer who have the task to collect and store them on a txt file.

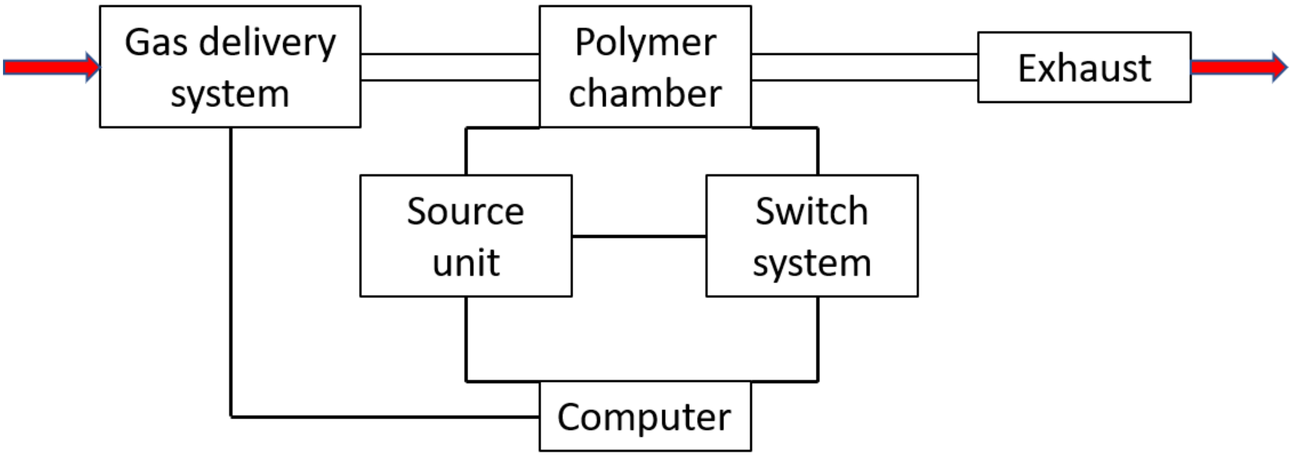

Figure 3.47: Experimental set-up scheme

3.6. IGORPro script

Considering the high number of data points collected for every single measurement the need of a script able to process them in a reasonable time was required; in fact, the data collected depends on the wait time, the total number of current values measured, and the averaging, the smoothing, reaching a total number of around 4300 data point for every sensor. Considering that every device employs 8 sensor the total number reach around 35’000 data point for every analyte, this means around 210’000 data point for the 6 analyte measurement and around 500’000 data point in the 14 analytes configuration.

IGOR Pro was the programme selected to meet this requirement. It is a scientific data analysis software developed by WaveMetrics Inc., originally thought for time series analysis but evolved to cover other application such as curve fitting and image processing. It comes with a fully functional programming language and compiler, but many functions are also accessible through menus. Other features include the possibility of extending the built-in functions with external operations allowing data acquisition, manipulation and analysis features, communication with external devices and in principle any other task that can be programmed in C or C++.

Various features are present inside of the script including:

- **Load function**; It is the main function of the script and it is able to load the data points from a txt file, extracting the path and splitting its name to store the data points into a folder tree (with sample name, solvent name and date). Once the folders are created the data points are inserted on a wave (the basic IGOR Pro instrument to process data) and the current measurements are converted on resistance through the formula:

$$R = \frac{V}{I} \tag{3.6}$$

The same data points are also smoothed, in case the noise is too high, and differentiated, to see any differences on the response peaks between different analytes. Then the current protocol is loaded into a wave and it is used to calculate the response, the dilution ratio and the analyte concentrations. Another feature of the load function is to mean the response waves and extract the standard deviation from those values, not just for all the 8 sensors but also for sensor 1 to 4 and sensor 5 to 8 (due to the fact that often the two electrode lines are coated with different material). The output of the function are a large number of waves including the current, the resistance and the response for every sensor on the device.

- **Resistance over time plot**; the function is able to plot for every sensor of the 8 considered, a graph.

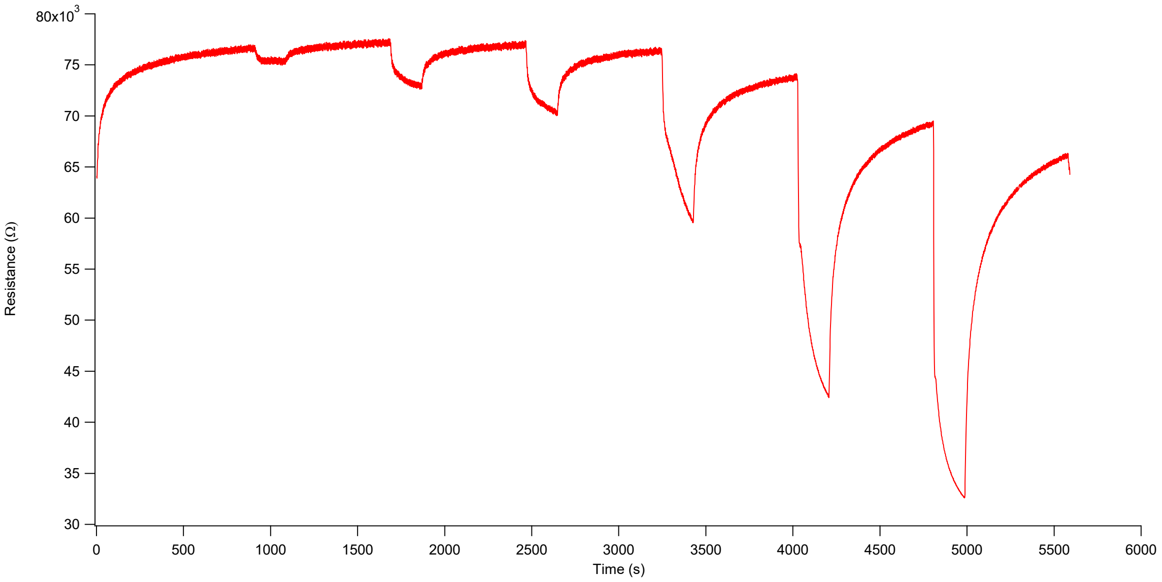

Figure 3.48: Resistance over time for water on cell 2, on PAni TE-II-17

- **Current over time plot**; the function is able to plot for every sensor of the 8 considered, a graph.

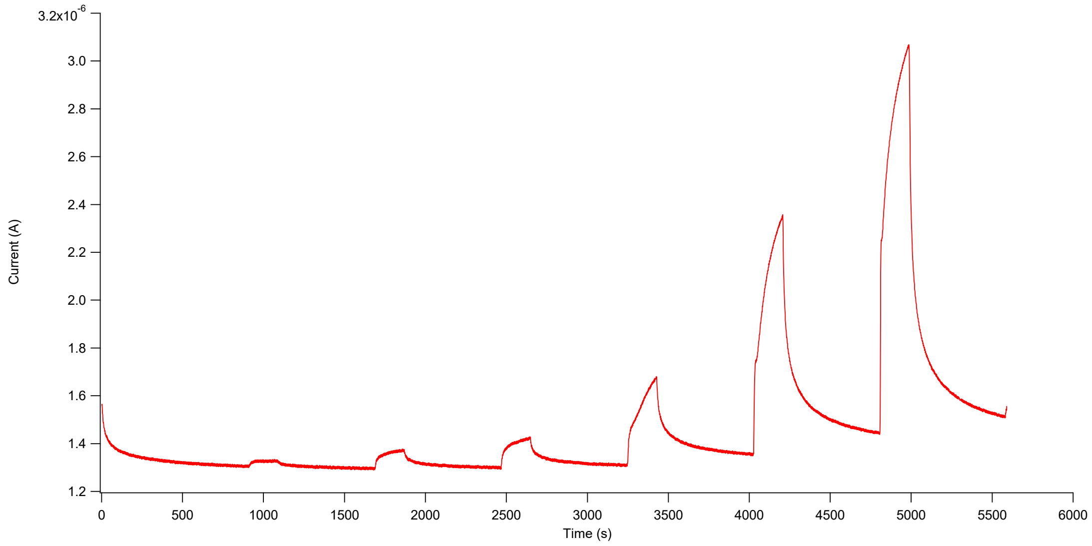

Figure 3.49: Current over time for water on cell 2, on PAni TE-II-17

- The derivative resistance over time plot; the function is able to plot for every sensor of the 8 considered, a graph.

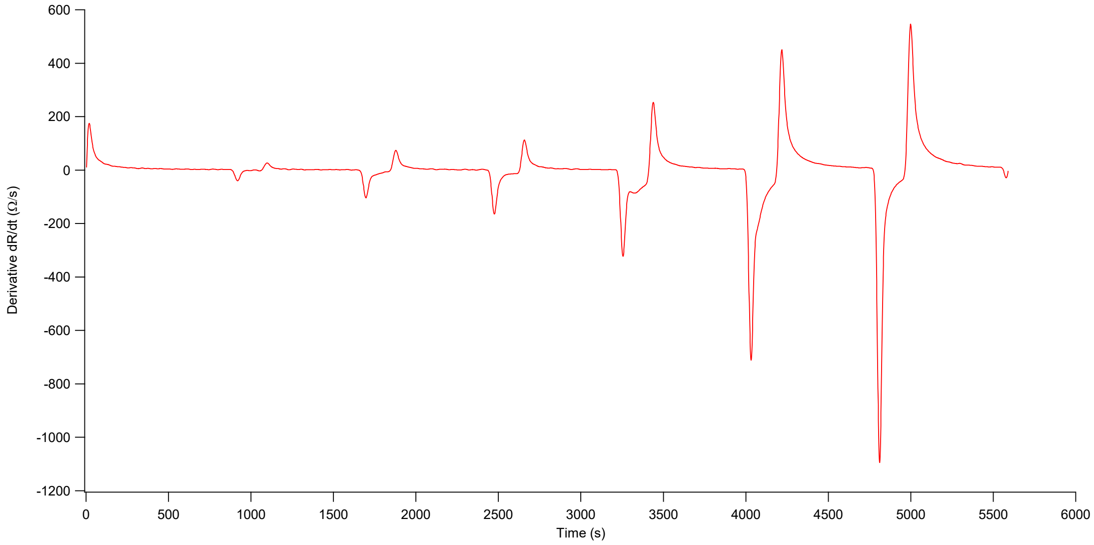

Figure 3.50: Derivative resistance over time for water on cell 2, on PAni TE-II-17

- The smoothed version of the first two plots, for every sensor.

- The response over concentration plot; the function is able to plot for every sensor of the 8 considered, a graph.

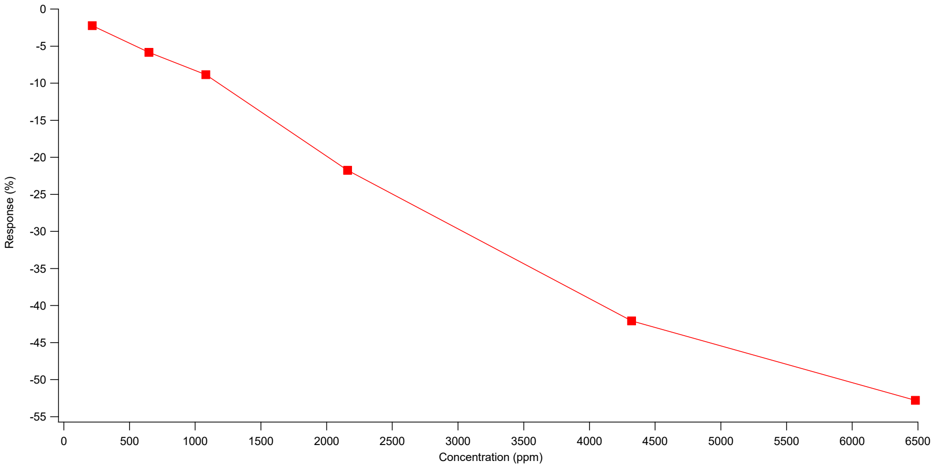

Figure 3.51: Response over concentration for water on cell 2, on PAni TE-II-17

- The Response over concentration with all the sensors of the device displayed on one graph.

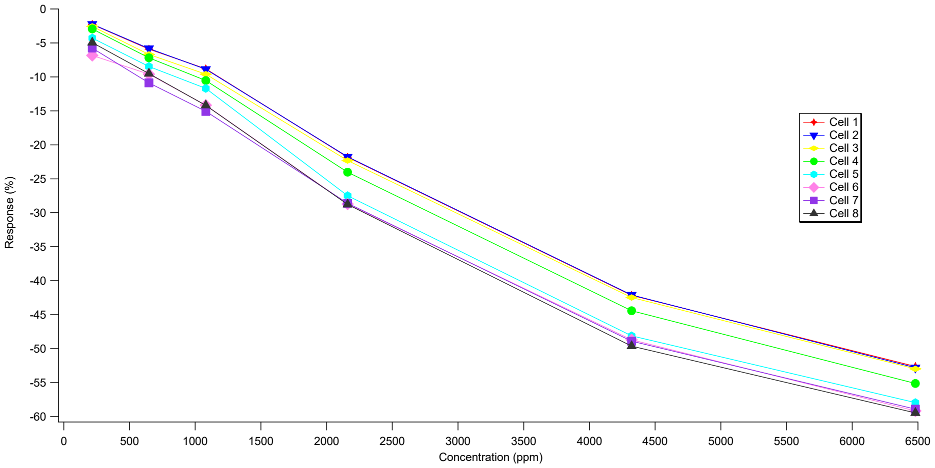

Figure 3.52: Response over concentration for water on PAni TE-II-17

- The response over concentration mediated over all the sensor with the standard deviation reported. The same plot is available also just for sensor 1 to 4 and 5 to 8.

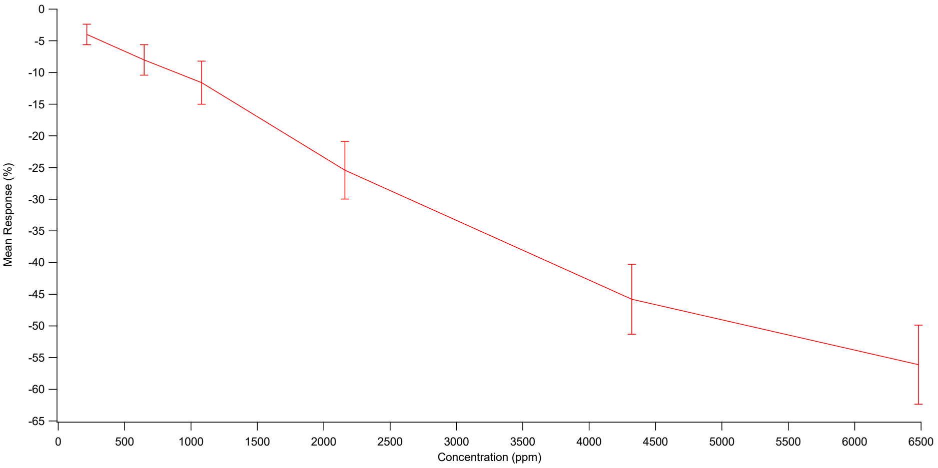

Figure 3.53: Response over concentration mediated between all the sensors for water on PAni TE-II-17

- The comparison over different analyte response over concentration for one single device, both for all the sensor mediated and the two-line sensors.

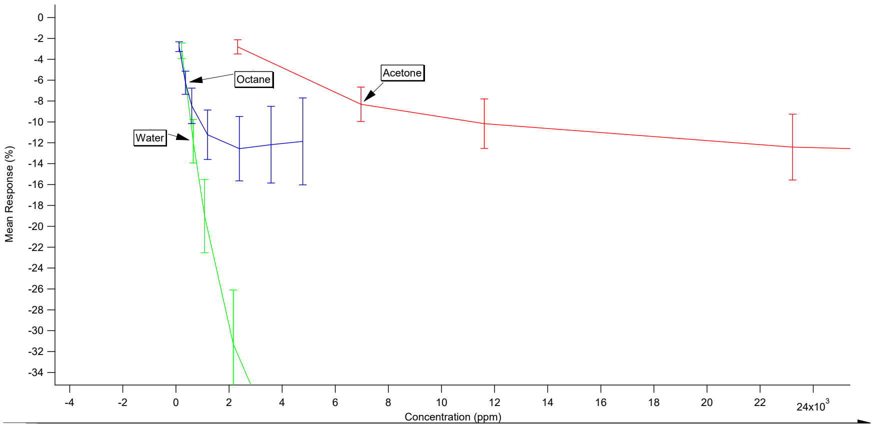

Figure 3.54: Comparison between different analytes mediated over the all sensors with the standard deviation reported for PAni TE-II-17

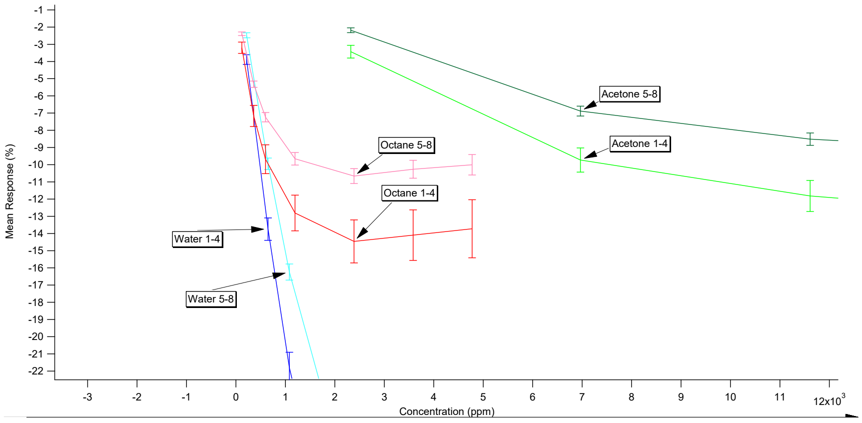

Figure 3.55: Comparison between different analytes mediated over sensors 1 to 4 and 5 to 8 with the standard deviation reported for PAni TE-II-17

- The comparison over different devices response over concentration for one single analyte, both for all the sensor mediated and the two-line sensors.

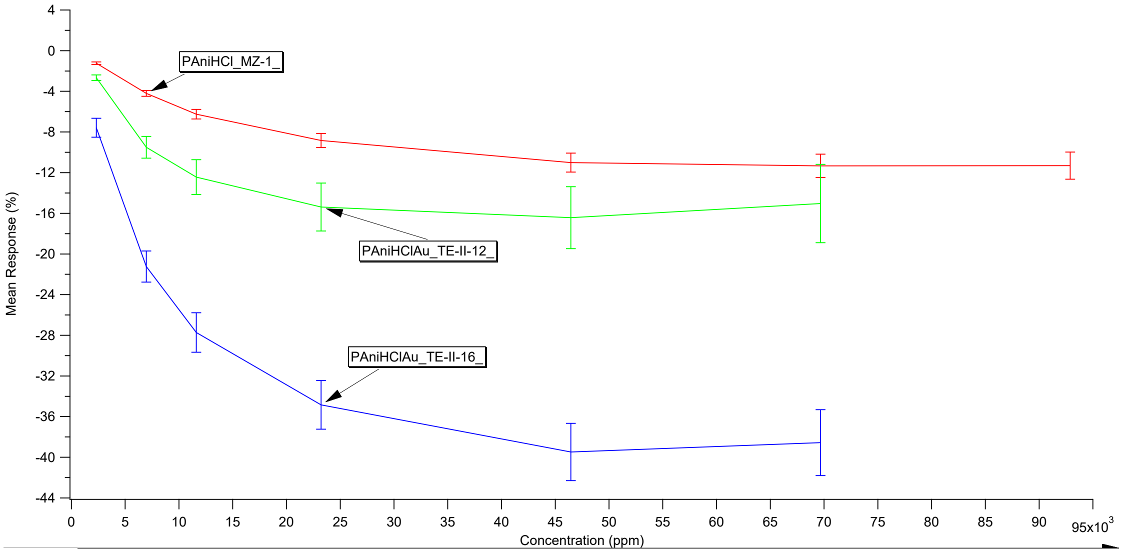

Figure 3.56: Comparison between different devices mediated over the all sensors with the standard deviation reported, for water.

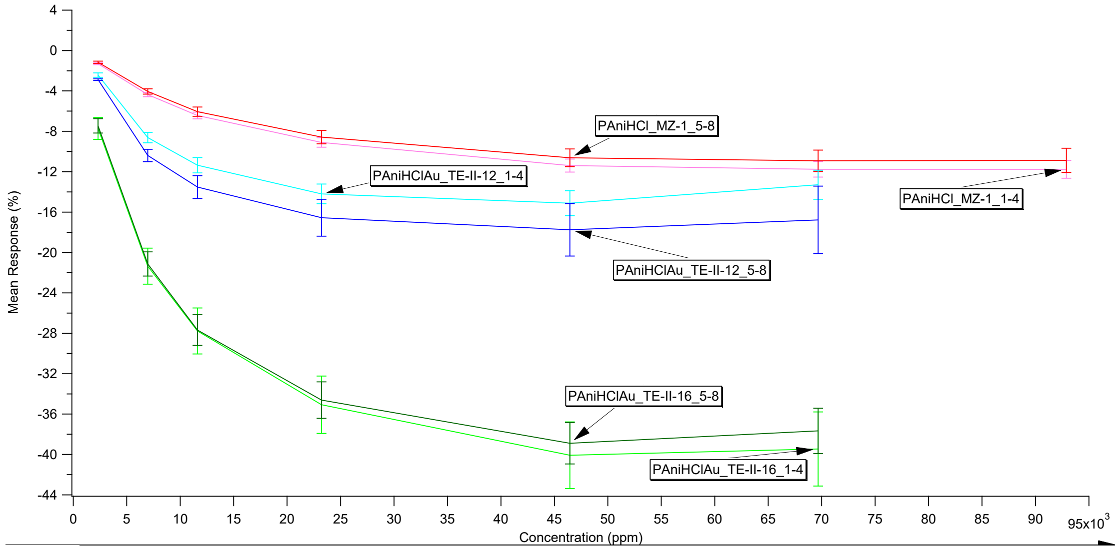

Figure 3.57: Comparison between different devices mediated over sensors 1 to 4 and 5 to 8 with the standard deviation reported, for water.

CHAPTER 4

RESULTS

The main aim of this thesis is to develop a gas sensor able to present better result in term of response and from there, sensitivity. A total number of 15 sample were tested but here are reported just the most important ones in terms of results. This chapter is then divided in three parts; In the first part are shown the first results achieved for the three materials tested while in the second these results are compared with the most promising one obtained. In the third part a comparison with the commercial polymeric e-nose for certain analyte is reported.

4.1. PEDOT:PSS

4.1.1. First measurements with PEDOT:PSS

The first material tested was PEDOT:PSS and especially the sample TE-I-59, blade coated on the sensor device and tested by the all 14 analytes case of study till a concentration of 40% of volume. The exposure time (so the response time) was 3 minutes, while the recovery time was 10 minutes. In the following plots the response over the different concentrations of an analyte are reported.

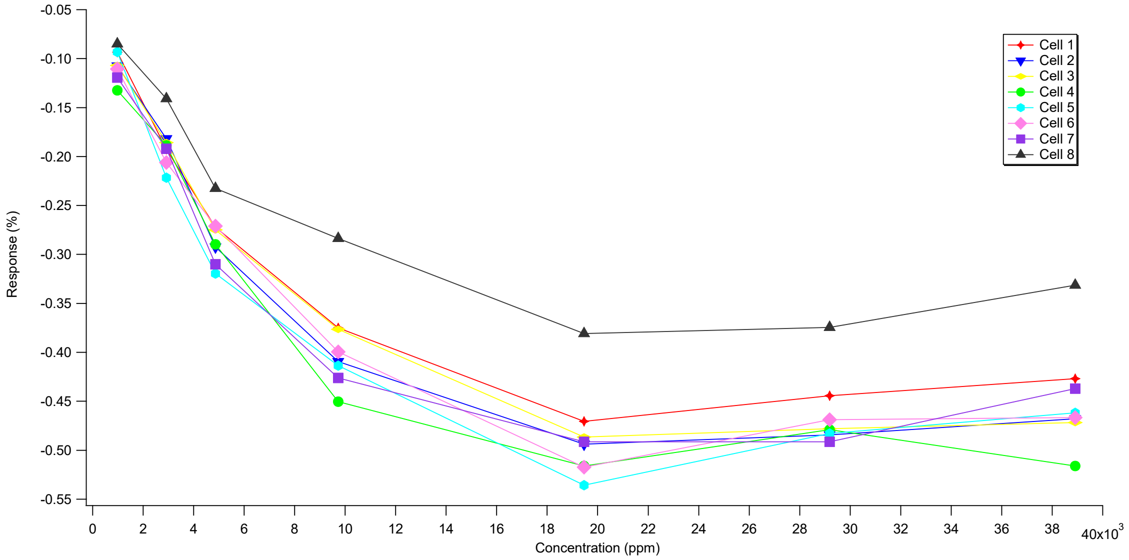

Figure 4.1: Response over concentration for Cyclohexane

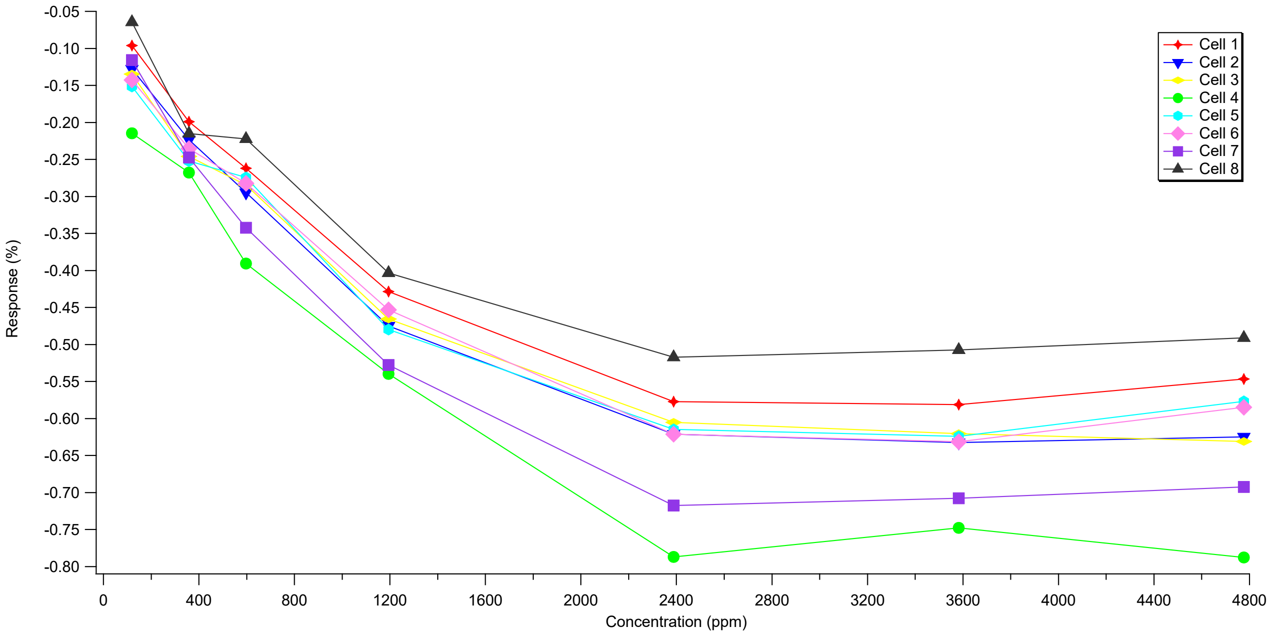

Figure 4.2: Response over concentration for Octane

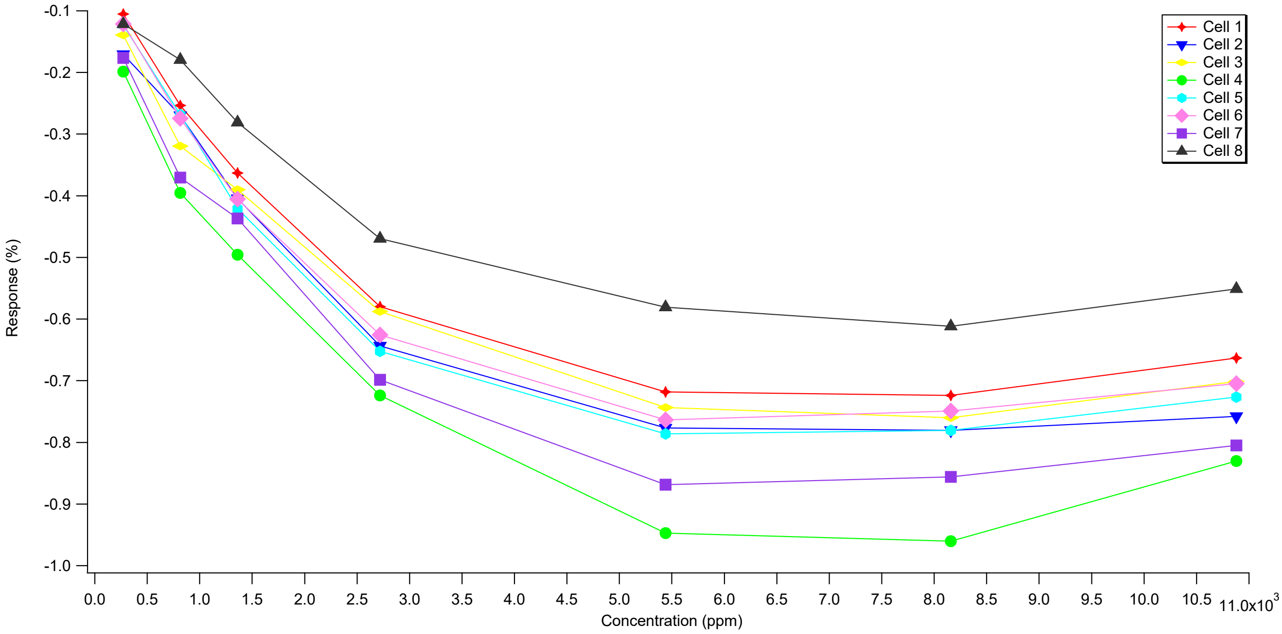

Figure 4.3: Response over concentration for Toluene

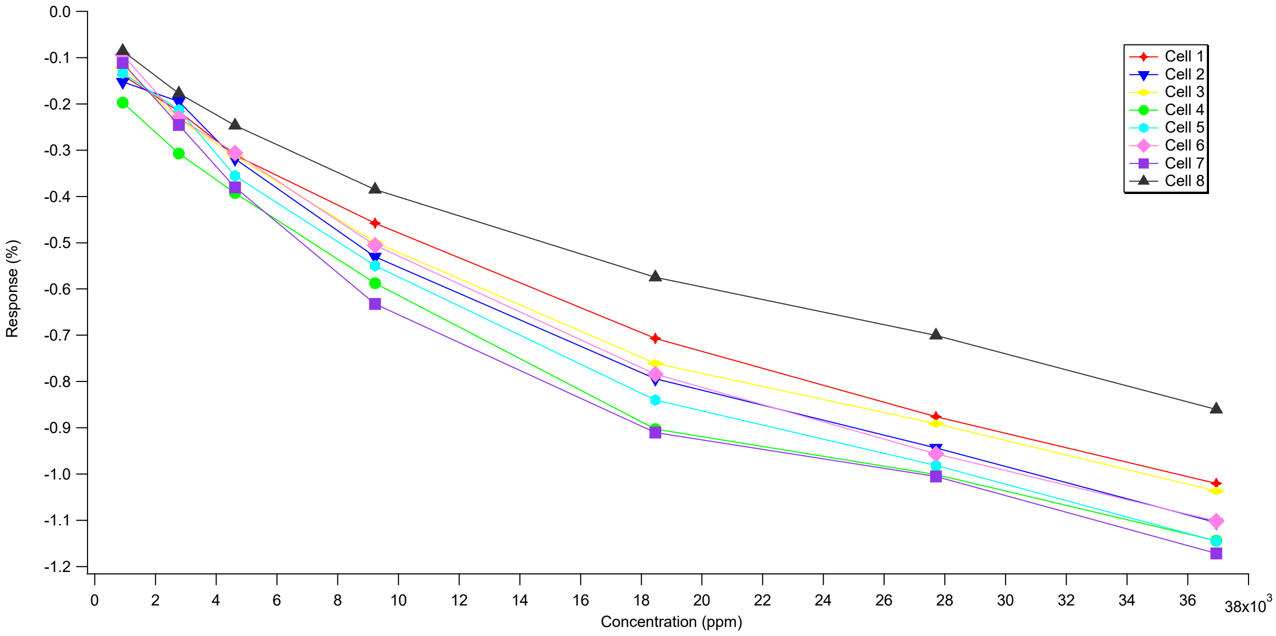

Figure 4.4: Response over concentration for Ethyl acetate

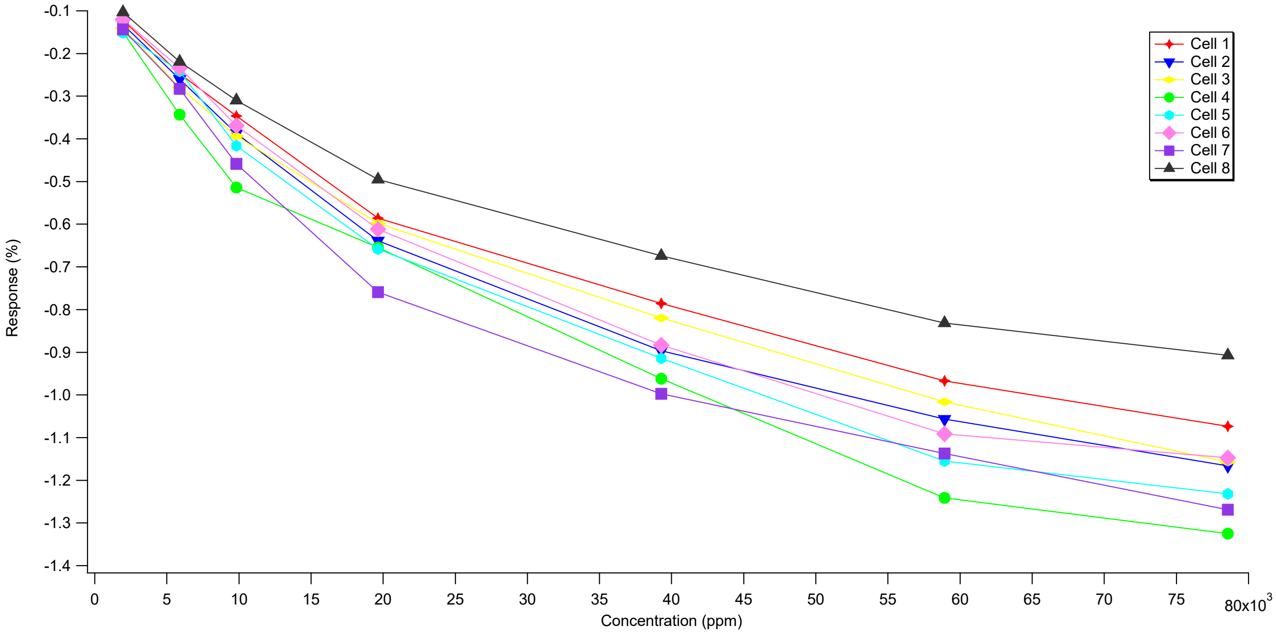

Figure 4.5: Response over concentration for Chloroform

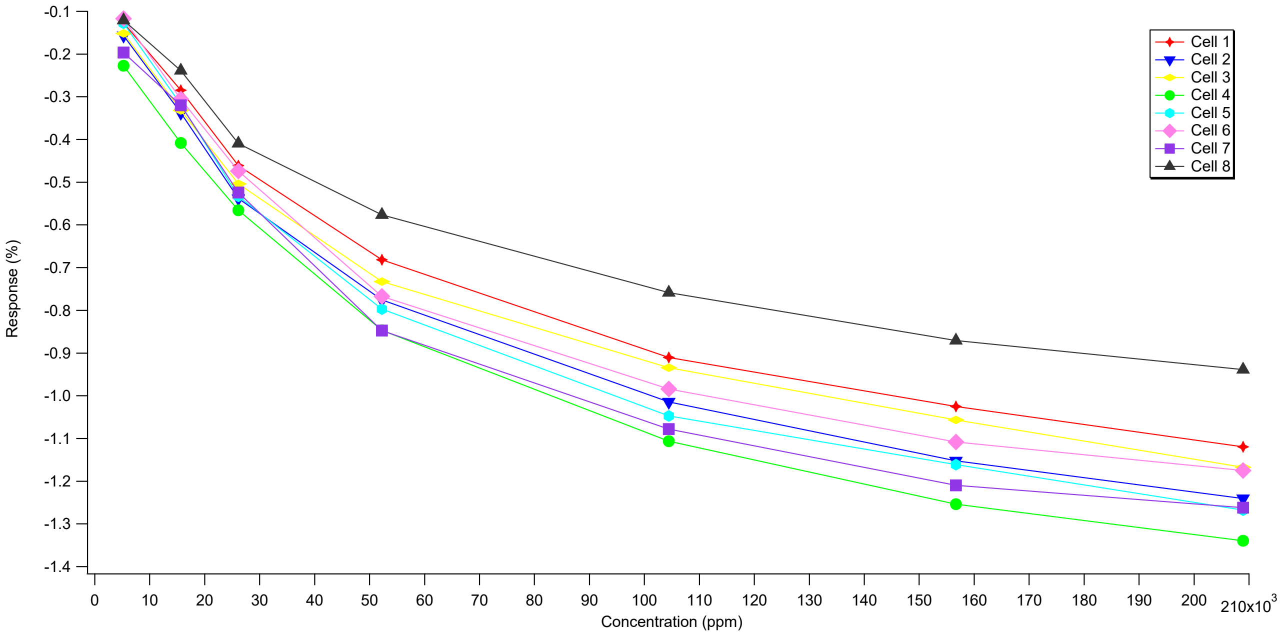

Figure 4.6: Response over concentration for Diethyl ether

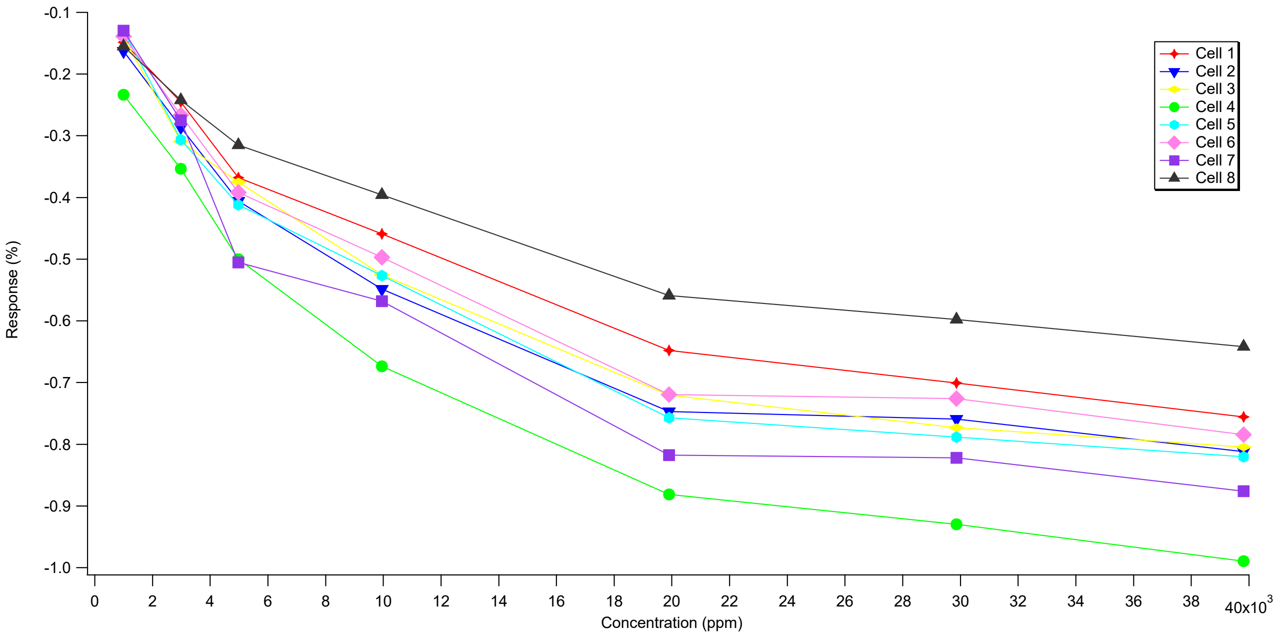

Figure 4.7: Response concentration time for 2-butanone

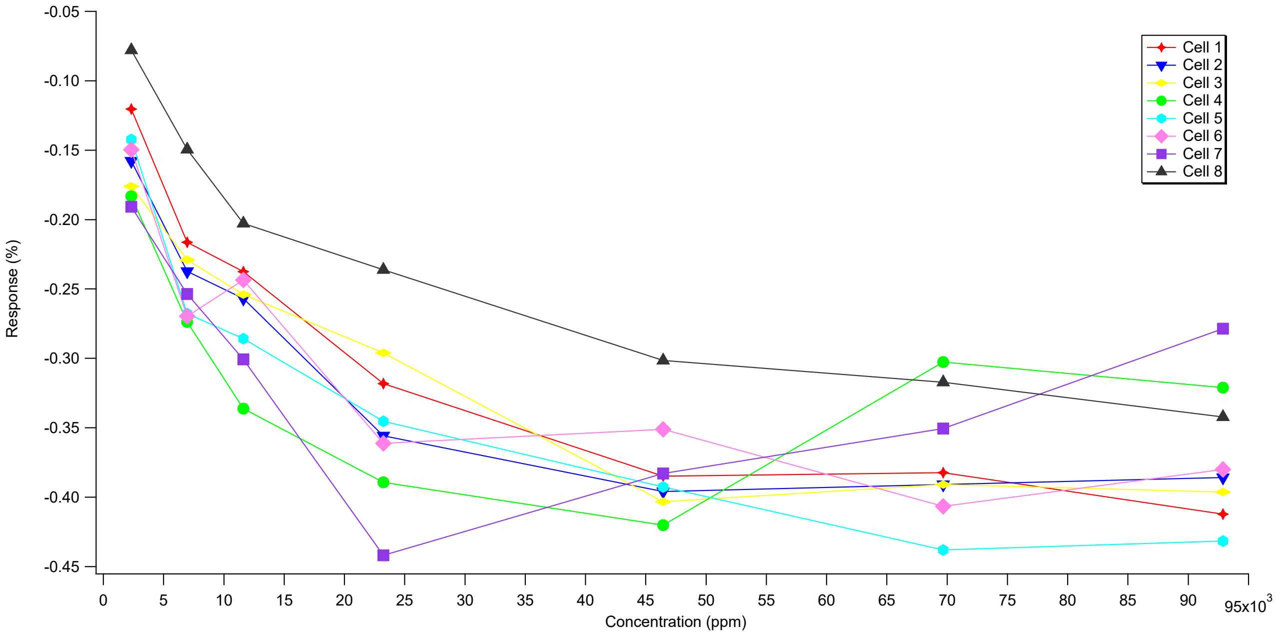

Figure 4.8: Response over concentration for Acetone

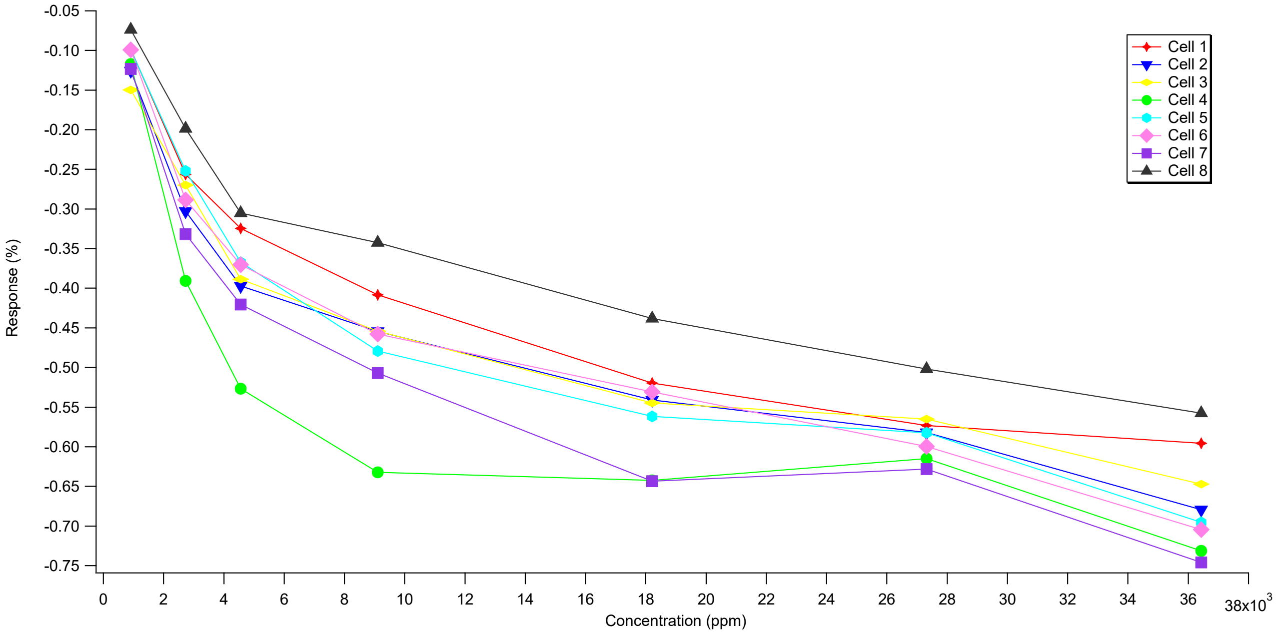

Figure 4.9: Response over concentration for Acetonitrile

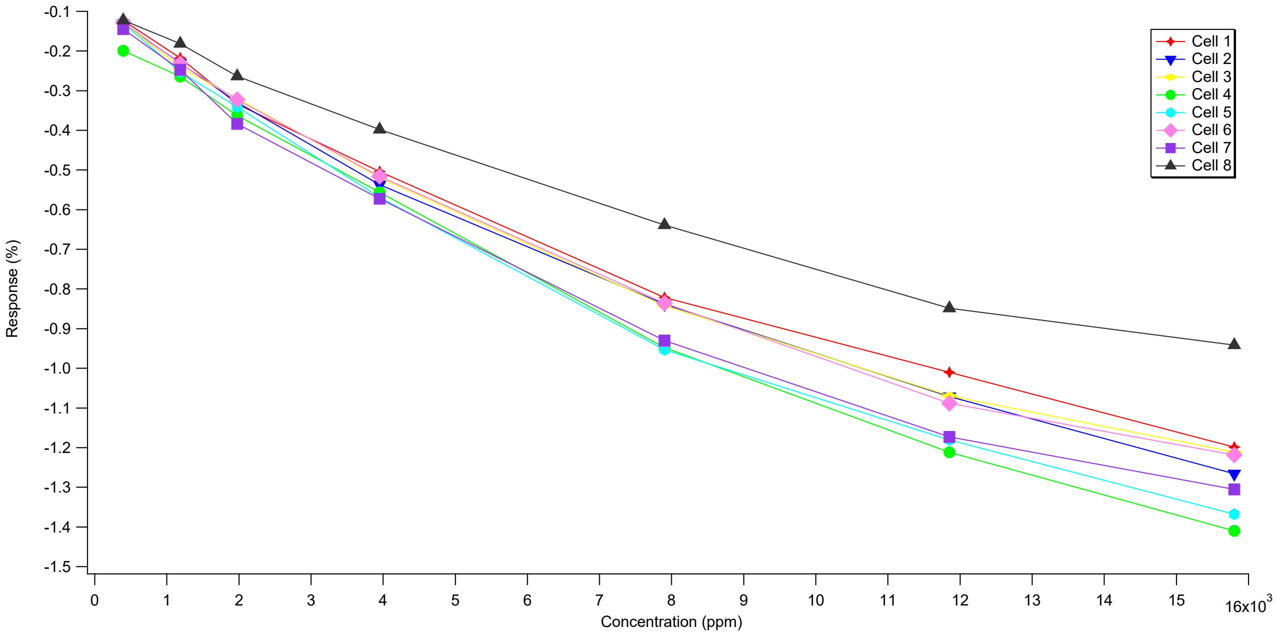

Figure 4.10: Response over concentration for 2-propanol

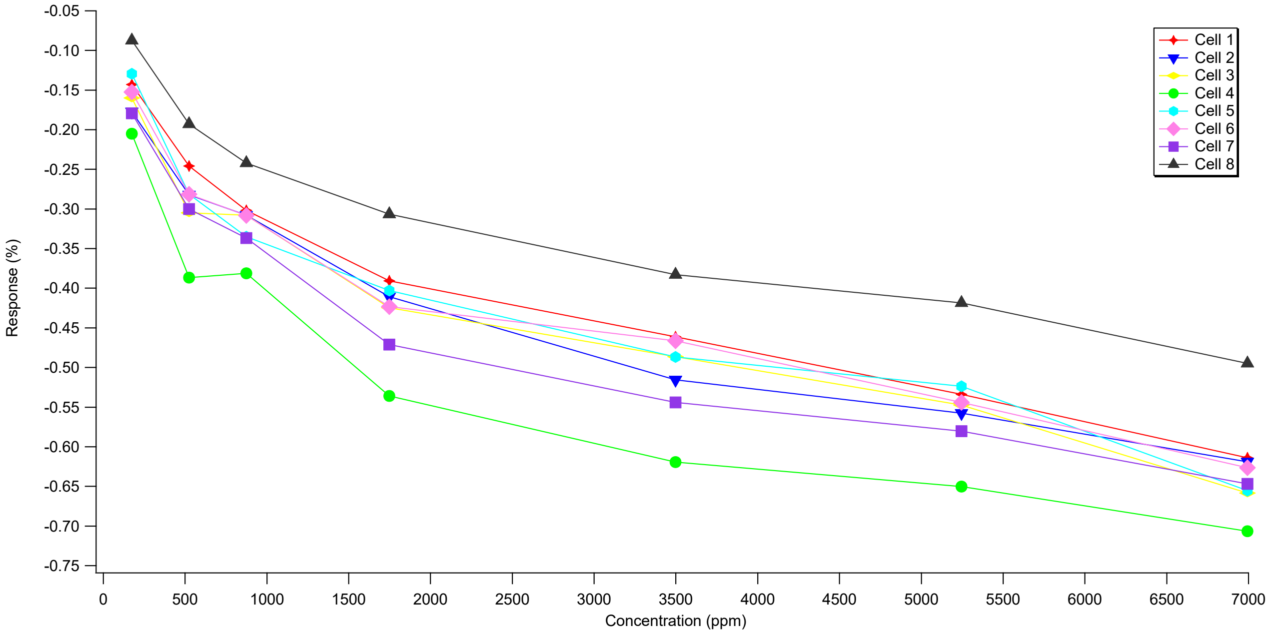

Figure 4.11: Response over concentration for 1-propanol

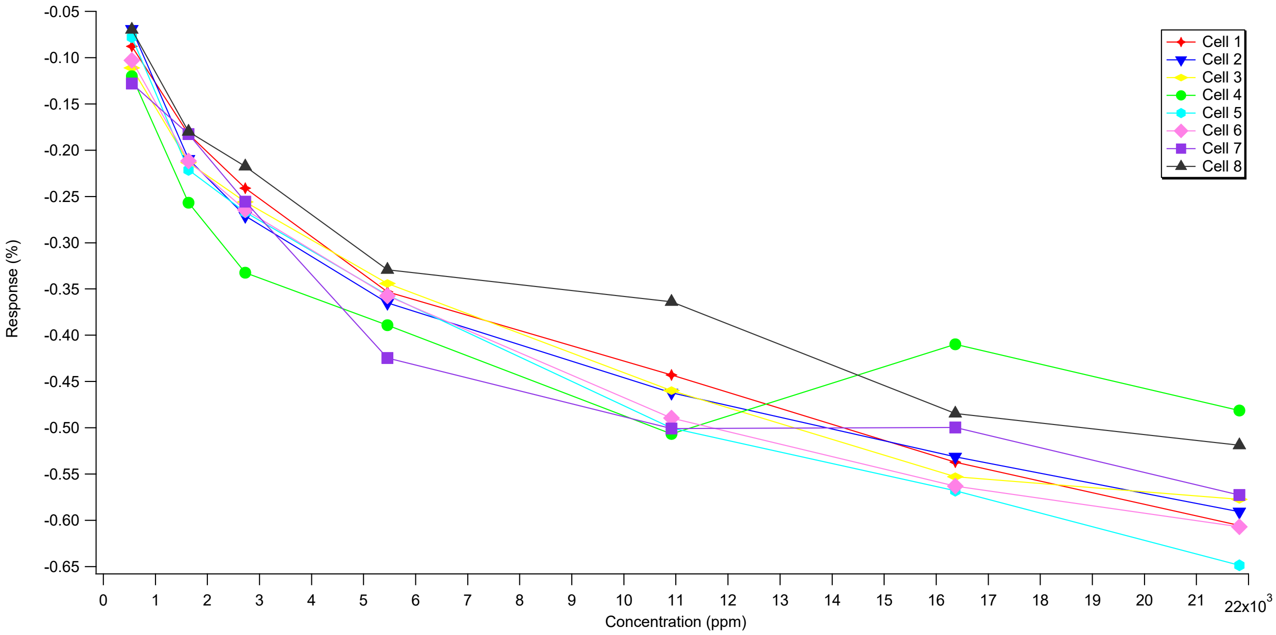

Figure 4.12: Response over concentration for Ethanol

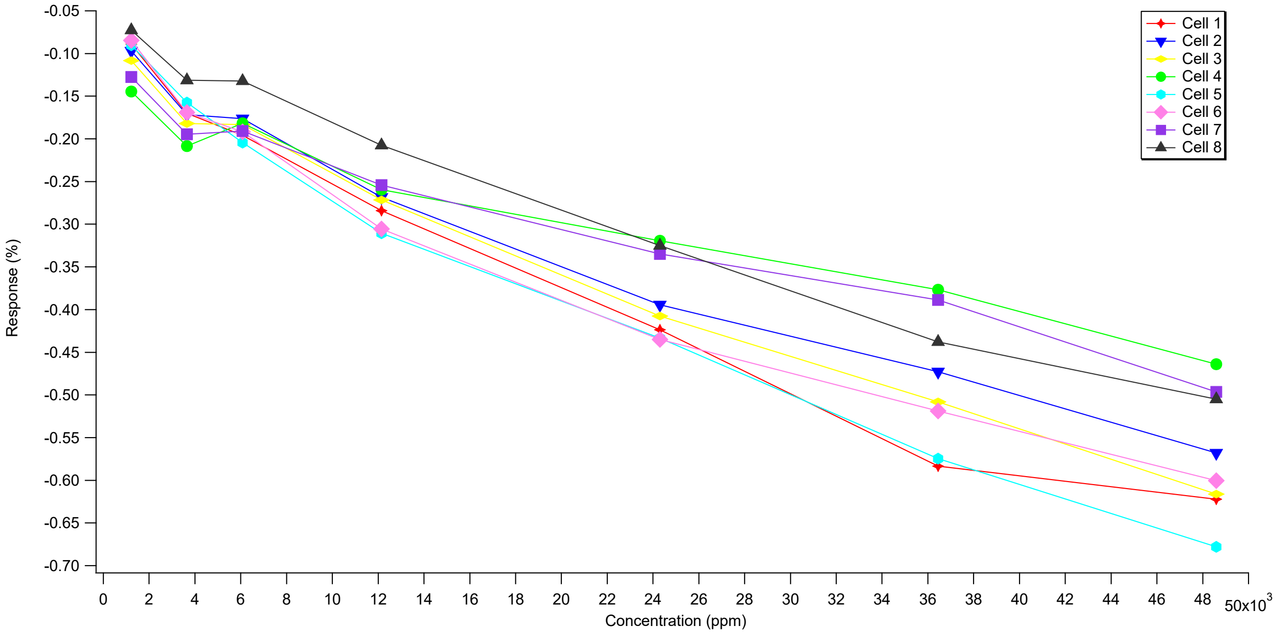

Figure 4.13: Response over concentration for Methanol

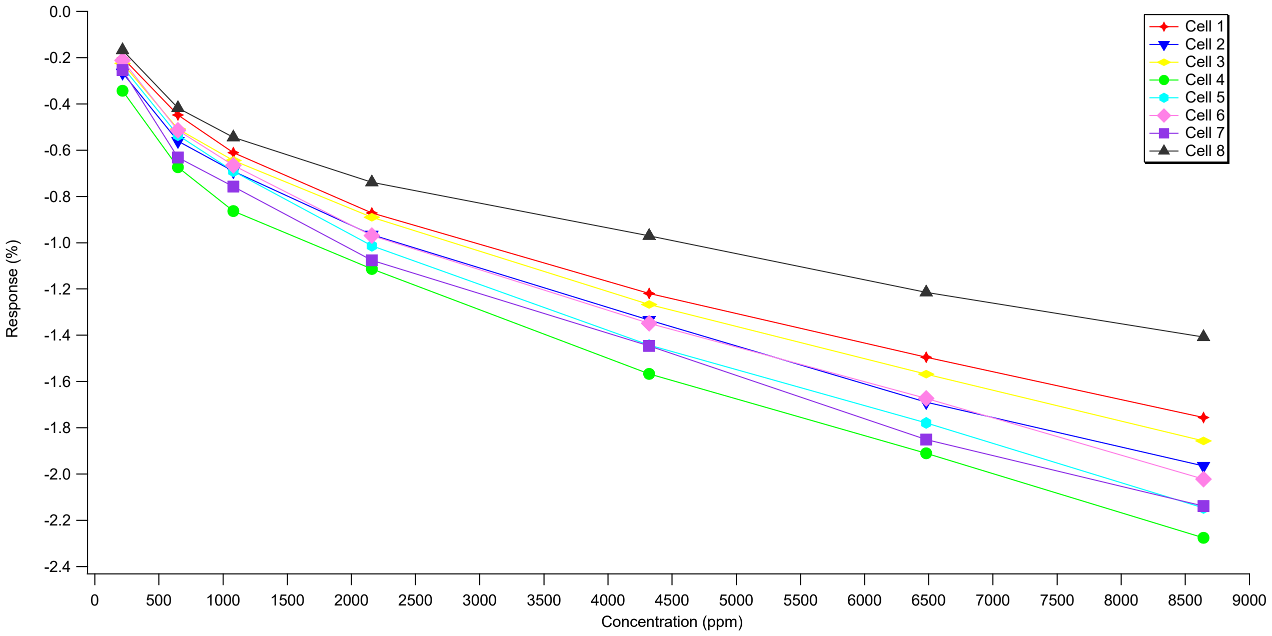

Figure 4.14: Response over concentration for Water

As it can be noticed on all the plots there is a trend on the cells (sensors) response and some cells, such as cell 4, present always better performances compared to other cells, such as cell 8. The reason of this behaviour can be researched on the flow diffusion entering on the polymer chamber.

4.1.2. Comparison between PEDOT:PSS samples

The first sample tested for PEDOT:PSS was TE-I-59, showing really low results in term of response. The next idea was to reduce the thickness of the blade coated active layer film to increase the response. The coated solution of TE-I-59 was then re-used to blade coat two extra samples, one with the same coating condition of TE-I-59, called TE-II-33, achieving a film thickness on a range between 100 and 200 nm, and one with a thinner film called TE-I-31, achieving a film thickness on a range between 15 and 30 nm. According with the test parameters, need to be reported that, due to the high difference in resistance among the TE-II-31 samples, cell 2, 3, 4 and 6 were not measured in order to compare lately the measurement with other material samples with a same degree of resistance. Different behaviours were seen variating the film thickness.

Cell	Resistance (Ω)
1	23.6
2	29.1
3	37.8
4	60.9
5	31.6
6	51
7	48.9
8	69.6

Table 4.1: Resistance value of TE-II-33

Cell	Resistance (Ω)
1	2325
2	350
3	426.7
4	560
5	1781
6	21.1
7	3790
8	4600

Table 4.2: Resistance values of TE-II-31

The first and not really well understood behaviour was the difference on the baseline of the two samples. For the first sample, TE-II-33, the baseline was measured over 30 hours of dry air exposure while TE-II-31 over 36.

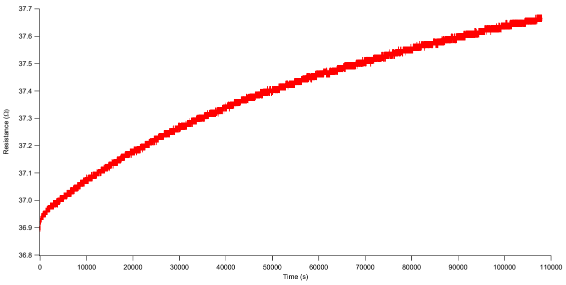

Figure 4.15: Baseline for TE-II-33, measured over 30 hours

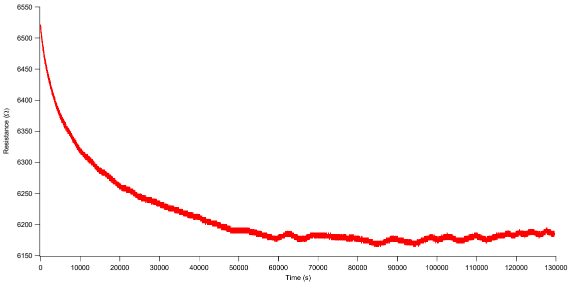

Figure 4.16: Baseline for TE-II-31, measured over 36 hours

The reason on these two different behaviours, even though the material is the same, can be researched on the time dependent desorption of the enviromental humidity on the thicker film (the polymer chamber is open to the environment when no flow is blown on the system), faster on the thinner film, or on a different conduction principle in the two cases. In fact, in the first case, the thicker film, the resistance increase all over the exposure time while in the second decrease, syntomous of an increasement of conductivity.

The other fenomenum noticed was the enhanced response value on the thinner film, as predicted.

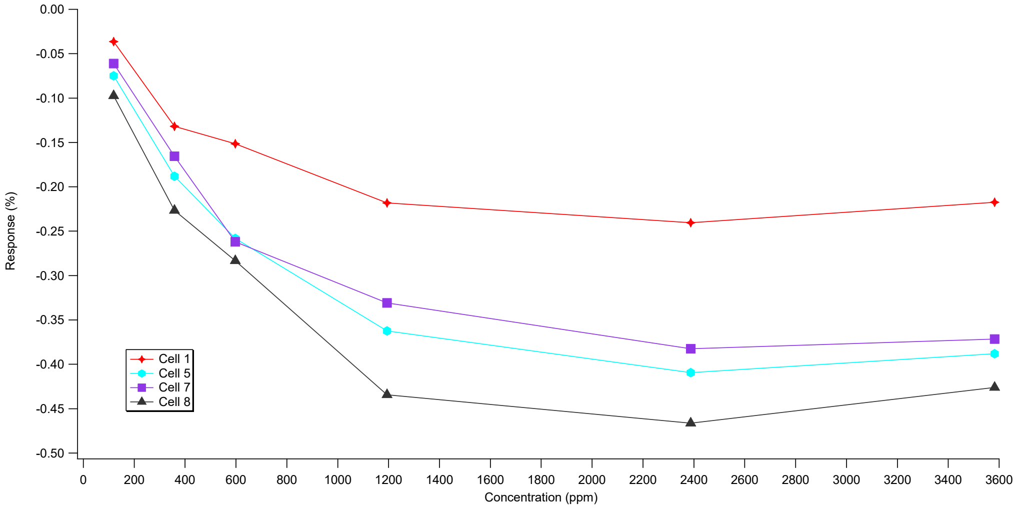

Figure 4.17: Response over concentration for Octane on TE-II-33

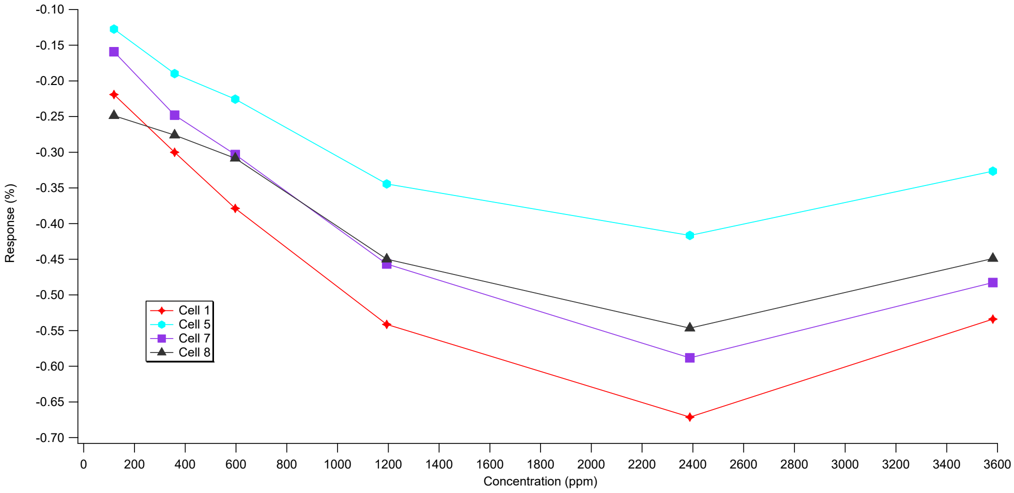

Figure 4.18: Response over concentration for Octane on TE-II-31

The case reported is for Octane, but the same behaviour was noticed all over the 6 analyte tested and the degree of increment was between 120 to 160 %.

4.2. Polypyrrole

4.2.1. First measurements with polypyrrole

The sample TE-II-24 is not the first sample tested for polypyrrole but it is the sample with the results more comparable with the other material tested; the other sample of polypyrrole will be discussed further in this chapter. The sample on this paragraph was drop-casted and tested over 6 analytes with a concentration max of 30% of volume of the solvent. The exposure time was 3 minutes and the recovery time 10. The response plots over the different concentrations are listed below.

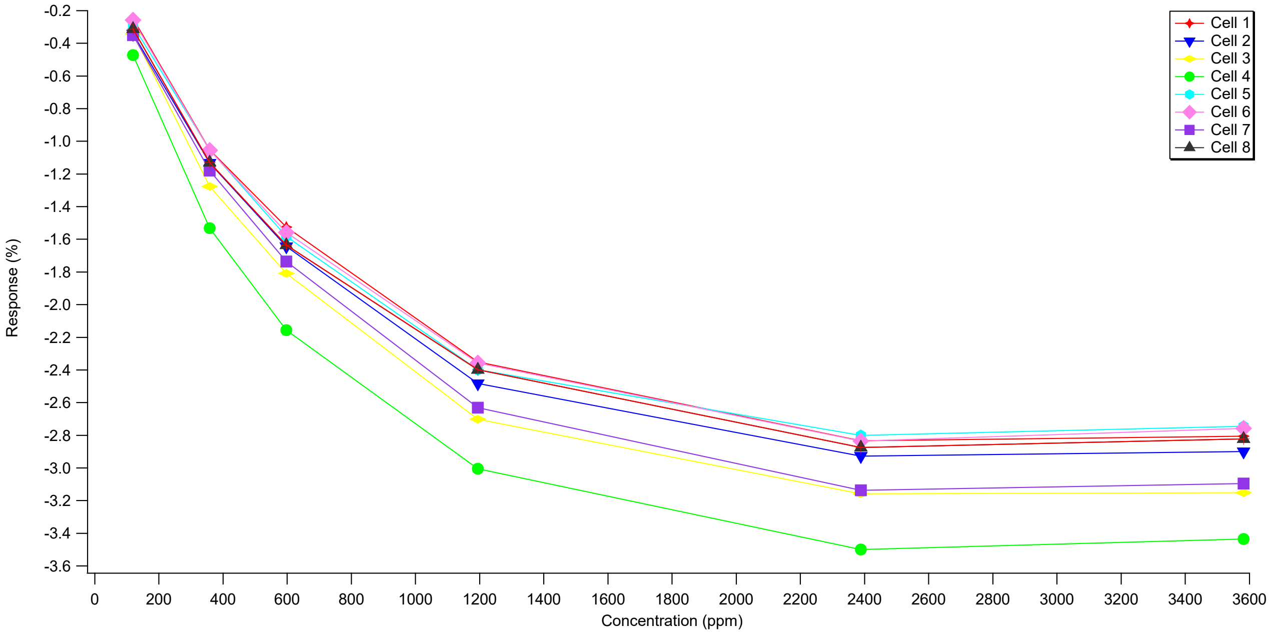

Figure 4.19: Response over concentration for Octane

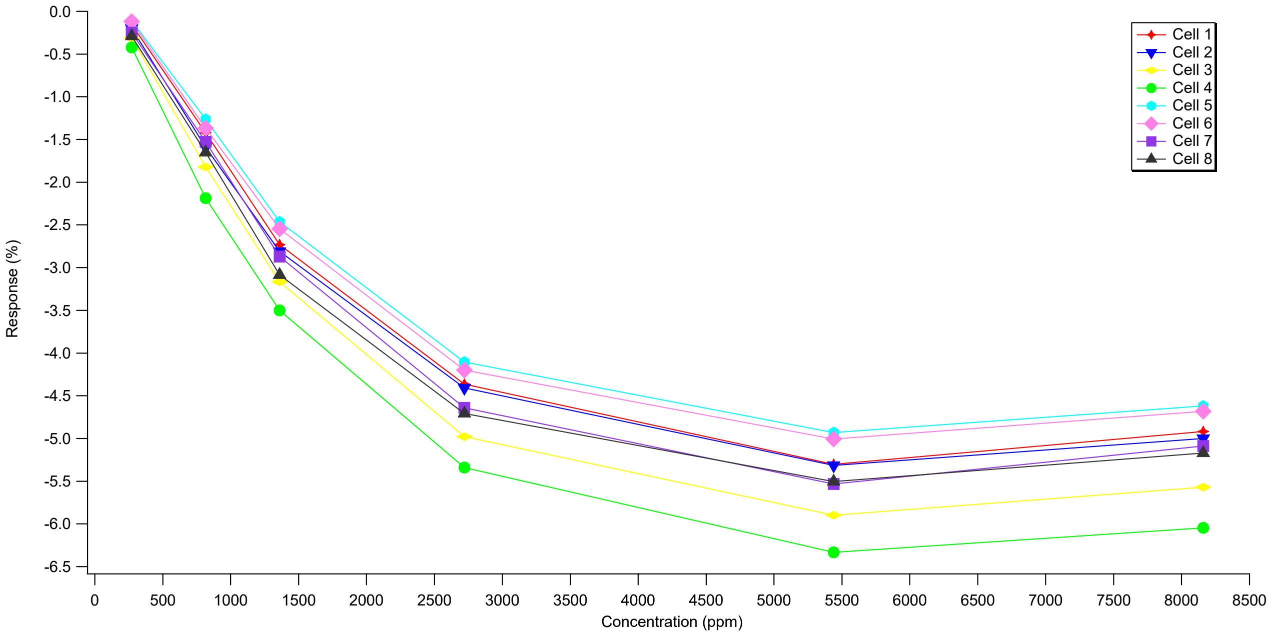

Figure 4.20: Response over concentration for Toluene

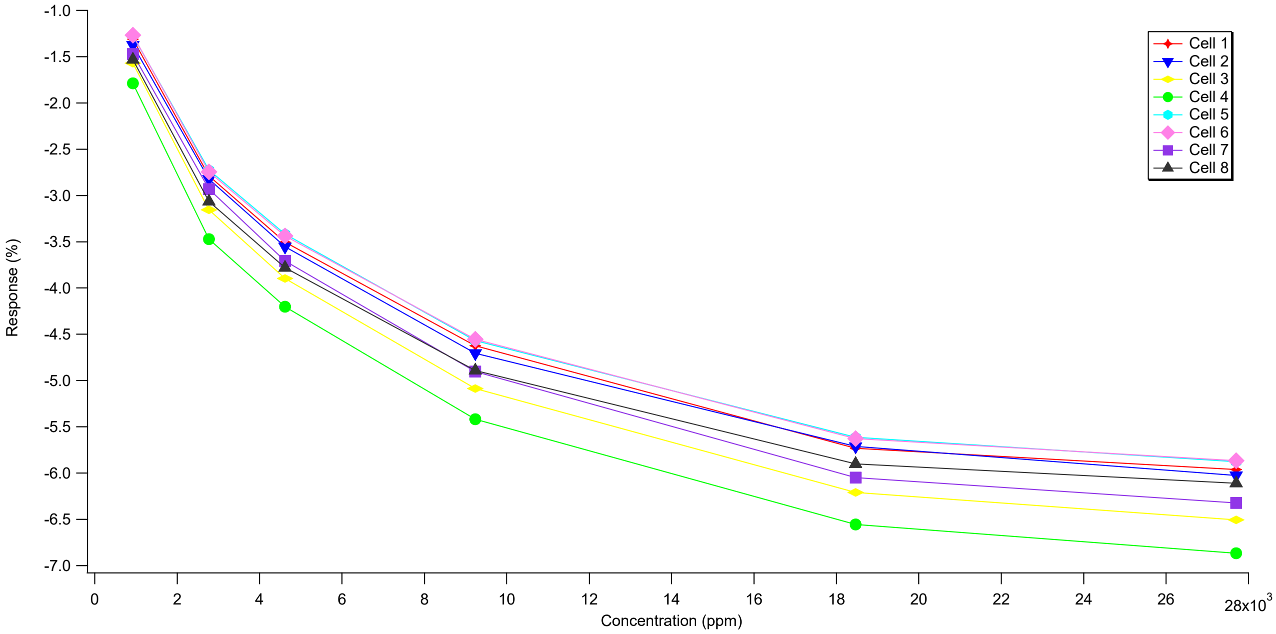

Figure 4.21: Response over concentration for Ethyl acetate

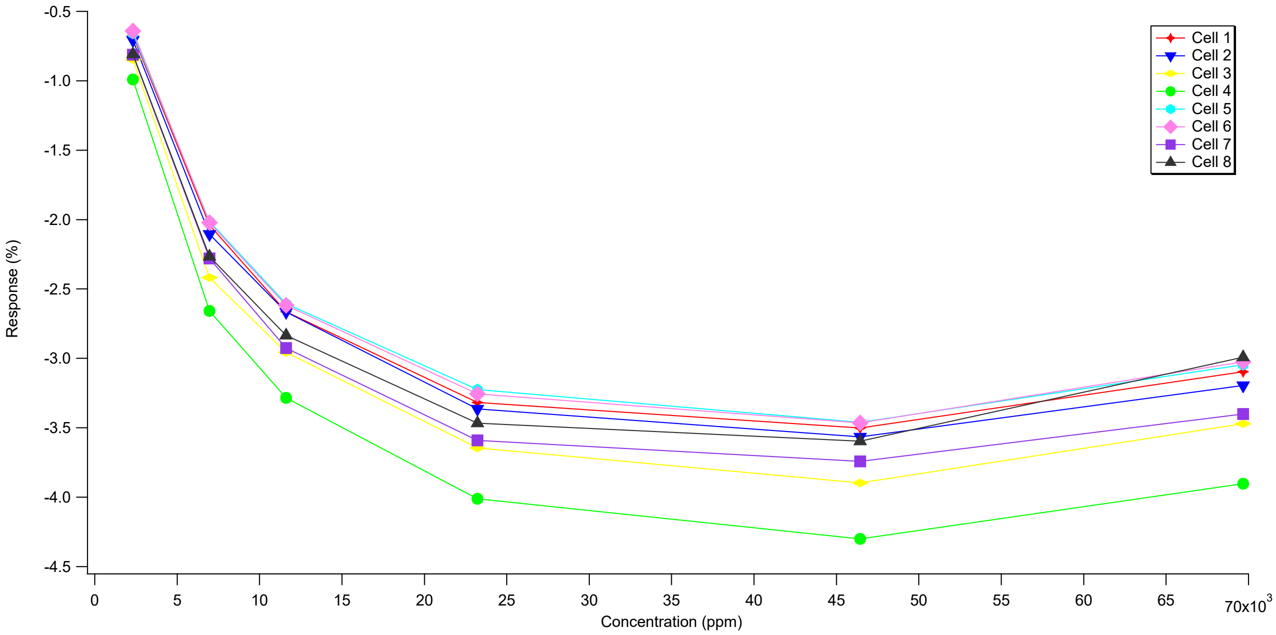

Figure 4.22: Response over concentration for Acetone

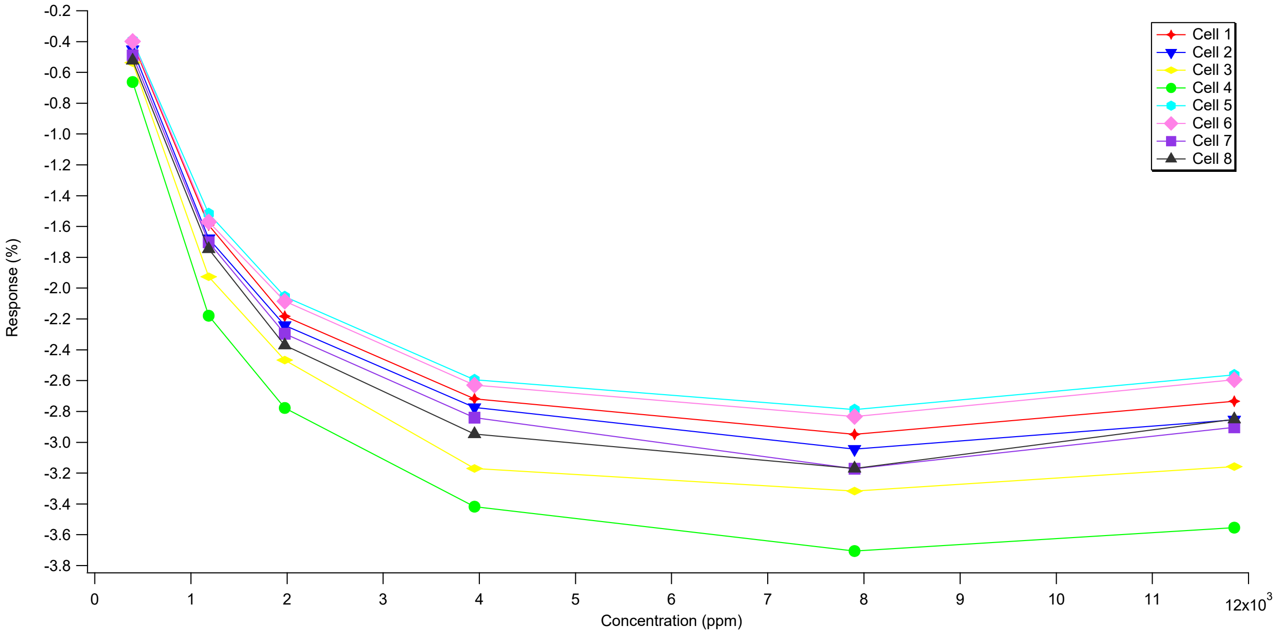

Figure 4.23: Response over concentration for 2-propanol

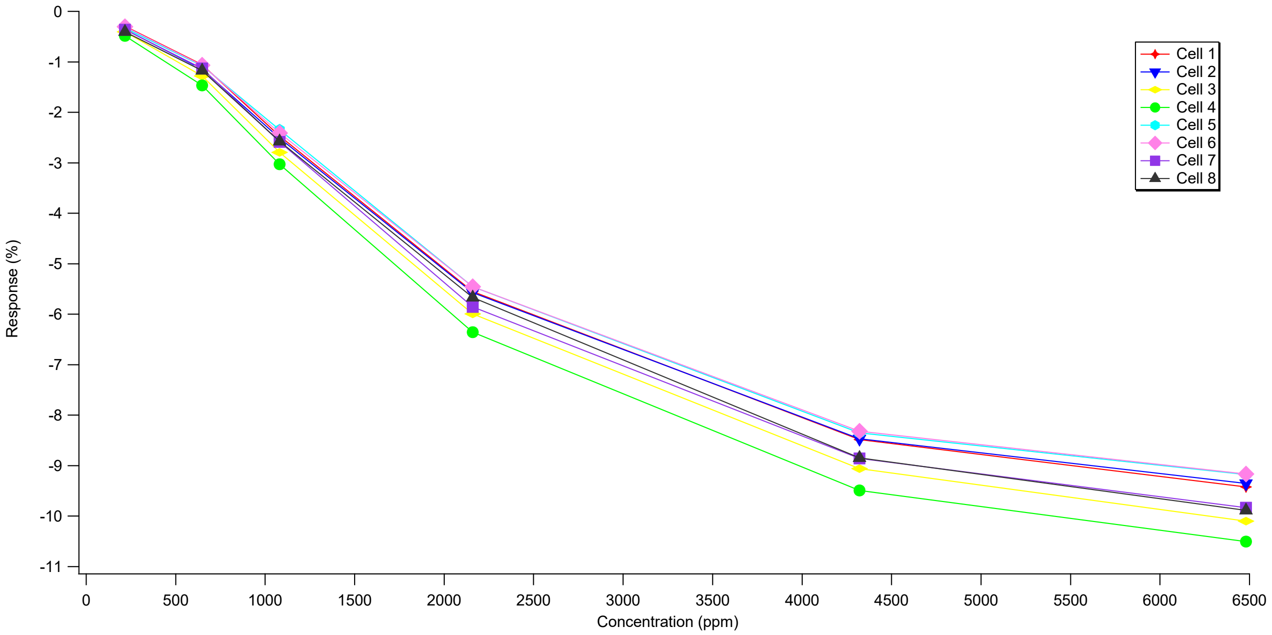

Figure 4.24: Response over concentration for Water

4.2.2. Comparison between polypyrrole samples

Another sample of polypyrrole was tested using a different dopant. This second sample, TE-II-20, was actually the first tested, but the results in term of response were extremely uncomplacent and dispersed. The reason was on the dispersion of the PPy polymer inside of the solution used to drop-cast the active layer, coagulated and not stable; In fact, the solution was just drop-casted and placed on the electrodes gap using a precision syringe. As usual the case of Octane is reported but the same behaviour was noticed on all the 6 analytes case of study.

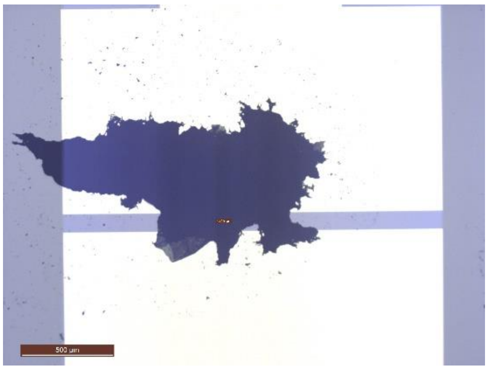

Figure 4.25: Sulfate doped PPy on cell 1 for TE-II-20

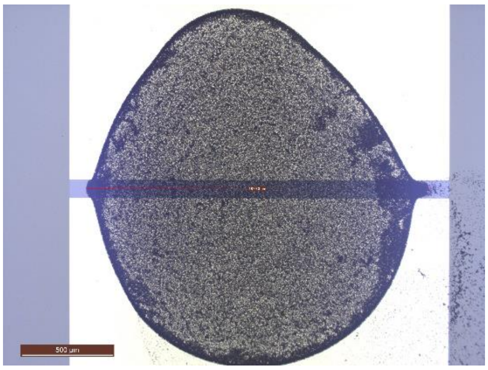

Figure 4.26: HCl doped PPy on cell 1 for TE-II-24

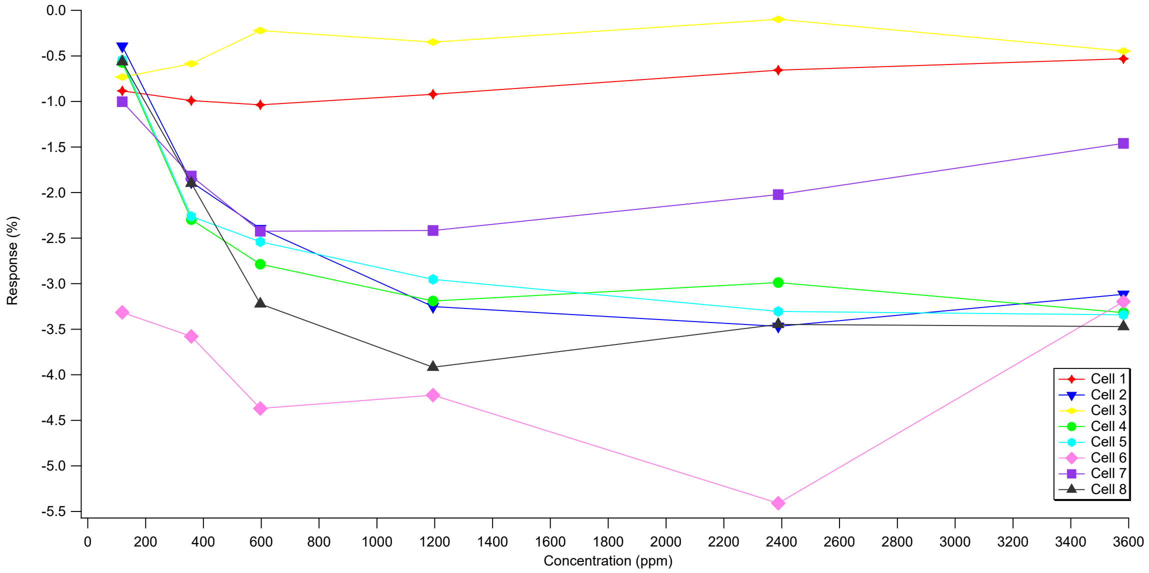

Figure 4.27: Response over concentration for Octane on TE-II-20

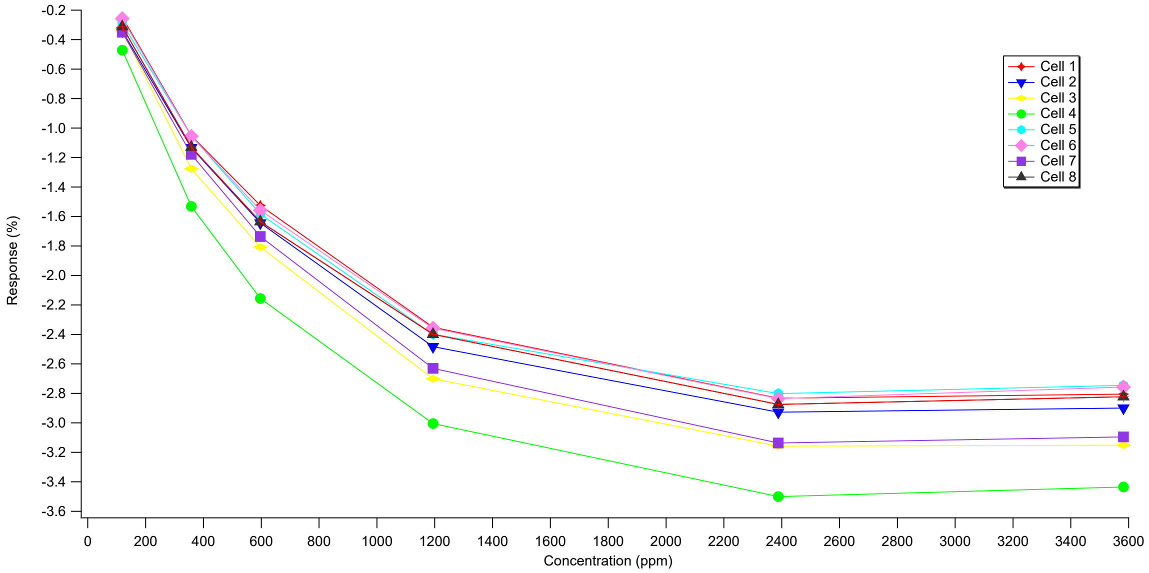

Figure 4.28: Response over concentration for Octane on TE-II-24

Even though the results of PPy TE-II-20 can’t be used an important and promising behaviour especially of cell 1, also found on some literature, was noticed.

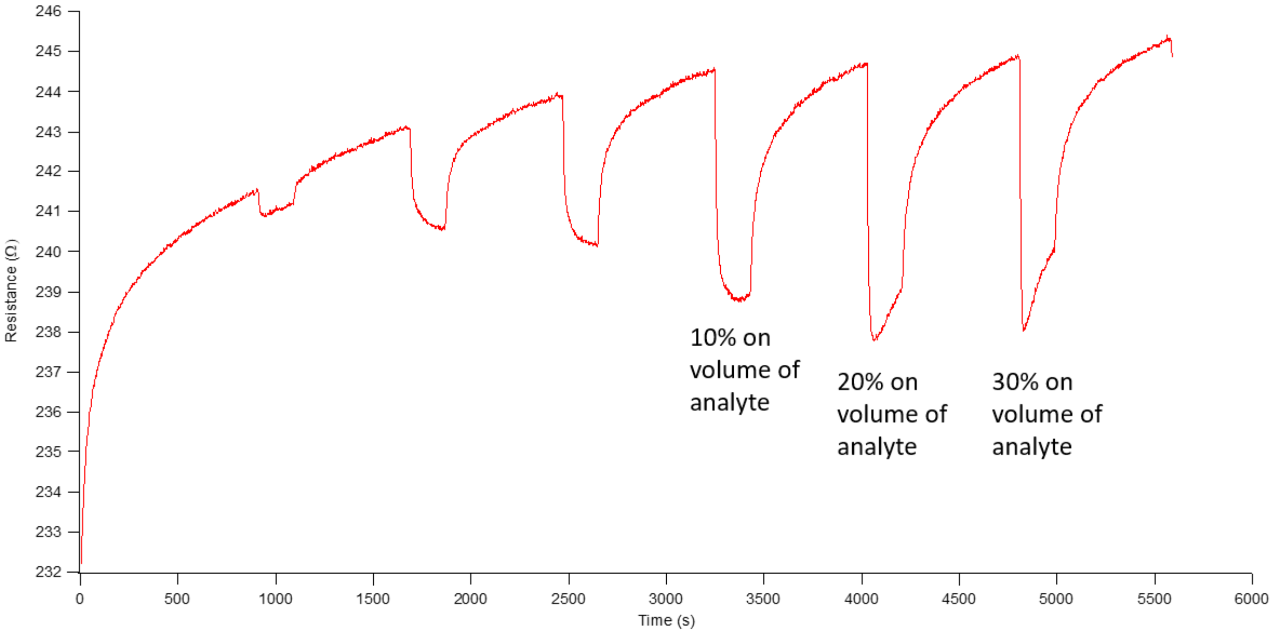

Figure 4.29: Resistance over time on cell 1, Octane for TE-II-24

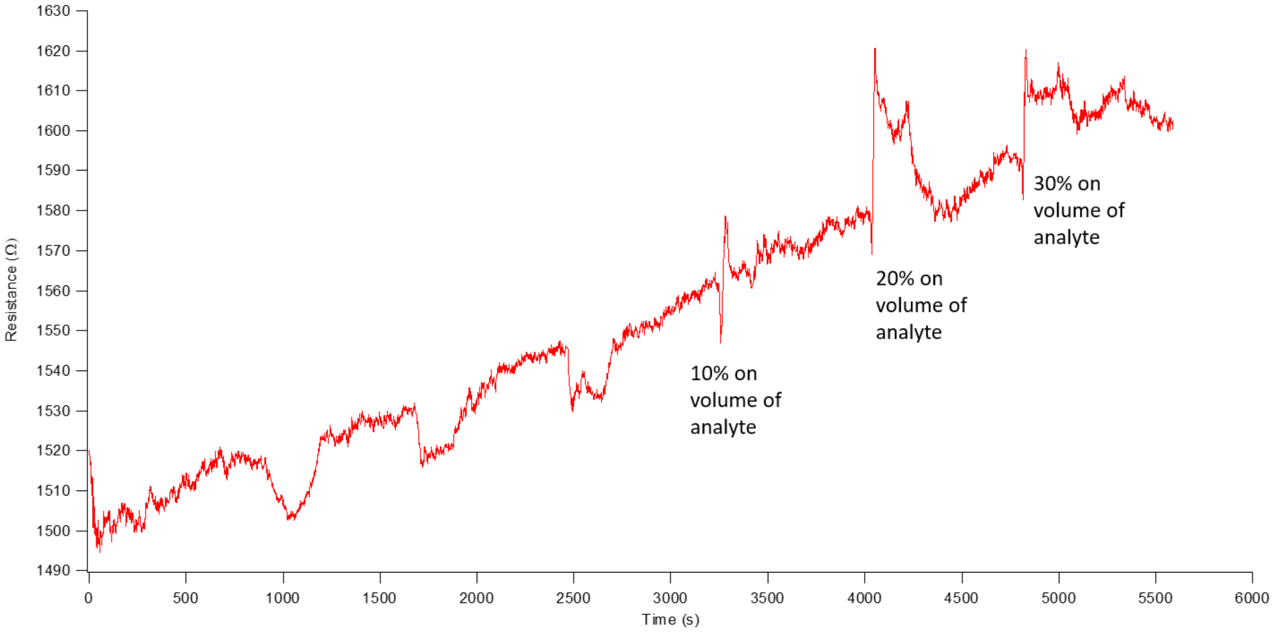

Figure 4.30: Resistance over time on cell 1, Octane for TE-II-20

Even though the sulphate doped sample present higher noise it is clear, comparing the peaks direction of the high concentration's analyte, that while in the first case there is a reduction of resistance due to the analyte doping of the active layer, in the second case an opposite tendency is present. Especially around 10% on volume of gaseous analyte there is a change on direction, suggesting a de-doping phenomenon. This behaviour is not only important to understand the different kind of reaction on the film but also a certain degree on selectivity among all the analytes.

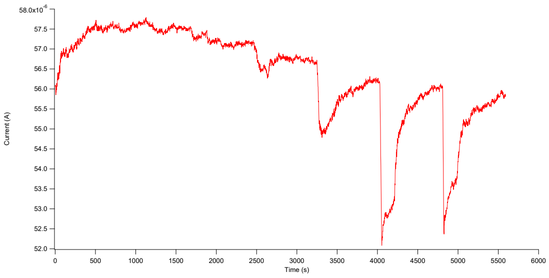

Figure 4.31: Resistance over time on cell 1, Toluene for TE-II-20

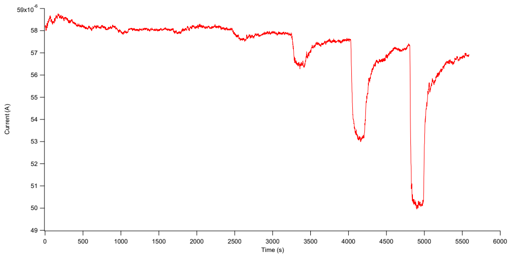

Figure 4.32: Resistance over time on cell 1, Ethyl acetate for TE-II-20

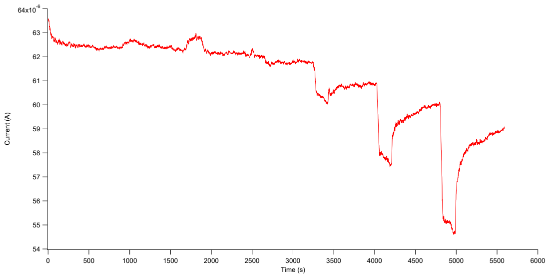

Figure 4.33: Resistance over time on cell 1, Acetone for TE-II-20

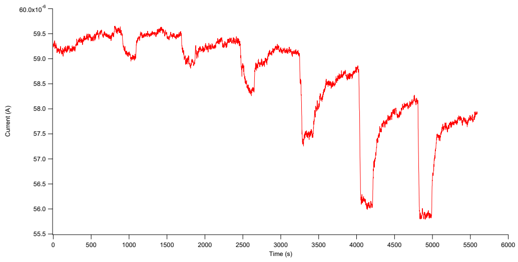

Figure 4.34: Resistance over time on cell 1, 2-propanol for TE-II-20

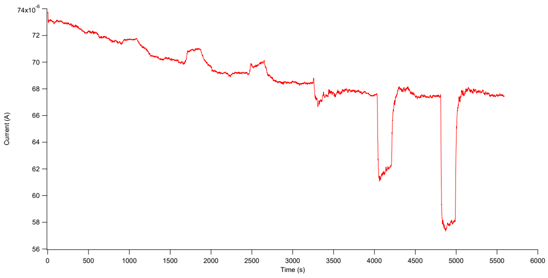

Figure 4.35: Resistance over time on cell 1, Water for TE-II-20

The reason of this statement is becouse the fixed concentration where there is a change on direction on the peaks on different analytes is different and finding this value can lead to a discrimination on the type of analaty sensed. The only problem is the usual high concentration where the variation occurs, but analizing the response over concentration plot a different trend is present for each analyte and from there a selection of the sensed substance is possible.

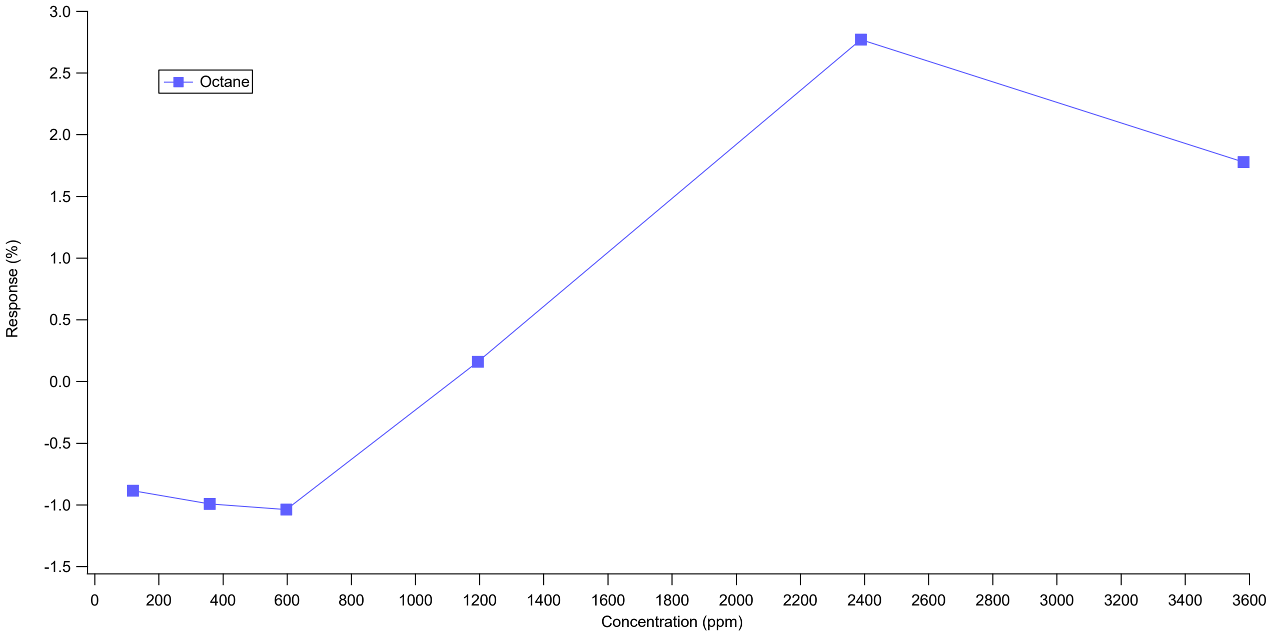

Figure 4.36: Response over concentration plot for Octane on TE-II-20

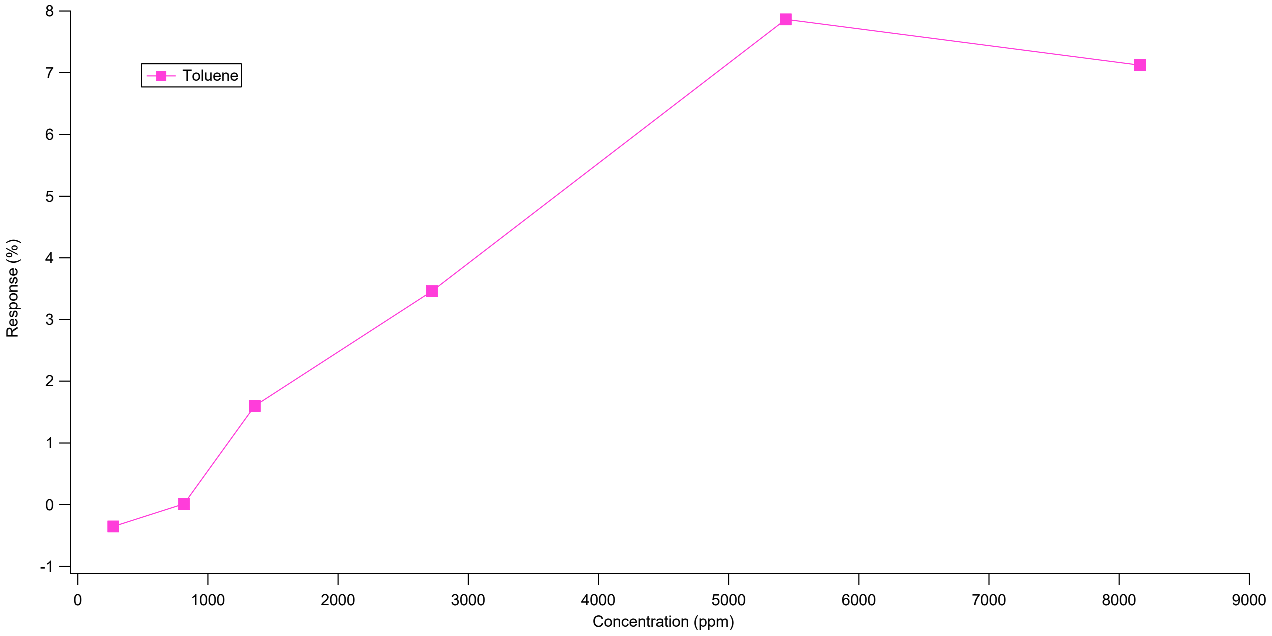

Figure 4.37: Response over concentration plot for Toluene on TE-II-20

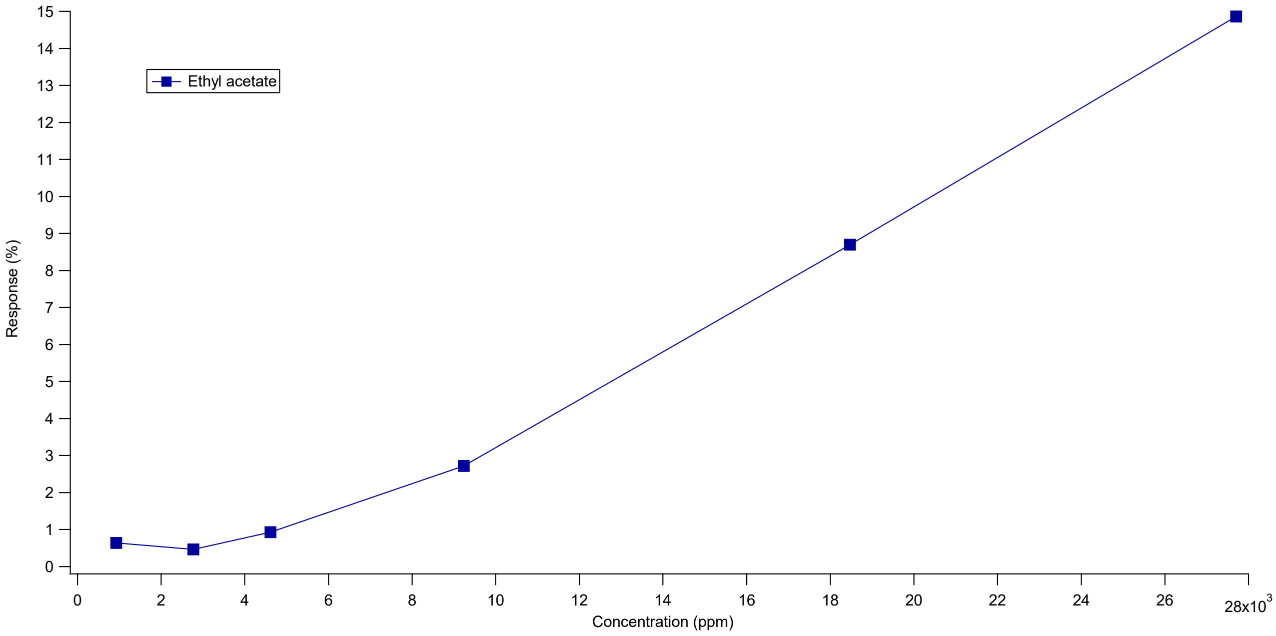

Figure 4.38: Response over concentration plot for Ethyl acetate on TE-II-20

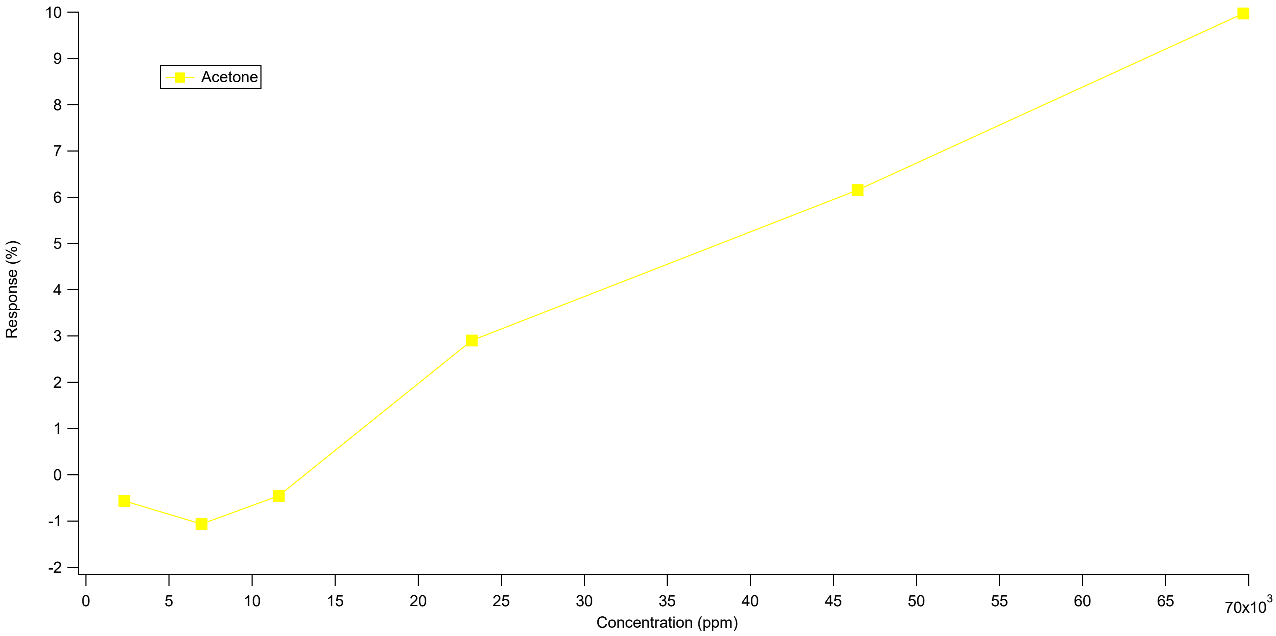

Figure 4.39: Response over concentration plot for Acetone on TE-II-20

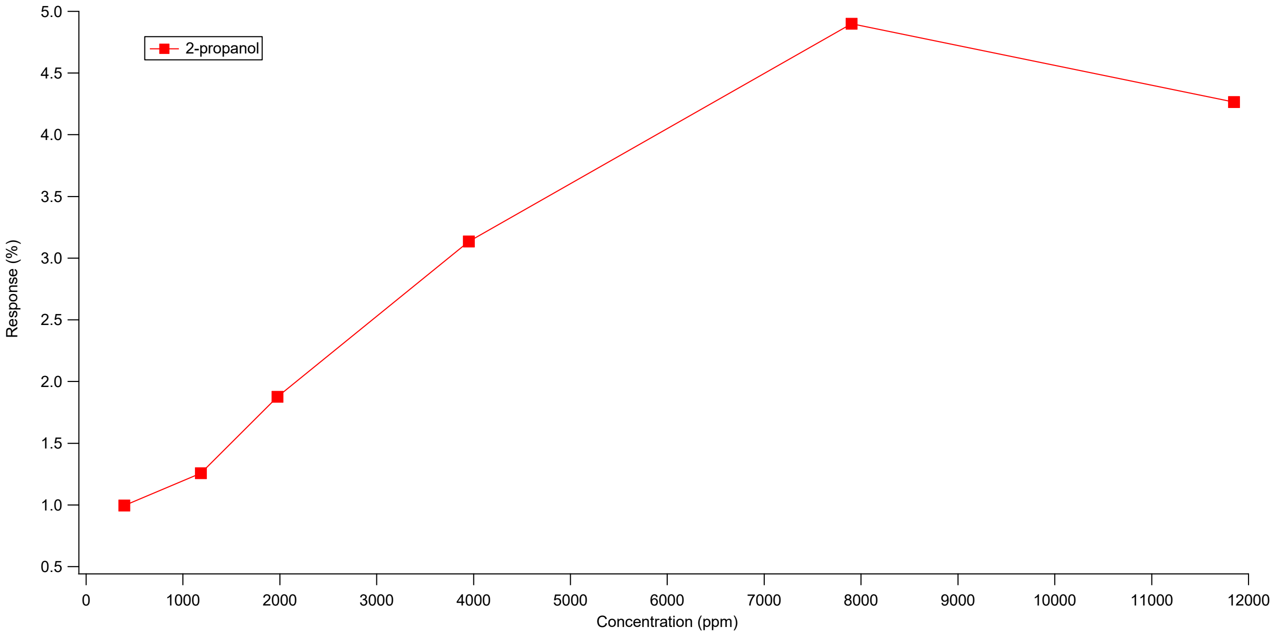

Figure 4.40: Response over concentration plot for 2-propanol on TE-II-20

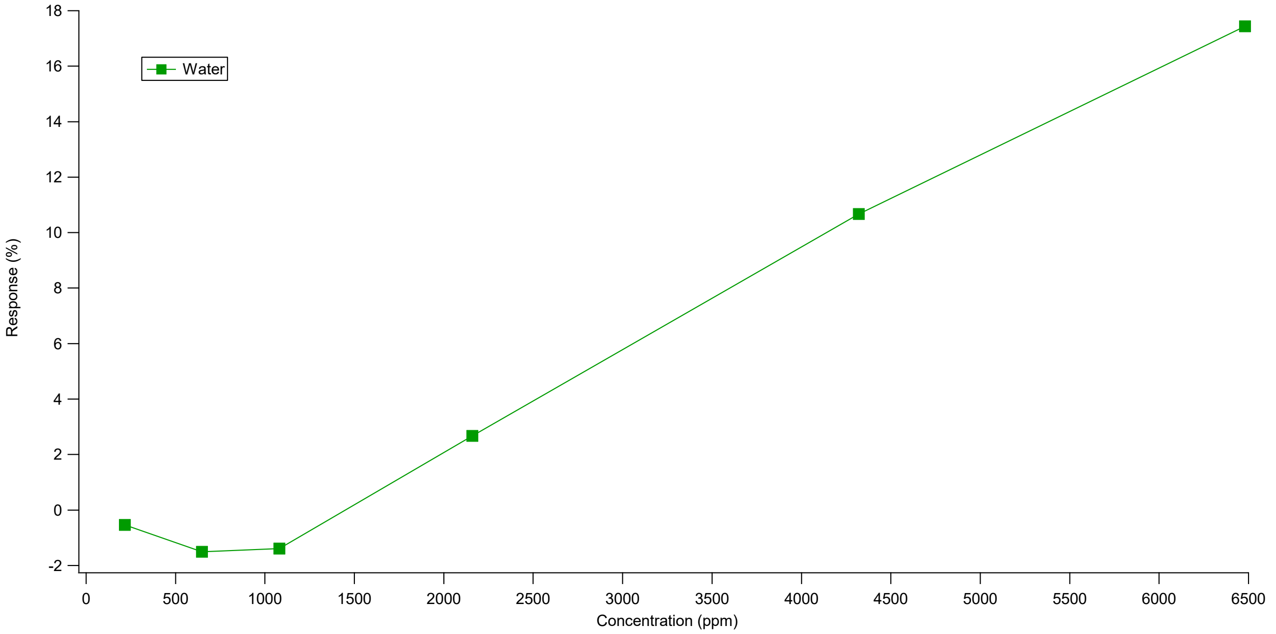

Figure 4.41: Response over concentration plot for Water on TE-II-20

4.3. Polyaniline

4.3.1. First measurements with polyaniline

In the case of polyaniline, due to the high number of different solutions prepared, the device was always coated with two different polymeric solution on the different sensor's lines. In particular, from cell 1 to cell 4 with one solution and from cell 5 to 8 with a different one. The first sample granting accurate results was TE-I-70. The sample was drop-casted and tested over the all 14 analytes with a maximum concentration of 40% on volume. As usual, the exposure time was 3 minutes and the recovery time 10. The results achieved are reported in the following plots.

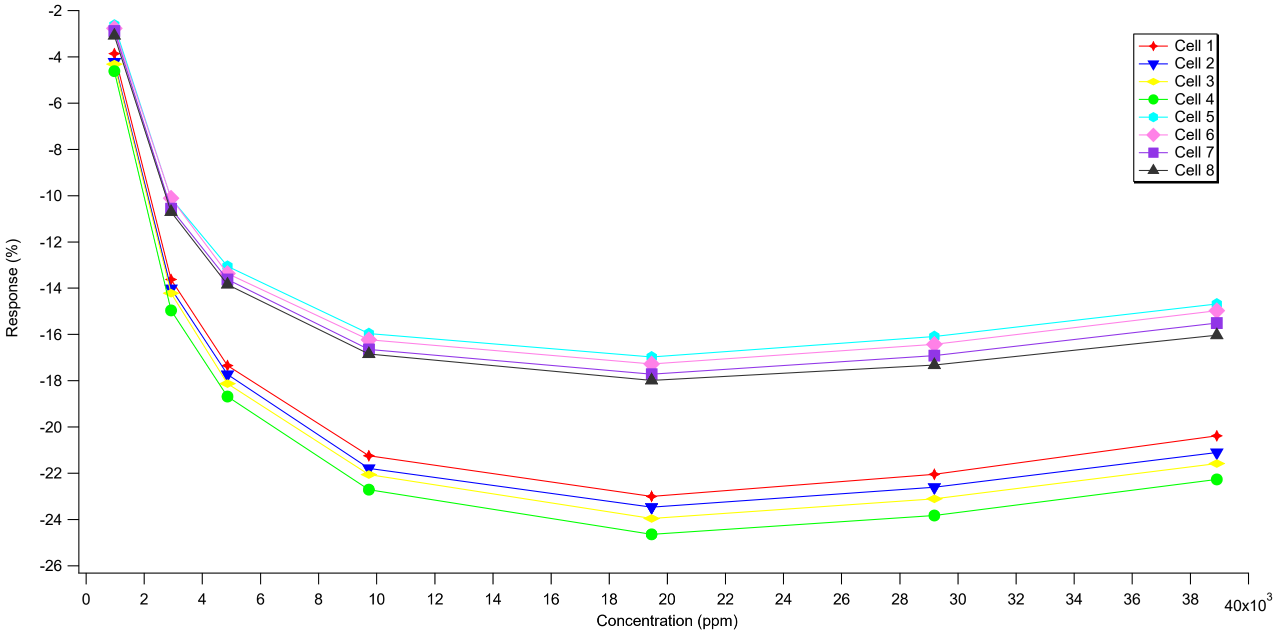

Figure 4.42: Response over concentration for Cyclohexane

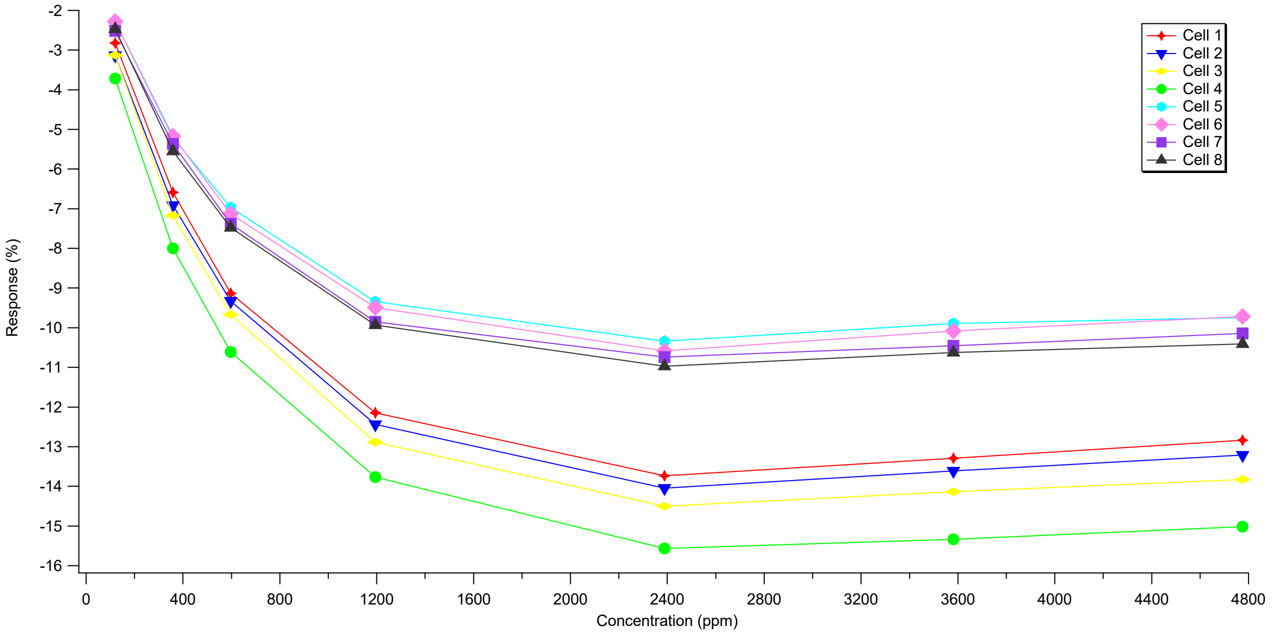

Figure 4.43: Response over concentration for Octane

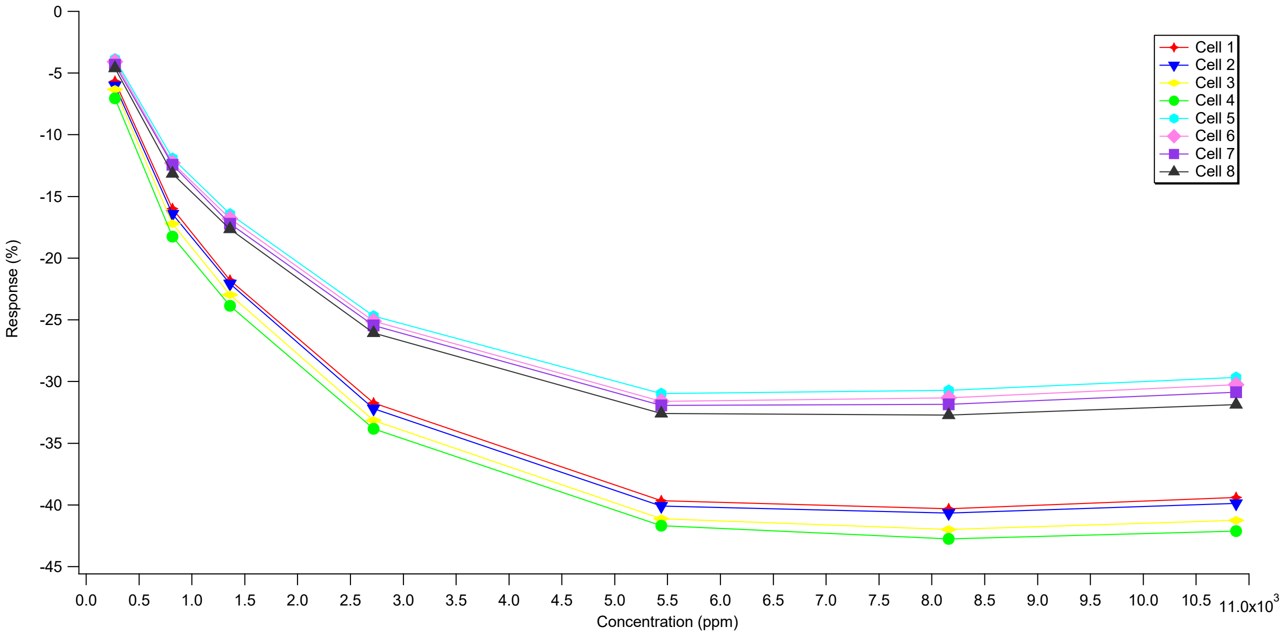

Figure 4.44: Response over concentration for Toluene

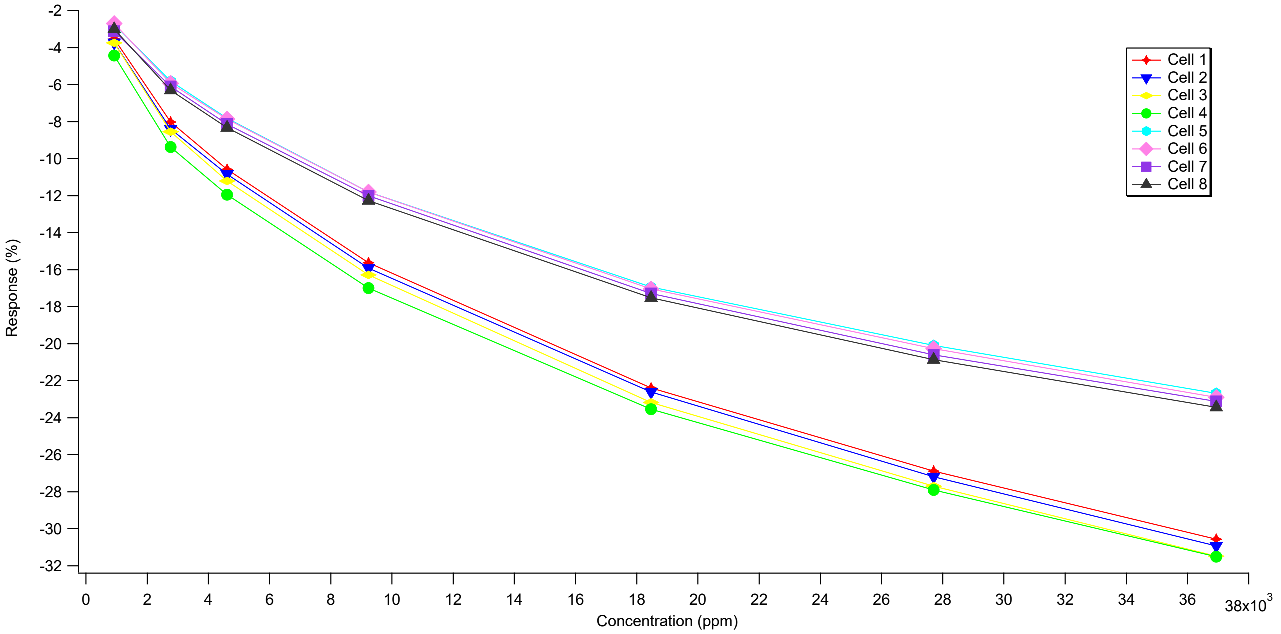

Figure 4.45: Response over concentration for Ethyl acetate

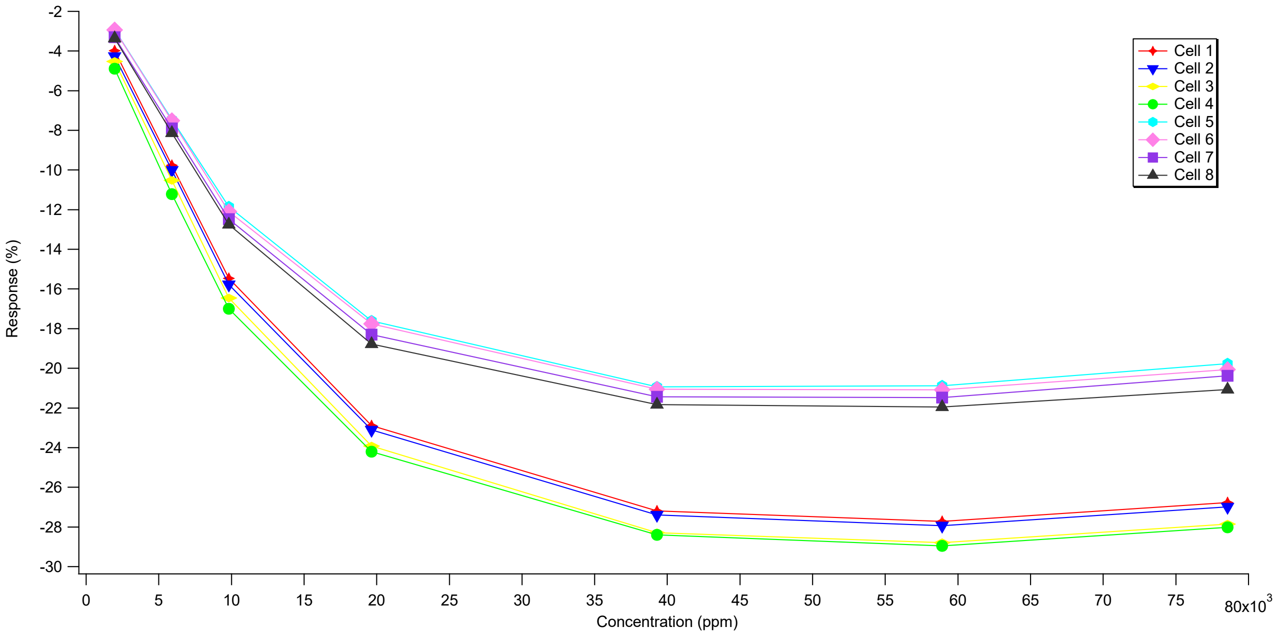

Figure 4.46: Response over concentration for Chloroform

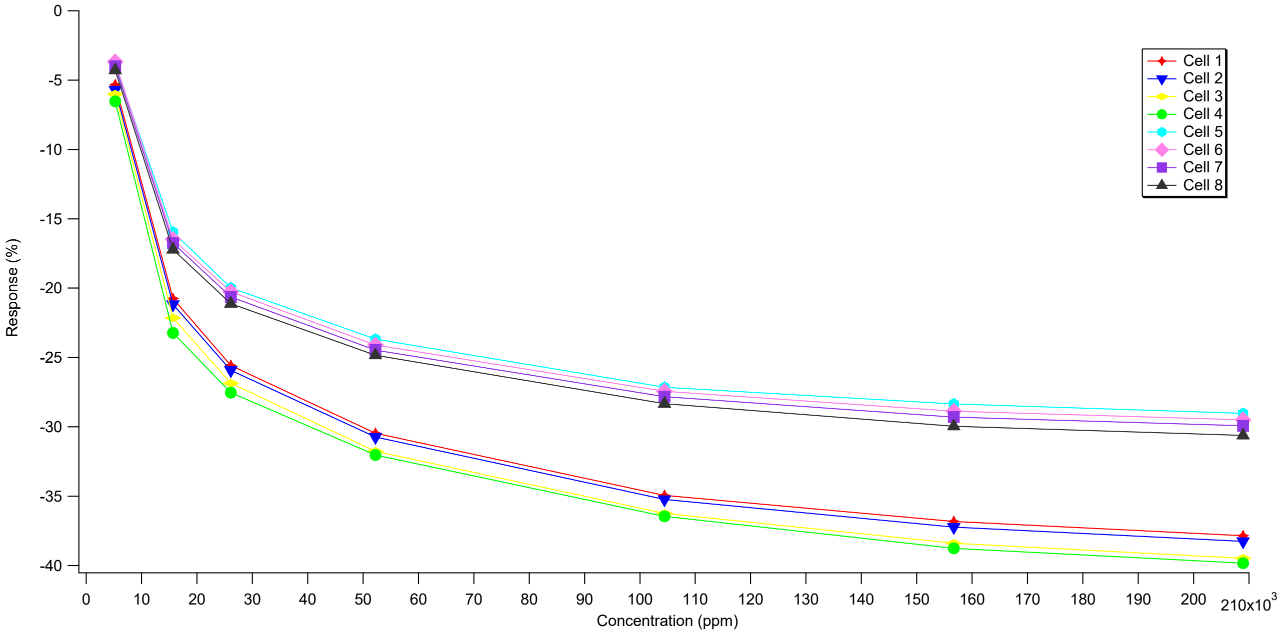

Figure 4.47: Response over concentration for Diethyl ether

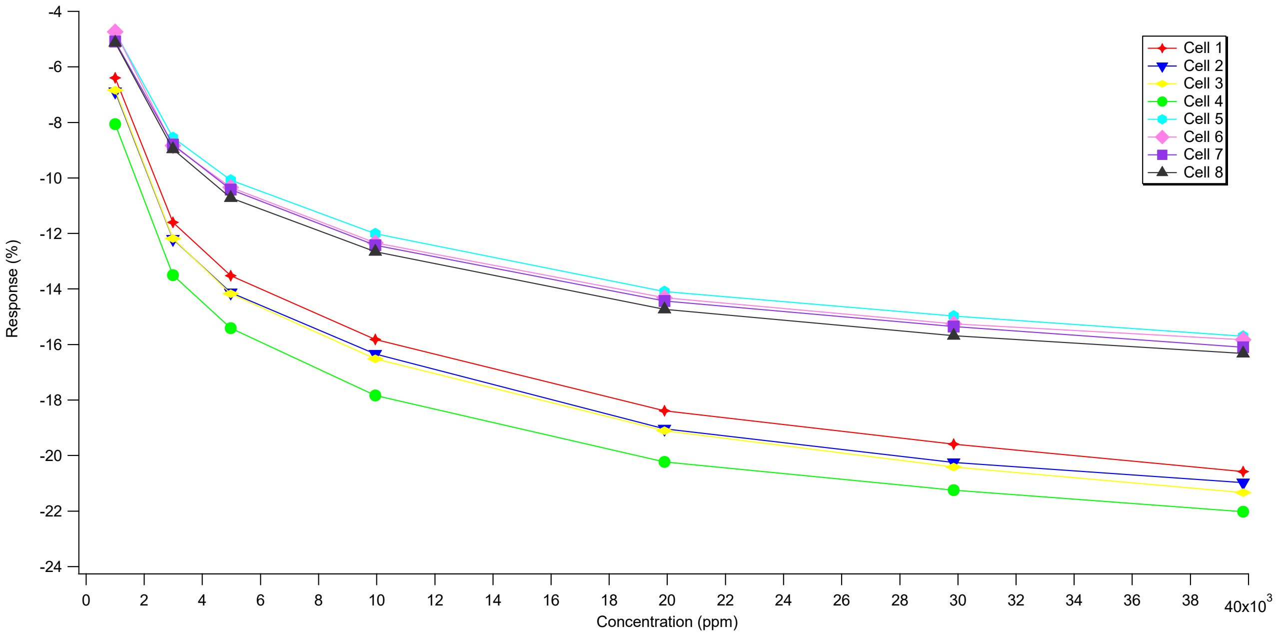

Figure 4.48: Response over concentration for 2-butanone

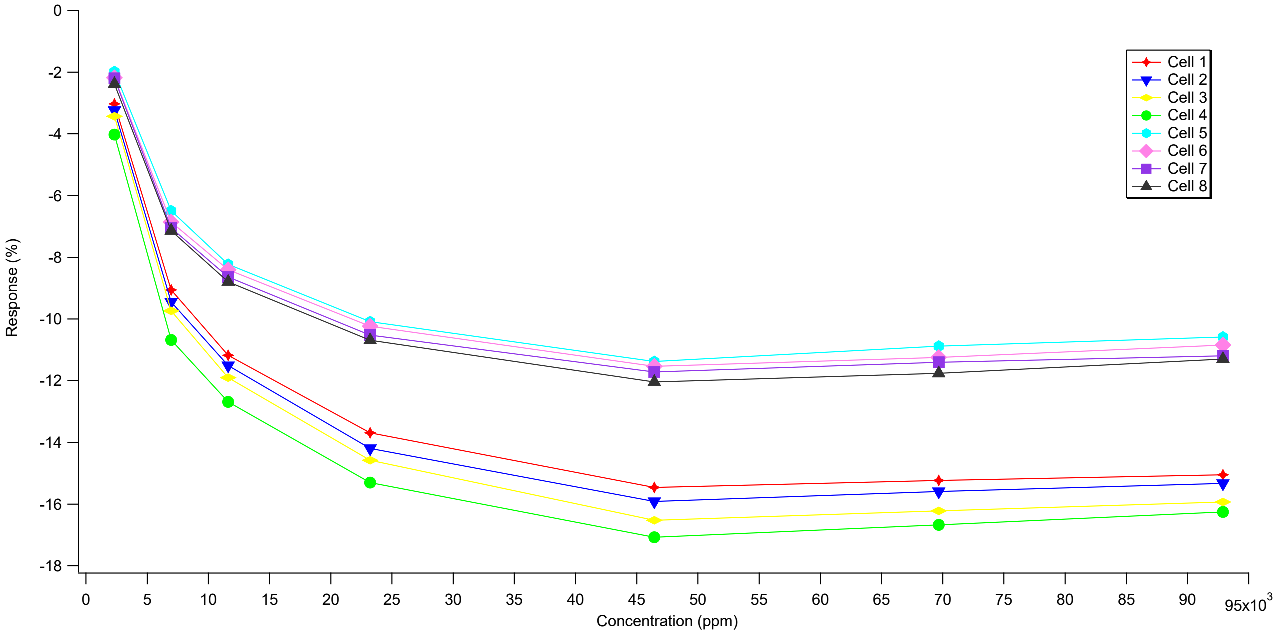

Figure 4.49: Response over concentration for Acetone

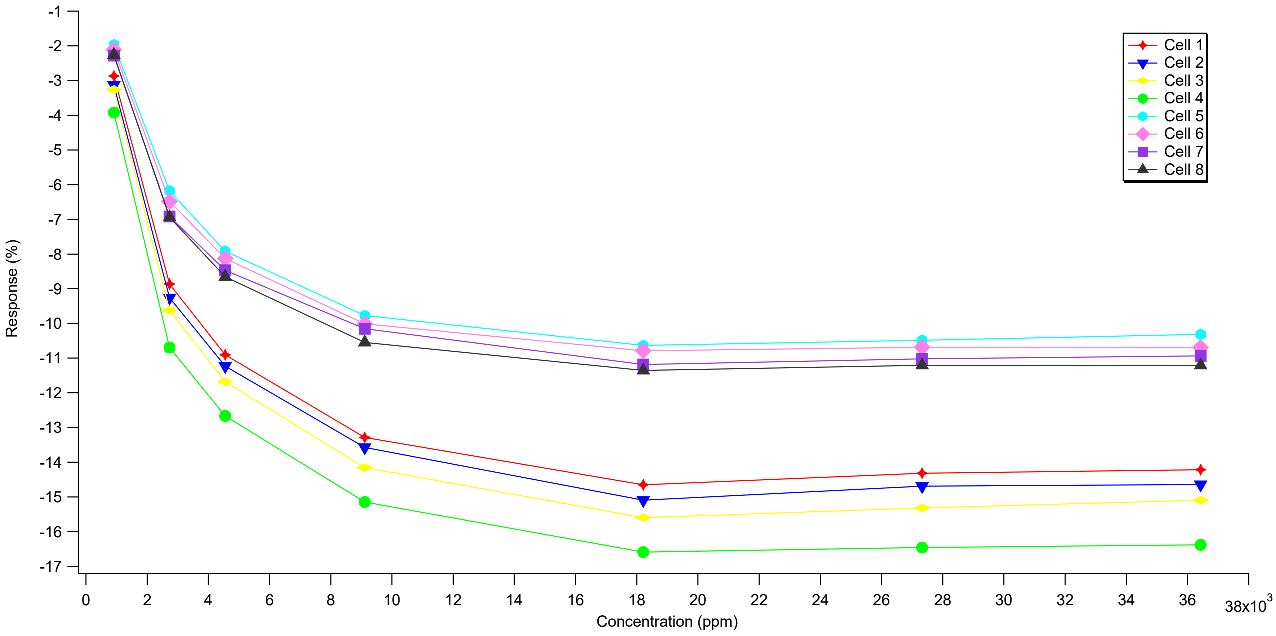

Figure 4.50: Response over concentration for Acetonitrile

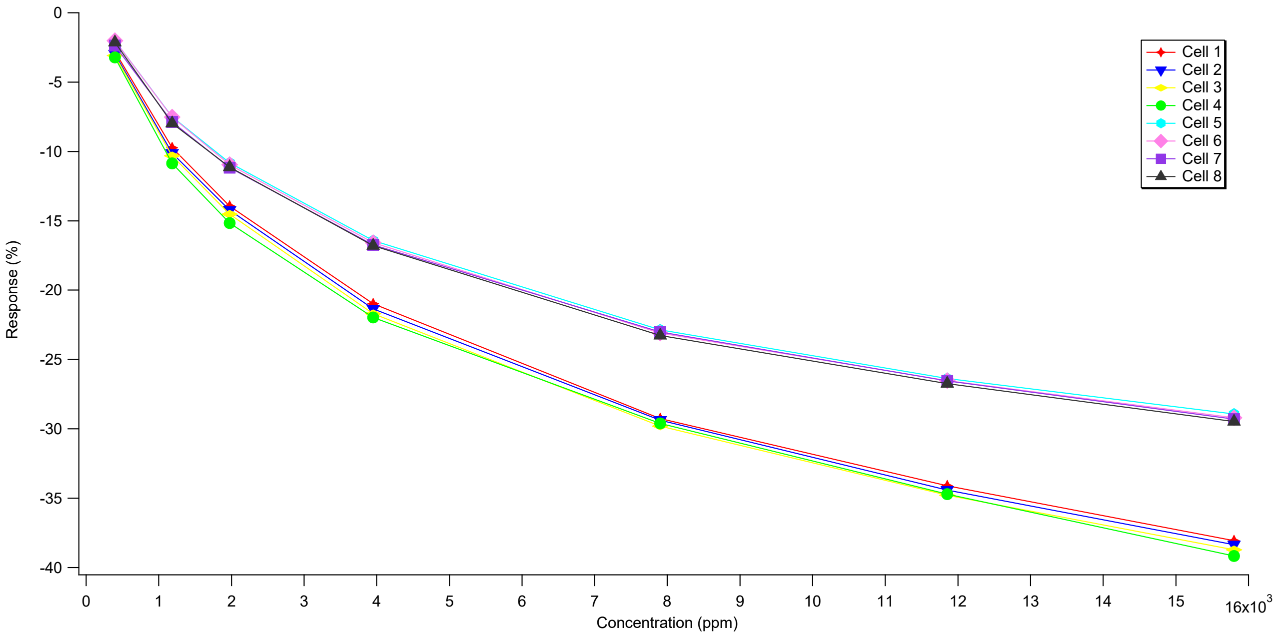

Figure 4.51: Response over concentration for 2-propanol

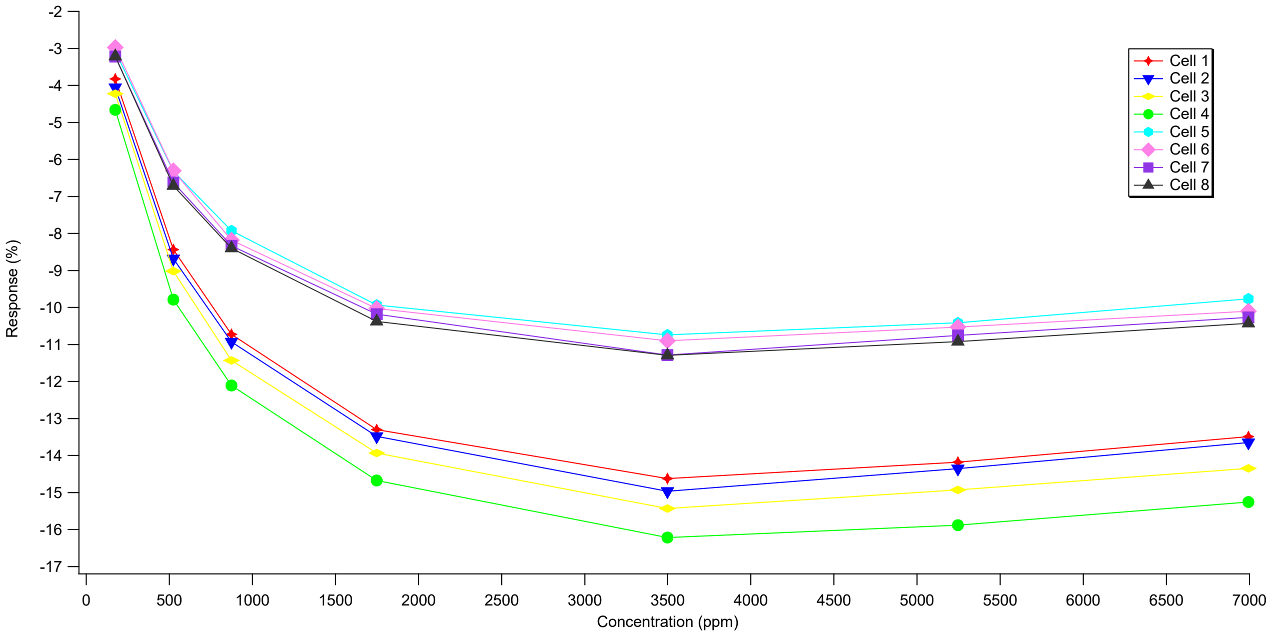

Figure 4.52: Response over concentration for 1-propanol

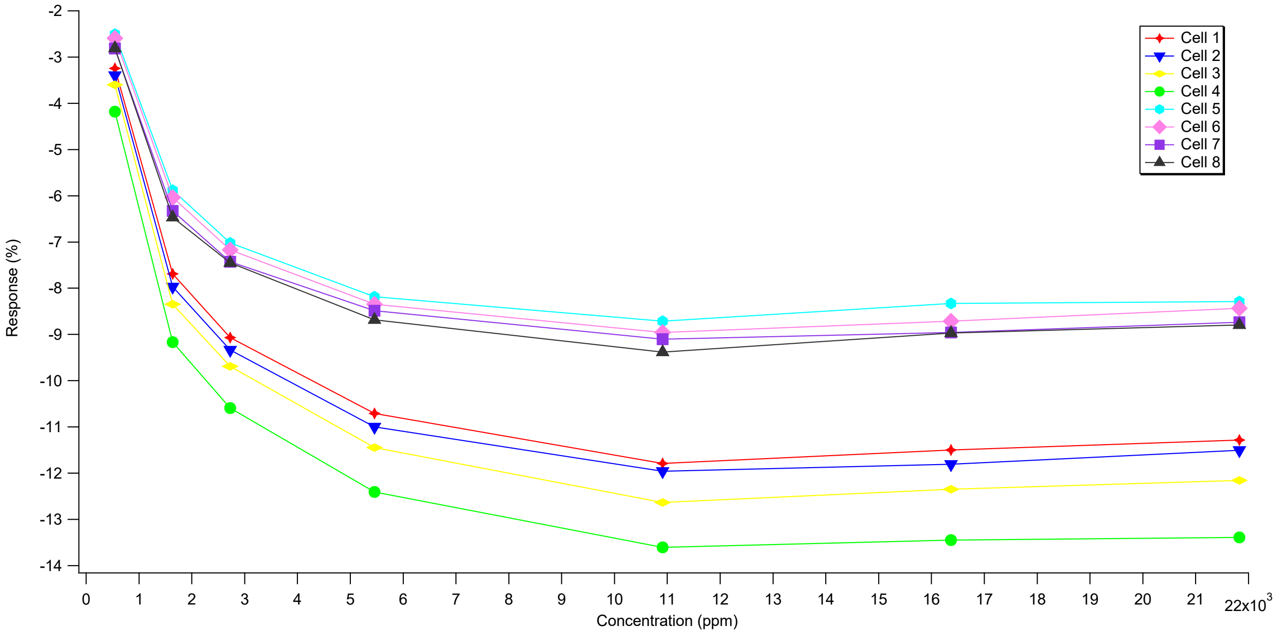

Figure 4.53: Response over concentration for Ethanol

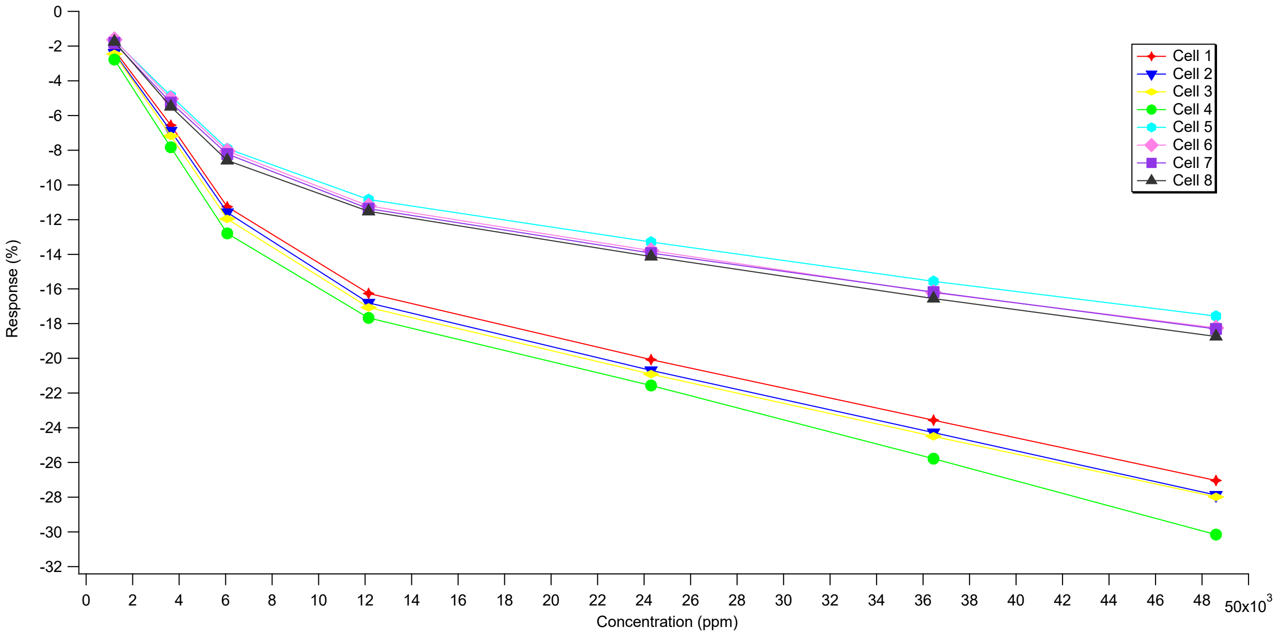

Figure 4.54: Response over concentration for Methanol

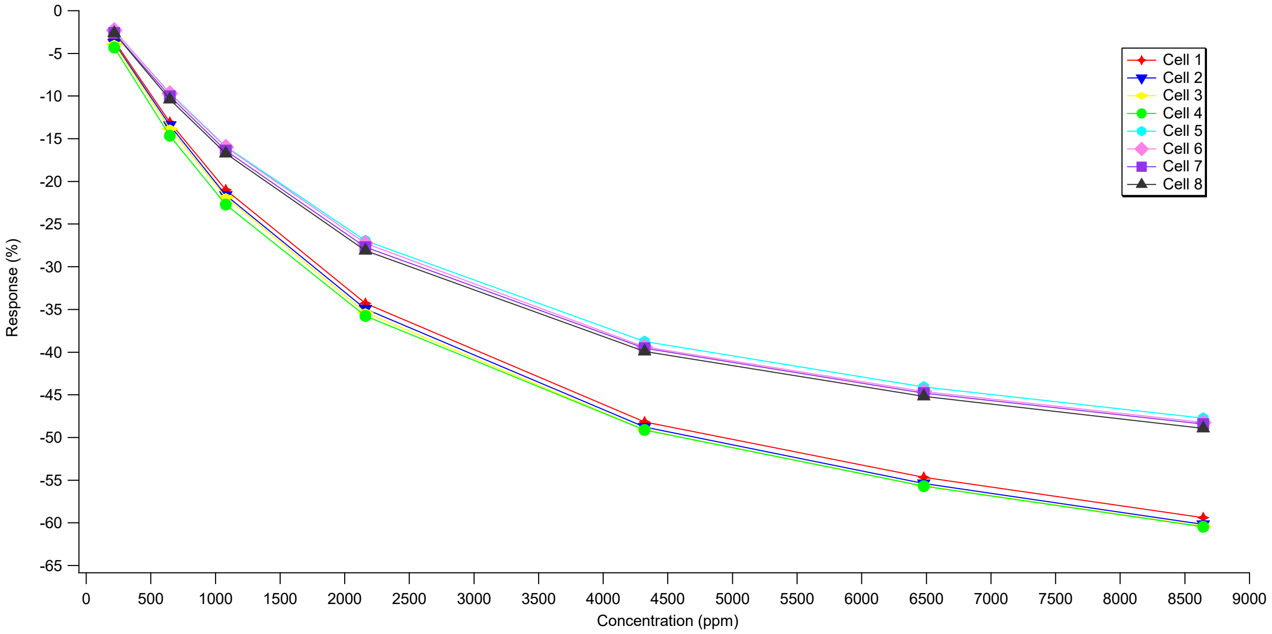

Figure 4.55: Response over concentration for Water

On the two electrode lines the polymer is prepared with two different oxidizers and doped with the same acid solution, HCl. As it can be noticed, the performances of the sensors on cell 1 to 4 are slightly better than cell 5 to 8 with a degree of improvement at low concentrations (1% on volume of gas analyte) around 40 %. The reason is clearly on the increase of oxidized spot on the polyaniline backbone attacked later by the acid dopant.

4.3.2. Comparison between PAni, PPy and PEDOT:PSS

The comparison is between the three different material, in particular between PAni TE-I-70, PPy TE-II-24 and TE-II-31 because of their performances. The plots are reported considering just the first 4 cells on PAni TE-II-70 due for the better responses achieved in that case and the all 8 sensors in the other case. The standard deviation among the different response value for each cell is also reported on the graph.

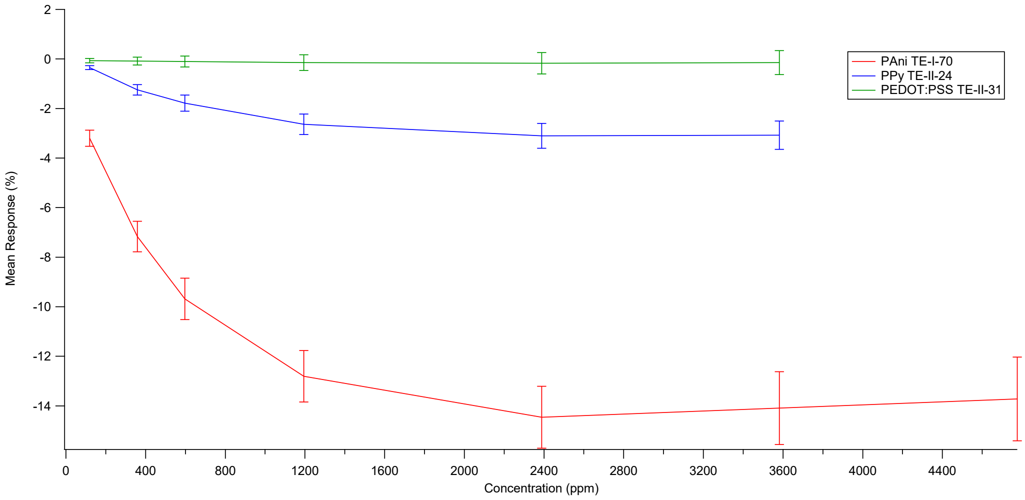

Figure 4.56: Response over concentrations for Octane compared between the different materials

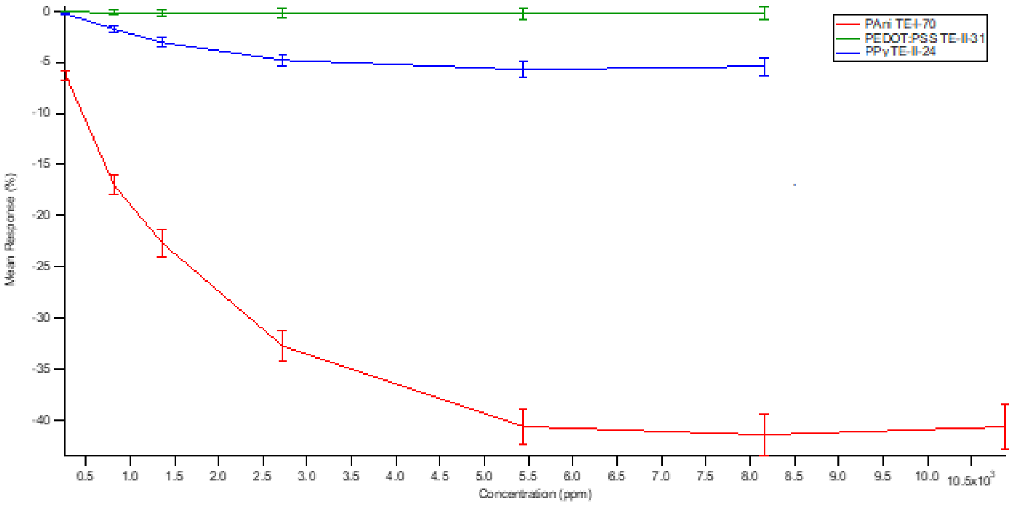

Figure 4.57: Response over concentrations for Toluene compared between the different materials

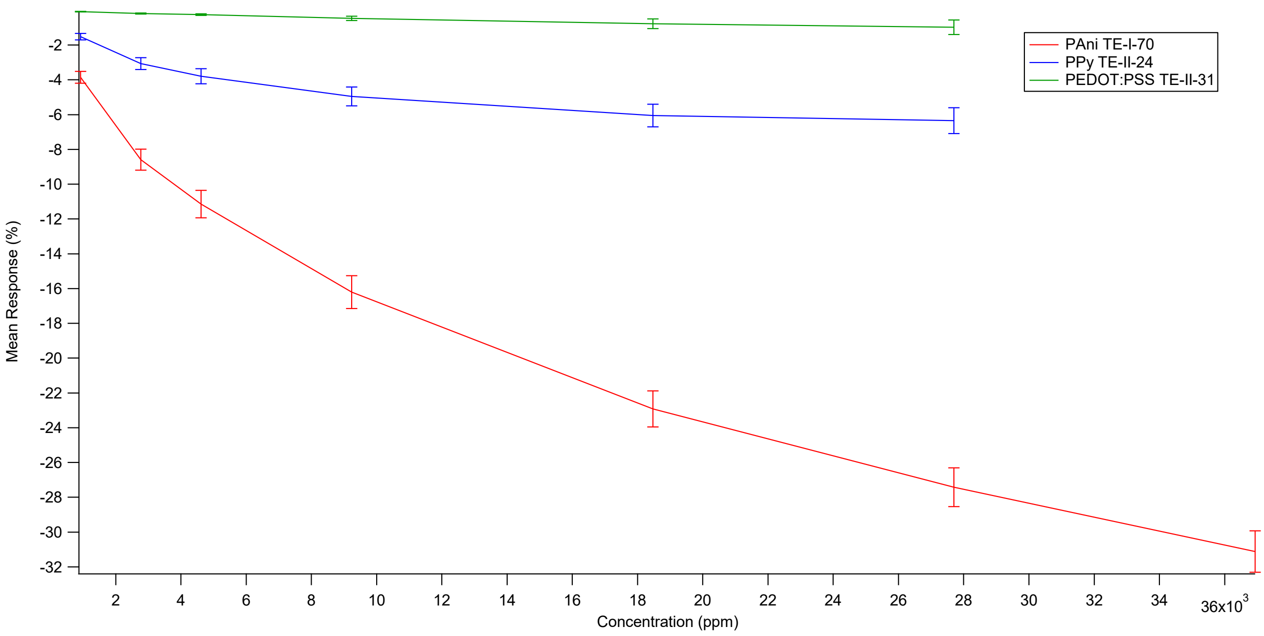

Figure 4.58: Response over concentrations for Ethyl acetate compared between the different materials

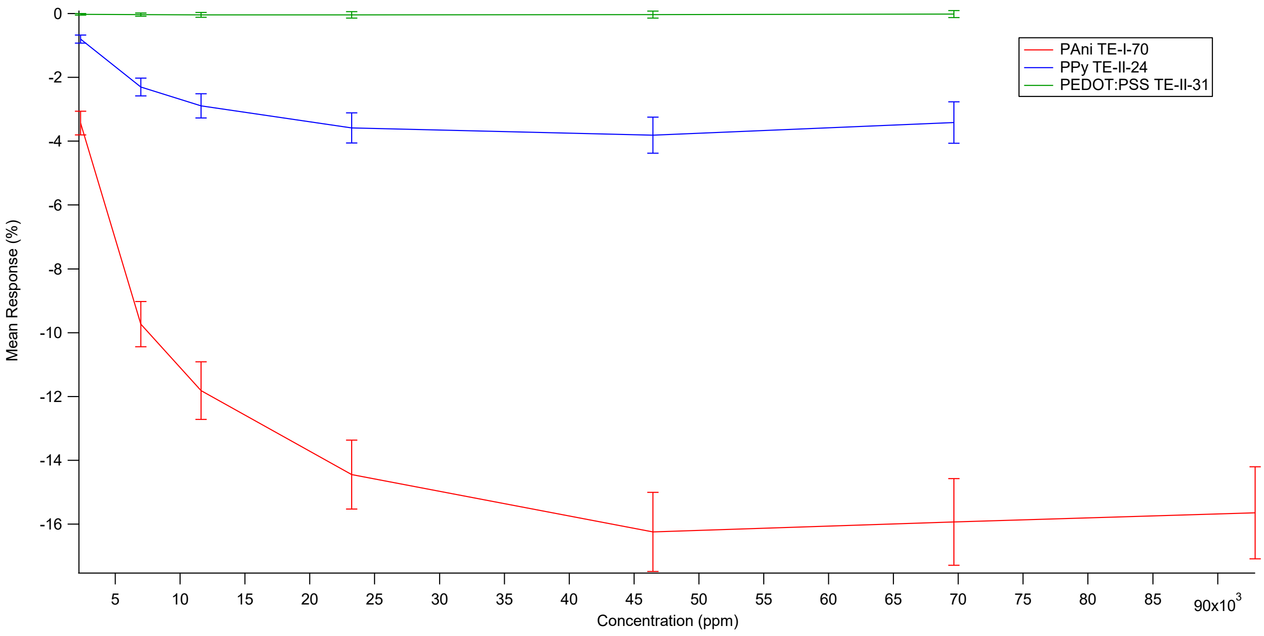

Figure 4.59: Response over concentrations for Acetone compared between the different materials

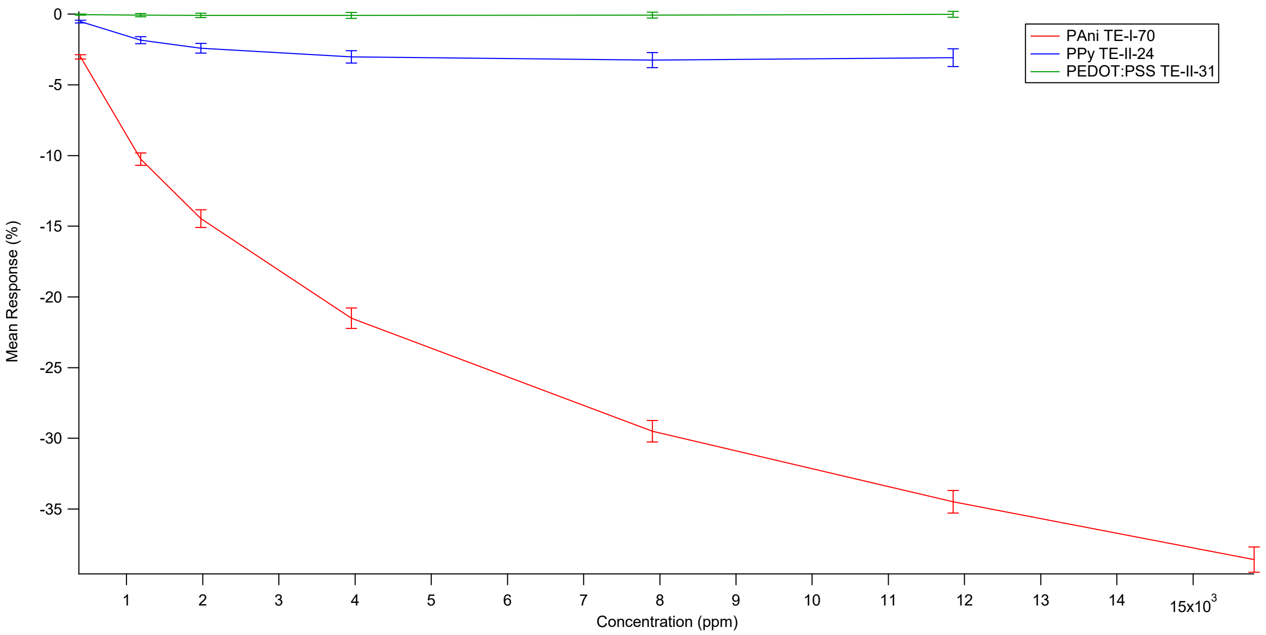

Figure 4.60: Response over concentrations for 2-propanol compared between the different materials

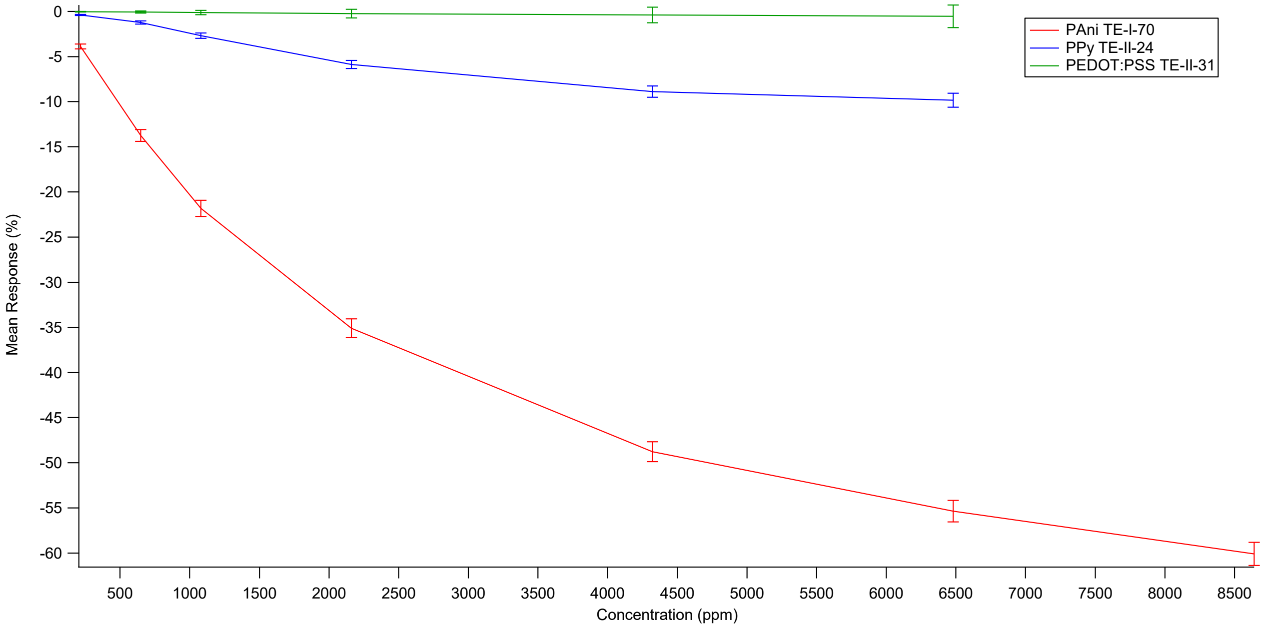

Figure 4.61: Response over concentrations for Water compared between the different materials

After analysing the responses over concentration plots for each analyte of the 6 tested, it was clear that polyaniline presented better performances in term of sensibility compared to the other polymers at the lowest concentration of analyte.

Analyte	**Response PAni TE-I-70 (%)**	**Response PPy TE-II-24 (%)**	**Response PEDOT:PSS TE-II-31 (%)**	**Level of increment PAni-PPy (%)**	**Level of increment PAni-PEDOT:PSS (%)**
Octane	-3.20	-0.33	-0.10	870	3100
Toluene	-6.26	-0.23	-0.13	2622	4715
Ethyl acetate	-3.86	-1.45	-0.02	166	19200
Acetone	-3.43	-0.77	-0.04	345	8475
2-propanol	-3.02	-0.48	-0.06	529	4933
Water	-3.89	-0.37	-0.05	951	7680

Table 4.3: Responses of the three material and level of increment compared to PAni TE-I-70.

4.3.3. Comparison with Cyranose 320

The cyranose 320 was tested inside of the laboratories of IBM upon the exposure of 4 analytes, cyclohexane, acetone, 2-propanol and water. The test was performed connecting the delivery system with a sealed PE tube directly with the sensor. The Cyranose 320 is connected to a computer where the variation of intensity of current is plotted over the time of analysis. The same parameters of exposure time (3 minutes) and recovery time (10 minutes) are set. The test was performed researching the minimum concentration detectable for each analyte (with the same percentage on volume of analyte in the total flow).

Analyte	**Cyranose 1% conc.**	**TE-I-70 1% conc.**	**Cyranose 3% conc.**	**TE-I-70 3% conc.**	**Cyranose 5% conc.**	**TE-I-70 5% conc.**	**Cyranose 10% conc.**	**TE-I-70 10% conc.**
Cyclohexane	0.11 %	4.62 %	0.29%	14.96 %	0.80%	18.68 %	Not tested	Not tested
Acetone	Not detected	/	0.20%	10.68 %	0.61%	12.69 %	Not tested	Not tested
2-propanol	Not detected	/	Not detected	/	0.17%	15.17 %	0.69%	21.96 %
water	0.17%	4.31 %	0.77%	14.66 %	Not tested	Not tested	Not tested	Not tested

Table 4.4: Comparison between Cyranose 320 results and TE-I-70 results at different percentages of analyte in the total flow of gas injected on the polymer chamber.

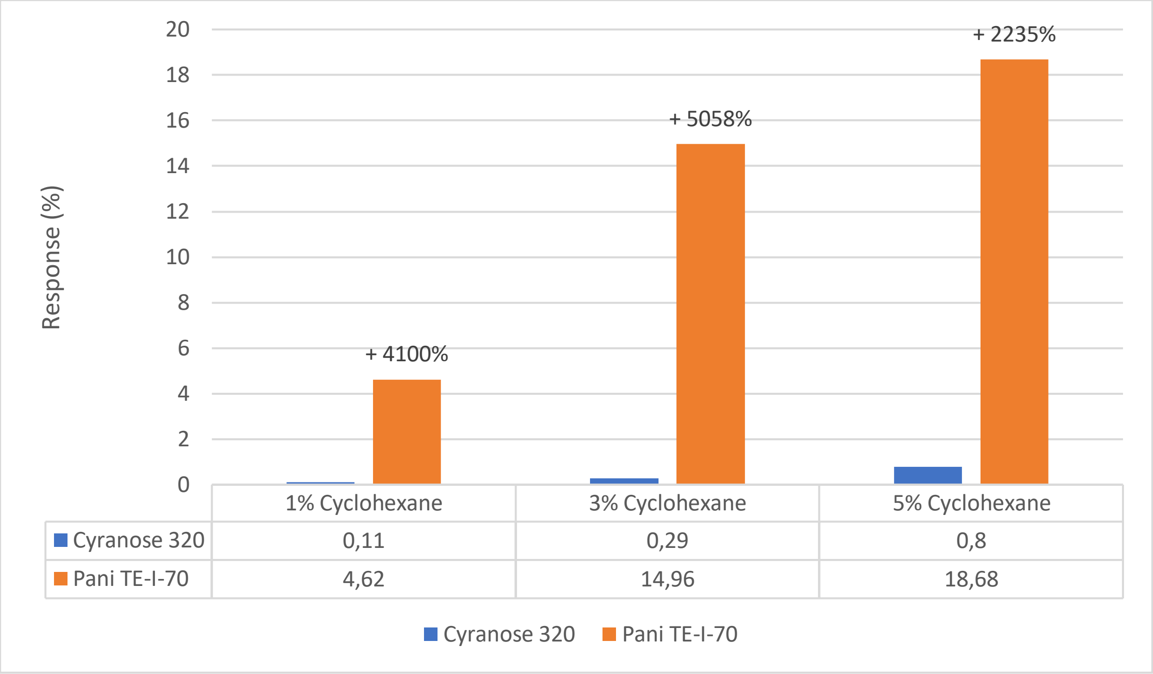

	1% Cyclohexane	3% Cyclohexane	5% Cyclohexane
🟦 Cyranose 320	0,11	0,29	0,8
🟧 Pani TE-I-70	4,62	14,96	18,68

Table 0.1: Comparison of cyclohexane response at different % of analyte on the total gas flow between Cyranose 320 and TE-I-70.

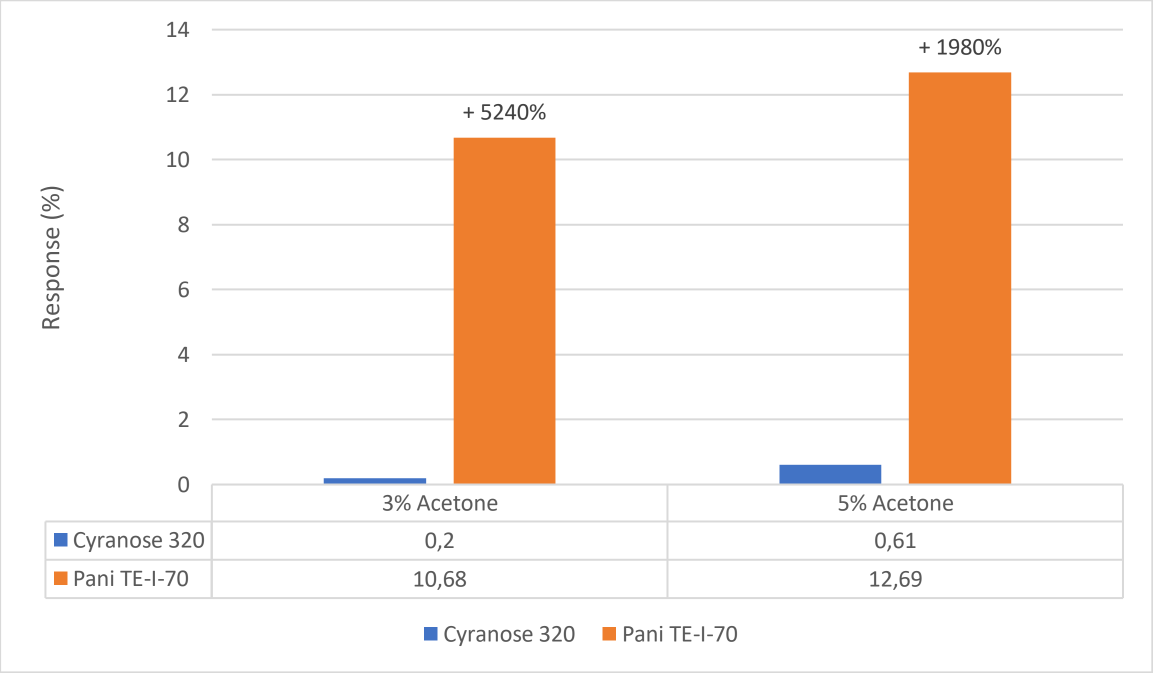

	3% Acetone	5% Acetone
🟦 Cyranose 320	0,2	0,61
🟧 Pani TE-I-70	10,68	12,69

Table 0.2: Comparison of acetone response at different % of analyte on the total gas flow between Cyranose 320 and TE-I-70.

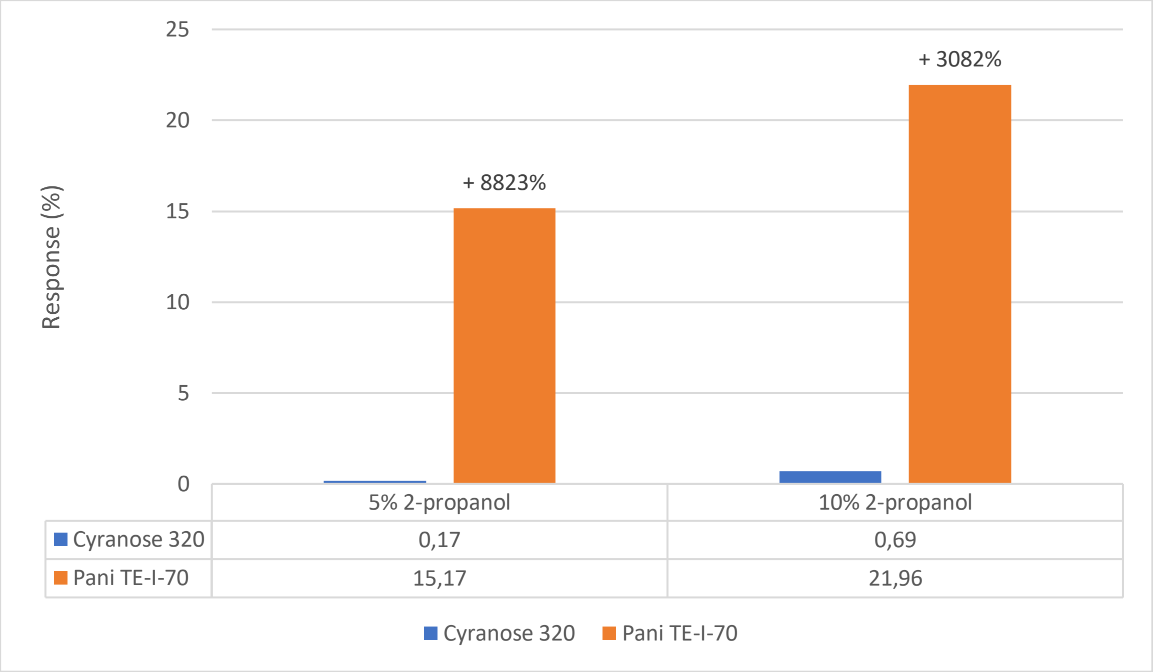

Table 0.3: Comparison of 2-propanol response at different % of analyte on the total gas flow between Cyranose 320 and TE-I-70.

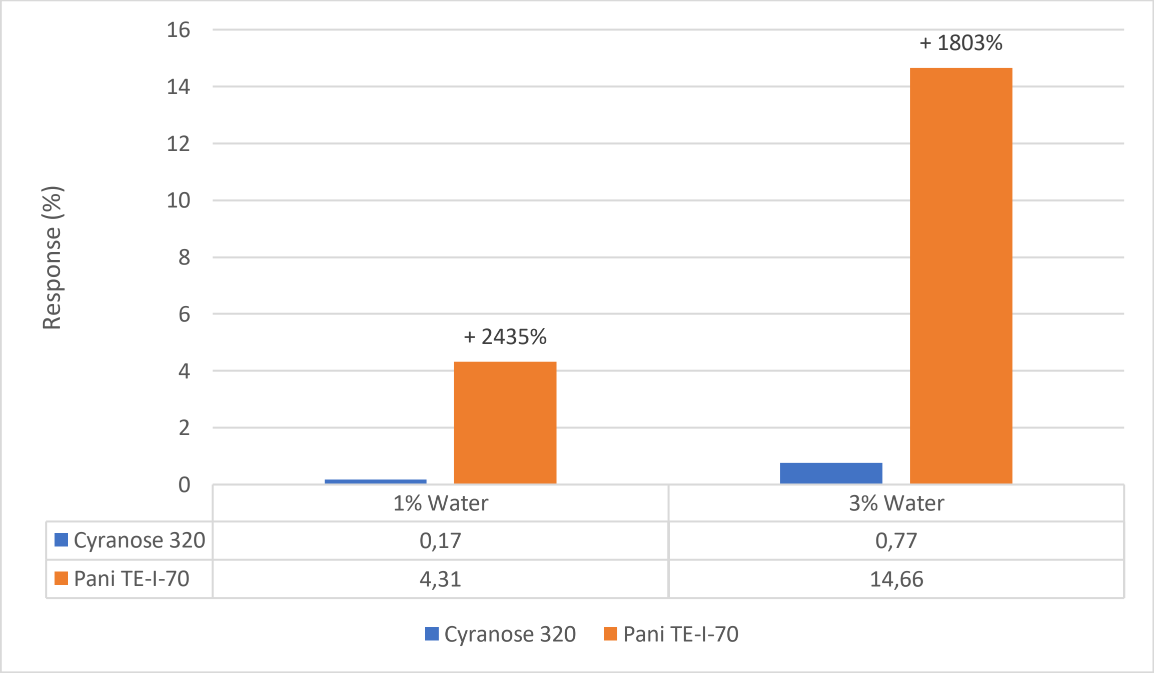

Table 0.4: Comparison of water response at different % of analyte on the total gas flow between Cyranose 320 and TE-I-70.

The results show clearly the better performances of the polyaniline sensor. The reason can be researched in the different conducting principles of the two devices; in fact, Cyranose 320 is fabricated using composite polymers charged with carbon black particles so the main principle of variation of resistance is due to the slow mechanism of swelling. In the case of the polyaniline the variation is imputable to mainly to secondary doping of the analyte, a faster and strong effect.

4.3.4. Further results with polyaniline

The next step was to use another oxidizer, Ammonium persulfate (APS), as oxidizer during the polymerization and comparing it with the previous one employed. The sample TE-II-10 was used where polyaniline prepared with APS was coated on cell 5 to 8 and the other oxidizer on cell 1 to 4.

The following plots are mediated between the two lines of coating with the standard deviation reported.

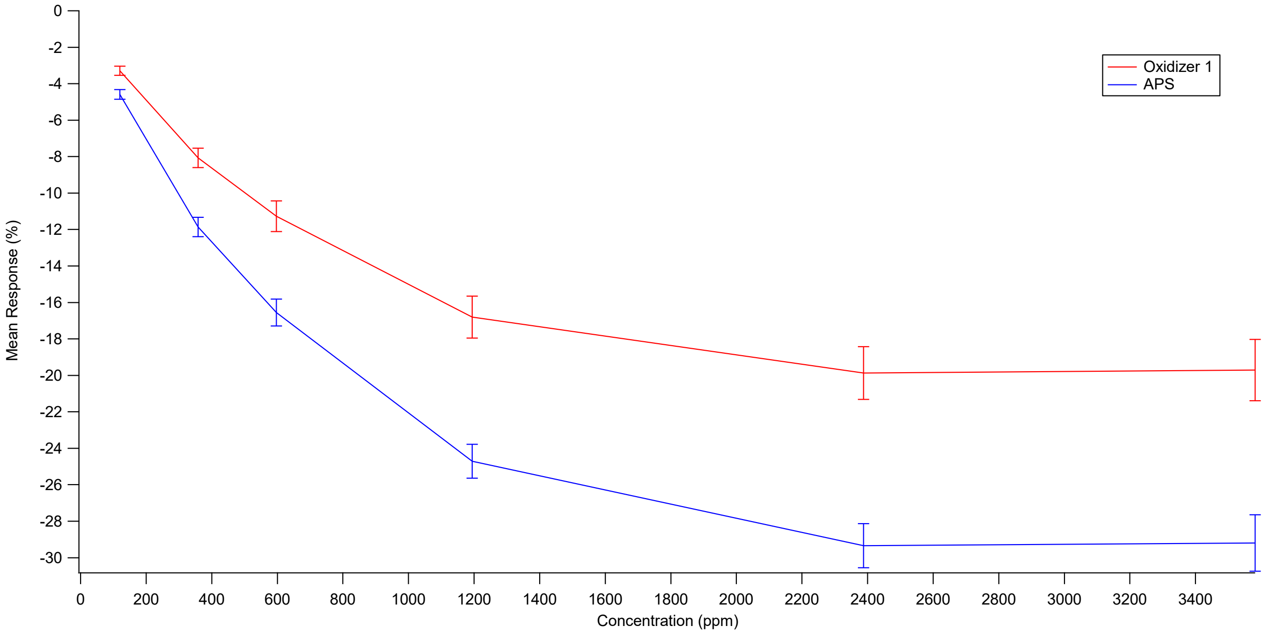

Figure 4.62: Response over concentrations for Octane compared between the different oxidizers

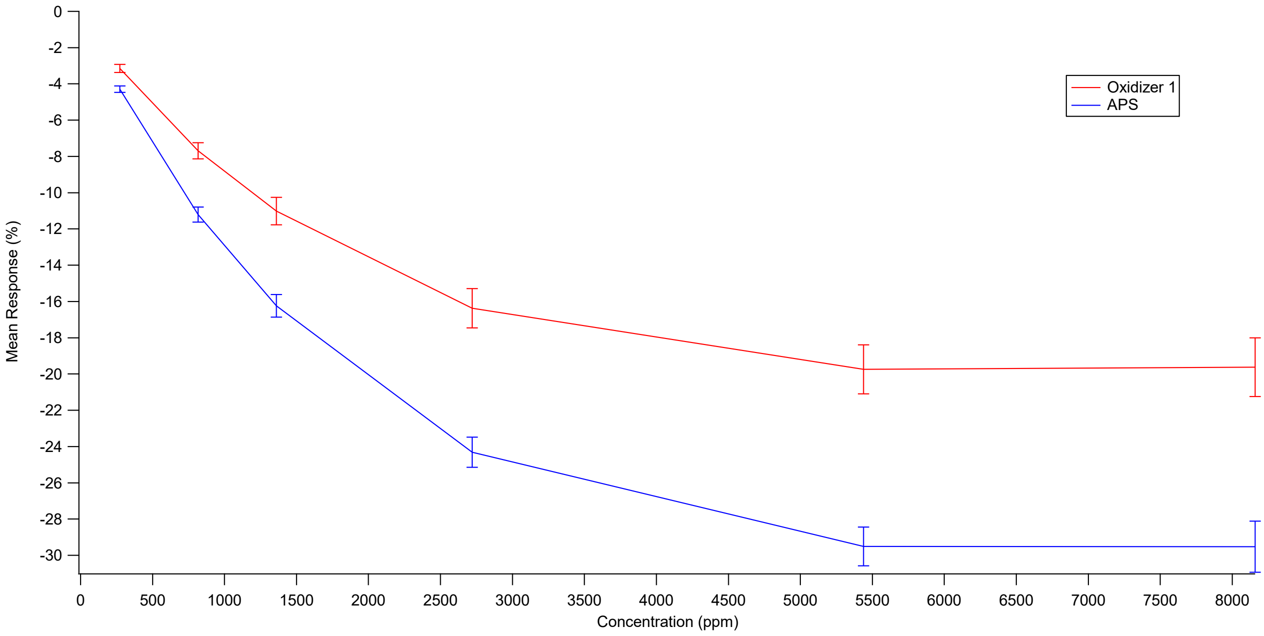

Figure 4.63: Response over concentrations for Toluene compared between the different oxidizers

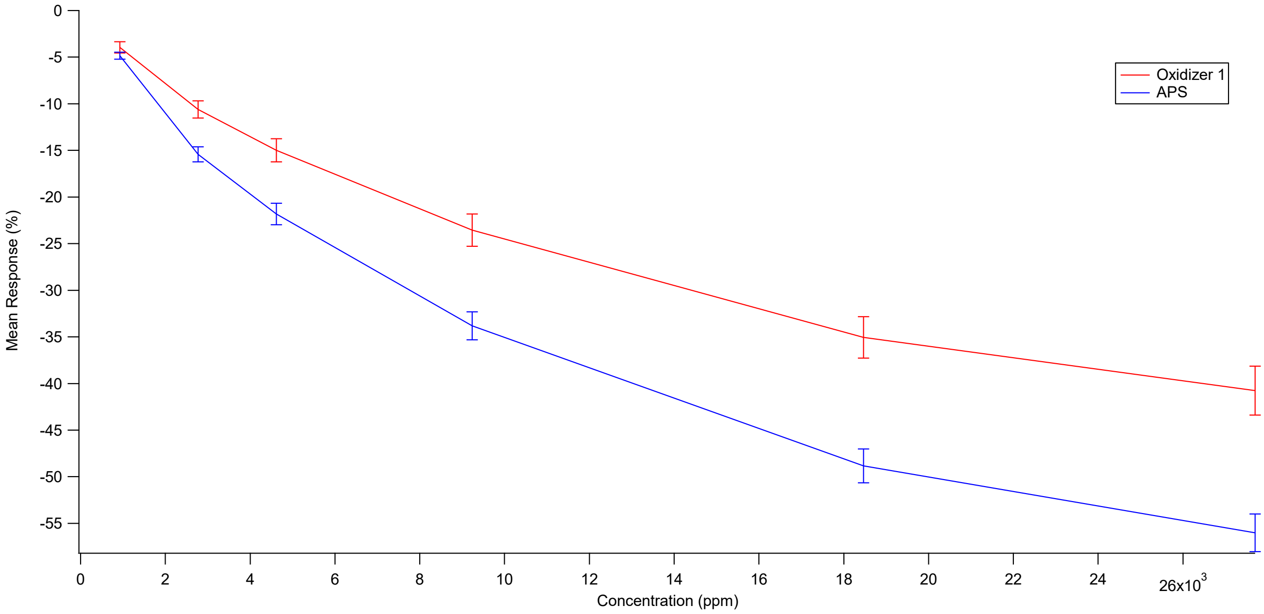

Figure 4.64: Response over concentrations for Ethyl acetate compared between the different oxidizers

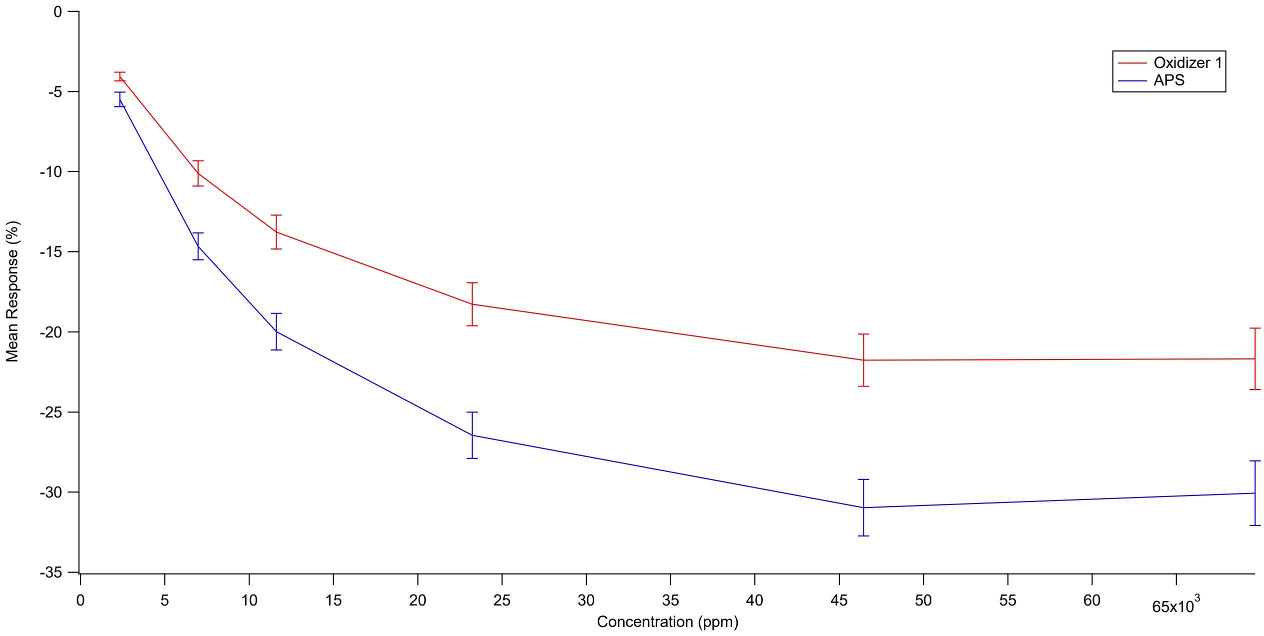

Figure 4.65: Response over concentrations for Acetone compared between the different oxidizers

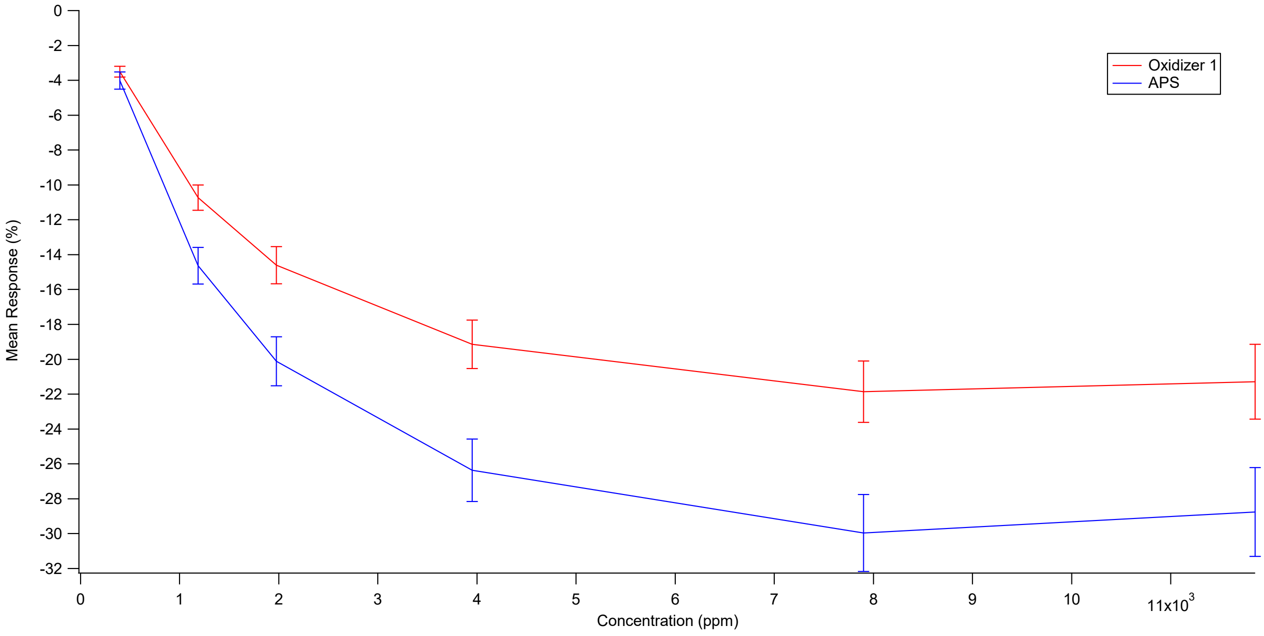

Figure 4.66: Response over concentrations for 2-propanol compared between the different oxidizers

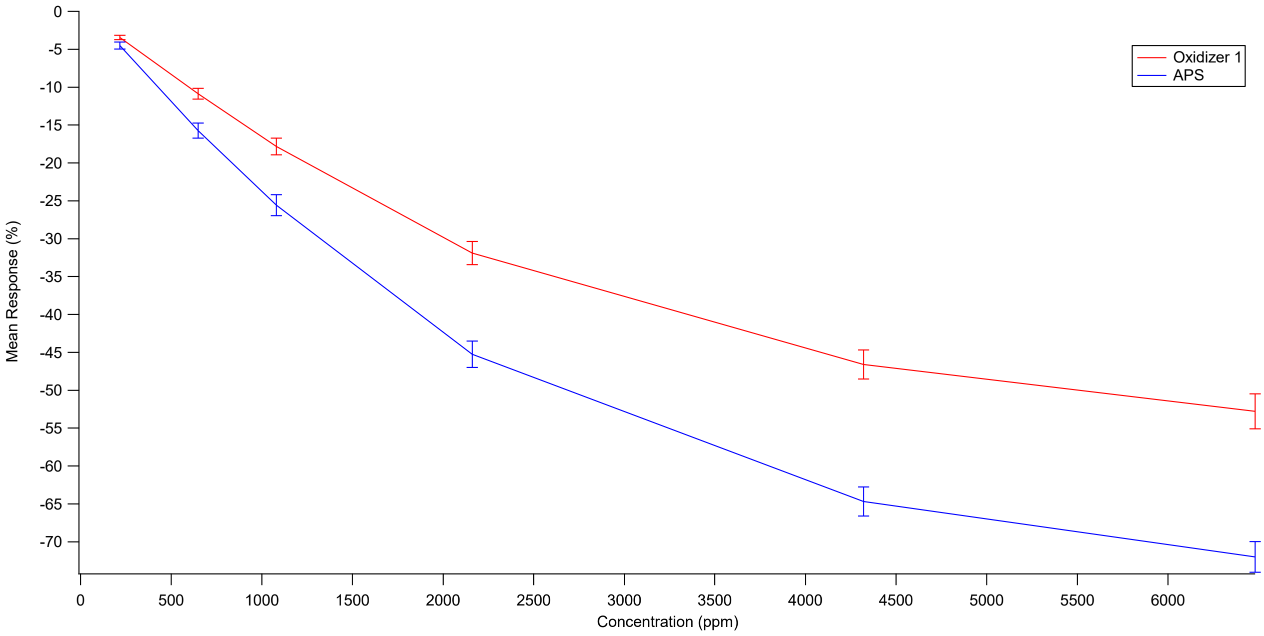

Figure 4.67: Response over concentrations for Water compared between the different oxidizers

Analyte	**Oxidizer 1 Response (%)**	**APS Response (%)**	**Level of increment (%)**
Octane	-3.29	-4.58	39%
Toluene	-3.15	-4.28	36%
Ethyl acetate	-3.94	-4.83	23%
Acetone	-4.06	-5.50	35%
2-propanol	-3.51	-4.02	15%
Water	-3.44	-4.47	30%

Table 4.5: Responses over the different analytes at 1% concentration on volume with the level of increment using APS

Polyaniline prepared with APS showed better performances in terms of response at low concentrations compared with the oxidizer previously used.

One of the additional parameters tested was the influence of the gap width on the response values. In this case the sample PAni TE-II-5 was drop-casted on a device with different electrode gaps (the usual gap is 100 µm) ; in particular the gaps were 1 µm for cell 1 and 5, 2 µm for cells 2 and 6, 5 µm for cells 3 and 7 and 10 µm for cells 4 and 8.

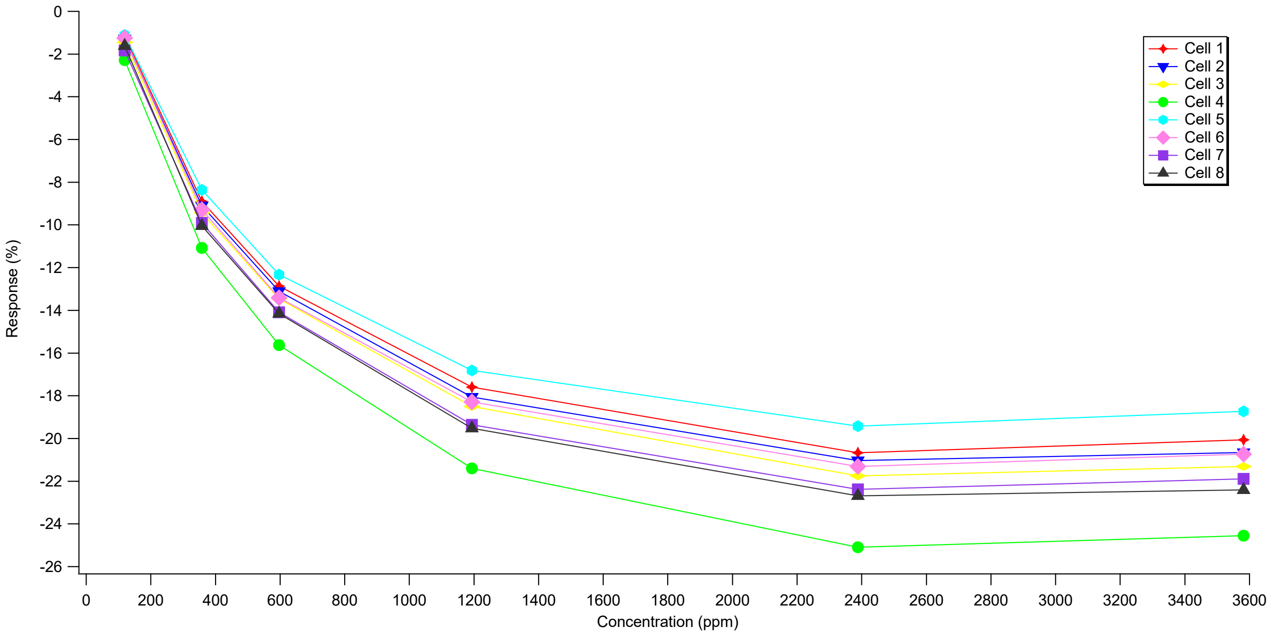

Figure 4.68: Response over concentration for the 8 cells on PAni TE-II-5, Octane.

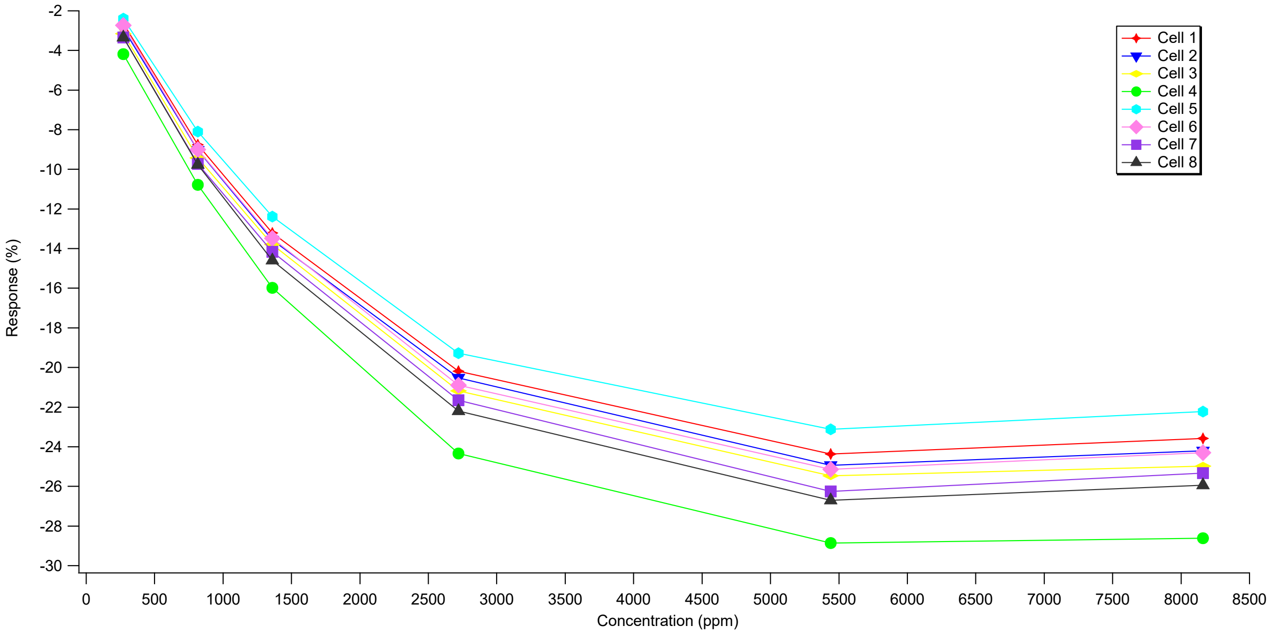

Figure 4.69: Response over concentration for the 8 cells on PAni TE-II-5, Toluene

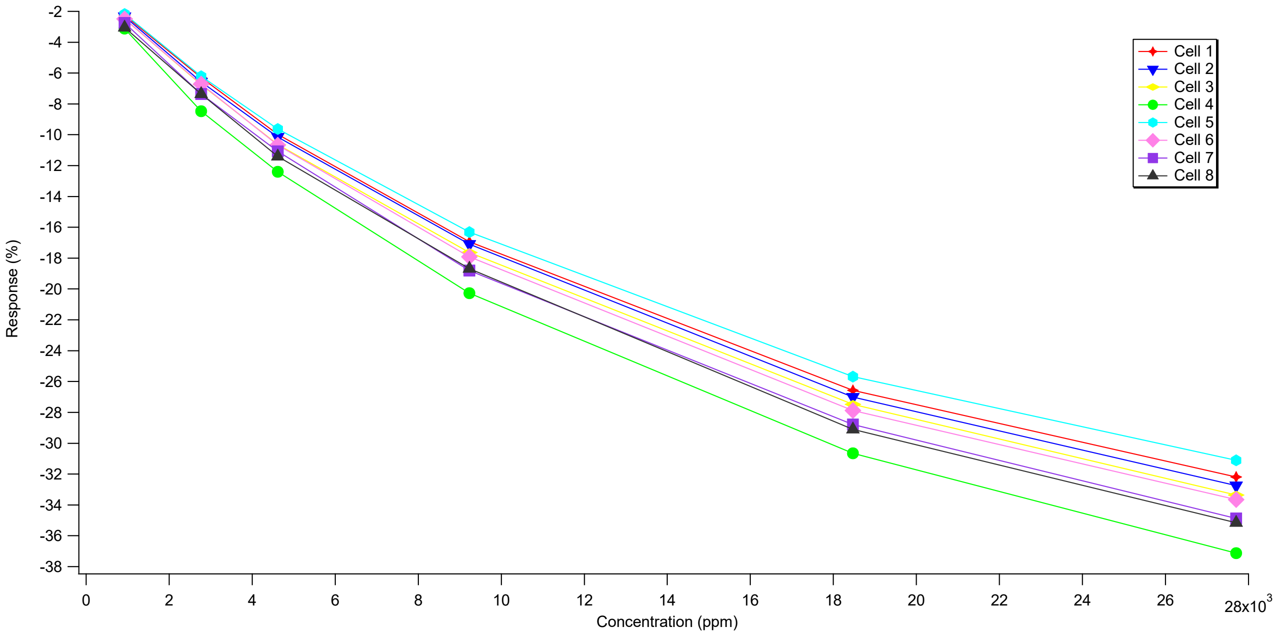

Figure 4.70: Response over concentration for the 8 cells on PAni TE-II-5, Ethyl acetate

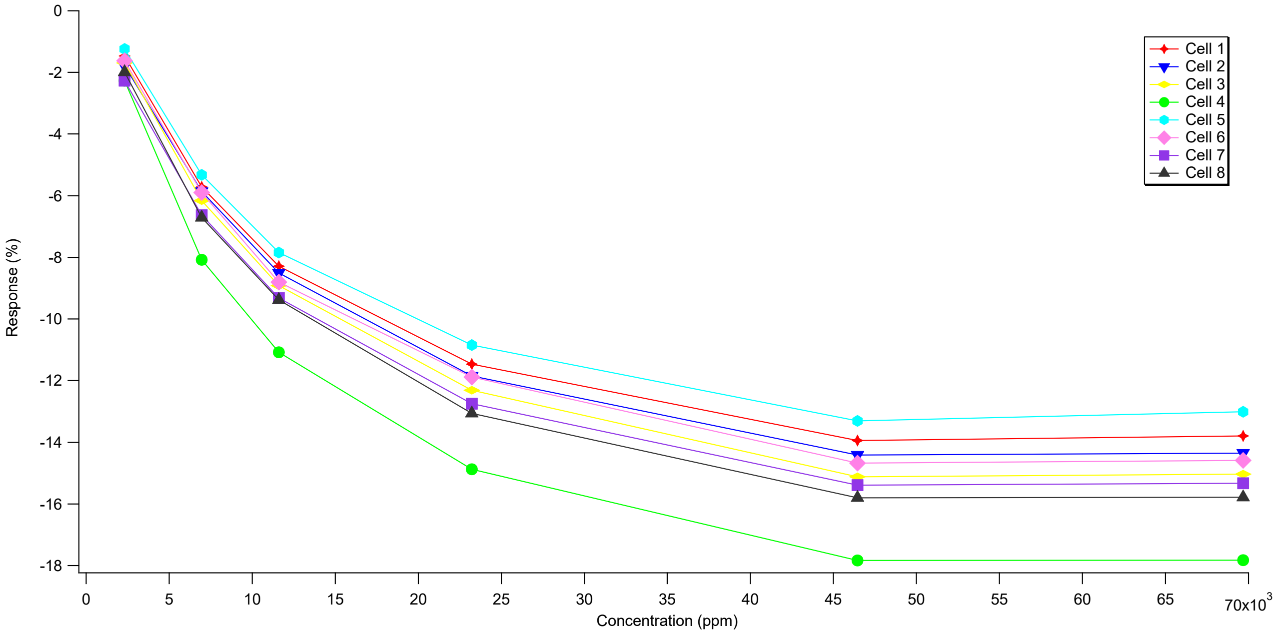

Figure 4.71: Response over concentration for the 8 cells on PAni TE-II-5, Acetone

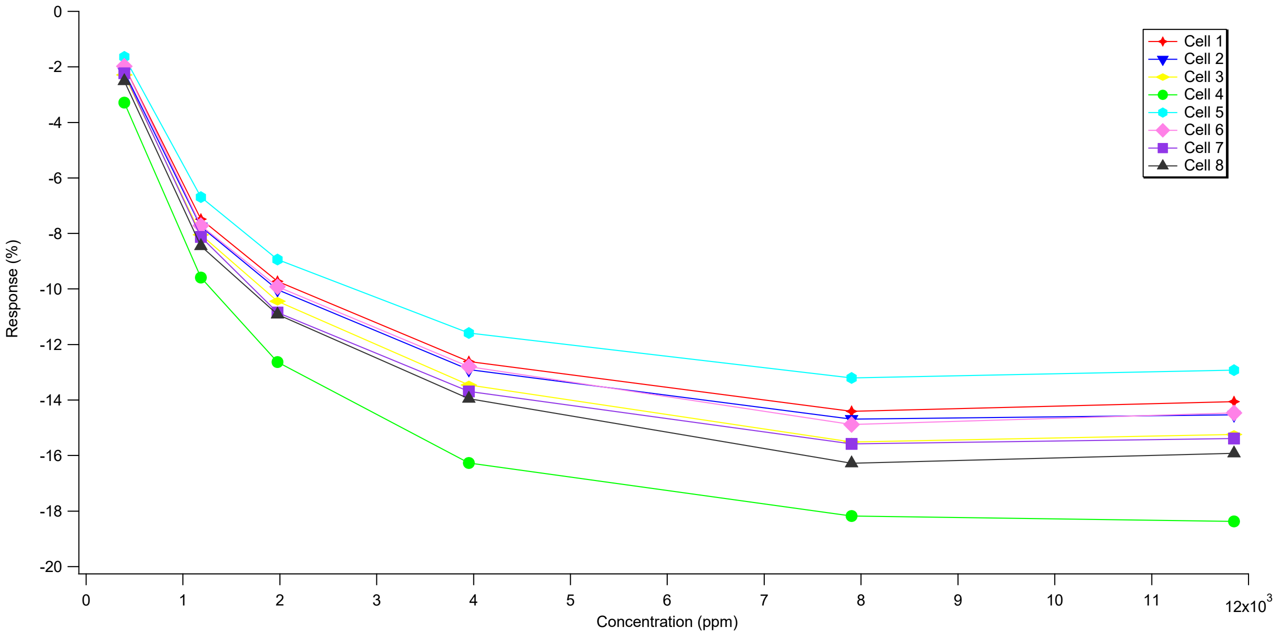

Figure 4.72: Response over concentration for the 8 cells on PAni TE-II-5, 2-propanol

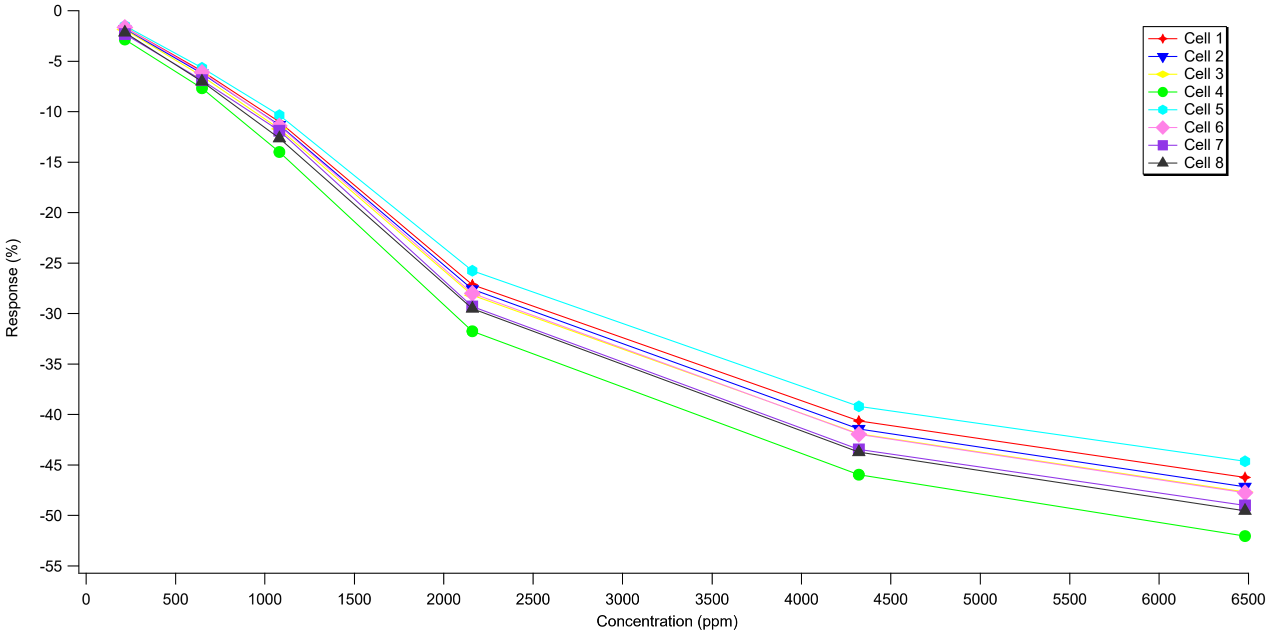

Figure 4.73: Response over concentration for the 8 cells on PAni TE-II-5, Water

No evidences of different responses were observed; In fact, the variation among the cells can be attributed more to the different flow entering on the polymer chamber than the gap itself according to the same increment of response over cells noticed in all the samples tested.

In order to increase the response, the option of adding some conductive nanoparticles was valuated; Gold nanoparticles were selected and dispersed on the polymer solution already as particles creating the sample TE-II-16. The solution coated was also more diluted compared to TE-II-10 granting a thinner film.

Cell	Thickness on PAni TE-II-10 (µm)	Thickness on PAni TE-II-16 (nm)
1	1.56	196
2	4.22	238
3	3.62	325
4	3.65	287
5	1.54	171
6	1.16	596
7	0.79	230
8	0.99	241

Table 4.6: Different thickness for each cell on PAni TE-II-10 and TE-II-16

In the following plots the response graphs are showed, comparing TE-II-10 cells 5-8 to TE-II-16 mediated over the all cells.

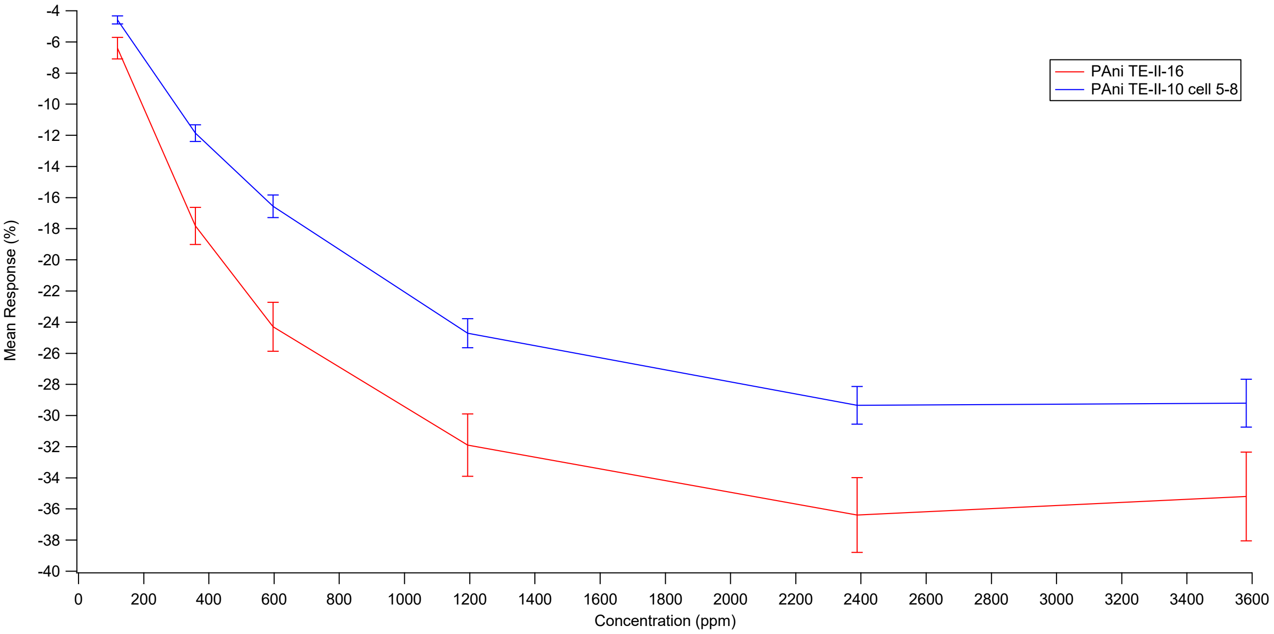

Figure 4.74: Comparison between PAni TE-II-10, cells 5 to 8, and PAni TE-II-16 for Octane

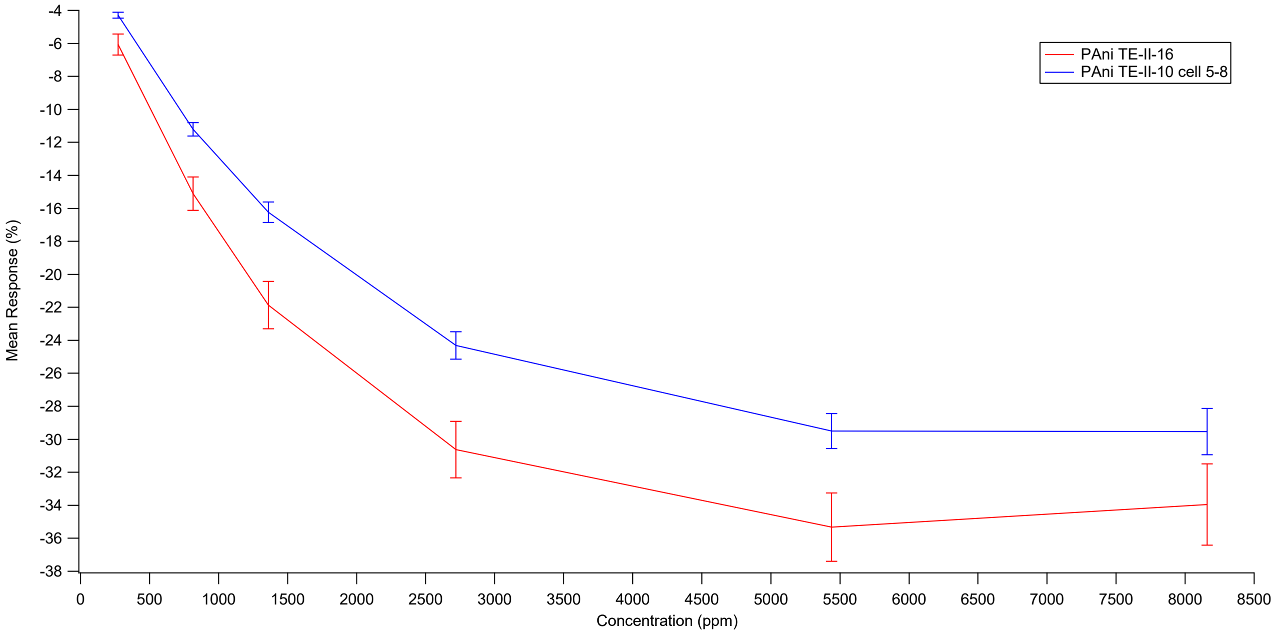

Figure 4.75: Comparison between PAni TE-II-10, cells 5 to 8, and PAni TE-II-16 for Toluene

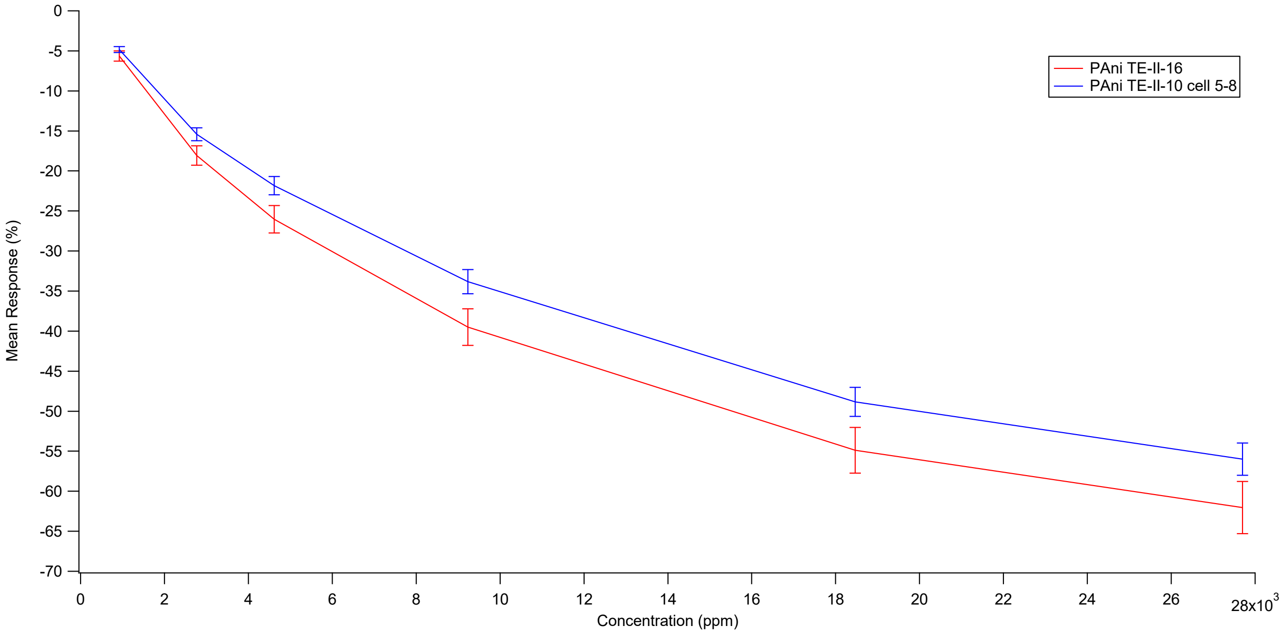

Figure 4.76: Comparison between PAni TE-II-10, cells 5 to 8, and PAni TE-II-16 for Ethyl acetate

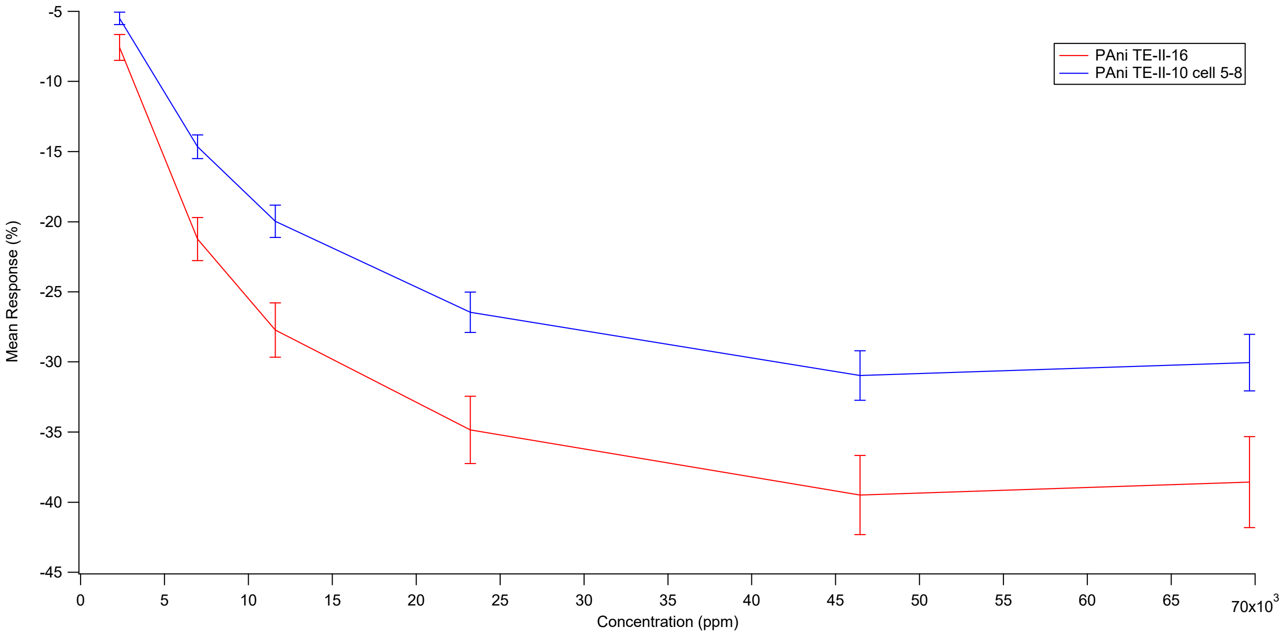

Figure 4.77: Comparison between PAni TE-II-10, cells 5 to 8, and PAni TE-II-16 for Acetone

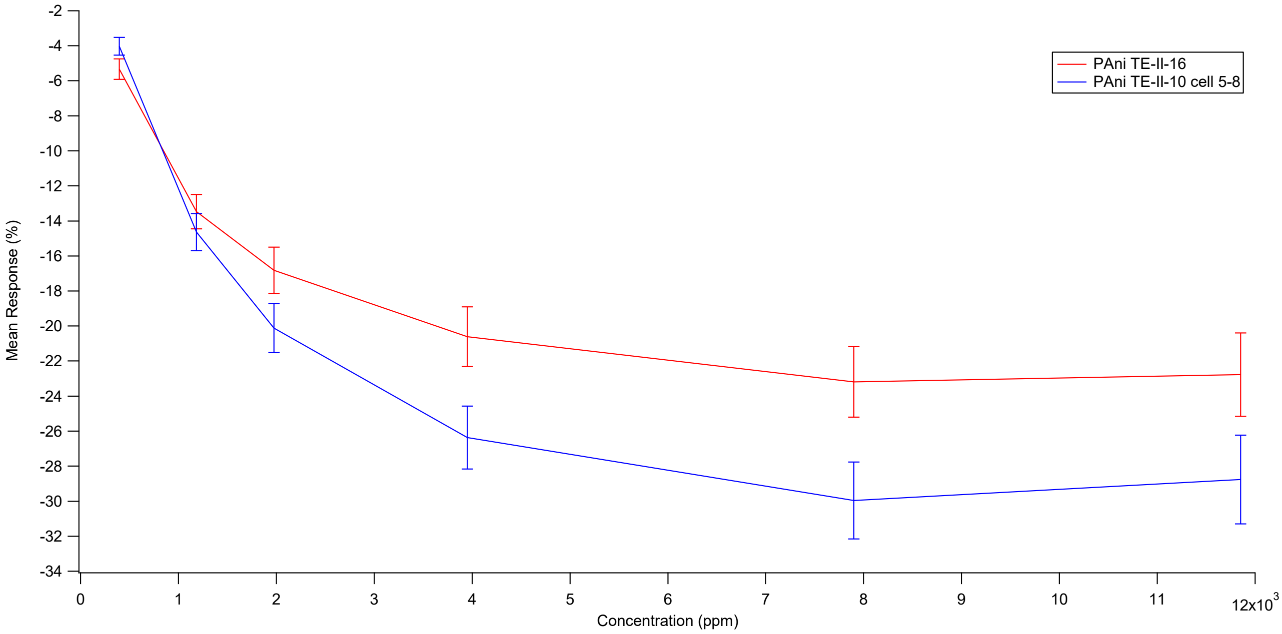

Figure 4.78: Comparison between PAni TE-II-10, cells 5 to 8, and PAni TE-II-16 for 2-propanol

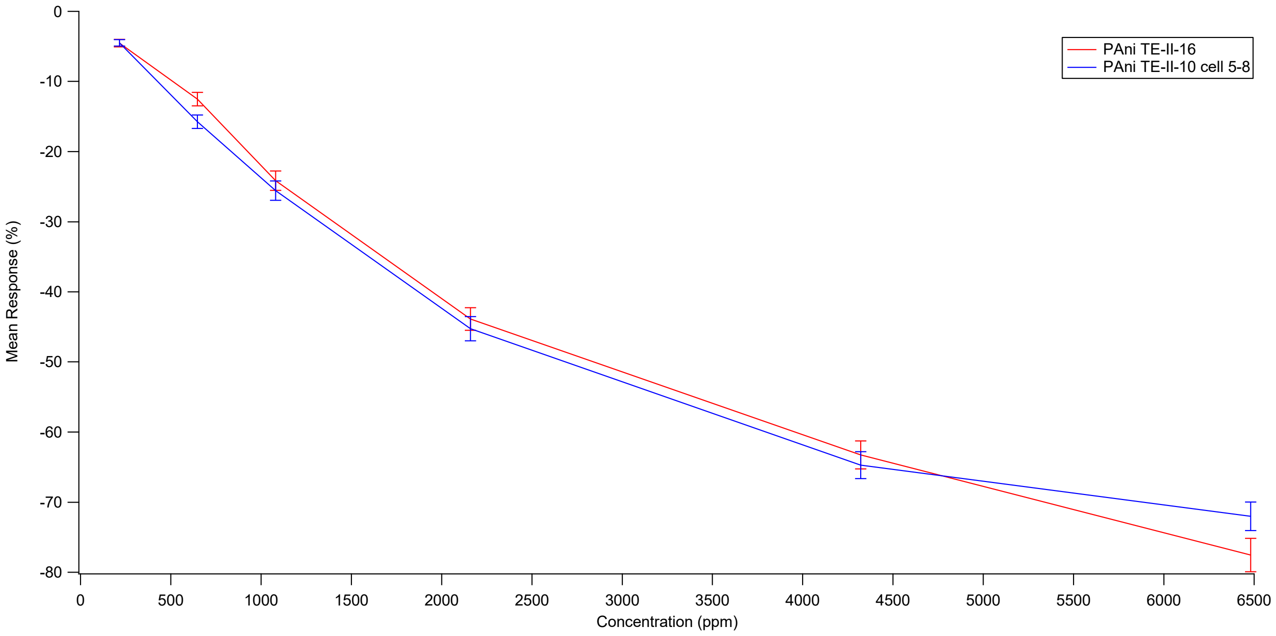

Figure 4.79: Comparison between PAni TE-II-10, cells 5 to 8, and PAni TE-II-16 for Water

Analyte	**Response TE-II-10 cell 5 to 8 (%)**	**Response TE-II-16 (%)**	**Level of increment (%)**
Octane	-4.58	-6.40	40
Toluene	-4.28	-6.08	42
Ethyl acetate	-4.83	-5.65	17
Acetone	-5.50	-7.58	38
2-propanol	-4.02	-5.32	32
Water	-4.47	-4.52	1

Table 4.7: Responses over the different analytes at 1% concentration on volume with the level of increment using the gold nanoparticles.

The reason of the increment does not just be researched on the gold nanoparticles presence but also on the thickness. This statement is, in this case, even more important because the initial solution with the devices were coated was different. In fact, many parameters can explain the increment and not just the two previously mentioned factors; Also, the PAni nanofibers diameter and the degree of doping occurred on the polymer can be a reason. Even the different resistance range (units of KΩ for PAni TE-II-10 and hundreds of KΩ for TE-II-16) could affect the results, not for itself, but because of the different parameters on the measuring set-up that can affect the response detection.

CHAPTER 5

CONCLUSIONS

In this conclusive chapter a summary of the whole thesis work need to be carried out to understand the key aspects of the project.

During the 5 months spent at IBM Almaden Research Center the development and fabrication of a gas sensors able to analyse different solvents was deeply investigated in order to create, in the future, a real e-nose device. The focus was on chemirsistors and especially, polymeric-based chemiresistors thanks to their high sensitivity toward a wide range of analytes, short response time, easy preparation, relatively good mechanical properties and extremely inexpensive cost.

Many efforts were put on the script developing, a code able to load and process the data points and saving all the time needed to understand and process the extremely high number of data points obtained as output from the experimental set-up.

According to literature, a deep and serious investigation on different conductive polymers in order to have a general idea of the performances of the different material was not described before. The fabrication started with the synthesis of the various polymers, especially polyaniline and polypyrrole, followed by the coating and the optimization of the gas delivery system and the customization of all the electronics. Once the device was ready to be used the testing step was carried out among a total number of 14 or 6 analytes, depending on the sample tested; Another important aspect of this operation was the previous absence of a research focused on a screen and sense of a high number of solvents on one single sample.

All the tests were based on DC measurements and all the parameters needed to be adjusted case by case according to the different value of resistance presented by the different device cells. The solvents tested were previously and well selected according to the different degree of polarity, from a polar solvent like water to a highly non-polar one like cyclohexane, and to the different chemical groups. The main aim of this work was to find a material able to present a high degree of response over different solvents and from here three different material were selected to the final testing procedure, polyaniline, polypyrrole and PEDOT:PSS.

The resistance variation showed a similar trend over the all materials, suggesting a connection between the conductive principle and the results achieved; In all the cases the response presented a likely linear behaviour at low concentrations and, gradually, a certain degree of curvature at high concentrations, symptom of a saturation on the active coated layer.

The first category of conductive polymers tested was PEDOT:PSS. The polymer presented a very low resistance, in the order of unit of Ω, but the wettability of the material made it a perfect suitable solution for blade coating. The response of the material showed, however really low results, always below 1% of variation of resistance upon the analyte exposure at low concentrations. A solution, due to the possibility of blasé coating, for the issue was researched on the decrement of the active layer thickness. The results after the optimization of the film width showed a big increment on the response, about 150% for each analyte, but still a variation of resistance under 1%. A curious phenomenon was also noticed with a thickness of the active layer around below 40 µm, namely an inversion of the baseline behaviour probably caused by a different rate of adsorption of the analyte on the thin film. A further investigation on the exact reason of this trend could lead to really important result on a sensor array to discriminate different analyte using different materials.

The next step was the employment of polypyrrole as conductive polymer active layer. The values of resistance in this case were around KΩ in most of the sensors and the polymer was drop-casted on the electrodes gaps carefully diluted to achieve values of thickness around hundreds of nm. The polymer was doped using different solution, ultrapure water and hydrochloric acid. While the sample doped with HCl presented results in line with the PEDOT:PSS measurements, just with a slightly better response around 1%, at low concentrations, the other sample showed a variation on the concavity of the sensing curve, suggesting an opposite behaviour of doping furnished by the adsorption of the analyte. Noticing the different concentration where this phenomenon occurs and the response plot it was possible to discriminate over the different analytes tested having a certain degree of selectivity. The sulphate-polymer initial solution was, however, highly instable with massive agglomerates in the media; A further investigation able to achieve a more stable solution is the main aim of this material study.

Polyaniline was the last tested and most promising material among all the conductive polymers; In fact, 10 of the 15 samples tested over the internship at IBM Almaden Research Center were polyaniline or functionalized polyaniline. The values of resistance in this case presented an wide range, from units of Ω almost to MΩ, even though the main target was usually KΩ and the polymer was drop-casted on the gaps. The basic polymer showed by itself the best values of response, from a minimum of 2% to a maximum of 7% at really low concentrations (in the order of magnitude of hundreds of ppm). Moreover, the sensor was compared with a commercially available sensor (Cyranose 320). The results showed better performances of conductive polymers compared to loaded polymer matrix sensors. Having as main objective the research of a conductive polymer showing good results of resistance variation at low concentrations, the main focus was carried out using this material so different oxidizers were employed to improve the performances; The choice felt lately on APS due to its higher oxidizing properties on polyaniline. Another parameter investigated was the dependence on the electrode gaps of the result achieved; Results showed no evidences of alteration of the response due to this parameter. The last two parameters investigated were the film thickness and the addition of conductive gold nanoparticles on the polymer during the polymerization. The contribute of both the variable showed improved response results suggesting the implementation of these techniques on future sensors.

In general, the future outlook in this investigation need to focus on all the three main aspects of sensing, namely the sensitivity, the selectivity and the stability. During the internship the research one of the focus was testing the various sample using a oven, to obtain concentrations in the order tens of ppm. Due to some technical problem with the heating system it was not possible to explore this path and a future investigation in this sense need to be carried out to observe a level of response even at low concentrations, so that the level of sensitivity of the material tested. Other solutions are the functionalization of the polymer, adding chemical group on the backbone or adding other nanoparticles on the material to improve the sensitivity or even the selectivity toward different analytes. To test the stability, the reproduction of the measurements carried out inside of the laboratories need to be done to confirm the results achieved, even testing with a certain degree of humidity. Many more properties, such as morphology of the polymer, composition and testing condition are strictly linked to the sensing performances and their optimization can lead, in the future, to create a array of polymeric sensors. Combining conductive polymers with other kind of material will grant the fabrication of a e-nose device able to give a unique fingerprint response to different VOCs and, with a recognition engine, make possible one eventual parallel usage of this technology with the human nose.

BIBLIOGRAFY

[1] Buratti, S. et al. (2018). "*E-nose, e-tongue and e-eye for edible olive oil characterization and shelf lifeassessment: A powerful data fusion approach"*.

[2] Baer, T. et al. (2018). *"Dior, J'adore": The role of contextual information of luxury on emotional responses to perfumes.*

[3] Gardner, J.W. and Baerlett, P.N. (1994). "*A brief history of electronic noses"*.

[4] Persaud, K.C. and Dodd, G. (1982). "*Analysis of Discrimination Mechanisms in the Mammalian Olfactory System Using a Model Nose"*. Nature, 299, 352-355.

[5] Ahmad, M. (2018). "*Olfactory nerve structure of olfactory nerve cells, function of olfactory nerve, olfactory bulb, olfactory tract"*. Web edition: https://www.medicosite.com/olfactory-nerve/.

[6] Nagle, T.H., S.S. Schiffman, and R. Gutierrez-Osuna (1998). "*The How and Why of Electronic Noses*". In: IEEE Spectr. 35.9, pp. 22–34.

[7] Leffingwell, J.C. (2014). *"Olfaction"*. Leffingwell & Associates. Web edition: http://www.leffingwell.com/olfaction.htm.

[8] Tudor Kalit, M. et al. (2014). "*Application of electronic nose and electronic tongue in the dairy industry"*.

[9] Wilson, A.D. and Baietto, M. (2009). "*Applications and Advances in Electronic-Nose Technologies"*.

[10] Dutta, R. et al. (2002). "*Bacteria classification using Cyranose 320 electronic nose"*.

[11] Wojciech, W. et al. (2017). "*Electronic noses: Powerful tools in meat quality assessment"*.

[12] Dave, D. et al. (2011). "*eat Spoilage Mechanisms and Preservation Techniques: A Critical Review*". American Journal of Agricultural and Biological Sciences, 6, 486-510.

[13] Cottone, N. (2017). *"La contraffazione causa una perdita di gettito di 5,7 miliardi"*. Il Sole 24 Ore, 7 August 2017.

[14] Shen, F. et al. (2016). "*Detection of Adulteration in Freshly Squeezed Orange Juice by Electronic Nose and Infrared Spectroscopy"*.

[15] Wang, Z. et al. (2019). "*Multivariate statistical analysis combined with e-nose and e-tongue assays simplifies the tracing of geographical origins of Lycium ruthenicum Murray grown in China"*.

[16] He, J. et al. (2017). "*A high precise E-nose for daily indoor air quality monitoring in living environment"*.

[17] Wilson, A.D. (2012). *"Review of Electronic-nose Technologies and Algorithms to Detect Hazardous Chemicals in the Environment"*. In: Procedia Technol. 1, pp. 453–463.

[18] Casalinuovo, I.A. et al. (2006). "*Application of Electronic Noses for Disease Diagnosis and Food Spoilage Detection".*

[19] Machado, R.F. et al. (2005). "*Detection of Lung Cancer by Sensor Array Analyses of Exhaled Breath".*

[20] Azzarelli, J.M. et al. (2014). "*Wireless gas detection with a smartphone via rf communication*". In: Proc. Natl. Acad. Sci. 111.51, pp. 18162–18166.

[21] Pearce, T.C. et al. (2004). "*Book Review: Handbook of Machine Olfaction*." In: Adv. Mater. 16.12, pp. 1028–1029.

[22] Devkota, J. et al. (2017). "*Review: SAW Sensors for Chemical Vapors and Gases*".

[23] Yuwono, A.S. et al. (2003). "*Odor Pollution in the Environment and the Detection Instrumentation".*

[24] Albert, K.J. et al. (2000). "*Cross-Reactive Chemical Sensor Arrays*". In: Chem. Rev. 100, pp. 2595-2626.

[25] Poole, C. (2012). "*GAS Chromatography*" Chap. 2. Elsevier Inc. Detroit, Michigan, USA. pp. 19-78

[26] Mellon, F.A. (2003). "*MASS SPECTROMETRY: Principles and Instrumentation*" In: Encyclopedia of Food Sciences and Nutrition (Second Edition). Academic Press. pp. 3739-3749.

[27] Aigner, R. et al. (1996). "*Si-planar-pellistor: designs for temperature modulated operation*" In: Sensor and Actuators B, 33, Elsiver Inc. pp.151-155.

[28] GCCSI, Global CSS Institute. "*Monitoring of hydrocarbons and organics*" Chap. 3.5 In: Feasibility of monitoring techniques for substances mobilised by CO2 storage in geological formations. Available online: https://hub.globalccsinstitute.com/publications/feasibility-monitoring-techniques-substances-mobilised-co2-storage-geological-34.

[29] Zhang, L. et al. (2014). "*A rapid discreteness correction scheme for reproducibility enhancement among a batch of MOS gas sensors*" In: Sensor and Actuators A, 205, pp. 170-176

[30] Thompson, J.E. (2016). "*Crowd-sourced air quality studies: A review of the literature & portable Sensors*".

[31] Ampuero, S. and Bosset, J.O. (2003). "*The Electronic Nose Applied to Dairy Products: A Review*". In: Sensors and Actuators B: Chemical, 94, 1-12.

[32] Taher, A. and Hamedsoltani, L. (2016). "*Managing of gas sensing characteristic of a reduced graphene oxide based gas sensor by the change in synthesis condition: A new approach for electronic nose design*". In: Materials Chemistry and Physics, 183, pp. 181-190

[33] Munstedt, H. and Z. Stary (2016). "*Is electrical percolation in carbon-filled polymers reflected by rheological properties?*" In: Polymer (Guildf). 98, pp. 51–60.

[34] Partridge, A.C., M.L. Jansen, and W.M. Arnold (2000). "*Conducting polymer-based sensors*". In: Mater. Sci. Eng. C 12.1, pp. 37–42.

[35] Rairigh, D. et al. (2009). "*CMOS Baseline Tracking and Cancellation Instrumentation for Nanoparticle-Coated Chemiresistors*". In: IEEE Transactions on Biomedical Circuits and Systems 3(5) pp. 267 – 276

[36] Huixia, L. et al. (2016). "*Development of ammonia sensors by using conductive polymer/hydroxyapatite composite materials*". In: Materials Science and Engineering: C Volume 59, pp. 438-444

[37] Arshak, K. et al. (2004). "A Review of Gas Sensors Employed in Electronic Nose Applications". In: Sensor Review: Volume 24, Number 2 ,pp. 181–198

[38] Bossart, E. (2011). "*The response time behaviour of pressure sensors: How is the response time defined and what is the definition of the rise time?*". Wika blog. Web edition: https://blog.wika.com/products/pressure-products/response-time-behaviour-rise-tim/.

[39] Seng Eu, K. and Meng Yap, K. (2014). "Overcoming Long Recovery Time of Metal-Oxide Gas Sensor With Certainty Factor Sensing Algorithm". 8th international conference on sensing technology, September 2-4, 2014, Liverpool, UK.

[40] Nylander, C. et al. (1983). Anal. Chem. Symp. Ser., 17, pp 203.

[41] Bai, Hua and Gaoquan Shi (2007). Gas sensors based on conducting polymers. Cabot, Co (2016). "*Black Pearl 2000 and Vulcan XC72 carbon black*". In: Cabot, pp. 2000–2001.

[42] Sangermano, M., Academic year 2016-2017. Scienza e Tecnologia dei Materiali Polimerici course slides.

[43] Treccani. Web version: http://www.treccani.it/export/sites/default/Portale/resources/multimedia/Lezioni_di_Scienze/legami_chimici2/LEZIONE_Legami_chimici_parte_seconda.pdf.

[44] Kittel, C. (1996). "*Semiconductor Crystal*". In: Introduction to Solid State Physics, Chap. 8 pp.185-218

[45] Rasmussen. S.C. (2015). "*Early history of polypyrrole: the first conducting organic polymer*". In: Bull. Hist. Chem., Volume 40, Number 1, pp 45-52.

[46] Malpicci, D. Istituto tecnico industriale Giulio Natta, academic year 2013-2014. "*ICPs: polimeri intrinsicamente conduttori*". Web version: http://www.nattabg.gov.it/wp-content/uploads/ArchivioDiplomati/LST_as13-14/5CLST/5CLST_MALPICCI_DANIELE.pdf.

[47] Thanh-Hai, L. (2017). "*Electrical and Electrochemical Properties of Conducting Polymers*". In: Polymers, Volume 9, issue 4, pp. 150-200.

[48] Kivelson, S. and Heeger, A.J. (1988). "Intrinsic conductivity of conductive polymers". In: Synthetic Metals, 22, pp. 371 - 384

[49] Manke, T. (2013). "Molecular Doping of Organic Semiconductors A Conductivity and Seebeck Study". Phd dissertation, Technische Universitat Dresden.

[50] Vigna, L. (2018). "Development of polymeric materials as gas sensors". Master degree thesis, Politecnico di Torino.

[51] Milone, A. (2018). "   ". Master degree thesis, Università del Salento.

[52] Mastragostino, M. and Soddu, L. (1990). “Electrochemical characterization of n-doped polyheterocyclic conducting polymers, polybithiophene”. In: Electrochimica Am, Vol. 35. No. 2. pp. 463-466.

[53] Snook, G.A. et al. (2011). “Conducting-polymer-based supercapacitor devices and electrodes”. In: Journal of Power Sources 196, pp. 1–12

[54] Mazzeu, M.A. et al. (2017). “Structural and Morphological Characteristics of Polyaniline Synthesized in Pilot Scale”. In: Journal of Aerospace Technology and Management, pp 345-402.

[55] Kalluri, S. (2013). “Electrospun nanofibers of polyaniline-carbon black composite for conductive electrode applications”. In: Trends in Polyaniline Research, Chap. 8.

[56] Blàha, M. et al. (2017). “Structure and properties of polyaniline interacting with H-phosphonates”. In: Synthetic Metals, volume 232, pp. 79-86.

[57] Aldaba, A.L. et al. (2018). “Polyaniline-coated tilted fiber Bragg gratings for pH sensing”. In: Sensors and Actuators B, 254, 1087–1093.

[58] Stejskal, J. et al. (2016). “Polypyrrole salts and bases: superior conductivity of nanotubes and their stability towards the loss of conductivity by deprotonation”. In: Royal Society of Chemistry.

[59] Al del Leon, R. (2015). “Conducting Polymers with Superhydrophobic Effects as Anticorrosion Coating”. In: Intelligent Coatings for Corrosion Control, 125, pp 87-101.

[60] Skodovà, J. et al. (2013). “Polypyrrole–silver composites prepared by the reduction of silver ions with polypyrrole nanotubes”. In: Polym. Chem., vol. 4, pp. 3610-3620.

[61] Benini, L. (2014). “Caratterizzazione di film sottili di PEDOT:PSS”. Master degree thesis. Alma Mater studiorum – Università di Bologna.

[62] Saghaei, J. et al. (2015). “Improvement of electrical conductivity of PEDOT:PSS films by 2-Methylimidazole post treatment”. In: Organic Electronics, vol. 19, pp. 70–75.

[63] Wiener, J. et al. (2013). “Preparation and Characterization of Conductive Cellulosic Fabric by Polymerization of Pyrrole”. In: Materials Sciences and Applications, vol. 4, pp. 649-655.

[64] Priyanka, K. et al. (2018). “Manufacturing Techniques of Perovskite Solar Cells”. In: Applications of Solar Energy, Energy, Environment, and Sustainability. pp. 341-364.

[65] Davis, R.L. et al. (2014). “Creating controlled thickness gradients in polymer thin films via flowcoating”. In: Langmuir 30.19, pp. 5637–5644.

[66] Khatami, N. et al. (2013). “Modeling of aerosol spray characteristics for synthesis of sensor thin film from solution”. In: Applied Mathematical Modelling, vol. 37, pp. 6389-6399.

[67] ATSDR Agency for toxic substances and disease registry (1997). “Public health statement chloroform”. Available online: www.atsdr.cdc.gov/.

[68] NIOSH National institute for occupational safety and health.

[69] Li, Y et al. (2012). “A novel surface acoustic wave-impedance humidity sensor based on the composite of polyaniline and poly(vinyl alcohol) with a capability of detecting low humidity”. In: Sensors and Actuators B, vol. 165, pp. 7– 12.

[70] Deng, Y. et al. (2018). “Chemically Modified Polyaniline for the Detection of Volatile Biomarkers of Minimal Sensitivity to Humidity and Bending”. In: Advanced healthcare materials, vol 7.